(NASA-CR-157749) DESIGN, MANUFACTURE, DEVELOPMENT, TEST, AND EVALUATION OF BORON/ALUMINUM STRUCTURAL COMPONENTS FOR SPACE SHUTTLE. VOLUME 1: DESIGN AND ANALYSIS (General Dynamics/Convair) 216 p 00/16 34452

Unclas

REPORT NO. GDCA-DBG73-006
CONTRACT NAS 8-27738

DESIGN, MANUFACTURE, DEVELOPMENT, TEST, AND EVALUATION OF BORON/ALUMINUM STRUCTURAL COMPONENTS FOR SPACE SHUTTLE

VOLUME I • DESIGN AND ANALYSIS

M. F. Miller
J. L. Christian
W. F. Wennhold

August 1973

Prepared Under
Contract NAS8-27738

Submitted to
National Aeronautics and Space Administration
GEORGE C. MARSHALL SPACE FLIGHT CENTER
Huntsville, Alabama

Prepared by
CONVAIR AEROSPACE DIVISION OF GENERAL DYNAMICS
San Diego, California

10011

FOREWORD

The following final report describes work performed on NASA Contract NAS 8-27738 by the San Diego Operation, Convair Aerospace Division of General Dynamics Corporation. The work was administered by the Materials Division of the Astronautics Laboratory, George C. Marshall Space Flight Center, Huntsville, Alabama 35812. Mr. F. P. Lalacona was the NASA project officer.

The program was conducted ty the Advanced Composites Group at Convair Aerospace, San Diego Operations. Principal designers for the program were A. F. Fujimoto, W. F. Wennhold, and R. E. Eckberg; the shear beam component fabrication was directed by C. R. Maikish. Other primary contributors to the program were:

Stress Analysis	E. E. Spier, G. Foelsch, R. Wilson
Design	D. Vaughan, J. D. Forest
Secondary Fabrication	M. Hersh, C. May, M. D. Weisinger, J. Christiana, M. Maximovich
Subcomponent Testing	N. R. Adsit
Nondestructive Evaluation	R. T. Anderson, R. Stewart
Environmental Studies	E. E. Keller

This report covers the entire program contract from 1 July 1971 to 30 June 1973.

Dr. M. F. Miller
Program Manager

J. L. Christian
Deputy Program Manager

PRECEDING PAGE BLANK NOT FILMED

Preceding page blank

TABLE OF CONTENTS

TABLE OF CONTENTS, Contd

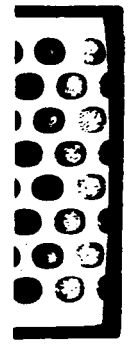

TABLE OF CONTENTS, Contd

LIST OF FIGURES

LIST OF FIGURES, Contd

LIST OF FIGURES, Contd

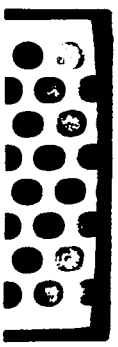

LIST OF TABLES

X74-10011

ABSTRACT

A program was performed to evaluate material properties, processing techniques, and fabrication characteristics of boron/aluminum (B/Al) to develop sufficient technology to permit the application of B/Al in reusable spacecraft with a high degree of confidence. The program included the design of three thrust structure components for the space shuttle, the testing of subcomponent specimens to verify design and joint fabrication concepts, and culminated in the design and fabrication of two components: a 1 by 0.96m (40 by 38 in.) shear beam weighing 35.4 kg (78 lb) designed for service at 366K (200F), and a 2 by 0.7m (80 by 29 in.) compression panel weighing 20.2 kg (44.4 lb) and capable of service up to 589K (600F). These structures successfully demonstrated that B/Al structural components could be fabricated and assembled using modified sheet metal technology and today's factory equipment. These panels have been shipped to NASA-MSFC where the shear beam will be structurally tested at room temperature and the compression panel at 589K (600F).

SECTION 1

INTRODUCTION

The application of advanced composites, both resin and metal-matrix, to aircraft and missile structure has become prevalent in recent years. It is clear that these high-strength, low-weight composite materials will find additional structural applications on future aerospace vehicles.

Several large aircraft and missile components have already been fabricated using metal-matrix composites as one of the key structural materials. The PRIME adapter for the Atlas booster (Reference 1), built in 1968, was the first major metal-matrix structure built: 1.2m (4 ft) in diameter and 2.1m (7 ft) high. During testing, failure (crippling of three stringers) occurred at 133% of ultimate design load (200% of limit load). The F-106 aircraft access door (Reference 2), built in 1969, was the first boron/aluminum (B/Al) structure to be flight tested. A duplicate test panel failed at 169% of design limit load. An F-111 aircraft fuselage bulkhead (Reference 3) consisted of BORSIC/6061-T6 Al with a titanium frame. The crossplied skin was stiffened with unidirectional zees, angles, and straight and joggled tees. During structural testing, failure occurred at 130% of design ultimate load. A dual OV1 support system truss structure (Reference 4), approximately 2m (80 in.) long and 0.8m (30 in.) square, was fabricated from seamless BORSIC/aluminum tubes. The spacer skins for the same system were fabricated from roll-formed crossplied skins 3.1m (10 ft) in length.

These test articles demonstrated that B/Al technology had progressed sufficiently to enable consideration of its use for space shuttle applications. Fabrication methods and joining techniques had been thoroughly examined and it was only necessary to optimize joining processes for large-scale structures, and to demonstrate the capability of metal-matrix structures to withstand the loading and environmental conditions encountered in space shuttle applications.

1.1 PROGRAM OBJECTIVES

The objectives of this program were to compare the use of B/Al in Space Shuttle applications with other structural materials and to evaluate material properties, processing techniques, and fabrication characteristics to develop sufficient technology to permit application of B/Al for space shuttle structural components with a high degree of confidence.

The program objective of demonstrating the applicability of B/Al composite structures for reusable spaceflight vehicles was achieved through a series of logical processes. It started with selecting and characterizing materials and proceeded with developing minimum design allowable data. Coincidental with this study, design and structural analysis of three structures were performed. Fabrication processes applicable to the

production of large-scale, metal-matrix structures were optimized, and selected subcomponents of a thrust structure shear web beam and a uniformly loaded compression panel were fabricated and tested to verify design and structural analysis, and to demonstrate the ability of developed joining methods to withstand both thermal and load cycling. A full-thickness component of the thrust structure shear web beam and a uniformly loaded compression panel were designed and fabricated for testing at MSFC.

The most significant accomplishment on the program was the successful fabrication of metal-matrix structures applicable to the space shuttle. These structures included such diverse sheet metal fabrication processes as forming, welding, brazing, drilling, sawing, riveting and heat treating of unidirectional and crossplied B/Al ranging in thickness from 1.78 mm (0.070 in.) to over 15.3 mm (0.60 in.). The two component test articles, a 1.0 × 0.96m (40 × 38 in.) shear beam and a 2.03 × 0.74m (80 × 29 in.) compression panel, demonstrated that B/Al structures similar to those required for reusable space flight vehicles could be fabricated with existing aircraft shop facilities using modified sheet metal technology.

1.2 ORGANIZATION

This report is divided into two volumes. The first volume details the design, stress analysis, and testing of structures examined during the program. Specifically, designs are presented for 9.2 × 3.1m (30 × 10 ft) and 1.0 × 0.96m (40 × 38 in.) shear beams, a 9.2 × 3.1m (30 × 10 ft) truss, and 3.1 × 3.1m (10 × 10 ft) and 2.0 × 0.7m (80 × 29 in.) compression panels as well as several subcomponent specimens. The second volume contains material characterization, process development, process and material specifications or guidelines, and manufacturing procedures used in the fabrication of component and subcomponent test articles.

1.3 COMPONENT TESTING

The two major component test specimens prepared during the program, a 1×0.96m (40×38 in.) shear beam and a 2×0.75m (80×29 in.) compression panel, are to be tested at NASA-MSFC. Because of scheduling difficulties at the Marshall Space Flight Center, it was not possible to perform these tests prior to issuance of this document. At the time of publication, no firm date had been established for testing the two components.

1.4 NEW TECHNOLOGY

In compliance with the New Technology clause of this contract, personnel assigned to work on the program were advised, and periodically reminded, of their responsibilities in the prompt reporting of items of New Technology. In addition, reports generated as a result of the contract work were reviewed by the Program Manager as a further means of identifying items to be reported.

Response was made to all inquiries by the company-appointed New Technology Representative, and when deemed appropriate, conferences were held with the New Technology Representative to discuss new developments arising out of current work that could lead to New Technology items. The New Technology Representative has the responsibility for transmitting reportable items of New Technology to the Technology Utilization Officer, as well as the annual and final reports specified in the Clause.

The Contractor believes the performance of personnel associated with the contract has been consistent with the requirements of the New Technology clause.

SECTION 2

SHEAR BEAM

2.1 INTRODUCTION

The general approach to the design was to use recognized structural advantages of boron/aluminum (B/Al) to the maximum extent possible. These advantages include a high crippling efficiency that results from its high effective modulus of elasticity, adaptability to proven design concepts, and compatibility with a number of joining methods. In addition, the potential of B/Al for specific property enhancement by heat treatment was used when required.

2.2 OBJECTIVES AND DESIGN CRITERIA

The task objective was to develop a B/Al shear web beam design for reusable spacecraft. The design requirements for the shear beam are shown in Figure 2-1. After final optimization of processes and materials and completion of design analysis, a selected component of the thrust structure shear web beam was fabricated at Convair for testing at NASA-MSFC.

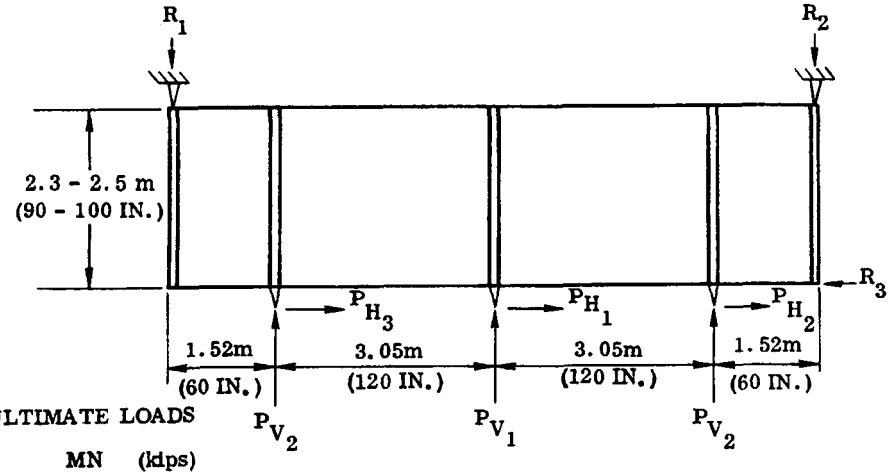

ULTIMATE LOADS

	MN	(kips)
P_{V_1}	2.01	453
P_{V_2}	1.47	330
P_{H_1}	.244	55
P_{H_2}	.489	110
P_{H_3}	0	0

1. MATERIAL IS BORON/ALUMINUM EXCEPT OPTIONAL FOR FITTINGS, ETC.
2. DESIGN TEMPERATURE 366K (200F).
3. P_{H_1} AND P_{H_2} APPLIED 30 CM (12 IN.) BELOW LOWER SURFACE OF LOWER CAP.
4. UPPER AND LOWER BEAM CAPS SUPPORTED LATERALLY AT LOAD INTRODUCTION POINTS.

Figure 2-1. Thrust Structure Shear Web Beam

The primary structural material for the beam was B/Al, with small amounts of titanium or other optional materials used for fittings, splices, etc. Four types of shear web beams were considered:

a. B/Al shear resistant beam.

b. Tension field B/Al beam.

c. Titanium web tension field beam.

d. Honeycomb shear web beam.

2.3 TRADE STUDIES

2.3.1 SHEAR RESISTANT B/Al BEAM DESIGN. The initial B/Al shear resistant beam selected for detail weights analysis is shown in Figure 2-2. The beam is 9.14m (360 in.) long and 2.54m (100 in.) deep, with stiffeners spaced on 12.7 cm (5 in.) centers. The beam caps, vertical stiffeners, and load introduction posts are fabricated from unidirectional B/Al. The web is fabricated from ST&A crossply ±45° material, tapered in thickness from the tension to compression beam cap. The beam caps and web are strain limited to 0.0038 m/m at ultimate load to meet the design requirements of 1.1 on yield and 1.4 on ultimate. The 12.7 cm (5 in.) stiffener spacing was selected based on the weight analysis of Figure 2-3. The spacing selected appears to be the minimum practical limits for design and fabrication considerations.

2.3.1.1 Web Design. Web gages for the selected design are shown in Figure 2-2. Each web panel is approximately 0.762m (30 in.) wide and spliced with a double row of spotwelds. The web thickness is maintained constant on the tension side of the beam and tapers on the compression side. Shear lag was not considered at the load introduction posts. Several iterations of the web gages were required to establish the minimum weight since the buckling strength is dependent on the secant modulus (E_S), which in turn is determined by the maximum strain levels attainable in the beam caps. The finite elements computer program was used in subsequent iterations to establish the true internal loads for the adjustment of web gages.

2.3.1.2 Vertical Stiffeners. The vertical stiffeners were sized to the I requirements shown in Table 2-1 for 12.7 cm (5 in.) spacing. The stiffeners are tapered from the tension cap to the compression cap utilizing the minimum section required to enforce a nodal point. Back-to-back Z- or J-sections were considered for ease of spotwelding the web. The sections can be fabricated in three segments and brazed together to form the desired cross section. The stiffener gage was selected with the limitation that it would be no thinner than 0.6 times the web thickness.

2.3.1.3 Compression and Tension Beam Caps. The compression and tension caps, shown in Figure 2-4, are fabricated from unidirectional B/Al. The beam cap is tapered from the center to the ends both in thickness and width along the length. The tension

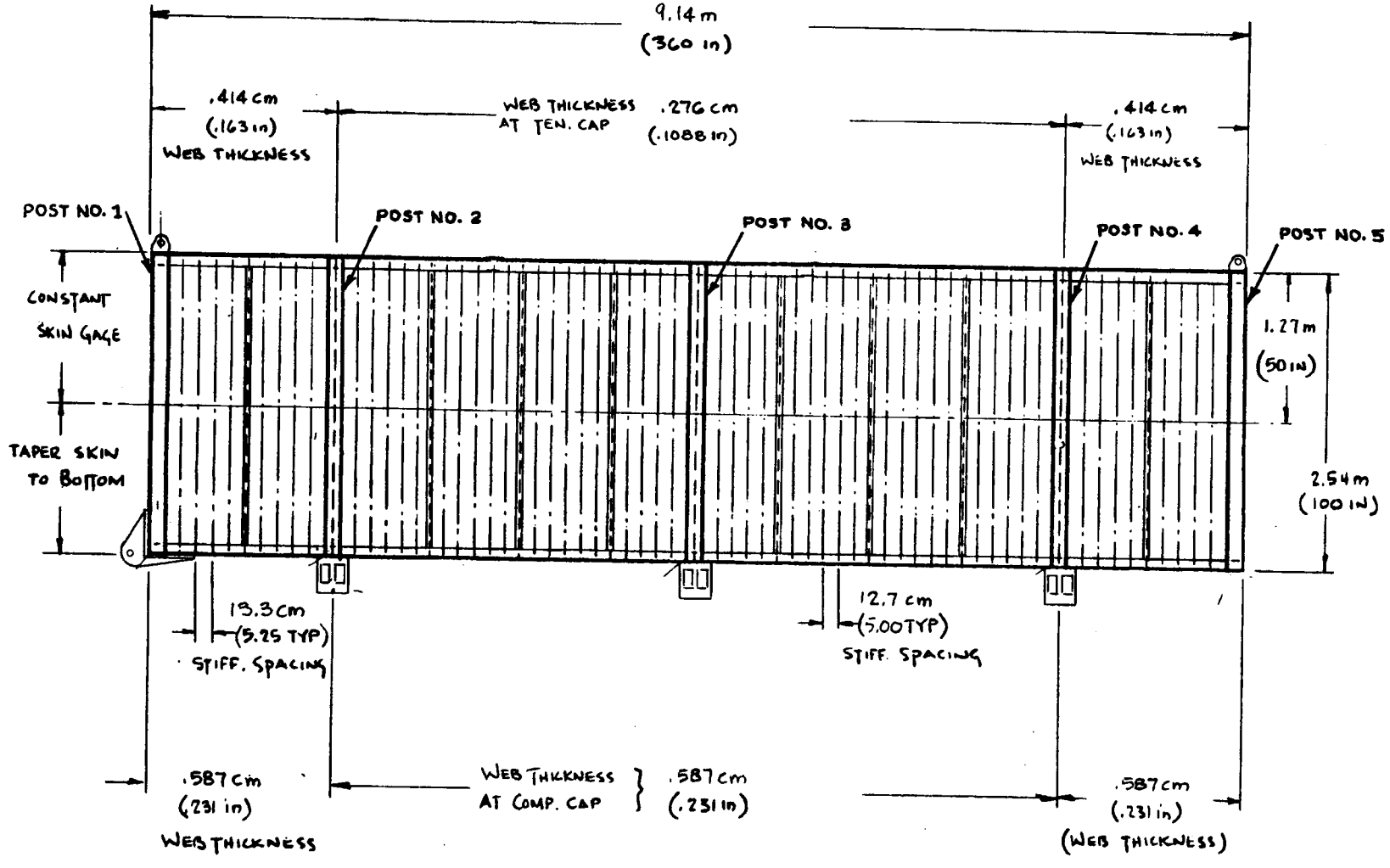

Figure 2-2. Shear Resistant Beam Web Gages

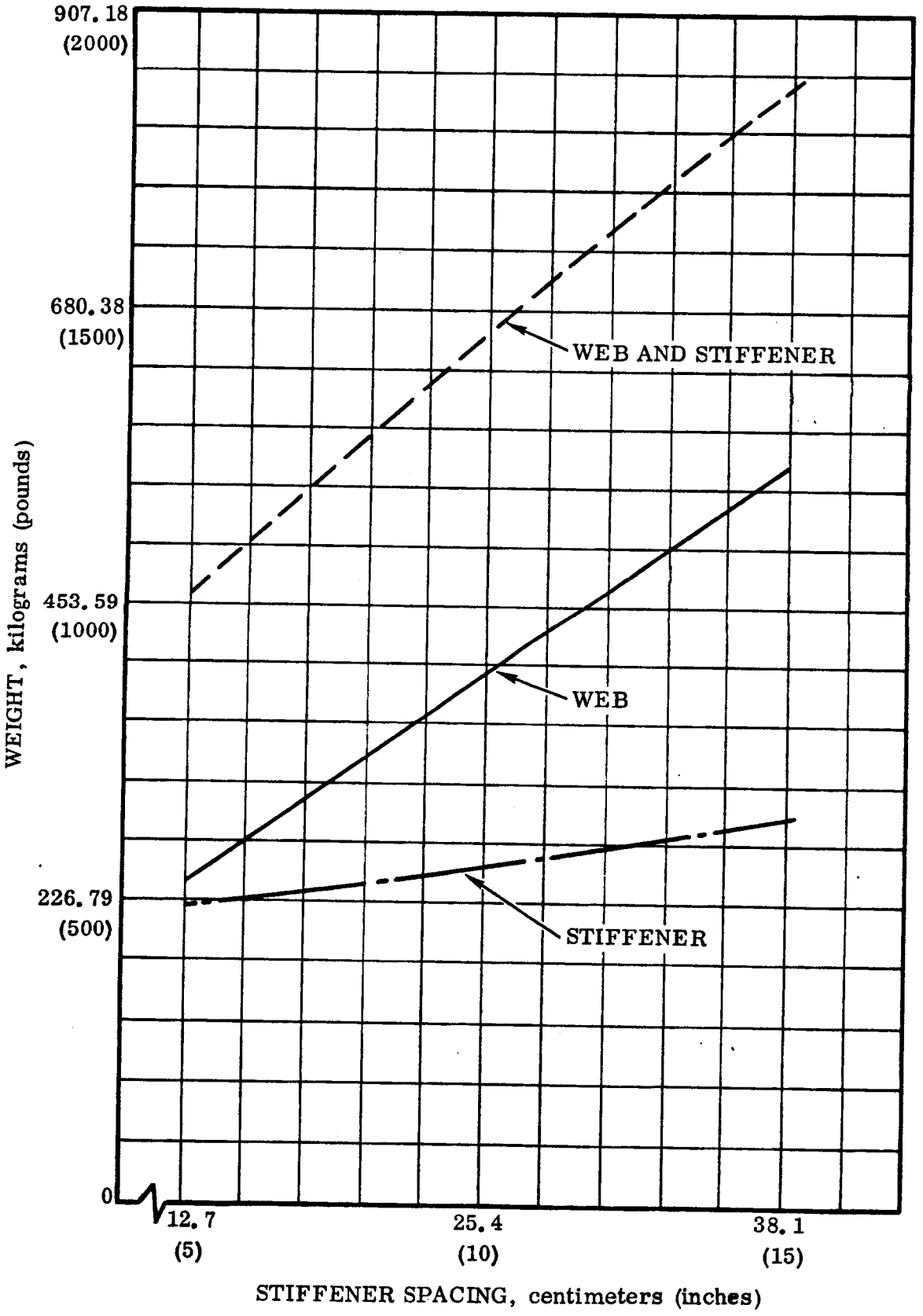

Figure 2-3. Shear Resistant Beam Stiffener Spacing Versus Web and Stiffener Weight

Table 2-1. Vertical Stiffener I-Section Requirements

Stiffener Spacing		Panel Thickness		I Required		Stiffener Area	
cm	in.	cm	in.	cm^4	$in.^4$	cm^2	$in.^2$
12.7	5	0.2764	0.1088	32.0	0.768	3.43	0.531
		0.4140	0.163	107.6	2.584	5.14	0.797
		0.5410	0.213	305.1	7.33	9.37	1.453
19.05	7.5	0.3454	0.136	54.9	1.32	4.03	0.625
		0.4851	0.191	151.1	3.63	7.56	1.172
		0.8280	0.326	757.5	18.20	17.89	2.773
		0.8636	0.340	857.4	20.60	18.65	2.891
25.4	10	0.4496	0.177	117.1	2.813	6.95	1.078
		0.5867	0.231	260.1	6.250	8.92	1.383
		1.1379	0.448	1900.8	45.668	30.70	4.758
		1.1735	0.462	2084.9	50.090	31.40	4.867
38.1	15	0.5867	0.231	229.7	5.518	8.62	1.336
		0.7595	0.299	497.8	11.96	13.50	2.094
		1.6942	0.667	5494.0	132.0	55.45	8.594

cap was sized to a maximum allowable stress of 786 MN/m^2 (114,000 psi) to limit the strain to 0.0038 m/m. The compression cap section was established on the basis of plate stability $F_{cr} = (t/b)^2 G_{xy}$, and the lateral stability requirements as a column over the maximum unsupported length. The upstanding legs for both caps were maintained at a constant depth for web and stiffener attachment. The thickness is limited by the shear strength of unidirectional B/Al. The upstanding leg is brazed to the beam caps.

2.3.1.4 Load Introduction Posts. The load introduction post cross-sections are shown in Figure 2-5. They consist of back-to-back channels spliced to the web with rivets. The overall sections are 13.2 cm (5.2 in.) wide, 7.62 cm (3 in.) deep and with a web thickness of 0.635 cm (0.25 in.). The flanges are brazed to the web to form the channel section. Post No. 2, 3, and 4 were sized for the combined compression load and moment resulting from the horizontal gimbal loads. The outboard posts (No. 1 and 5) were sized for compression only. The loads were assumed to be uniformly sheared into the webs. The finite element computer program was used in subsequent interations to establish the post internal loads. The output was used to establish the desirability of tapering the parts in the final design.

2.3.2 B/Al TENSION FIELD BEAM. The B/Al tension field beam design is shown in Figure 2-6. The overall beam configuration is similar to that of the shear resistant design with the primary difference being in the size of the beam caps and the shear web panel aspect ratio. The load introduction points and reaction points are identical to those of the shear resistant beam design. The design study was done only in sufficient detail to obtain a weight comparison with the other beam concepts.

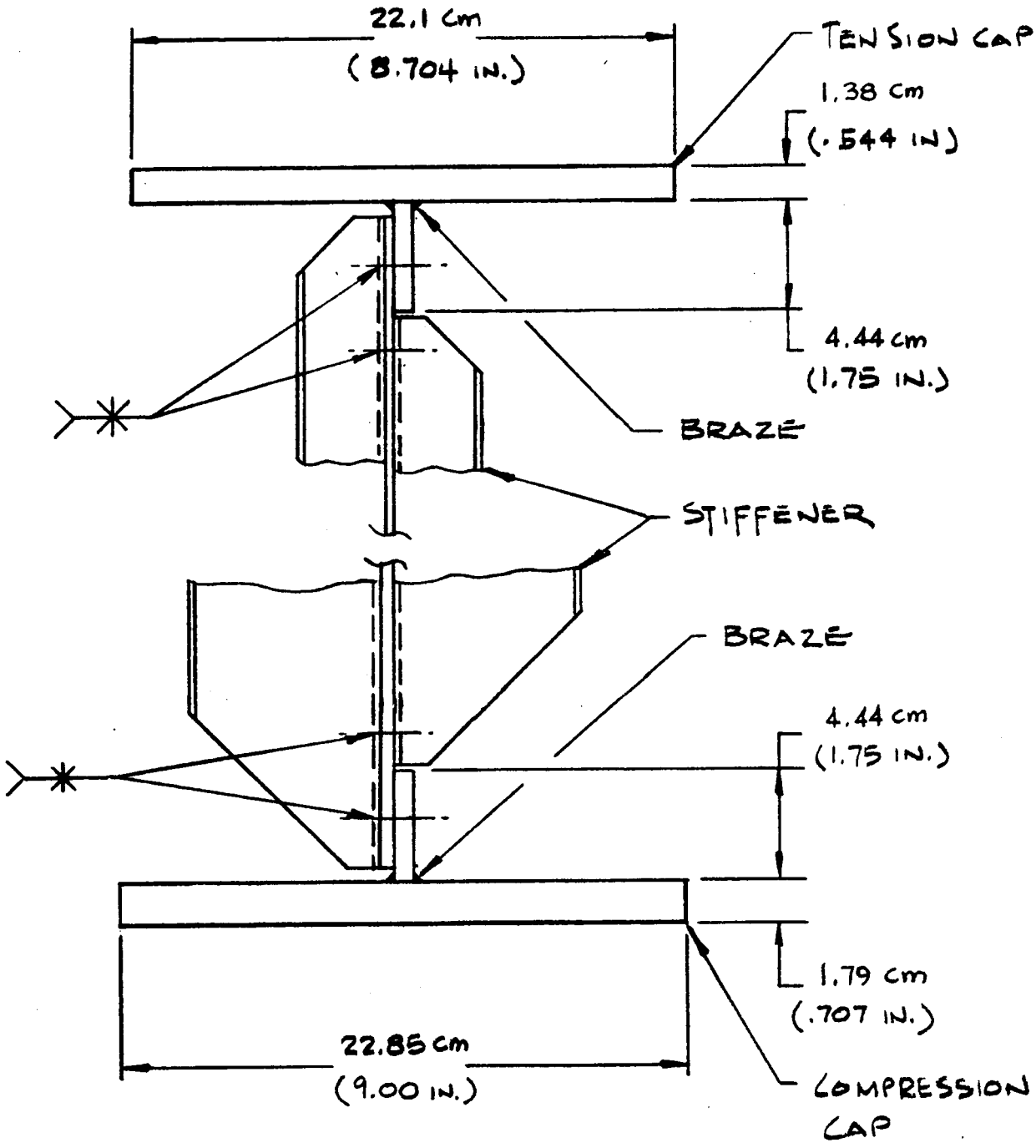

Figure 2-4. Shear Resistant, Tension and Compression Beam Cap Cross Section

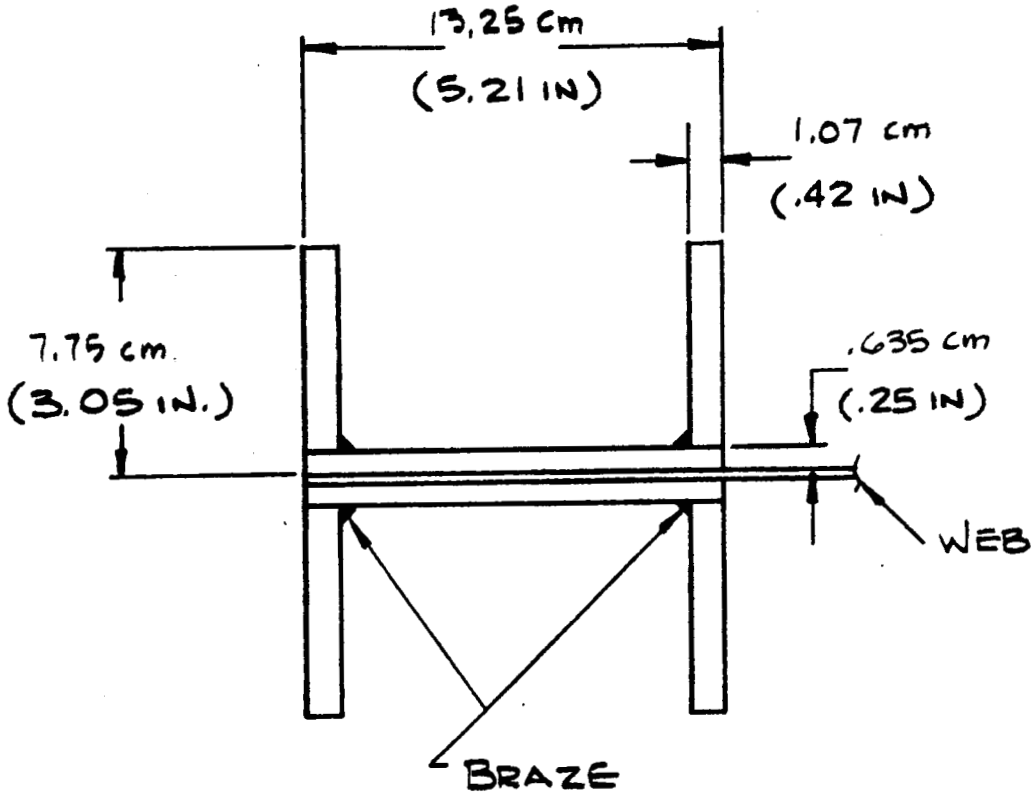

OUTBOARD LOAD REACTION POST # 1 & 5

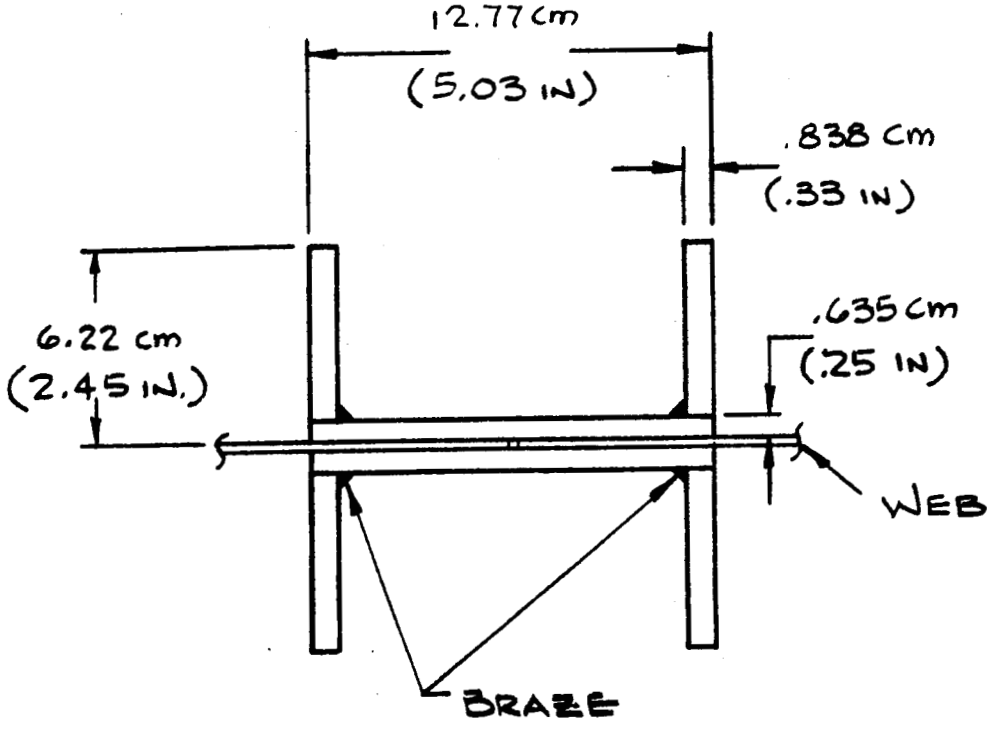

ENGINE THRUST POST # 2 - 4

Figure 2-5. Shear Resistant Beam Load Introduction Posts

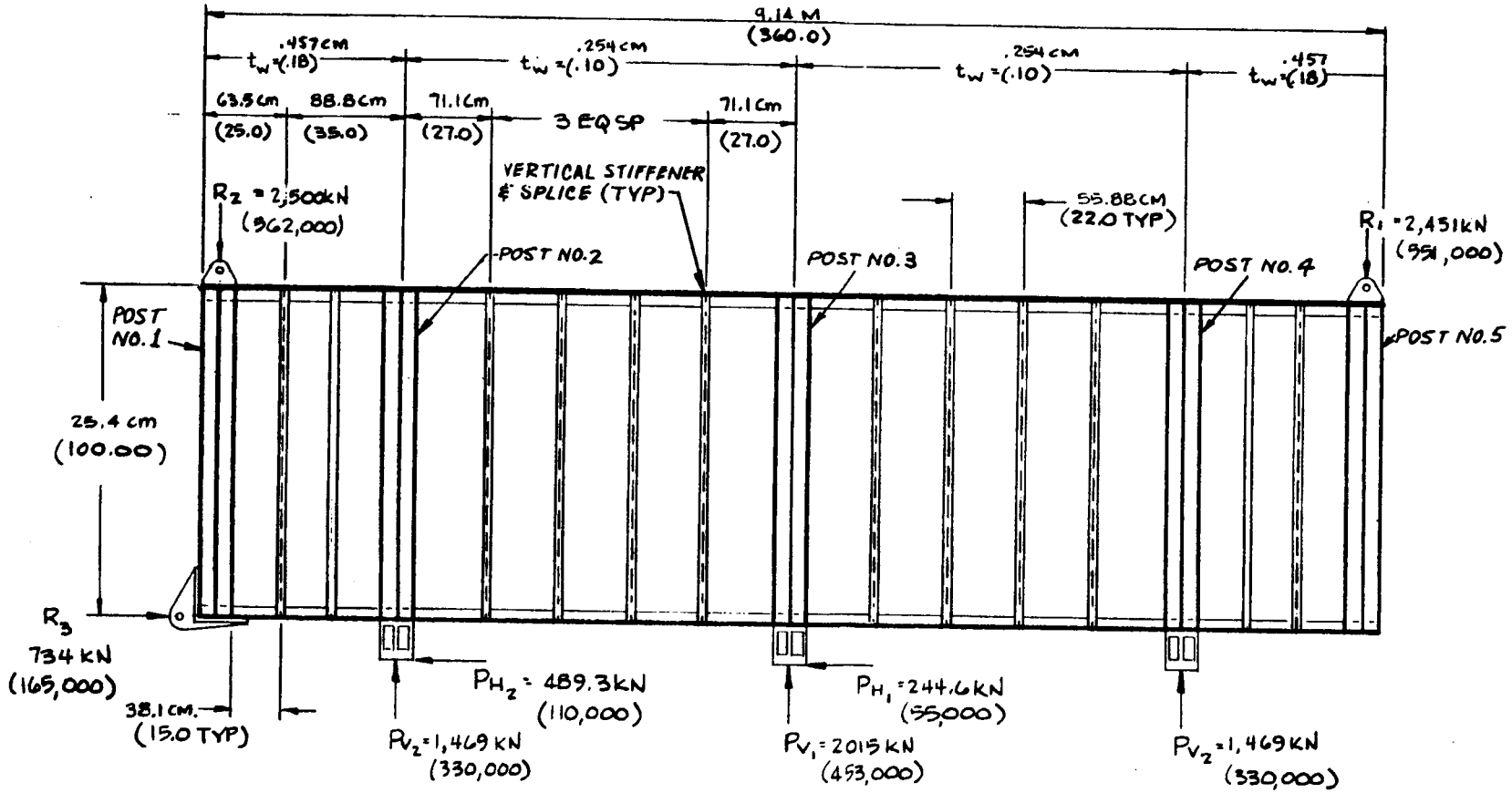

Figure 2-6. B/Al Tension Field Beam

The design was based on the analysis method of NACA Technical Note 2661. The tension field web was designed to a loading ratio of $\tau/\tau_{cr} = 2.1$ and 8.68 for the outboard and inboard bays respectively. The panel aspect ratios selected were 6.7:1 and 5:1 with diagonal tension angles of 43 and 41 degrees.

2.3.2.1 Web Design. The panel widths were kept relatively small for both the inboard and outboard bays to maintain a small diagonal tension factor since no data was available on the safe limits of diagonal tension for crossply B/Al. Available test data covers a range of τ/τ_{cr} up to 10. The panel sizes used were 50.8 cm (20 in.) wide and 0.254 mm (0.10 in.) thick for the center bays and 38.1 cm (15 in.) wide and 0.457 cm (0.18 in.) thick for the outboard bays. τ_{cr} was established from the equation:

$$\tau_{cr} = K_S \frac{\pi^2 E}{12(1-\mu^2)} (t/b)^2$$

where K_S = 5.5 and 5.4 for the center and outboard bays respectively.

The maximum web shear stress for the panels selected were 158.6 MN/m^2 (23,000 psi) and 213.8 MN/m^2 (31,000 psi) for the inboard and outboard panels respectively. The diagonal tension stresses were 317.2 MN/m^2 (46,500 psi) and 434.4 MN/m^2 (63,000 psi). The panels were assumed to be spotwelded to the vertical stiffeners and the beam caps; thus, no allowances were made for decreased allowables for attachment.

No allowances were made in the establishment of the web gages for the strain compatibility at the attachment interface between the web and beam caps. Up to the web buckling stress, a uniform shear flow was used over the effective web depth. Maximum available sheet width was considered to be 91.5 cm (36 in.); thus, web splices were provided for an increment no greater than 91.5 cm (36 in.).

2.3.2.2 Beam Caps. The beam caps are fabricated from unidirectional B/Al. The caps were sized to the combined external bending moment and diagonal tension loads. The caps are tapered from the beam centerline to the outboard ends. The upstanding legs are maintained at a constant depth of 10.16 cm (4 in.) and 7.62 cm (3 in.) for the compression and tension caps to allow fastener attachment of the vertical stiffeners and provide the moment of inertia for the tension field secondary bending stresses. Typical beam cap sections are shown in Figure 2-7. The average compression and tension stresses at the beam centerline are 602 MN/m^2 (87,400 psi) and 710 MN/m^2 (103,000 psi) respectively. At the outboard load introduction points, post No. 2 and 4, the stresses are 548.5 MN/m^2 (50,600 psi) and 527 MN/m^2 (76,700 psi). The secondary bending stresses on the compression flange resulting from diagonal tension are small, 115 MN/m^2 (16,700 psi) at the centerline and 55.1 MN/m^2 (8,000 psi) at post No. 2 and 4. The small secondary bending stresses result from the small diagonal tension factor (K) and the close stiffener spacing. The relatively inefficient beam cross section at post

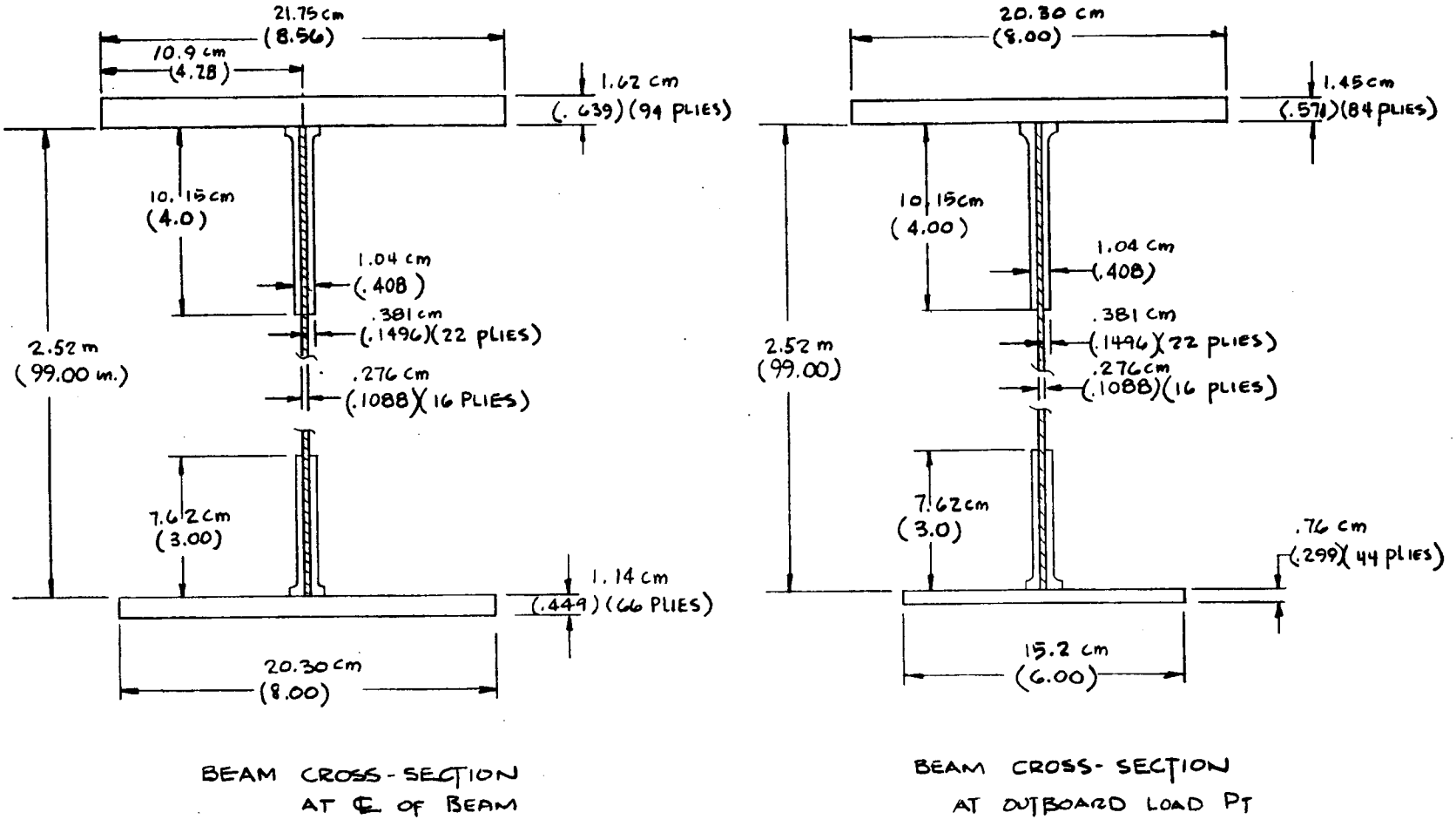

Figure 2-7. Tension Field Beam Caps

No. 2 and 4 resulted from maintaining a wide beam cross section for lateral instability as a column together with maintaining a constant upstanding leg depth for the web and stiffener attachment.

The combined secondary bending and compressive stresses at the beam centerline, post No. 3 is 716 MN/m^2 (104,000 psi) as compared to an allowable stress of 820 MN/m^2 (119,000 psi). At the outboard load points, post No. 2 and 4, the combined stress is 516 MN/m^2 (75,000 psi) with a large margin indicating that further refinements can be made to the beam caps for reduced weight.

2.3.2.3 Vertical Stiffeners. The vertical stiffener design shown in Figure 2-8 was sized to the requirements of NACA TN 2661. The stiffeners resist the vertical component of the diagonal tension that tends to pull the beam flanges together, and thus they were sized as a column. Double uprights (stiffeners on each side of web) were selected. The stiffener spacing generally coincides with the web splice; thus, the stiffeners were made an integral part of the splice. The splice material was ST&A ± 45° cross-ply B/Al with the upstanding leg and flange material unidirectional B/Al. Brazing was selected as the means of fabricating the detail stiffeners with attachment to the web by rivets or spot-welds. The stiffeners were assumed to be capable of being joggled for attachment to the beam caps as shown. Identical stiffeners were used for both the inboard and outboard bays resulting in a conservative design for the outboard bay.

2.3.2.4 Load Introduction Posts. The load introduction posts consist of back-to-back UD B/Al channels that are spliced to the web with rivets. The overall channel sections are 25.4 cm (10 in.) wide and 7.62 cm (3 in.) deep with a web thickness of 0.762 cm (0.30 in.). The flanges are brazed to the web to form the channel section (Figure 2-9). The load introduction posts No. 2 and 4 were sized for the combined compression load and moments resulting from the horizontal engine gimbal loads. Since the web is in the buckled state, the horizontal loads were assumed to be reacted at the compression and tension beam caps. The compression loads were assumed to be uniformly sheared into the web and the posts were sized as a column to the equation from Reference 5.

$$ql = \frac{2\pi^2 EI}{l^2}$$

The allowable column stress was established using the Johnson-Euler equation. The local crippling stresses were established from the equations $F_{cr} = (t/b)^2 G_{xy}$ for one unloaded edge free, three sides simple support, and $F_{cr} = \frac{2\pi^2}{tb^2} (\sqrt{D_{11} D_{22}}) + D_{12} + 2 D_{66}$ for the web elements.

The end bay of a tension field beam is normally made shear resistant to react the horizontal component of diagonal tension. In this design configuration, the large reaction

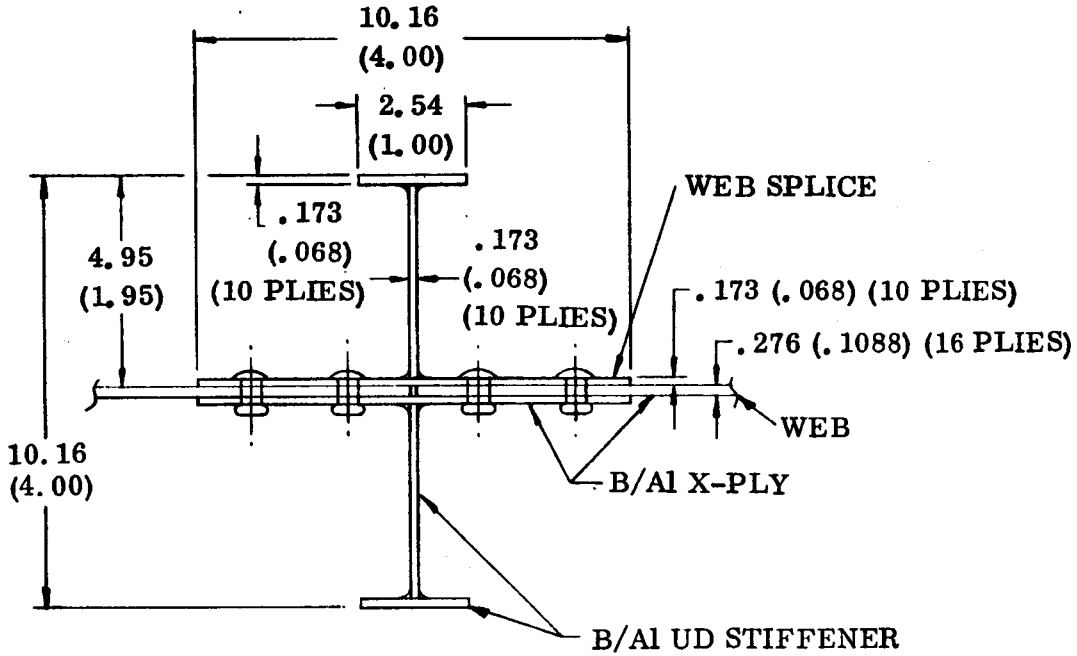

TYPICAL VERTICAL STIFFENER

MEASUREMENTS IN CENTIMETERS (INCHES)

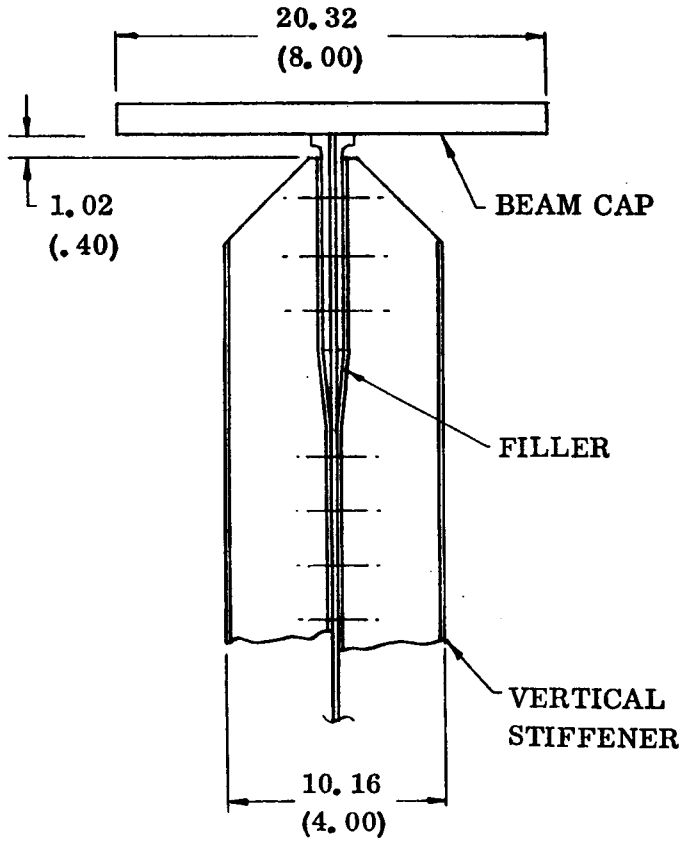

TYPICAL BEAM CAP &

VERTICAL STIFFENER JOINT

Figure 2-8. Tension Field Beam Vertical Stiffener

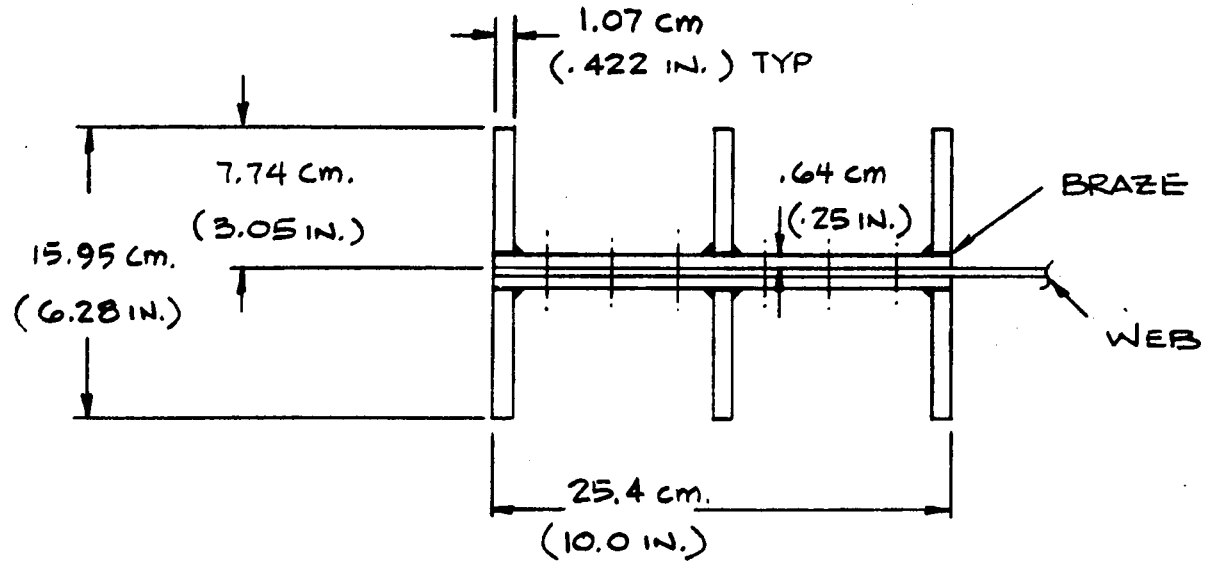

OUTBOARD LOAD REACTION
POST NO. 1 & 5

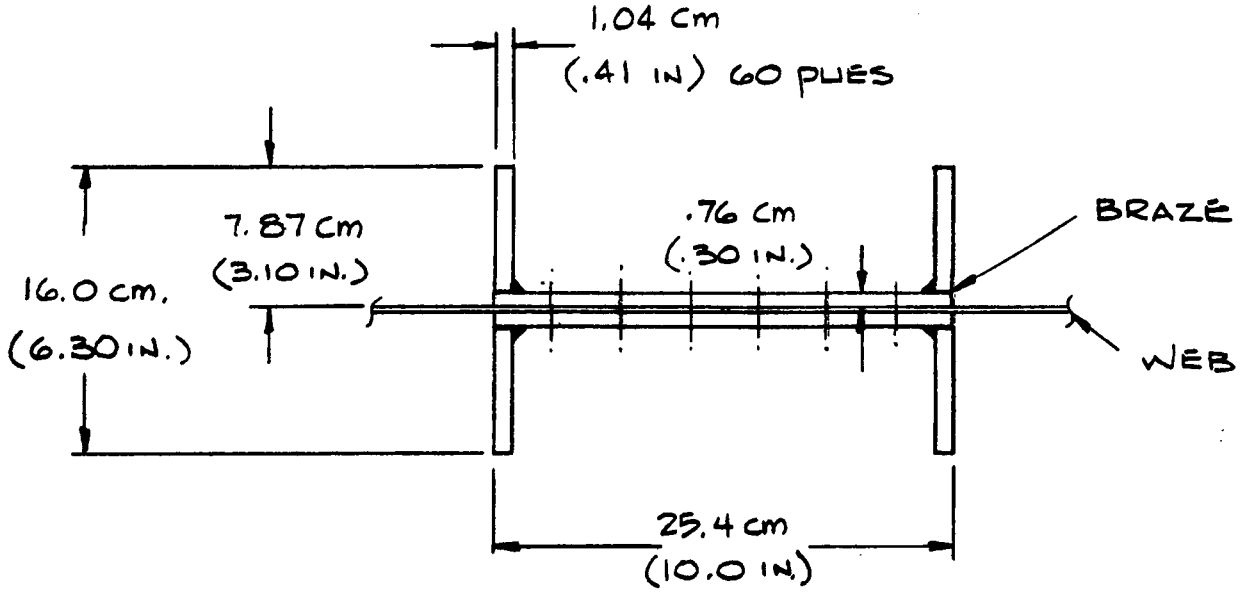

ENGINE THRUST LOAD
POST NO. 2, 3, & 4

Figure 2-9. Tension Field Beam Load Introduction Columns

loads at post No. 1 and 5, together with the small diagonal tension factor, led to the consideration of utilizing the end posts as a beam to react the horizontal component of diagonal tension with less weight penalty than a shear resistant end bay. For this design iteration, the columns were made a constant section to react the horizontal component of diagonal tension. The end posts were sized for the interaction of combined bending and compression. The allowable column stresses were established in a similar manner to that described for the inboard posts.

2.3.3 TITANIUM WEB, TENSION FIELD BEAM. Titanium alloy Ti-6Al-4V was considered for the web of a shear beam. The web thickness and stiffener spacings were selected to obtain efficient tension field webs. The method of analysis was taken from Reference 5. Stiffener spacings of 25 cm (10 in.) and 33 cm (13 in.) were chosen for the maximum and minimum shear loadings, respectively. An important parameter in the analysis of these tension field beams is τ/τ_{cr}, where τ is the applied shear stress and τ_{cr} is the buckling shear stress. This ratio of τ/τ_{cr} can be permitted to be quite high for static loading. However, because of fatigue considerations it has been limited to around 5 for airliners. For military aircraft and missiles, this ratio could be much greater. For Space Shuttle, τ/τ_{cr} has been arbitrarily limited to 25. For 33 cm (13 in.) wide panels, the web thickness is 0.152 cm (0.060 in.) with a τ/τ_{cr} of 22. For 25 cm (10 in.) wide panels, the web thickness is 0.38 cm (0.150 in.) with a τ/τ_{cr} of 4. The theory presented in NACA TN 2661 is for an entire structure being of the same material. Consequently, some of the simple equations have been partially modified to account for B/Al flanges and stiffeners with a titanium web. These original equations from Reference 5, Section 3, are presented showing the appropriate modifications:

	Original		Modified
Upright Stress:	$\sigma_U = -\dfrac{k\tau \tan\alpha}{\dfrac{A_{U_e}}{dt} + 0.5(1-k)}$	(30a)	$\sigma_U = -\dfrac{k\tau \tan\alpha}{\dfrac{E_U A_{U_e}}{E_{WEB}\,dt} + 0.5(1-k)}$
Flange Stress:	$\sigma_F = -\dfrac{k\tau \cot\alpha}{\dfrac{2A_F}{ht} + 0.5(1-k)}$	(30b)	$\sigma_F = -\dfrac{k\tau \cot\alpha}{\dfrac{2E_F A_F}{E_{WEB}\,ht} + 0.5(1-k)}$
Strains:	$\epsilon_F = \dfrac{\sigma_F}{E}$		$\epsilon_F = \dfrac{\sigma_F}{E_F}$

Original	Modified
$\epsilon_U = \frac{\sigma_U}{E}$	$\epsilon_U = \frac{\sigma_U}{E_U}$
$\epsilon = \frac{1}{E}(\sigma_1 - \mu\sigma_2)$	$\epsilon_{WEB} = \frac{1}{E_{WEB}}(\sigma_1 - \mu\sigma_2)$

These equations are to be used in the formula for the tension field angle:

$$\tan^2 \alpha = \frac{\epsilon - \epsilon_F}{\epsilon - \epsilon_U} \qquad (30c)$$

where

U = upright (vertical) stiffener

f = flange (cap)

k = tension field factor

A = area

h = height

t = thickness

τ = shear stress

σ = normal stress

The design was analyzed only in sufficient detail to establish a weight comparison with the B/Al design. The beam caps, vertical stiffeners, and load introduction posts from the B/Al design were selected for a first-cut design and found to meet the load requirements. These weights were therefore used in the weight summary discussed in Section 2.3.5.

2.3.4 ADDITIONAL CONCEPTS

2.3.4.1 Unidirectional B/Al Tension Field Design. A secondary concept, which fulfills the study desirability for an all B/Al shear beam, would utilize unidirectional material for a tension field web. A considerable saving in weight is anticipated for this configuration. However, the uncertainties associated with the development of this shear beam make it an undesirable selection for primary development in this study. Some consideration was given to design of a subelement test specimen to evaluate the feasibility of the concept. For this concept to be a consideration for the space shuttle shear beam design, the loading must be in the most part nonreversible.

2.3.4.2 Honeycomb-Stiffened Shear Web Beam. A honeycomb core sandwich was considered for the web of the shear beam. The configuration considered consists of large panels without stiffeners between adjacent posts. The sandwich material considered was heat resistant aluminum honeycomb core (Table 2-3 in Reference 2) with a facing material of ±45° crossplied B/Al. Analysis indicated that a core thickness of 3.7 cm (1.5 inches) with a core density of 49.6 kg/m^3 (3.1 lb/ft^3) was required together with a facing thickness one-half the required thickness for the shear resistant stiffened beam.

Several factors were taken into consideration prior to any detailed design work. These included the poor adhesive bondline reliability when exposed to cyclic applications of temperature and load, and the potentially overweight structures resulting from proper provisions for mechanical attachments. Because of these considerations, and the more promising concepts described above, further examination of a honeycomb-stabilized beam was discontinued.

2.3.5 WEIGHT SUMMARY. A weight summary of the three main concepts studied is shown in Table 2-2. On a weight comparison basis, the semi-tension field beam offers the lightest weight structure. This is primarily the result of the added load carrying capability of the web beyond the critical buckling load. The web plus stiffener weight of the shear resistant beam is substantially greater than for the tension field design. The close stiffener spacing used in the shear resistant design allowed for relatively thin gages as indicated by the weight comparison.

Table 2-2. Summary Weights Shear Web Beam

Component	Shear Resistant		Tension Field			
	B/Al Web		B/Al Web		Titanium Web	
	kg	lb	kg	lb	kg	lb
Web	235.6	519.51	196.4	433	276.7	610
Compression Cap	76.8	169.37	85.7	189	76.2	168
Tension Cap	48.7	107.46	53.1	117	47.6	105
Vertical Stiffeners	369.8	818.44	47.6	105	75.7	167
Web Splice	16.8	37.10	—	—	—	—
Load Introduction Posts	115.9	255.5	240.4	530	240.4	530
Total Weights	863.6	1907.4	633.2	1374	716.6	1580

The vertical stiffener weight shown indicates that the stiffener weight for the shear resistant design is five times as heavy as the tension field vertical stiffeners. This appears to be contrary to what one would expect since there is no appreciable load transfer in the stiffeners of the shear resistant design. The stiffeners serve only to divide the web into smaller panels. On the tension field beams, the vertical stiffeners must react the vertical web tension stresses tending to pull the beam flanges together -- resulting in compression forces in the vertical stiffeners. The extremely close stiffener spacing required in the shear resistant beam to obtain a high critical buckling stress and relatively thin gages results in a large I-section to enforce node points at the stiffeners. NACA TN 3782 shows that the EI/bD increases rapidly with a/b ratios beyond 5, thus resulting in the large stiffener weights for the shear resistant design.

The compression beams cap weights of the three designs are shown to be equal. The beam caps of a tension field beam would normally require a greater area than for a shear resistant beam because of the secondary bending loads from the diagonal tension and the added compression loads in the beam cap. The shear resistant beam caps, however, were constrained to a maximum strain of 0.0038 m/m, and this, together with the low transverse shear strength of unidirectional B/Al, resulted in a thick upstanding beam cap leg. The leg depth was sized to that required for attachment. Thus the effective strength of the unidirectional material is not fully utilized.

The load introduction posts are shown to be heavier for the tension field designs. This resulted from utilizing the end load introduction posts to react the horizontal component of the web diagonal tension.

From a weight, cost, and manufacturing standpoint, the titanium shear web beam with unidirectional B/Al caps appears to be the most efficient design concept; however, the tension field all-B/Al design appears to be lighter than the titanium design. The two designs are competitive from the weight standpoint.

The undesirability of the tension field design concept is its fatigue life. No data is available on the fatigue life of a B/Al tension field beam in the gages being considered. It was decided by NASA-MSFC that additional work beyond the scope of the present program would be required to verify this design concept. Because the titanium web panel did not show a gross weight saving over either the B/Al tension field or shear resistant panels, and because the program objective was to demonstrate the fabricability of essentially all-B/Al structures, NASA-MSFC felt this concept was not consistent with this goal. Therefore, by NASA direction, the remainder of the design work on the shear web beam was on the shear resistant concept using a $\pm 45°$ crossply B/Al web.

2.4 FINAL DESIGN SHEAR WEB BEAM

The final design of the shear resistant shear web beam is shown in Figure 2-10. The basic preliminary design drawing was modeled for the finite element computer program. The model is shown in Figure 2-11. The member areas, web thicknesses, cap areas, load introduction posts, and vertical stiffeners were iteratively adjusted to the final design values.

2.4.1 WEB DESIGN. The fiber orientation of the preliminary design was modified from ±45° to a 90°, ±45° layup to increase the material allowables in the direction of primary tension and compression loading. The basic B/Al skin gages were not altered significantly from the values used in the preliminary sizing. The early finite element computer program indicated that the web was being stressed above the material allowables in compression and tension. Two options were available to modify the design: 1) increase the beam cap areas and thereby reduce the web strain, or 2) revise the fiber orientation to tailor the web strength to the loading. It was found necessary both to increase the beam cap areas by 25% and to revise the fiber orientation to a 90°, ±45° layup in selective sections of the web as shown in Figure 2-12.

It was determined that increasing the web-gage does not have significant effect in decreasing the web stress. This becomes obvious since the beam I-section is not significantly increased. The longitudinal web stress results from the beam cap strains. The web is material allowable critical on the tension side (F_{TU}) and compressive buckling critical on the compression side of the beam.

The web splice locations were modified from the preliminary design drawings to areas away from the high load introduction posts.

2.4.2 FINAL BEAM CAP DESIGN. The final design beam caps, tension and compression, were modified from an all-composite T-section to that shown in Figure 2-13. Subelement tests conducted during the design iterations indicated that the design configuration for the beam cap to upstanding leg braze joint cannot be satisfactorily joined in thick sections. A backup joint design that was successfully tested (see Section 3.4.3) utilizing a titanium web attachment was incorporated in the final design. In addition, the original design indicated a need to increase the compression and tension cap areas to reduce the web stresses below 490 MN/m^2 (70 ksi) in the localized areas near the upper and lower beam caps. The tension- and compression-beam caps vary in both thickness and width; they are fabricated from unidirectional B/Al. The tension cap has a cross-sectional area of 27 cm^2 (4.75 in^2) at the beam centerline and 10.9 cm^2 (1.75 in^2) directly adjacent to the outboard lateral extremities. At the lateral extremities the cap member has special configuration provisions for attachment to the beam end post and load fitting. The compression cap has a cross-sectional area of 48 cm^2 (7.0 in^2) at the beam centerline and 16 cm^2 (2.55 in^2) at its lateral extremities.

FOLDOUT FRAME

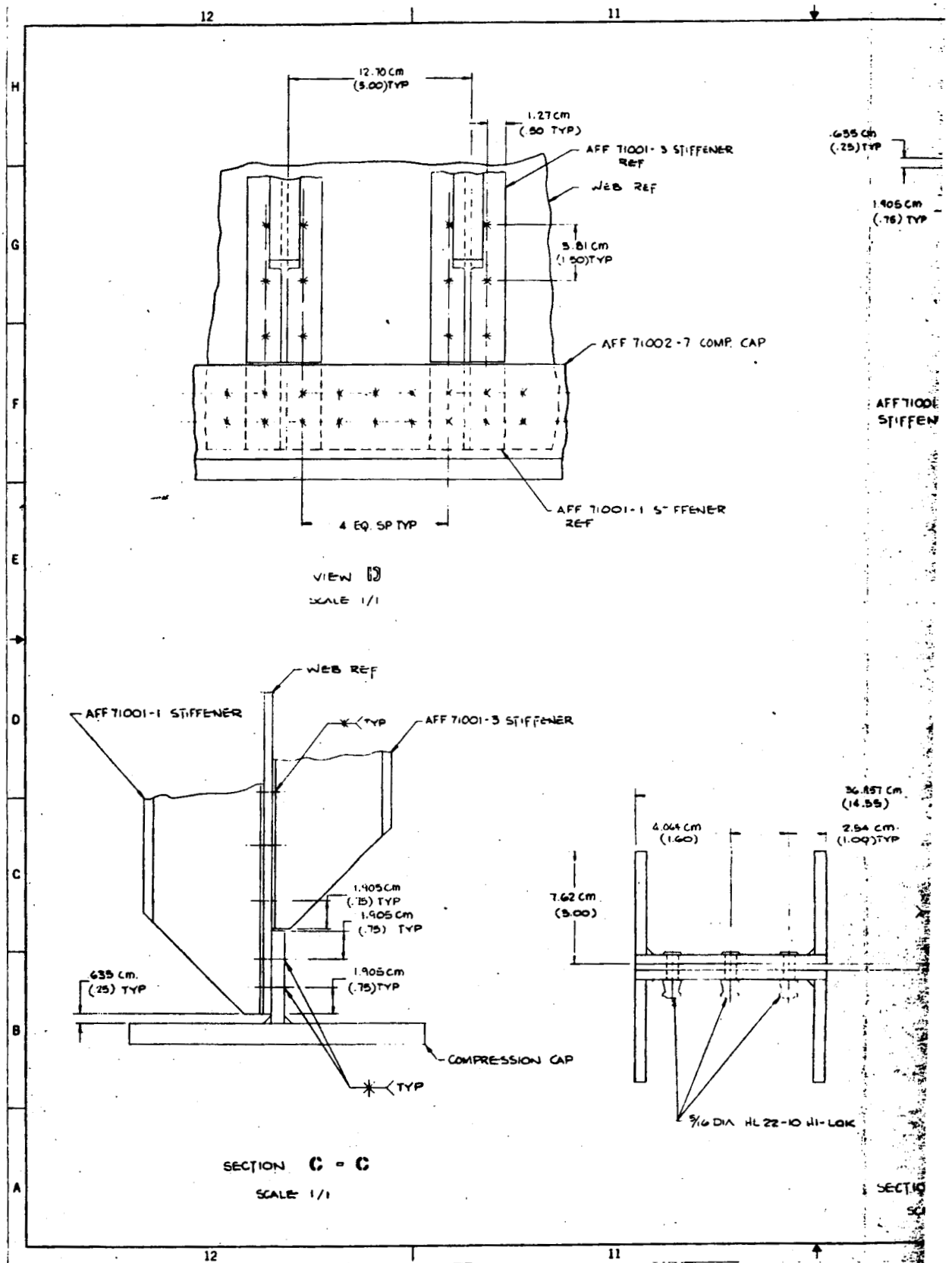

2-19/20 - A

FOLDOUT FRAME 2

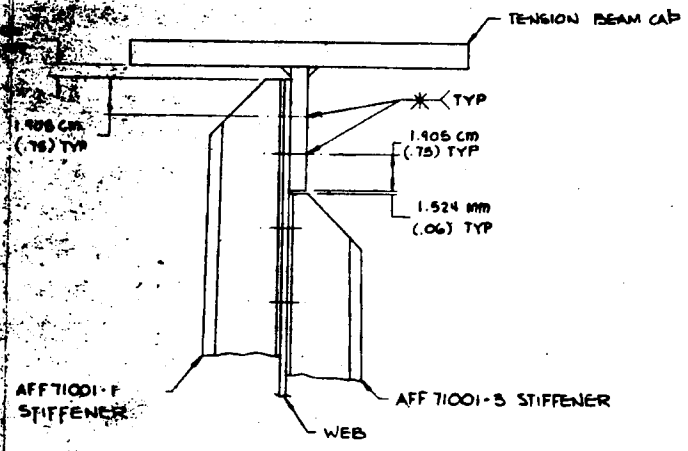

SECTION C2 - C2
SCALE 1/1

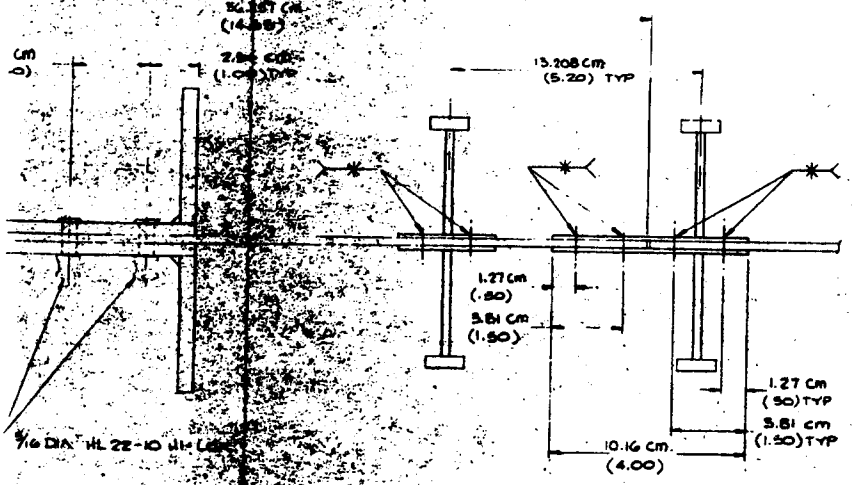

SECTION B - B
SCALE 1/1

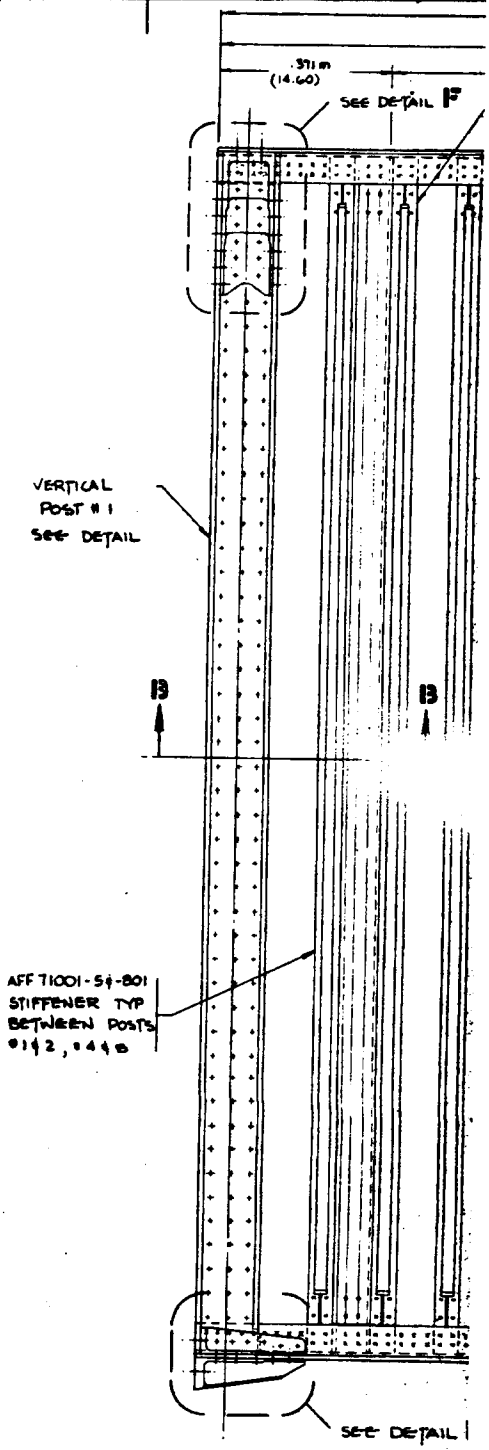

14170

2-19/20-B

FOLDOUT FRAME 2

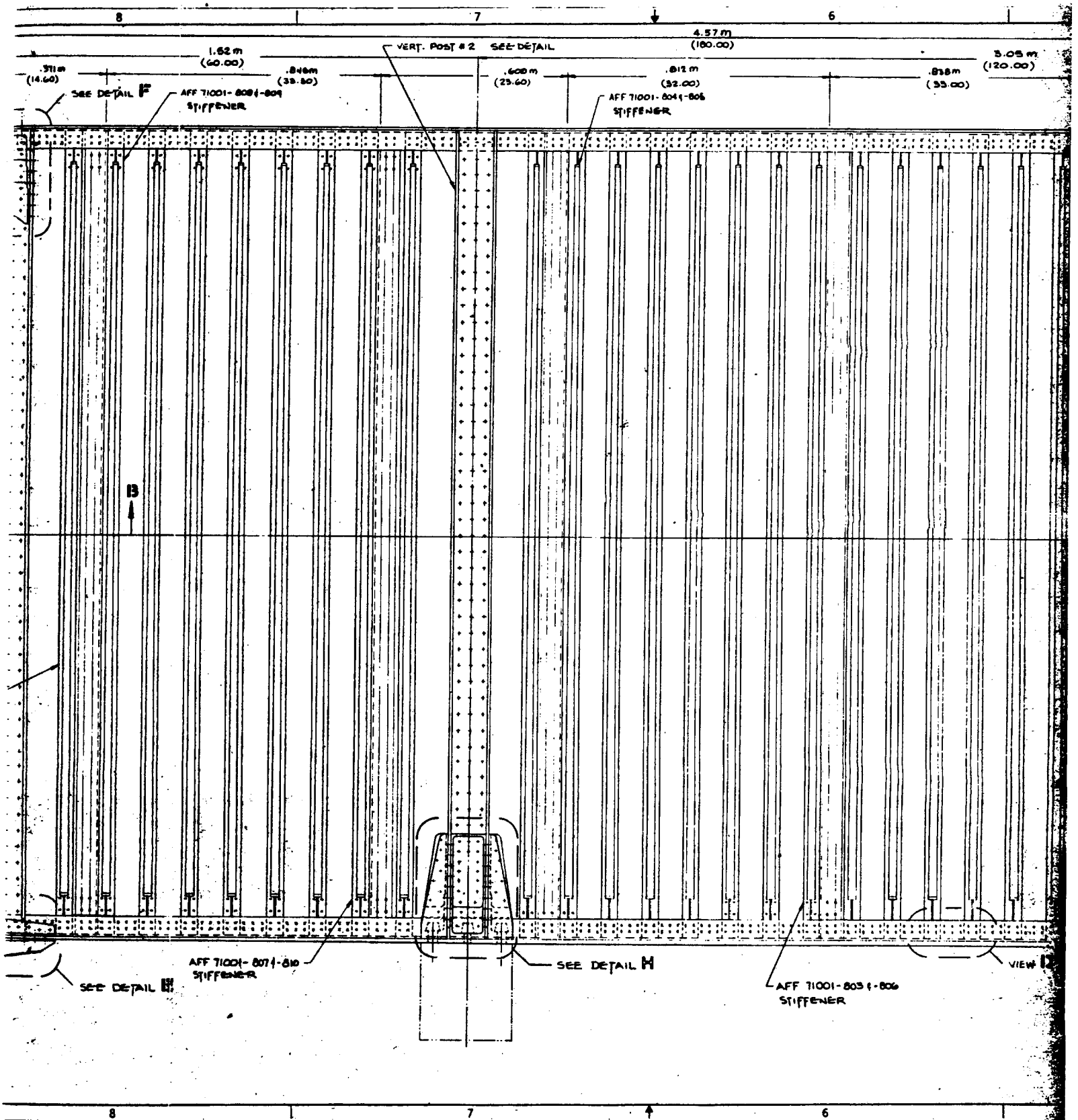

2-19/20-B

2-19/20-C

FOLDOUT FRAME 3

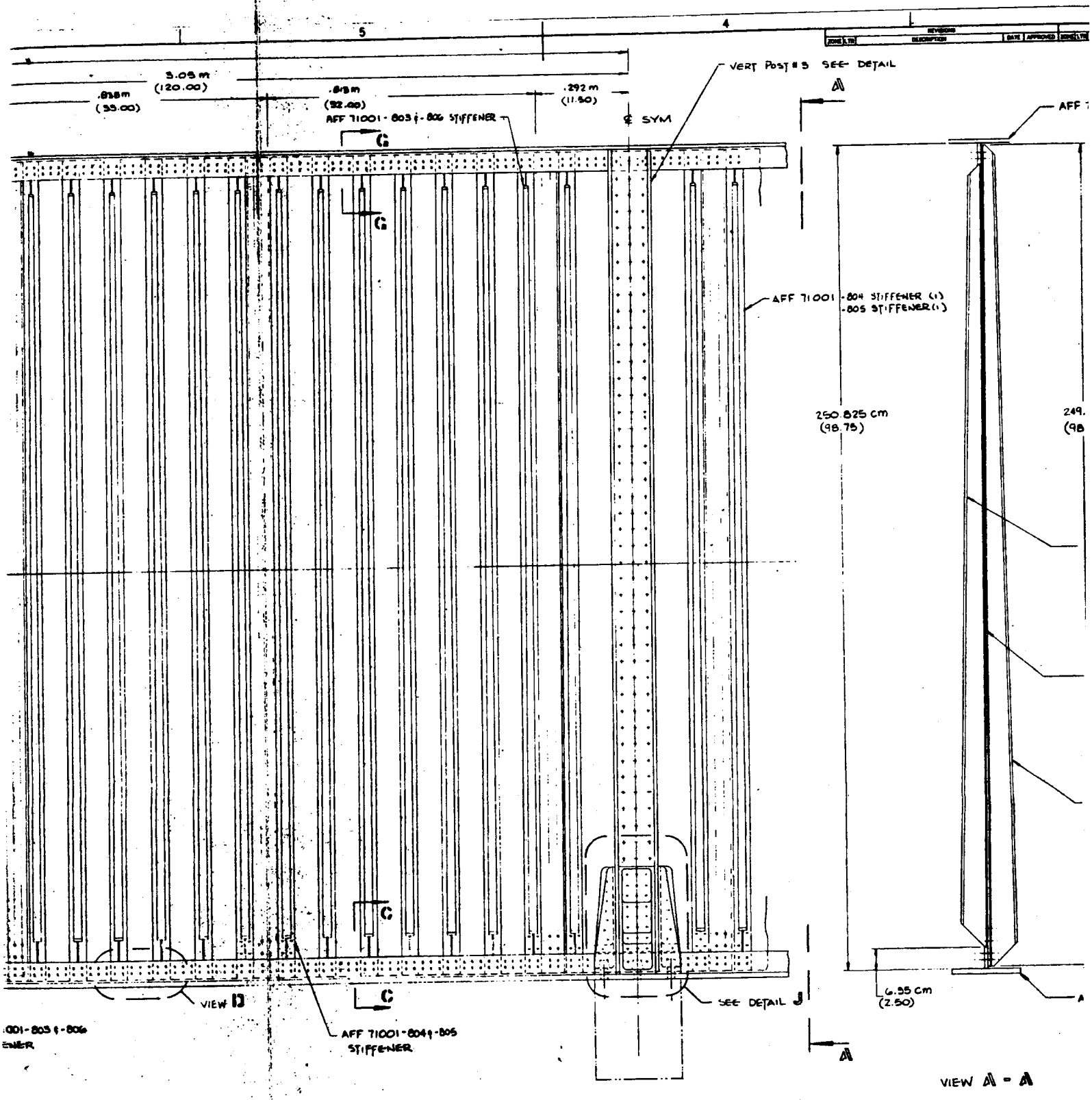

14170

2-19/20 -D

FOLDOUT FRAME
4

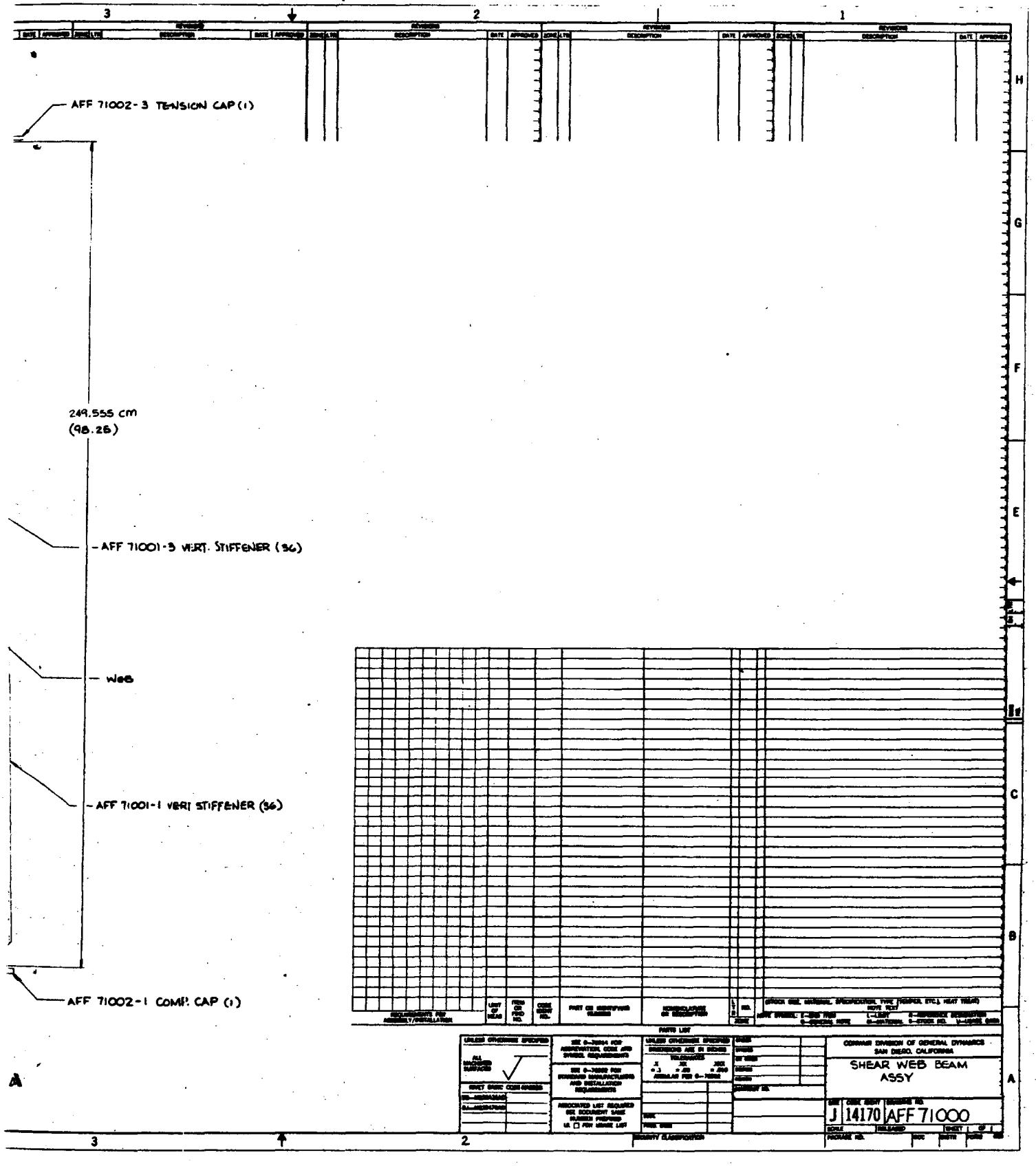

Figure 2-10. Shear Web Beam Assembly

FOLDOUT FRAME

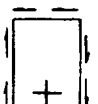

SHEAR
SIGN CONVENTION

NOTES: 1. NODES
2. ELEME
3. NUMBE
MATE

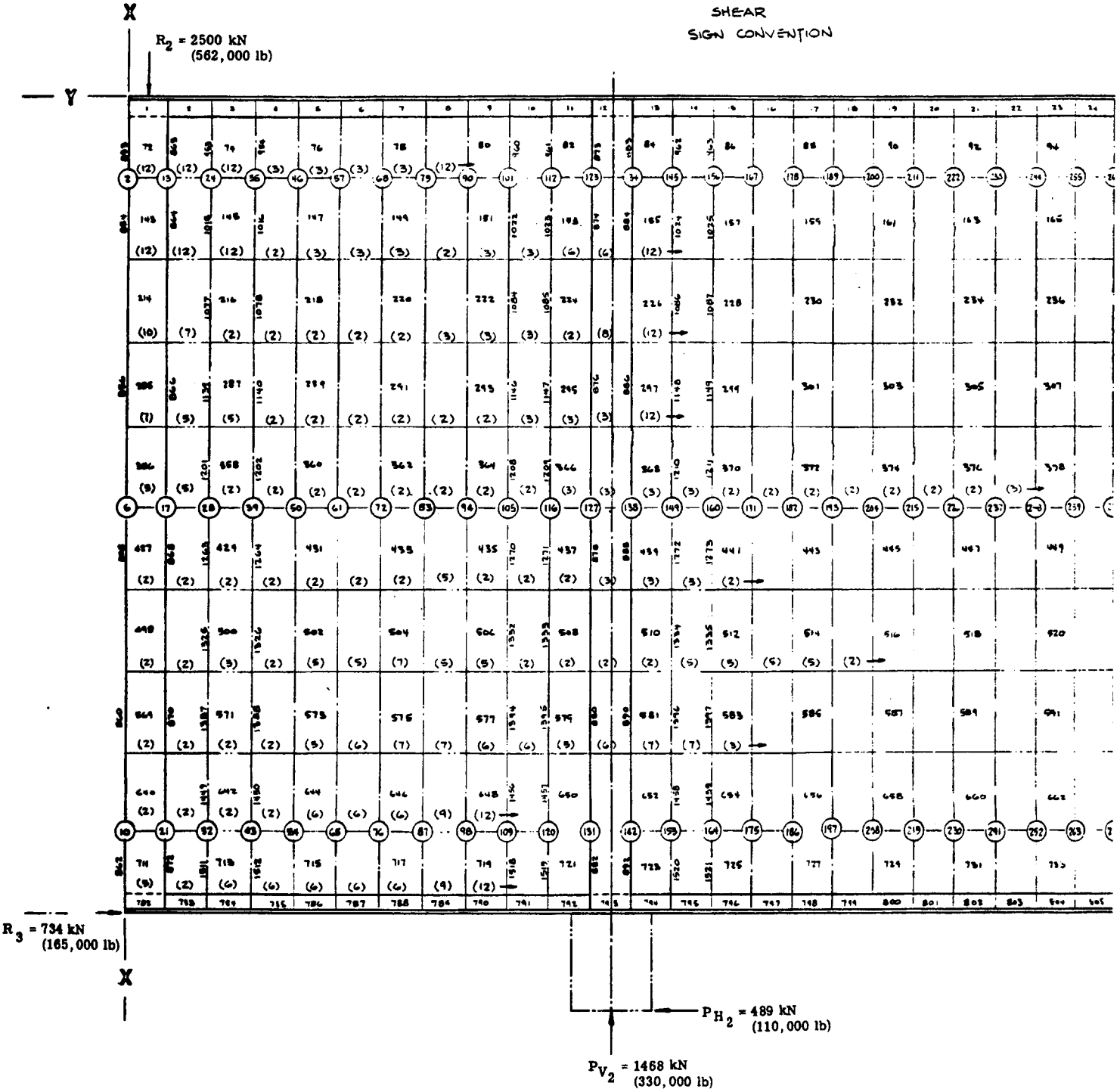

2-21 H

NOTES: 1. NODES INDICATED IN CIRCLE

2. ELEMENT NUMBERED FROM 1 TO 1572

3. NUMBERS IN PARENTHESIS INDICATE WEB MATERIAL DESIGNATIONS

FOLDOUT FRAME 2

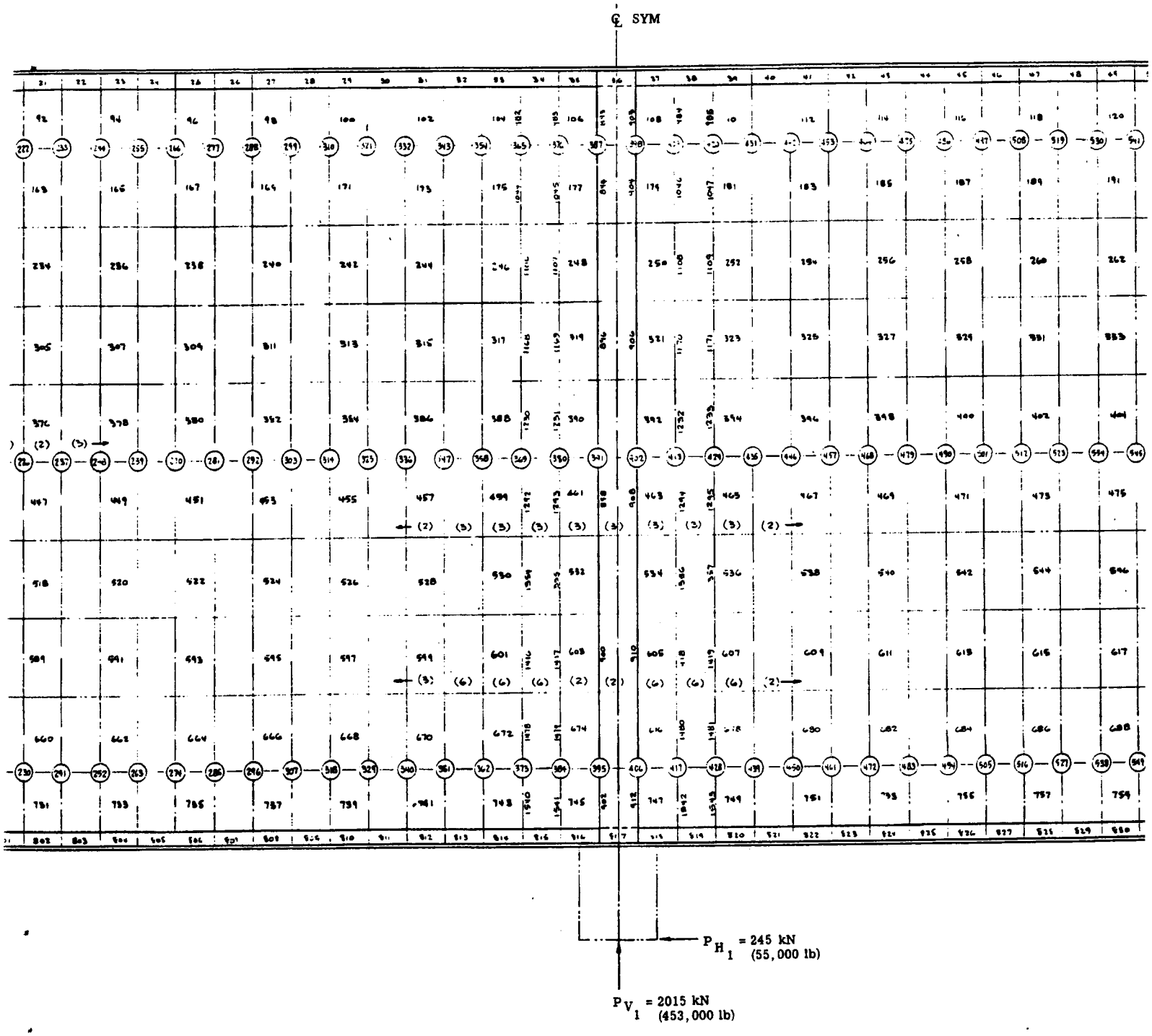

A

2-21

B

FOLDOUT FRAME 3

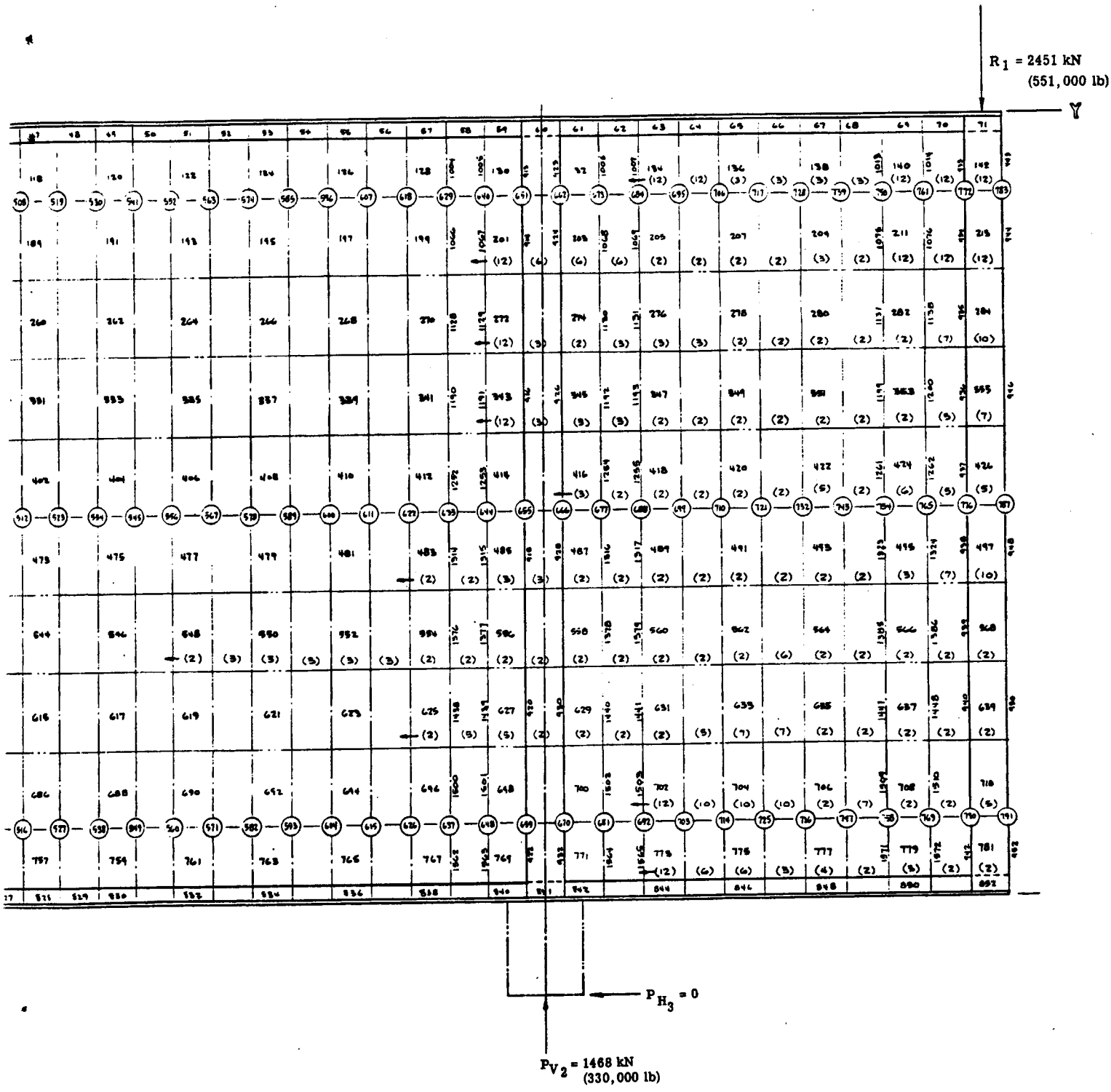

Figure 2-11. Shear Beam Geometry Node Points, Element and Web Material Design for Computer Program

FOLDOUT FRAME

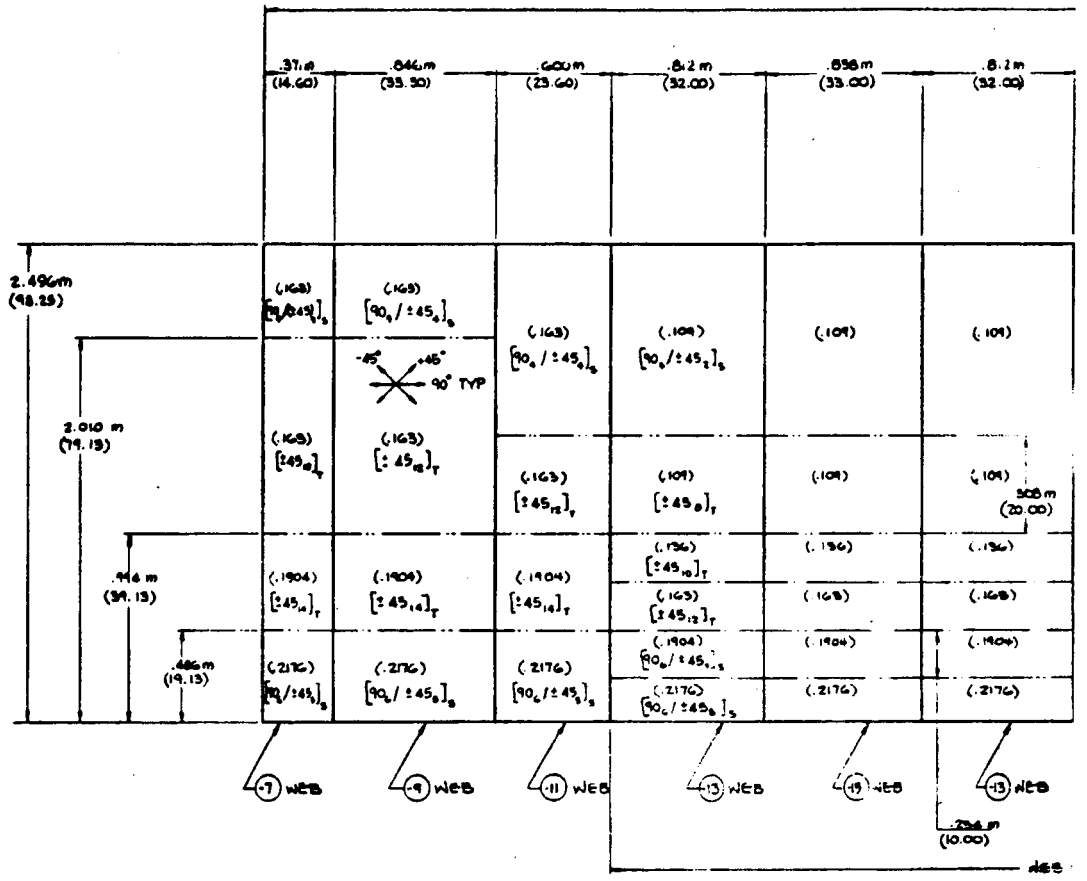

DIMEN
EXCEPT

2-22 A

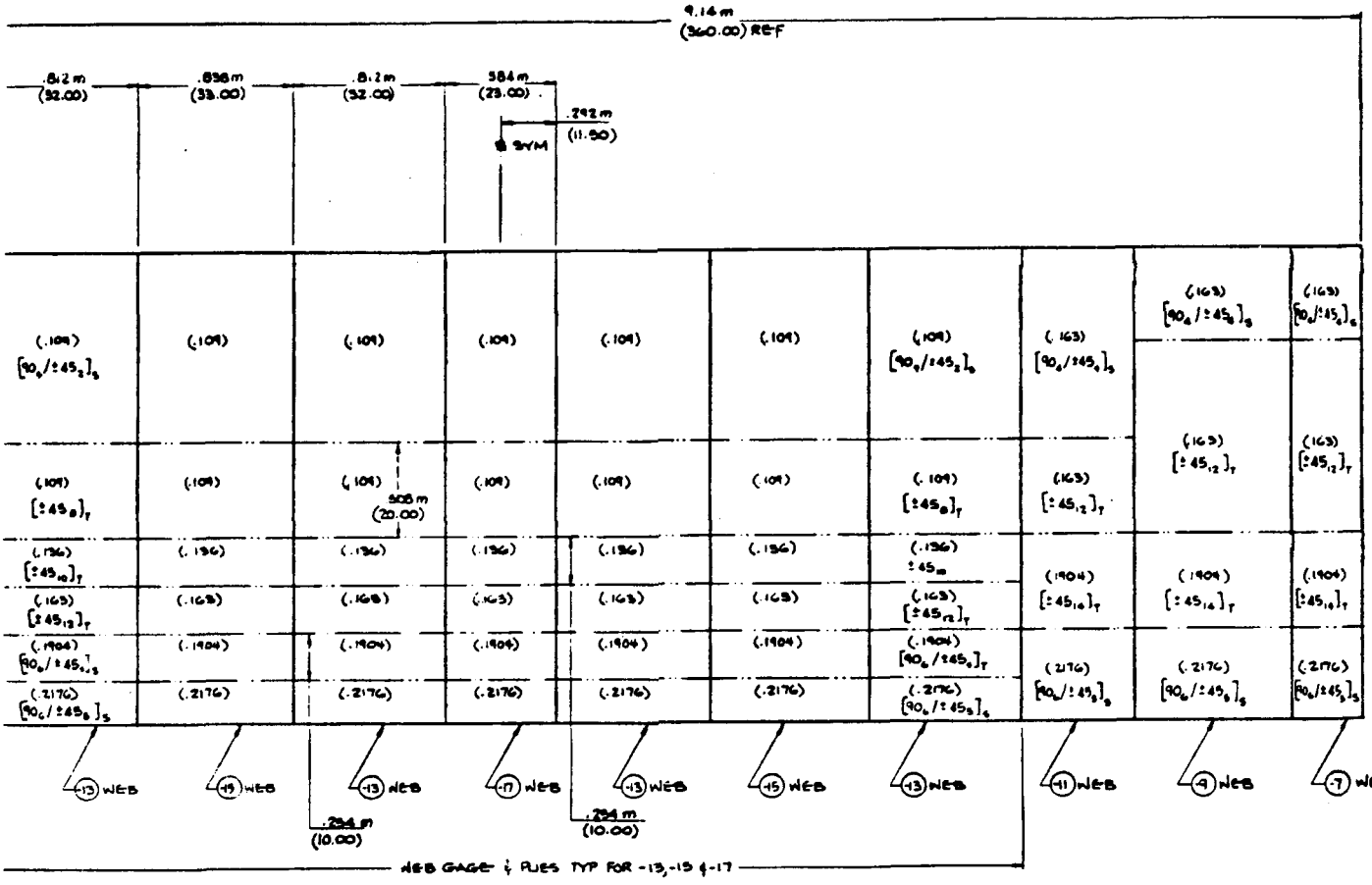

DIMENSIONS ARE METERS (INCHES)
EXCEPT WEB GAGE (SEE TABLE)

CONVERSION WEB G	
INCHES	M
.109	2.
.136	3.
.163	4.
.1904	4.
.2176	5.

1. MATERIAL T
HEAT TREAT
NOTES: ARE AS SH

SIZE	SECURITY CLASSIFICATION	DRAWING NO	SH
14170			

FOLDOUT FRAME 2

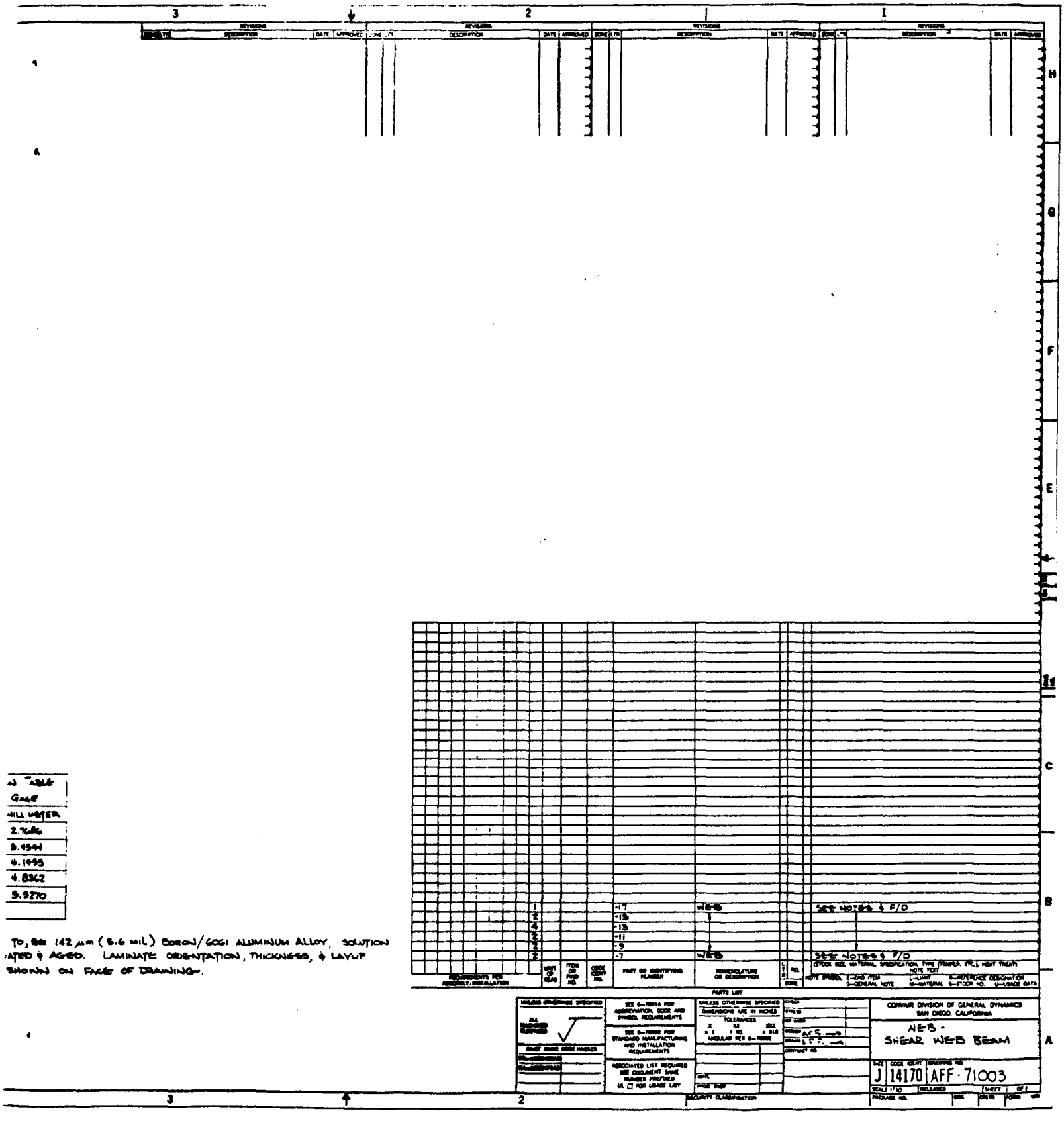

ABLE
GAGE
MIL METER
2.7486
3.4544
4.1995
4.8362
5.5710

TO, BE 142 μm (5.6 MIL) BORON/6061 ALUMINUM ALLOY, SOLUTION ATED & AGED. LAMINATE ORIENTATION, THICKNESS, & LAYUP SHOWN ON FACE OF DRAWING.

Figure 2-12. Web-Shear Web Beam

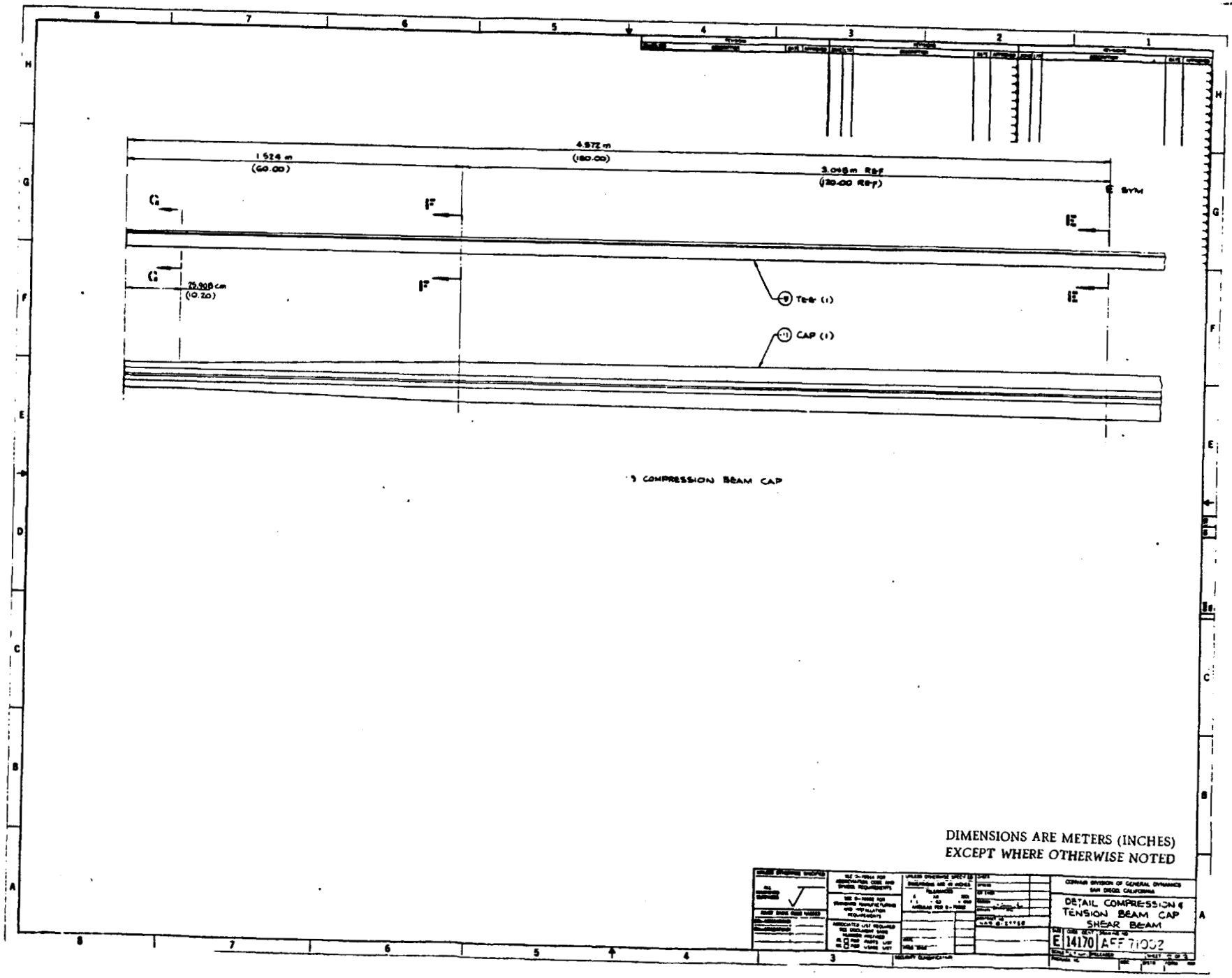

2-23/24 A

Figure 2-13. Compression and Tension Beam Cap

2.4.3 FINAL DESIGN VERTICAL AND HORIZONTAL STIFFENERS. A final weights review of the total beam indicated that additional weight savings might be realized by the addition of horizontal stiffeners, which decreases the stiffness requirements of the vertical stiffeners.

The original all-B/Al shear resistant shear web beam consisted of 12.5 cm (5 in.) spacings on vertical stiffeners that were 2.54m (100 in.) in height. This resulted in a beam having more weight in the stiffeners than in the web and caps combined. The primary reason for this weight was the a/b ratio for the individual panel, i.e., a/b = 20. The spacing, b, could not be increased beyond 12.5 cm (5 in.) without causing an exponential weight increase in the web. A study was made incorporating horizontal stiffeners to decrease a, the vertical stiffener length. Table 2-3 shows the I required as the member of horizontal stiffeners is increased.

Table 2-3. Web Stiffener I Requirements

a/b	No. of Lateral Supports	$\frac{EI}{bD}$	I Required							
			Center Bay				End Bay			
			Lower		Upper		Lower		Upper	
			cm^4	in^4	cm^4	in^4	cm^4	in^4	cm^4	in^4
20	0	3650	235.5	5.658	30.1	0.724	235.5	5.658	98.2	2.36
10	1	1680	108.4	2.604	13.7	0.329	108.4	2.604	45.2	1.087
6.67	2	1030	66.5	1.597	8.4	0.202	66.5	1.597	27.7	0.666
5.0	3	700	45.2	1.085	5.7	0.137	45.2	1.085	18.9	0.453
4.0	4	500	32.3	0.775	4.07	0.0978	32.3	0.775	13.5	0.3235

It can be seen that the stiffness requirements decrease substantially with an increased number of horizontal stiffeners. Table 2-4 compares the weights of the individual components for no horizontal stiffeners and three horizontal stiffeners. The primary reason for the decreased stiffener weight is the reduced cross-sectional area (Table 2-3) because of a decrease in stiffness requirements.

The design was modified to incorporate three horizontal stiffeners as shown in Figure 2-14. The stiffeners increase the design and manufacturing complexity, requiring a splice joint at each stiffener intersection, but this is compensated by the thinner overall gages required. The three horizontal stringers have basically the same stiffness modulus requirement as the vertical stringers at their point of intersection. They are configured to provide this rigidity from one side of the beam web only, thus allowing the vertical stiffeners on the other web face to be continuous from the tension to compression beam cap. The vertical stringers were resized to the revised stiffness requirements and designed from unidirectional B/Al of 1.8 mm (0.068 in.) thickness.

Table 2-4. Weight Summary for Shear Beam

Component	B/Al Shear-Resistant Beam			
	No Horizontal Stiffeners		Three Horizontal Stiffeners	
	kg	lb	kg	lb
Web	236	520	236	520
Compression Cap	77	169	77	169
Tension Cap	48	108	48	108
Vertical Stiffeners	371	818	205	451
Horizontal Stiffeners	-	-	40	88
Splice	17	37	17	37
Posts	116	256	116	256
Fittings	53	116	53	116
Total	918	2024	792	1745

The Con Braz joining process is used to attach these section elements. The stringers are spot welded to both sides of the web. Variations in stringer modulus requirements are satisfied by tapering the height of the stiffener. Back to back vertical stringers are used to provide the web splice joint. These stringers are unique in that they have a crossply skin attachment cap that is of twice the normal width.

2.4.4 FINAL DESIGN THRUST BEAM POST FITTINGS. Each of the load introduction and load reaction post fittings and their attachments were designed using a 1.15 fitting factor on ultimate load. The fasteners chosen are such that the shear strength to bearing strength ratio of the joint is 1.20. The beam web is critical in bearing and in fact is the basis of the design criteria. The bearing allowable used was 550 MN/m^2 (80 ksi) at 366K (200F) reduced from a nominal room temperature value of 690 MN/m^2 (100 ksi). The material selected for all load introduction and load reaction fittings is titanium. The fitting weights are shown in Table 2-5.

Table 2-5. Titanium Load Introduction and Reaction Fittings

	Weight	
	kg	lb
Post No. 1 and 5 Lower End Fittings (2)	5.17	11.4
Post No. 1 and 5 Upper End Fittings (2)	9.53	21.0
Post No. 2 and 4 Load Introduction Fitting	26.04	57.4
Post No. 3 Load Introduction Fitting	12.11	26.7
Total Fitting Weights	52.84	116.5

FOLDOUT FRAME

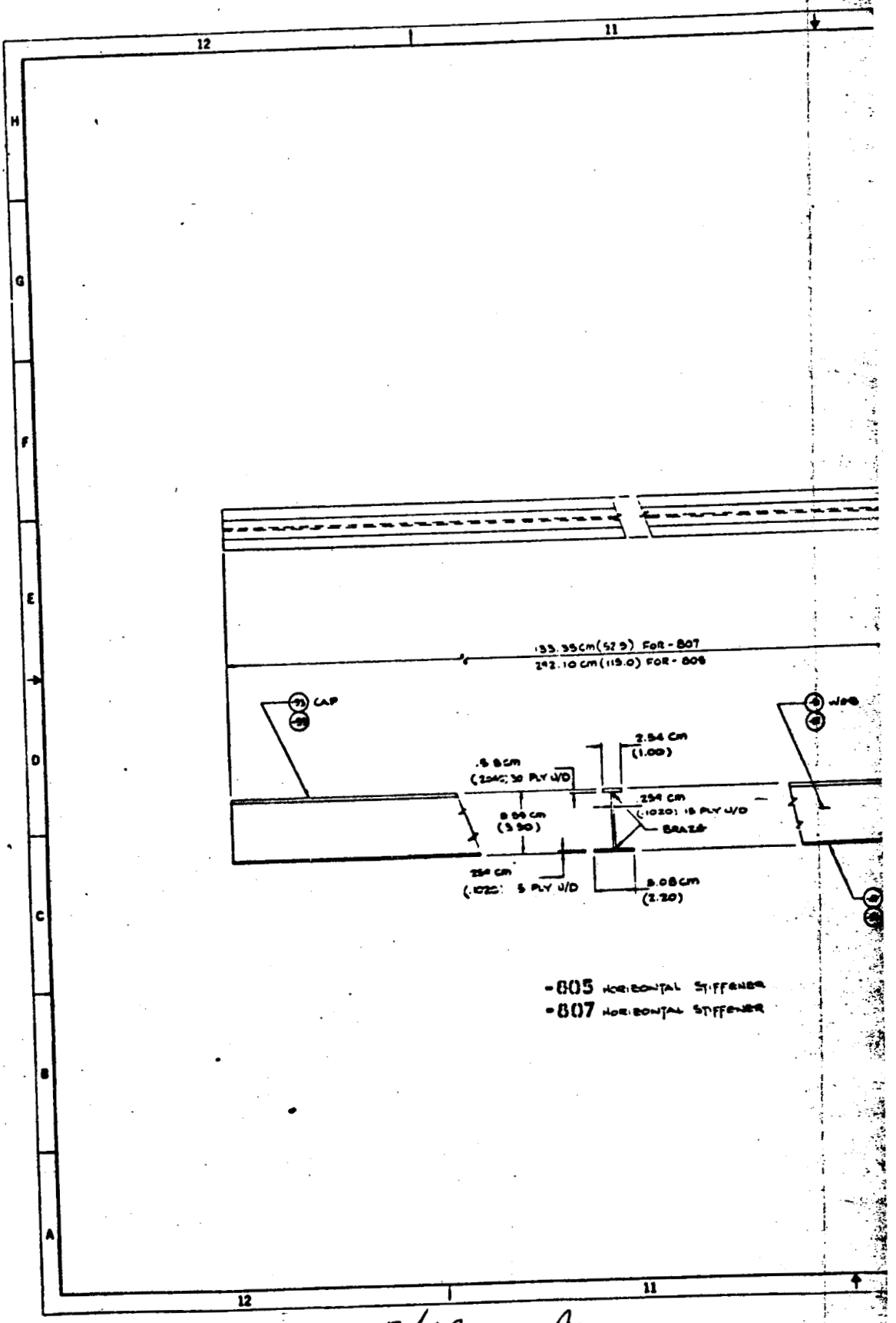

2 - 27/28 - A

FOLDOUT

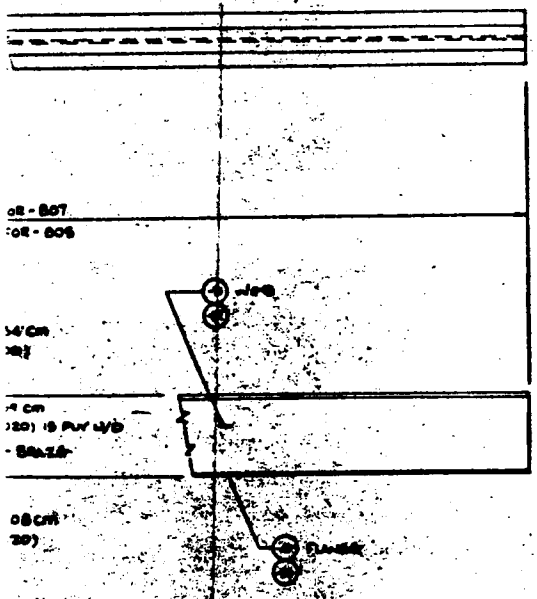

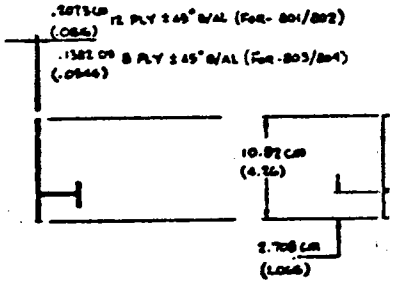

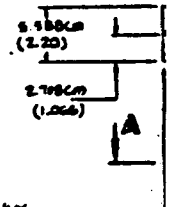

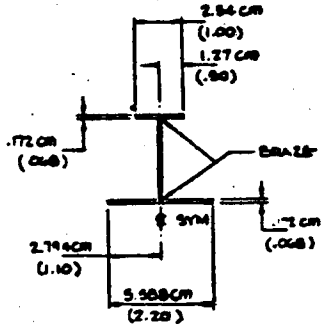

SECTION B-B
SCALE 1/1

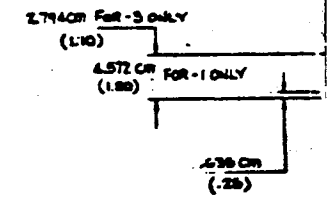

		14170		

2-27/28 -B

FRAME 2

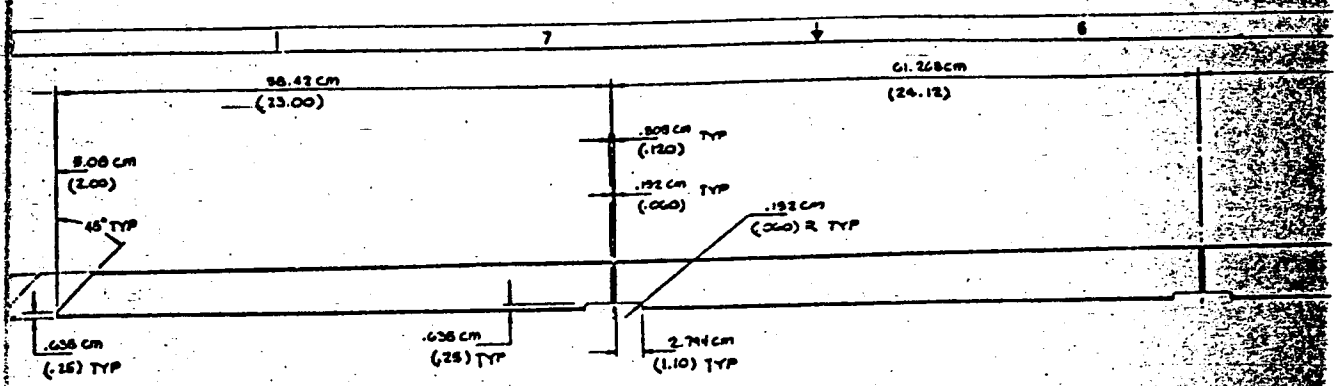

-17 OUTBOARD BAY STIFFENER (M/F -1)
-25 INBOARD BAY STIFFENER (M/F -3)
-33 OUTBOARD BAY SPLICE (M/F -801/802)
-36 OPP.
-41 INBOARD BAY SPLICE (M/F -803/804)
-42 OPP

-19 OUTBOARD BAY STIFFENER (M/F -1)
-27 INBOARD BAY STIFFENER (M/F -3)
-35 OUTBOARD BAY SPLICE (M/F -801/802)
-38 OPP
-43 INBOARD BAY SPLICE (M/F -803/804)
-44 OPP

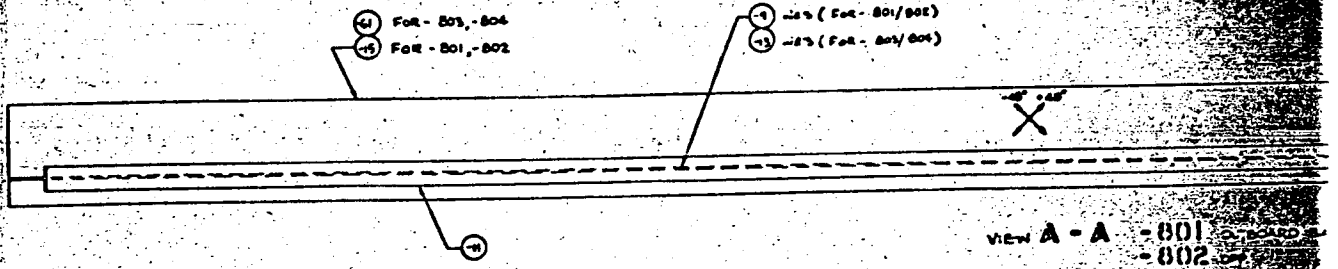

VIEW A - A -801 OUTBOARD
-802 OPP
-803 INBOARD
-804 OPP

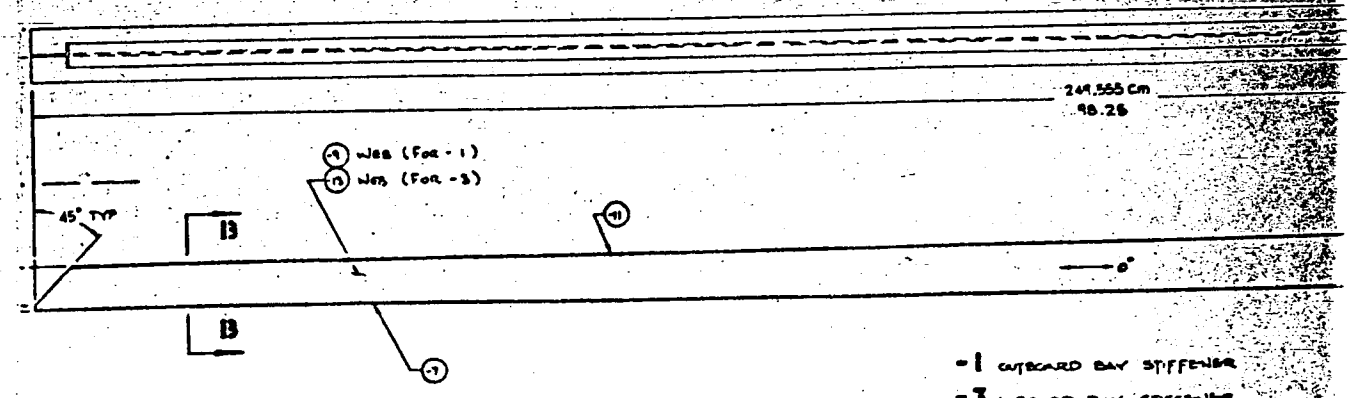

-1 OUTBOARD BAY STIFFENER
-3 INBOARD BAY STIFFENER

2-27/28 - C

FOLDOUT FRAME 3

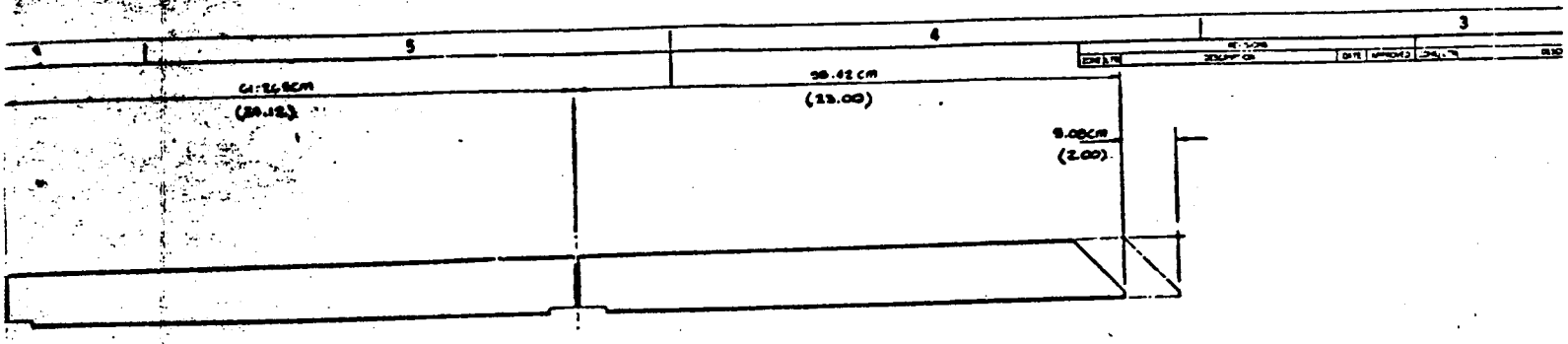

- 21 OUTBOARD BAY STIFFENER (M/F-1)
- 29 INBOARD BAY STIFFENER (M/F-5)
- 37 OUTBOARD BAY SPLICE (M/F-801/802)
- 38 OPP
- 45 INBOARD BAY SPLICE (M/F-803/804)
- 46 OPP

- 23 OUTBOARD BAY STIFFENER (M/F-1)
- 31 INBOARD BAY STIFFENER (M/F-5)
- 39 OUTBOARD BAY SPLICE (M/F-801/802)
- 40 OPP
- 47 INBOARD BAY SPLICE (M/F-803/804)
- 48 OPP

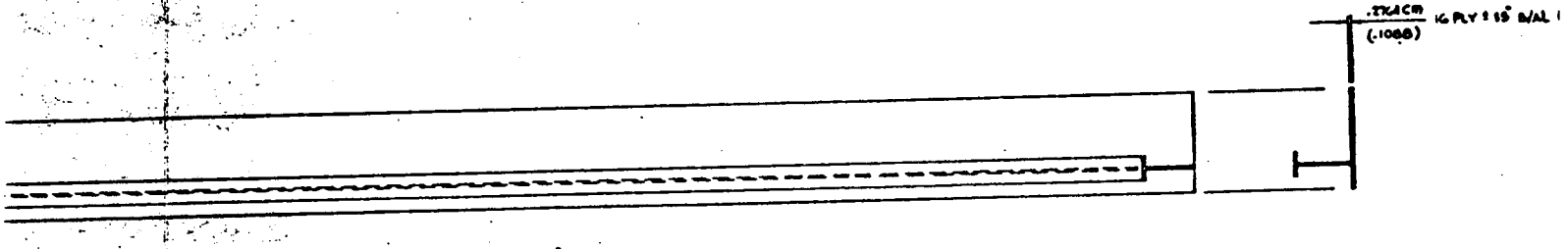

1 OUTBOARD BAY SPLICE STIFFENER (SAME AS-1 EXCEPT AS SHOWN)
2 OPP
3 INBOARD BAY SPLICE STIFFENER (SAME AS-5 EXCEPT AS SHOWN)
4 OPP

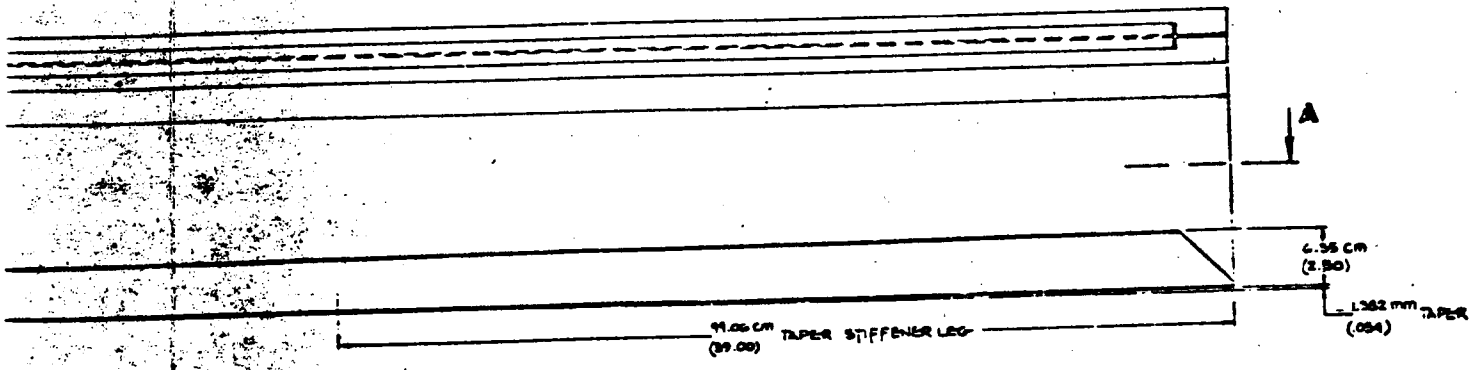

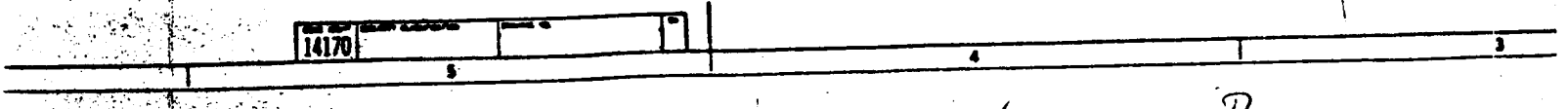

2-27/28 D

FOLDOUT FRAME 4

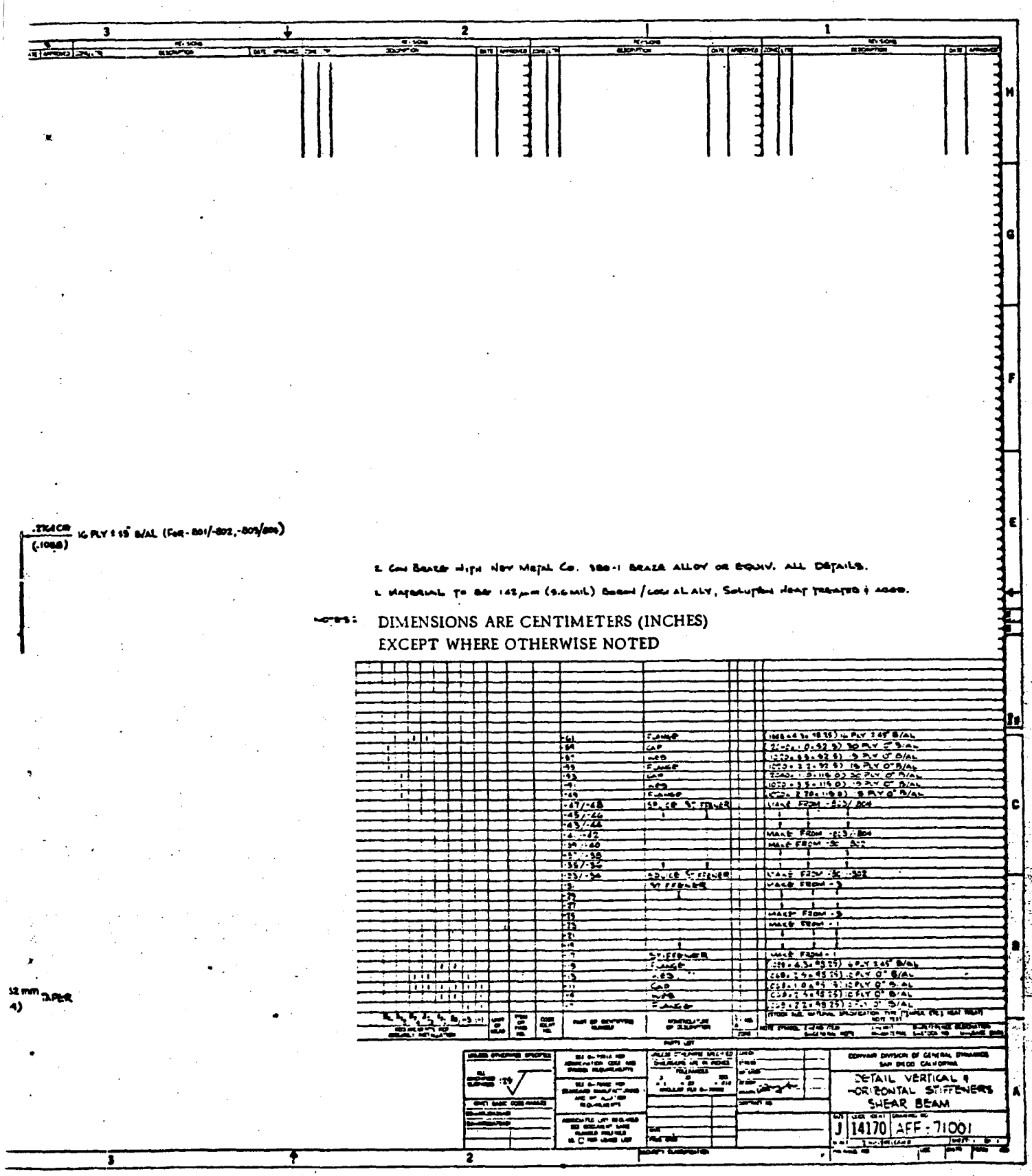

Figure 2-14. Vertical and Horizontal Stiffeners

Post No. 1 (Lower End) Load Reaction Fitting. The entire load at this point is introduced into the lower beam cap via a set of three separate but joined fittings. Provisions for four attaching bolts were made to mate the beam to the surrounding structure. The inherent design of these fittings is such that an allowance is made for some misalignment of the introduction load.

Post No. 1 and 5 (Upper End) Load Reaction Fittings. The load reaction fitting consists of two open-ended bathtub fittings bolted back to back and nested in the post channels. The entire load is assumed to be dumped into the post which in turn sheds the load into the web. Provision for four bolts were made to attach the beam to the surrounding structure. This allows provisions for some misalignment of the reaction load.

Post No. 2 and 4 Load Introduction Fittings. These consist of two open-ended bathtub fittings and four half bathtub fittings bolted to the web and post channels. These are the most heavily loaded fittings due to the introduction of large side loads, 3800 N (110 kips). Large tensile loads 1410 N (41.2 kips) on the reversible moment reaction fittings require four 2.9 cm (0.750 in.) diameter bolts to handle the shear load due to the large side introduction load.

Post No. 3 Load Introduction Fitting. The fittings for this load introduction point are similar to those at post No. 2 and 4 except they are lighter because of the smaller side introduction load 1900 N (55 kips).

2.4.5 FINAL DESIGN TAPERED THRUST BEAM POST. The tapered columns were designed on the assumption that the column load is sheared uniformly into the web. This assumption provides a conservative column, and the load should shear out more rapidly at the load introduction end and drop off down the column length.

To determine the buckling loads of the columns, the Boeing method for columns of variable EI (a process of numerical integration of a differential equation by a series of successive approximations) was used.

The fastener pattern and sizing was designed to carry the shear distribution obtained from the first computer iteration of the shear web beam. The final iteration, which included the tapered column effects, indicates a slightly higher shear distribution in the areas of the load introduction and reaction points. It is expected, however, that these maximum shear stresses will not exceed the allowable of the ±45° B/Al web. Should the allowable be exceeded, the web may be thickened up locally on one side in this area, and the columns could be stepped to accommodate. This step could be built into the column web during layup or could be machined into it after consolidation.

A weight saving of 6 to 8% (Table 2-6) was realized in tapering the columns to within practical limits, when compared to respective constant cross-section columns. Additional weight savings could be achieved by tapering the columns in more frequent steps, but this would involve more complicated and expensive tooling, and would only result in a small additional weight savings in each column.

Table 2-6. Column Weights

Post No.	Tapered Weight kg	Tapered Weight lb	Constant X-Section Weight kg	Constant X-Section Weight lb	Weight Saved %
1	25.3	55.8	27.1	59.5	6
2	21.0	46.3	22.8	50.3	8
3	23.4	51.3	25.3	55.6	7
4	21.0	46.3	22.8	50.3	8
5	25.3	55.8	27.1	59.5	6
Total	116.0	255.5	125.1	275.3	

2.5 SHEAR BEAM ANALYSIS

The shear beam is designed to be shear resistant, where the web material is ±45° ST&A B/Al except in regions of high normal stresses. In these areas, combinations of unidirectional and ±45° crossplies are employed. Because of the high compressive and shear stresses, the vertical stiffener spacing is small. In addition, three horizontal stiffeners were added to reduce the aspect ratios (length to width) of the panels. This permits the use of much lighter stiffeners primarily to support the panels in shear. To keep the normal stresses in the web within reasonable bounds, the cap stresses in the UD B/Al are limited to levels below 620.6 MN/m^2 (90,000 psi). The load introduction posts are tapered in cross section to attain minimum weight. The present analysis of the shear beam indicates a very near optimum design. Precise optimum design is impossible due to layup requirements in the crossply web; i.e., the minimum thickness change of the ±45° material includes four layers.

2.5.1 BORON/ALUMINUM MATERIAL PROPERTIES. All structural elements of the shear beam, except for the web, are constructed from unidirectional B/Al. The web consists of two different ST&A B/Al crossplies. The mechanical properties of these materials are:

Material A: UD ST&A B/Al

F_{tu_x} = 1276 MN/m^2 (185,000 psi)

F_{tu_y} = 224 MN/m^2 (32,500 psi)

ϵ_{u_x} = 0.0061 m/m (0.0061 in/in)

ϵ_{u_y} = 0.002 m/m (0.002 in/in)

E_{t_x} = 214 GN/m^2 (31 x 10^6 psi)

E_{t_y} = 121 GN/m^2 (17.5 x 10^6)

$F_{su_{xy}}$ = 55 MN/m^2 (8000 psi)

G_{xy} = 41 GN/m^2 (6×10^6)

ν_{xy} = 0.3

ν_{yx} = 0.169

Material B: ±45° ST&A B/Al

F_{tu_x} = F_{tu_y} = 248 MN/m^2 (36,000 psi)

ϵ_{u_x} = ϵ_{u_y} = 0.010 m/m (0.010 in/in)

E_{t_x} = E_{t_y} = 172 GN/m^2 (25×10^6 psi)

$F_{su_{xy}}$ > 39 MN/m^2 (56,000 psi)

G_{xy} = 69 GN/m^2 (10×10^6 psi)

ν_{xy} = ν_{yx} = 0.31

Material C: 37.5% 0°, 62.5% ±45° ST&A B/Al

F_{tu_x} = 620 MN/m^2 (90,000 psi)

F_{tu_y} = 233 MN/m^2 (33,750)

E_{t_x} = 179 GN/m^2 (26×10^6 psi)

E_{t_y} = 1486 N/m^2 (21.5×10^6 psi)

$F_{su_{xy}}$ = 262 MN/m^2 (38,000 psi)

G_{xy} = 67 GN/m^2 (9.7×10^6 psi)

ν_{xy} = 0.32

ν_{yx} = 0.265

} 0° fibers in X-direction

Material properties at 366k (200F)

Assume all stiffnesses and strengths to be 90% of room temperature allowables.

The elastic/inelastic behavior of Material B (±45° ST&A B/Al composite) is shown in the stress-strain curve of Figure 2-15. The plasticity factor $\eta = E_{sec}/E$ is plotted versus stress as shown in Figure 2-16. The elastic/inelastic behavior of Poisson's ratio is shown in Figures 2-17 and 2-18, where Poisson's ratio is plotted versus stress and plasticity factor, respectively.

2.5.2 STIFFNESS MATRIX OF MATERIAL B (±45° ST&A B/Al) LAMINATES. For symmetrical and balanced composite laminates, the elastic stretching constitutive equations are in the form

$$\begin{Bmatrix} \sigma_x \\ \sigma_y \\ \tau_{xy} \end{Bmatrix} = \frac{1}{t} \begin{bmatrix} A_{xx} & A_{xy} & 0 \\ A_{xy} & A_{yy} & 0 \\ 0 & 0 & A_{66} \end{bmatrix} \begin{Bmatrix} \epsilon_x \\ \epsilon_y \\ \gamma_{xy} \end{Bmatrix} \tag{1}$$

where the orthotropic stretching stiffness matrix components are

$$A_{xx} = \frac{E_x t}{(1-\nu_{xy}\nu_{yx})}, \quad A_{yy} = \frac{E_y t}{(1-\nu_{xy}\nu_{yx})}, \quad A_{xy} = \nu_{yx} A_{xx}, \quad A_{66} = Gt \tag{2}$$

when test data are available whereby E_x, E_y, ν_{xy}, and ν_{yx} are known.

Also, the bending constitutive equations are in the form

$$\begin{Bmatrix} M_x \\ M_y \\ M_{xy} \end{Bmatrix} = \begin{bmatrix} D_{xx} & D_{xy} & 0 \\ D_{xy} & D_{66} & 0 \\ 0 & 0 & D_{66} \end{bmatrix} \begin{Bmatrix} \chi_x \\ \chi_y \\ \chi_{xy} \end{Bmatrix} \tag{3}$$

where the orthotropic bending stiffness matrix components are

$$D_{xx} = \frac{E_x t}{12(1-\nu_{xy}\nu_{yx})}, \quad D_{yy} = \frac{E_y t^3}{12(1-\nu_{xy}\nu_{yx})}$$

$$D_{xy} = \nu_{yx} D_{xx}, \quad D_{66} = \frac{G_{xy} t^3}{12} \tag{4}$$

and χ is the curvature change. Curves for stretching and bending matrix components are shown in Figures 2-19 through 2-25.

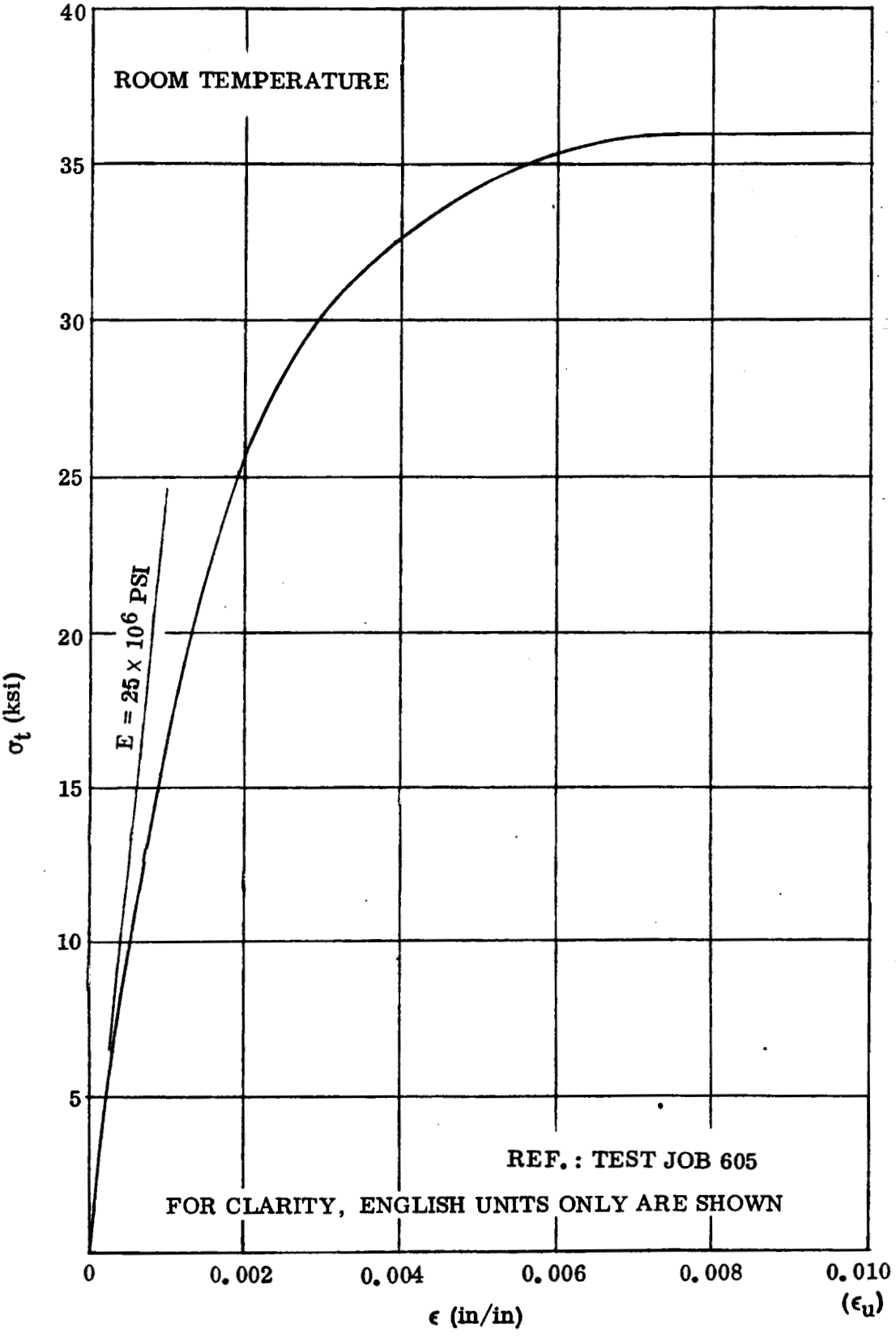

Figure 2-15. Stress/Strain Curve of Heat Treated ±45° B/Al

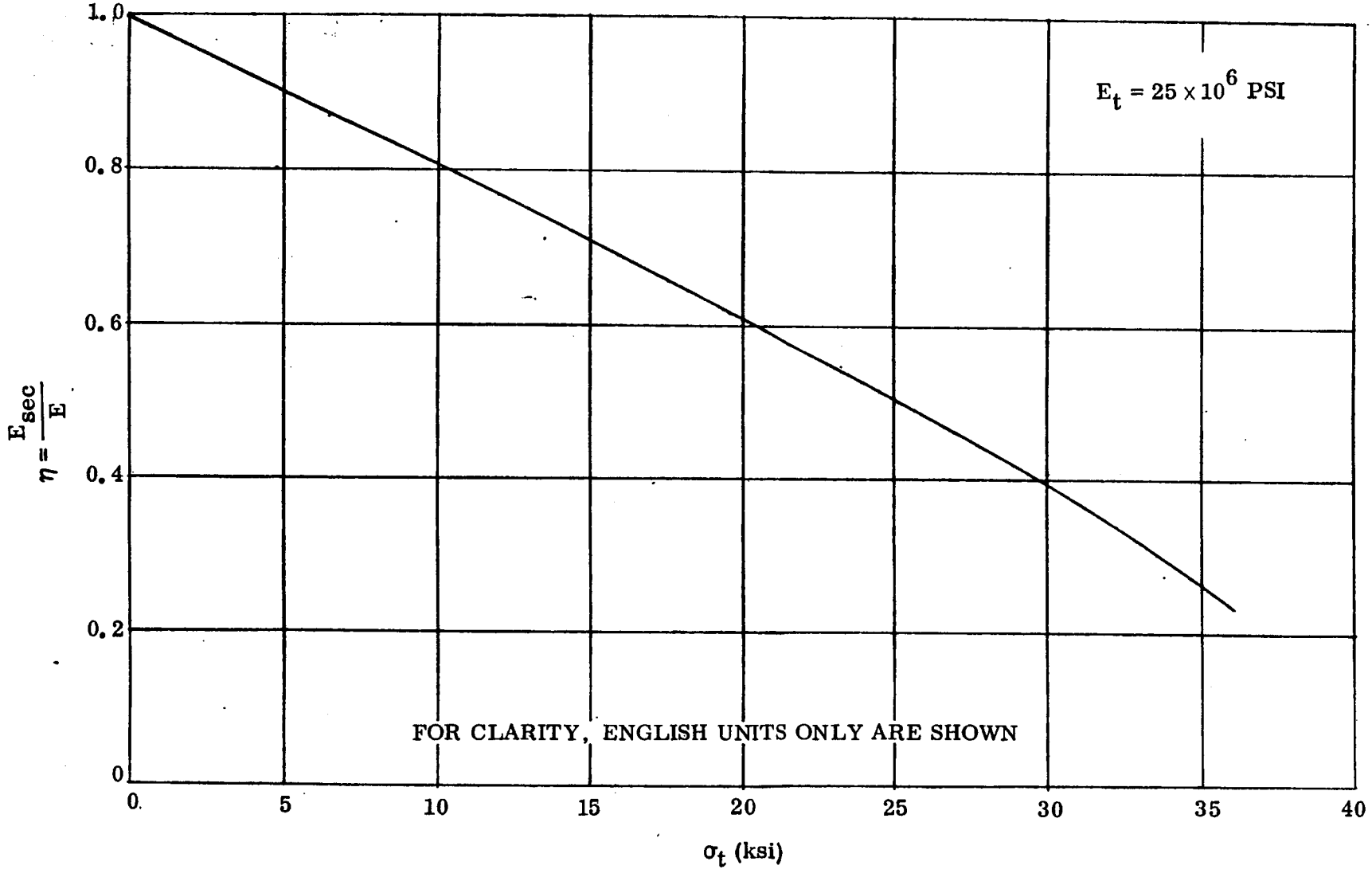

Figure 2-16. Secant Modulus of ±45° Heat Treated B/Al

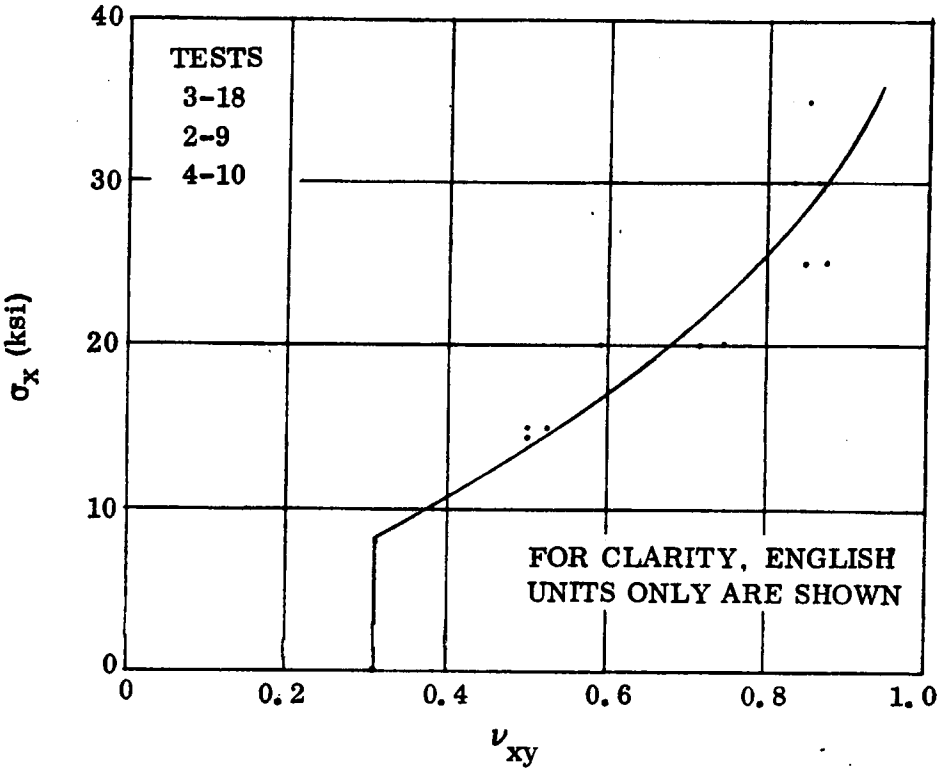

Figure 2-17. Poisson's Ratio for ±45° Heat Treated B/Al

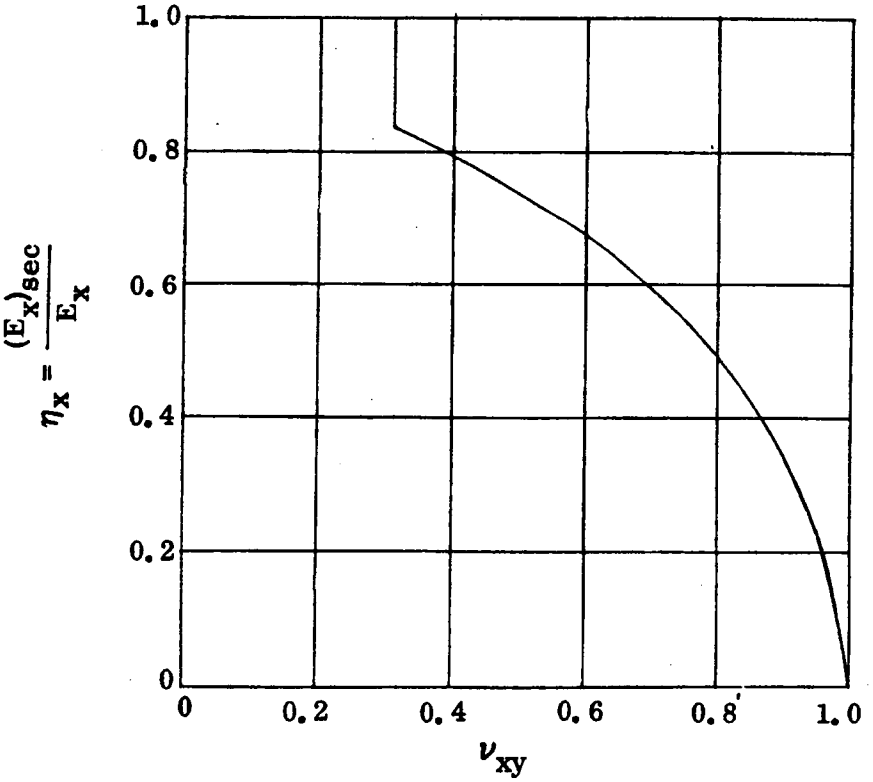

Figure 2-18. Poisson's Ratio Versus Plasticity Factor for ±45° Heat Treated B/Al

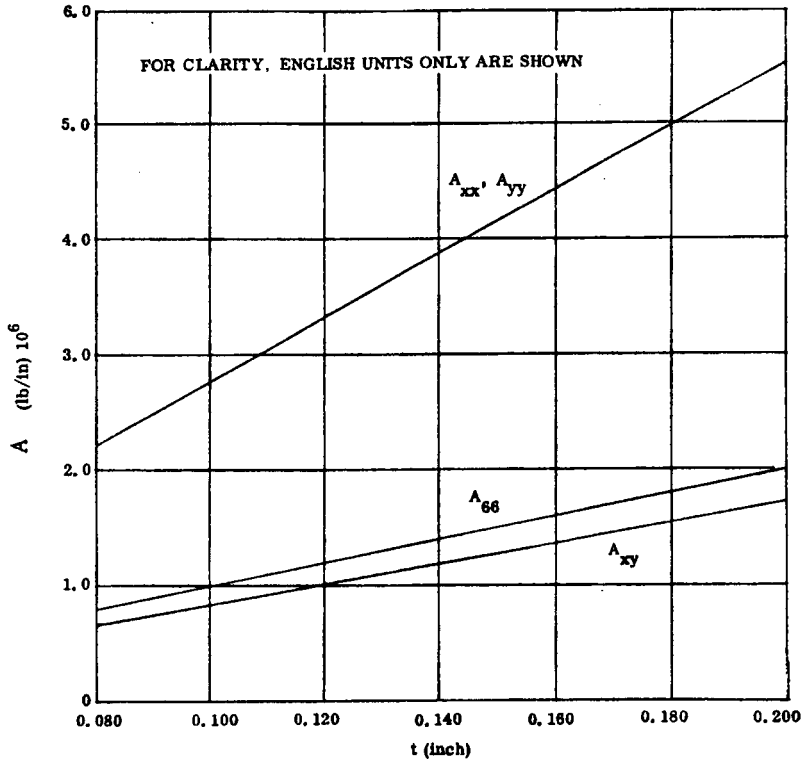

Figure 2-19. Stiffness of ±45° Heat Treated B/Al Plates

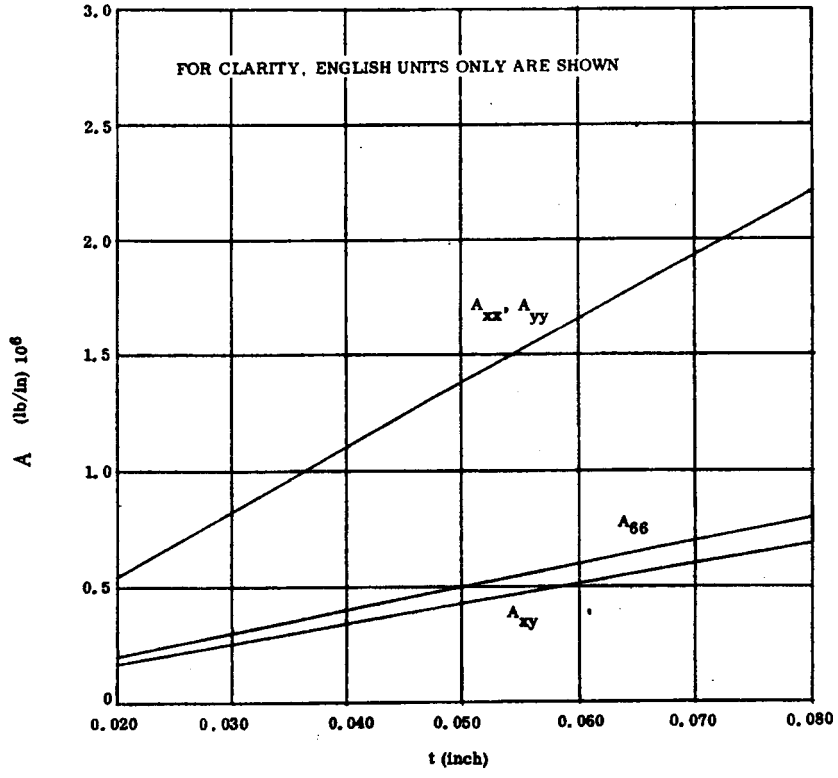

Figure 2-20. Stiffness of ±45° Heat Treated B/Al Plates

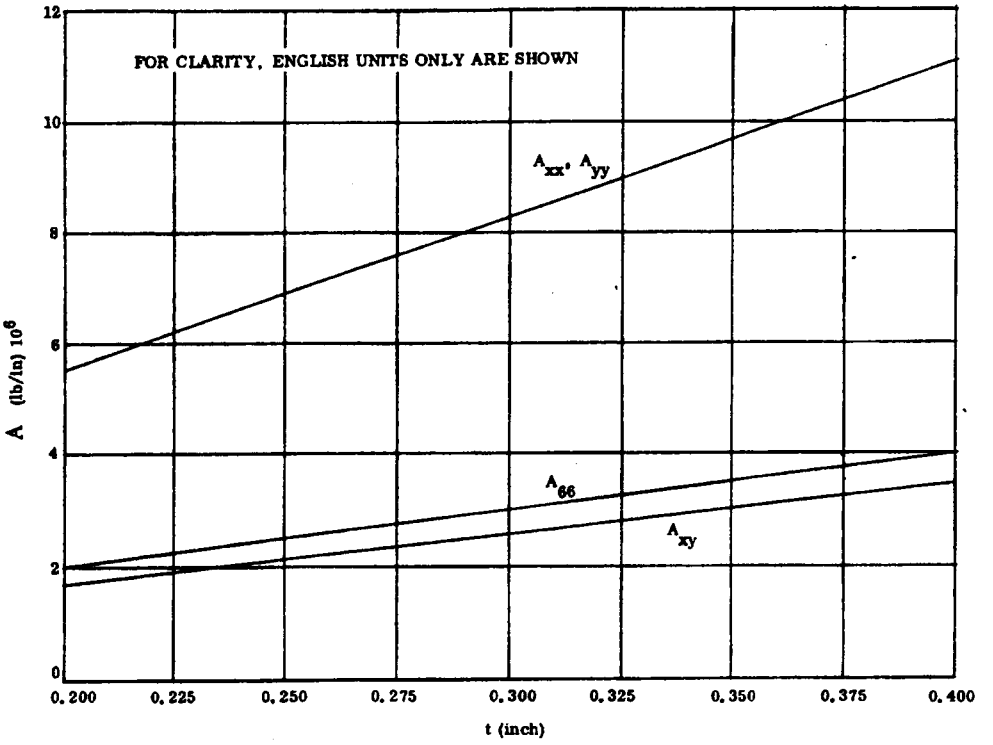

Figure 2-21. Stiffness of ±45° Heat Treated B/Al Plates

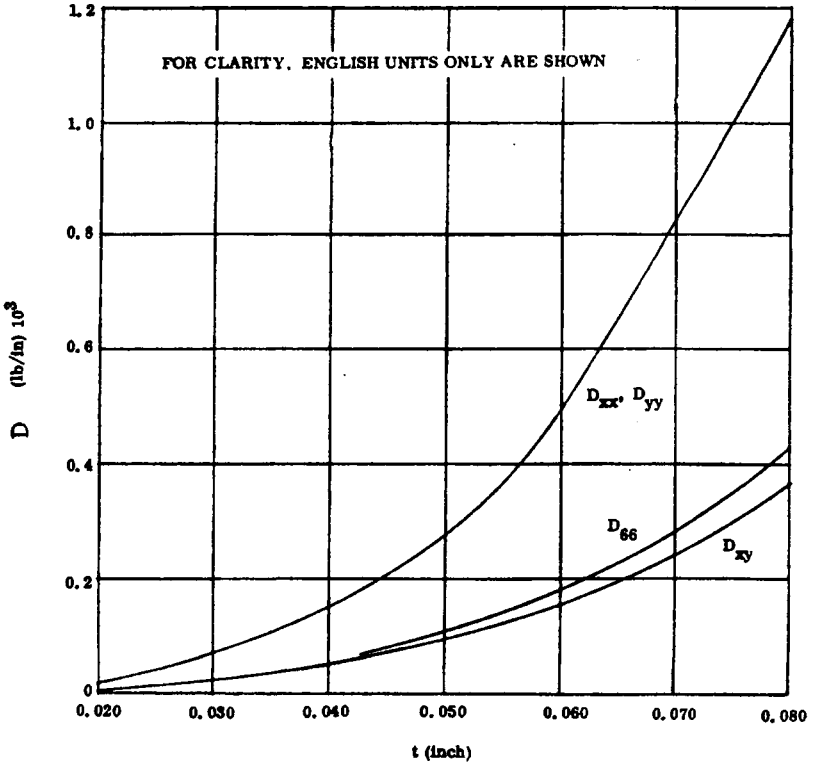

Figure 2-22. Stiffness of ±45° Heat Treated B/Al Plates

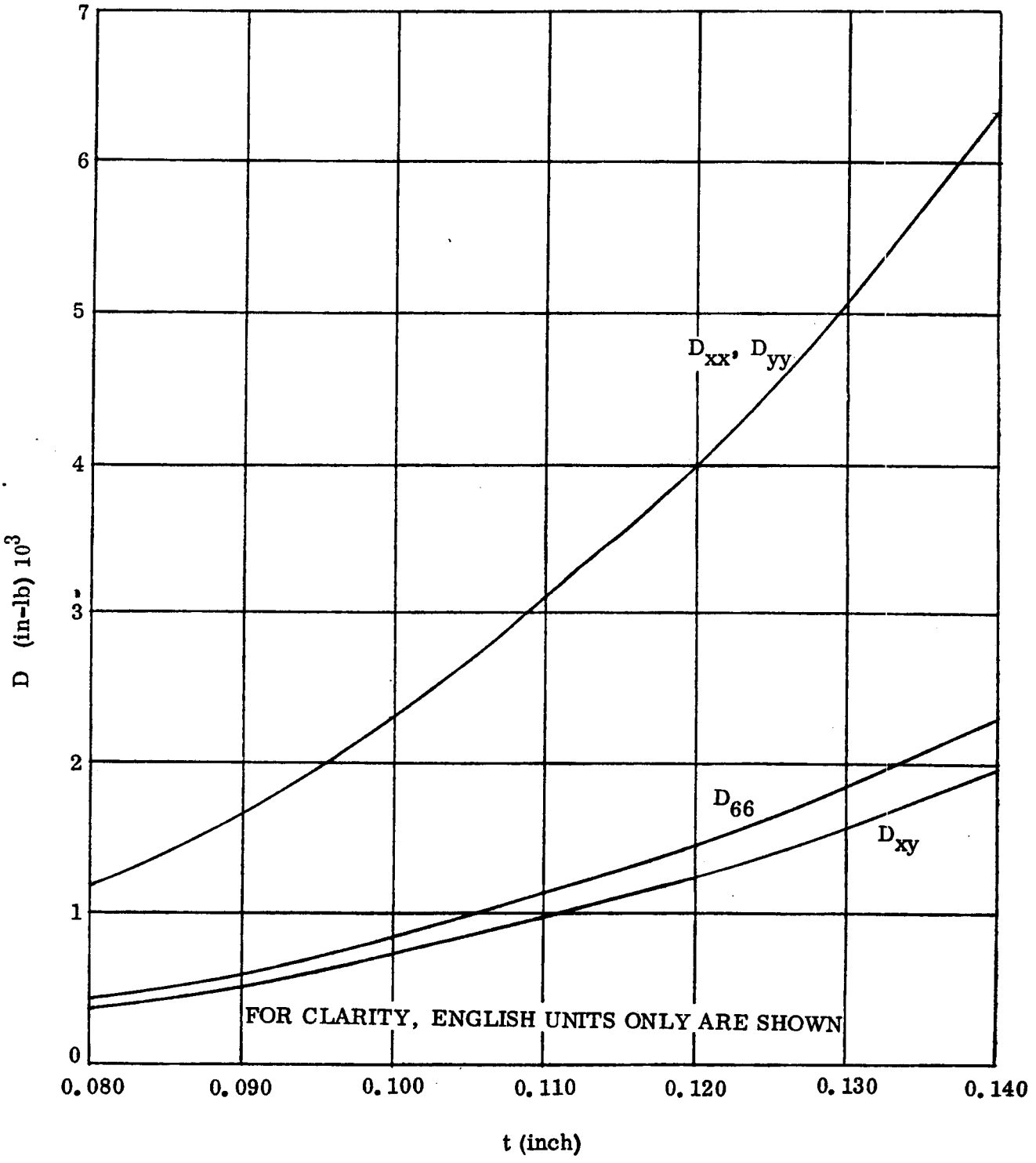

Figure 2-23. Elastic Constants of ±45° Heat Treated B/Al Plates

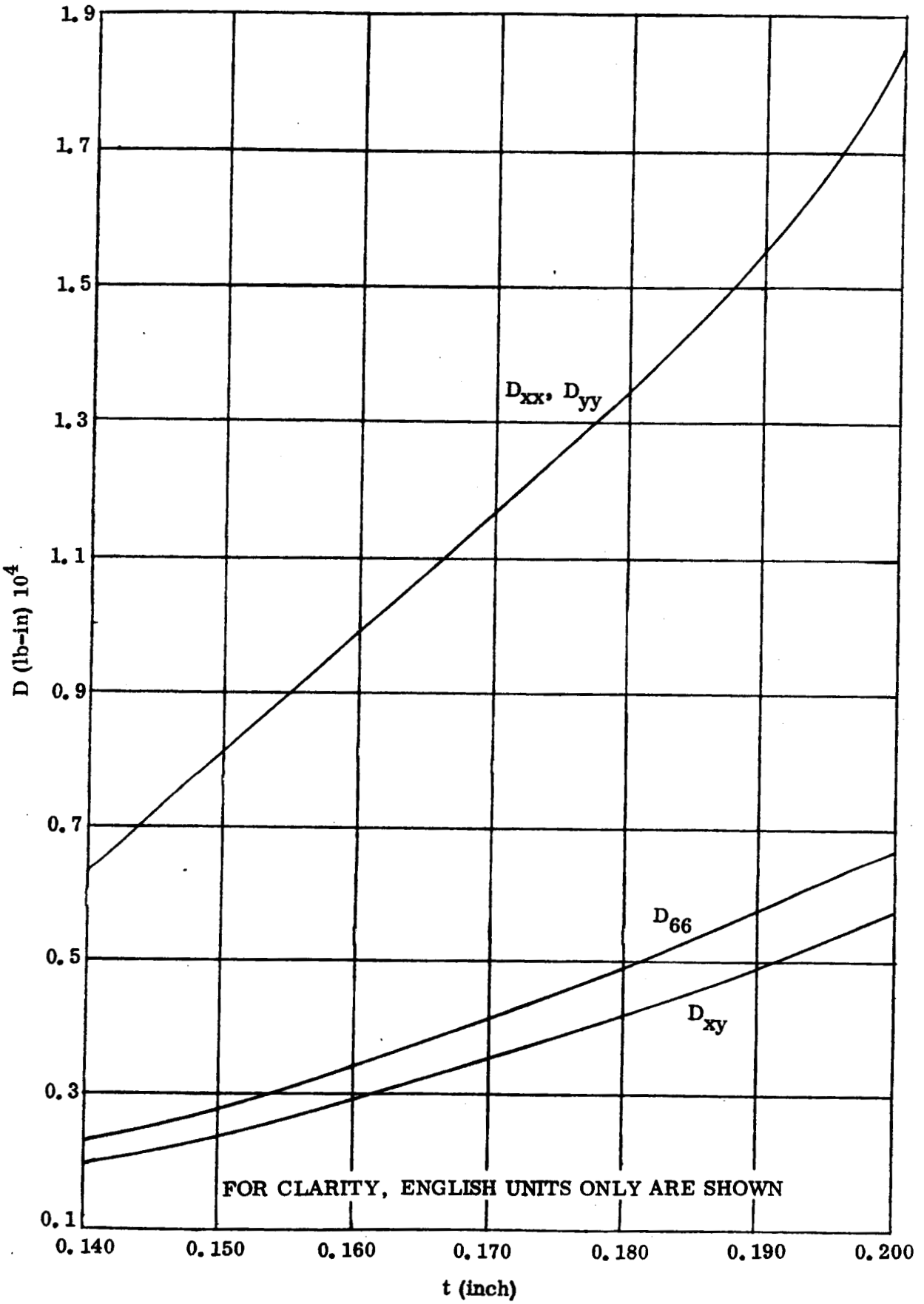

Figure 2-24. Elastic Constants of ±45° Heat Treated B/Al Plates

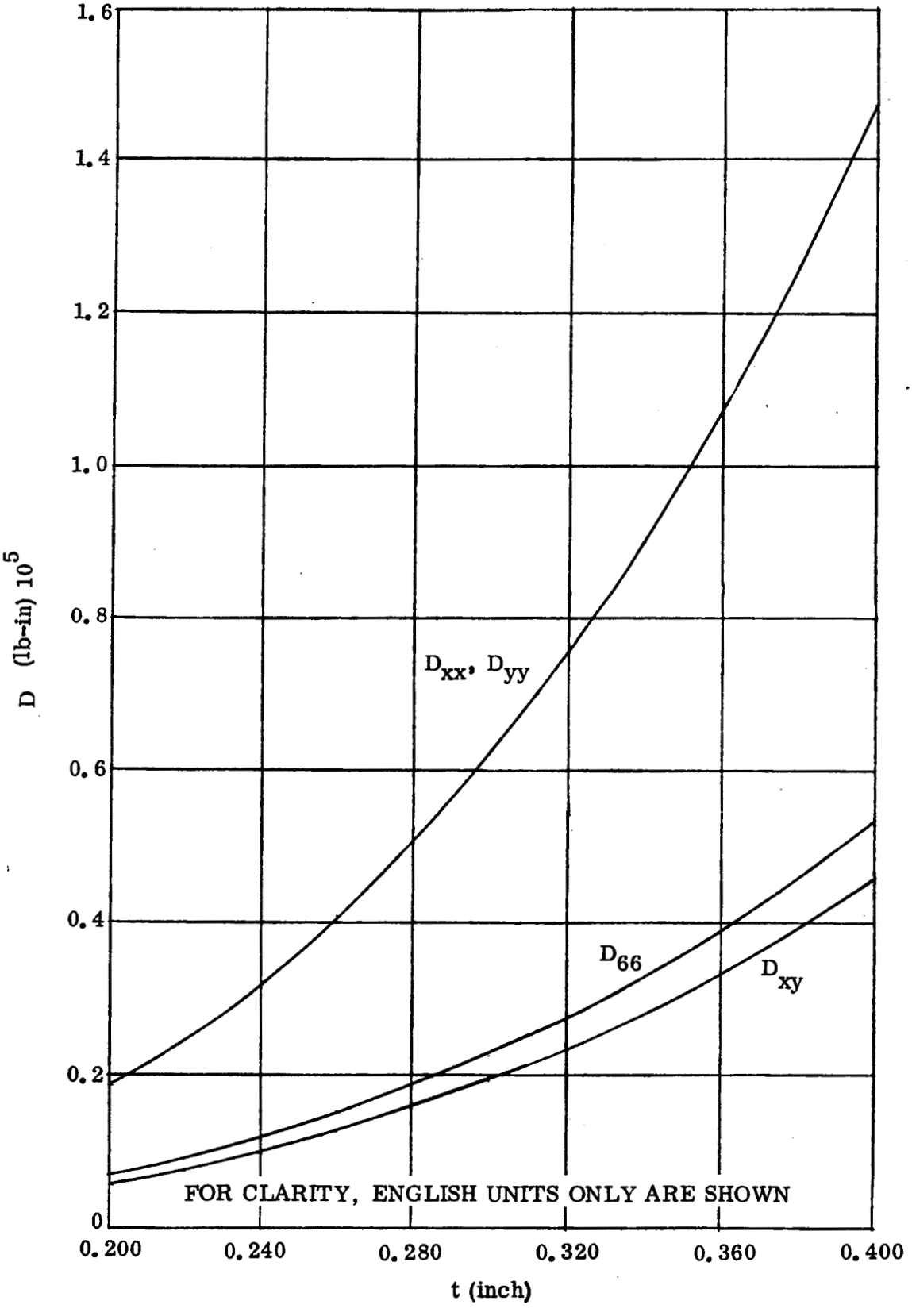

Figure 2-25. Elastic Constants of ±45° Heat Treated B/Al Plates

For the inelastic stress properties indicated in Figures 2-15 through 2-18, inelastic stiffness matrices must be substituted in the constitutive Equations 1 and 3. Accordingly, these matrices become

$$\left[A^I\right] = \begin{bmatrix} A^I_{xx} & A^I_{xy} & 0 \\ A^I_{xy} & A^I_{yy} & 0 \\ 0 & 0 & A^I_{66} \end{bmatrix} \tag{5}$$

$$\left[D^I\right] = \begin{bmatrix} D^I_{xx} & D^I_{xy} & 0 \\ D_{xy} & D_{yy} & 0 \\ 0 & 0 & D^I_{66} \end{bmatrix} \tag{6}$$

where

$$A^I_{xx} = \frac{\eta_x E_x t}{(1-\nu_{xy}\nu_{yx})^I}, \qquad A^I_{yy} = \frac{\eta_y E_y t}{(1-\nu_{xy}\nu_{yx})^I}$$

$$A^I_{xy} = \sqrt{\nu^I_{yx} A^I_{xx} \nu^I_{xy} A^I_{yy}}, \qquad A^I_{66} = G_{xy} t \tag{7}$$

and

$$D^I_{xx} = \frac{\eta_x E_x t^3}{12(1-\nu_{xy}\nu_{yx})}, \qquad D^I_{yy} = \frac{\eta_y E_y t^3}{12(1-\nu_{xy}\nu_{yx})^I}$$

$$D^I_{xy} = \sqrt{\nu^I_{yx} D^I_{xx} \nu^I_{xy} D^I_{yy}}, \qquad D^I_{66} = \frac{G_{xy} t^3}{12} \tag{8}$$

Convenient curves for the stiffness matrix components for Material B at room temperature are presented in Figures 2-26 through 2-29. These curves represent the best available data at this time. Actually, material properties taken from biaxial test data should be used.

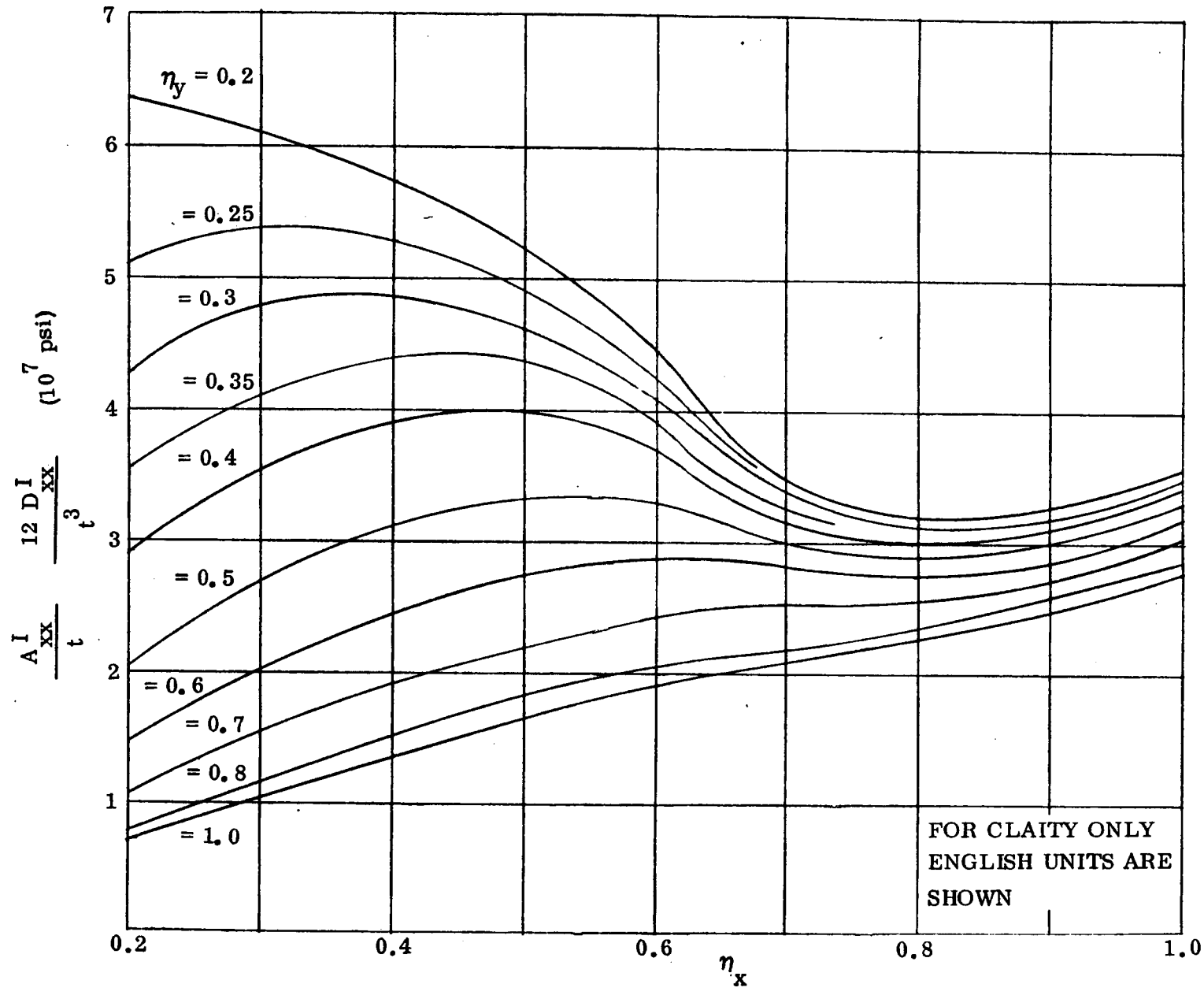

Figure 2-26. Inelastic Constants for ±45° Heat Treated B/Al

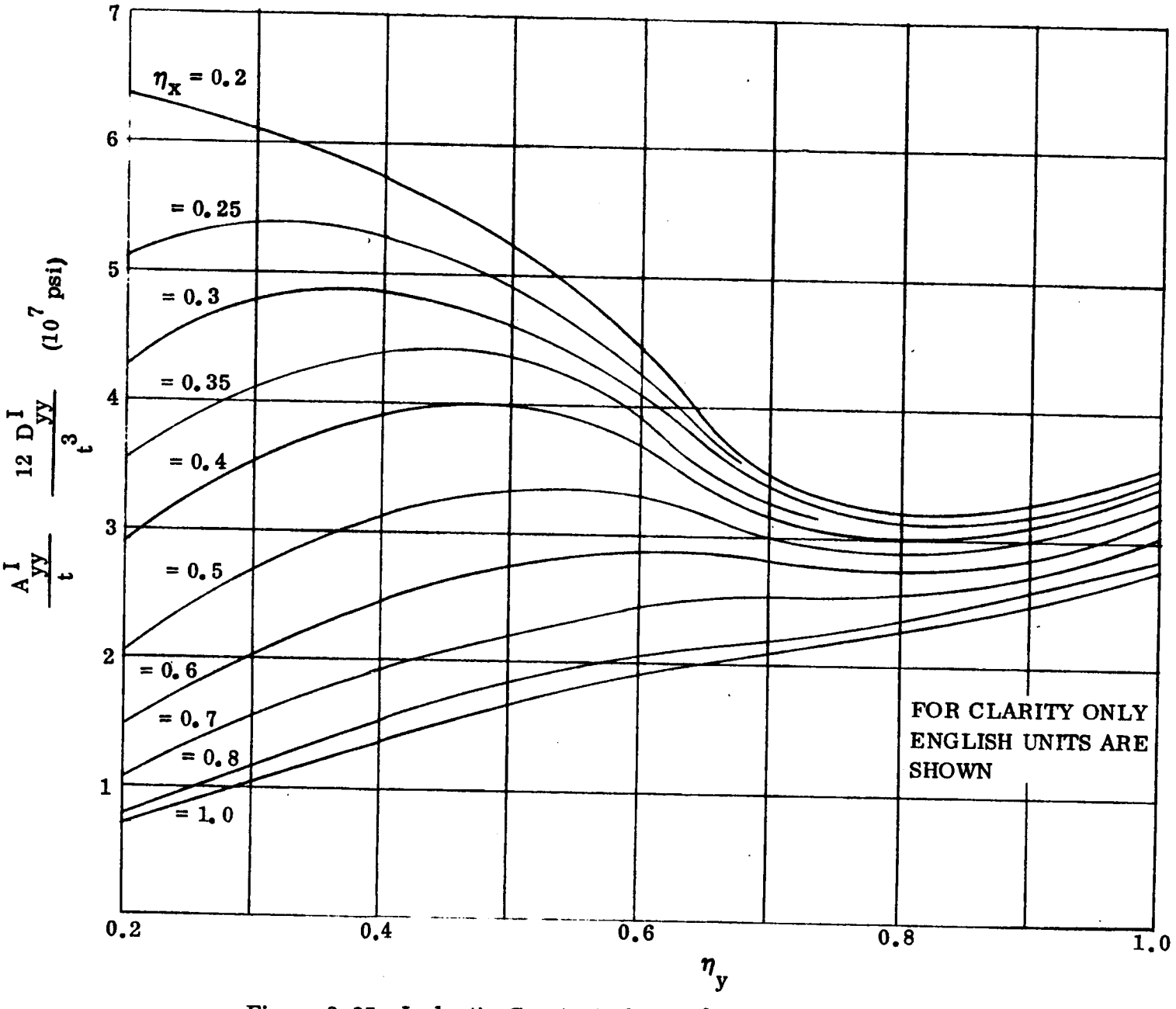

Figure 2-27. Inelastic Constants for ±45° Heat Treated B/Al

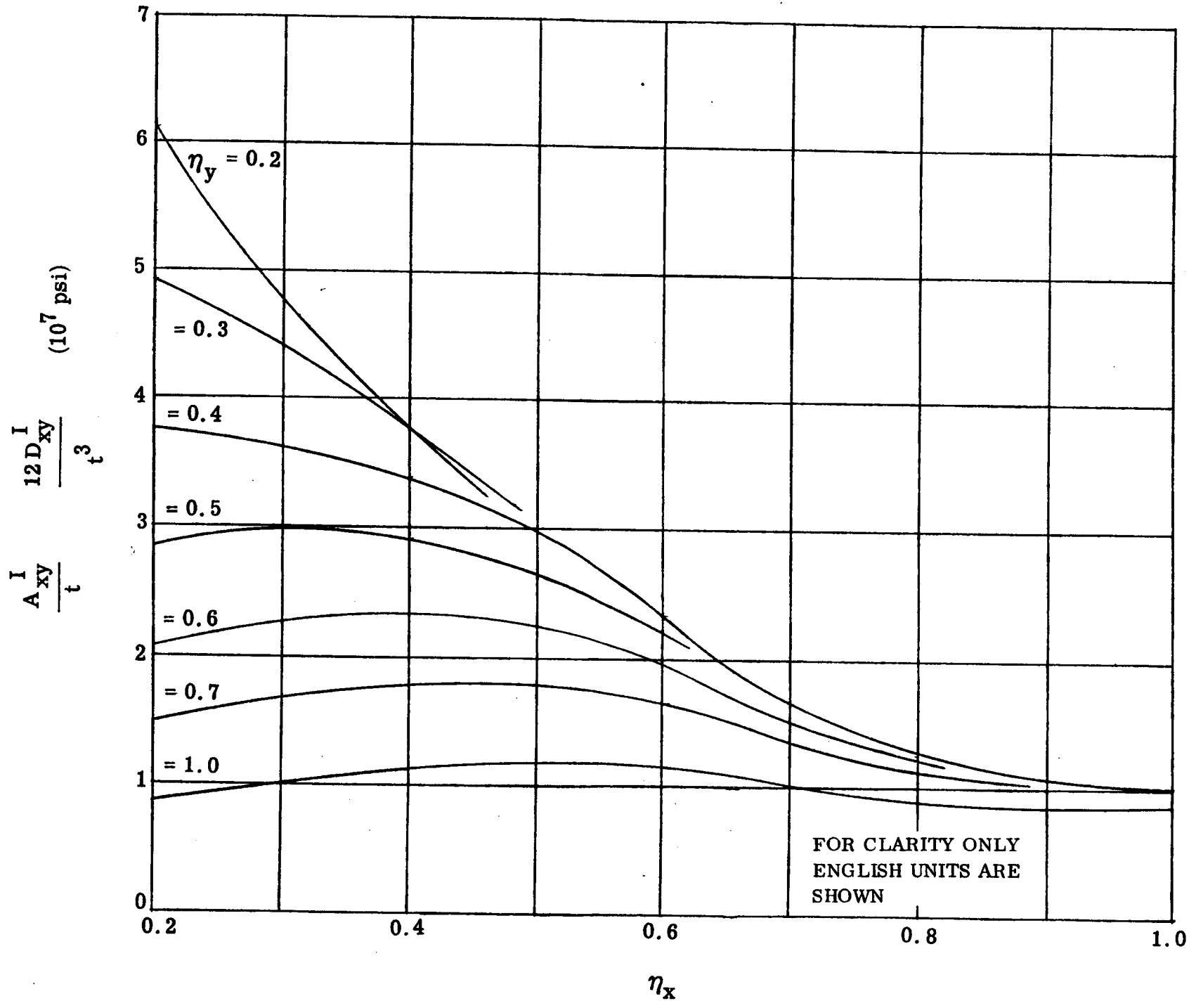

Figure 2-28. Inelastic Constants for ±45° Heat Treated B/Al

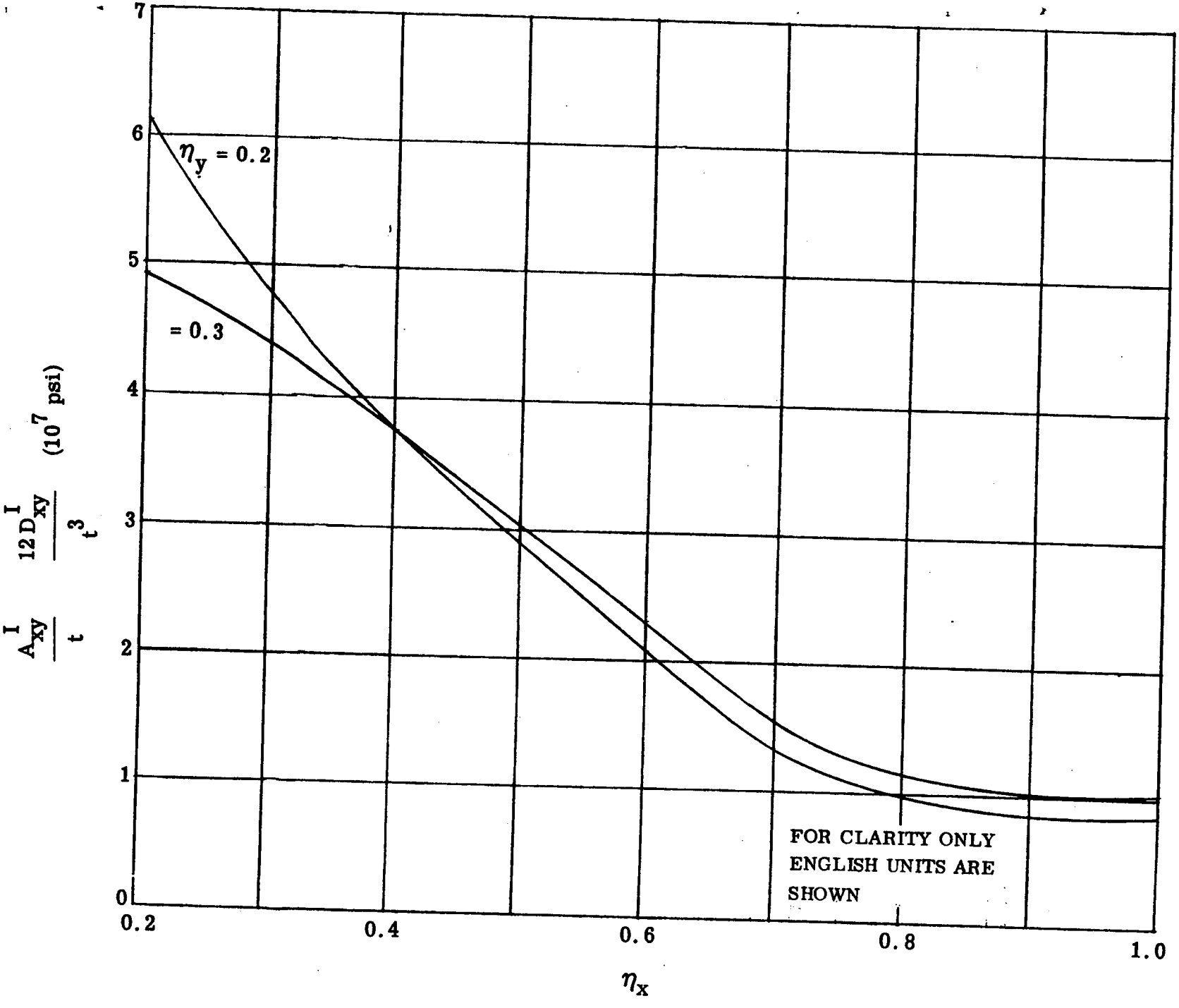

Figure 2-29. Inelastic Constants for ±45° Heat Treated B/Al

2.5.3 PLANE STRESS FINITE ELEMENT ANALYSIS OF SHEAR BEAM. Internal loads of the shear beam were obtained by the use of a plane stress finite element computer program (Number P5543). Inelastic stress states in the ±45° solution treatment plus age (ST&A) B/Al web were obtained by an iteration process where the inelastic stiffness matrix components (A^I_{ij}) were obtained from Figures 2-26 through 2-29. A convenient means of expediting the iteration process was accomplished by the use of Figures 2-30 through 2-32. Figure 2-30 shows the values of A^I_{xx}, A^I_{xy}, and A^I_{yy} for one-inch thickness at 366K (200F) for all combinations of η_x and η_y. To minimize the number of inelastic values to be input to the computer program, combinations of nearly equal inelastic constants have been grouped together and given a reference number as shown in Figures 2-31 and 2-32. Material numbers 1 and 12 have been reserved for materials A and C, respectively. Starting with an elastic computer run, several iterations were performed with corrected inelastic A^I_{ij} terms to arrive at a realistic stress distribution in the beam. The sign convention, node numbers, element numbers, and final material numbers used in the web are indicated in Figure 2-11. Material Number 1 (Material A) is not shown, but is used in the caps, stiffeners, and posts. High stresses occurred in the vicinity of load introduction points; these are highly conservative since the theory within the computer program cannot account for hole deformations at the fasteners. These deformations permit the introduced load to be sheared into the web in a more uniform manner. Accordingly, these particular high stresses are ignored.

The stretching stiffness matrix for Material C, which is Material 12 in the computer program is obtained below:

Material Designation 12 (Material C): 37.5% 90°, 62.5% +45° ST&A B/Al at 366K (200F)

$E_x = 0.9 \times 21.5 \times 10^6 = 133\ GN/m^2\ (19.35 \times 10^6\ psi)$

$E_y = 0.9 \times 26 \times 10^6 = 161\ GN/m^2\ (23.4 \times 10^6\ psi)$

$F_{tu_x} = 0.9 \times 33,750 = 209\ MN/m^2\ (30,375\ psi)$

$F_{tu_y} = 0.9 \times 90,000 = 558\ MN/m^2\ (81,000\ psi)$

$G = 0.9 \times 9.7 \times 10^6 = 60\ GN/m^2\ (8.73 \times 10^6\ psi)$

$F_{su} > 0.9 \times 44,750 > 277.7\ MN/m^2\ (40,275\ psi)$

$\nu_{xy} = 0.265$

$\nu_{yx} = 0.32$

η_x	0.4	0.5	0.6	0.7	0.8	0.9	1.0
1.0	3.4 1.0 1.4	3.3 1.0 1.7	3.2 1.0 1.9	3.0 1.0 2.1	2.9 1.0 2.3	2.8 0.9 2.5	2.8 0.9 2.8
0.9	3.1 1.1 1.4	3.0 1.1 1.7	2.9 1.1 2.0	2.7 1.0 2.1	2.6 1.0 2.3	2.5 0.9 2.5	2.5 0.9 2.8
0.8	3.0 1.3 1.5	2.9 1.3 1.8	2.8 1.2 2.0	2.6 1.1 2.2	2.4 1.0 2.4	2.3 1.0 2.6	2.3 0.9 2.9
0.7	3.2 1.7 1.9	3.0 1.6 2.2	2.8 1.5 2.4	2.5 1.4 2.5	2.2 1.2 2.6	2.1 1.1 2.7	2.1 1.0 3.0
0.6	3.7 2.3 2.5	3.3 2.2 2.8	2.9 2.0 2.9	2.4 1.7 2.8	2.0 1.5 2.8	2.0 1.3 2.9	1.9 1.1 3.2
0.5	4.0 3.0 3.1	3.3 2.7 3.3	2.8 2.3 3.3	2.2 1.8 3.0	1.8 1.6 2.9	1.7 1.4 3.0	1.7 1.2 3.3
0.4	3.9 3.4 3.9	3.1 2.9 4.0	2.5 2.3 3.7	1.9 1.8 3.2	1.5 1.6 3.0	1.4 1.3 3.1	1.4 1.1 3.4

η_y

Note:
Values shown (top to bottom) are A_{xx}^I, A_{xy}^I, A_{yy}^I lb/in $\times 10^7$ for one-inch thickness.
For clarity, only English units are shown.

Figure 2-30. A_{xx}^I, A_{xy}^I, and A_{yy}^I as a Function of Combined η_x and η_y at 366K (200F)

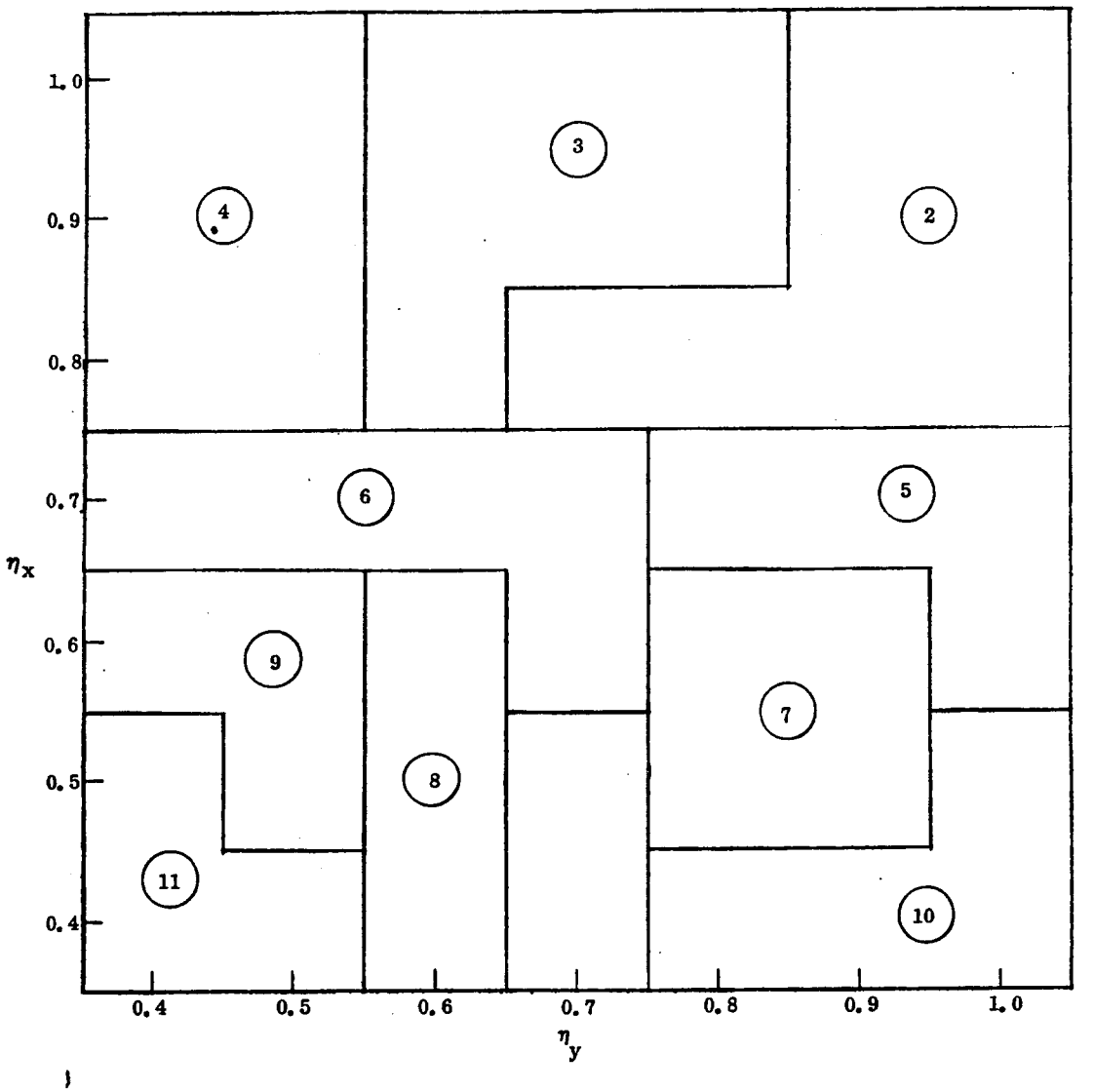

$$\textcircled{2}\begin{Bmatrix} A^I_{xx} \\ A^I_{xy} \\ A^I_{yy} \end{Bmatrix}_{avg} = \begin{Bmatrix} 2.53 \\ 0.95 \\ 2.59 \end{Bmatrix} \quad \textcircled{3}\begin{Bmatrix} A^I_{xx} \\ A^I_{xy} \\ A^I_{yy} \end{Bmatrix}_{avg} = \begin{Bmatrix} 2.87 \\ 1.04 \\ 2.10 \end{Bmatrix} \quad \textcircled{4}\begin{Bmatrix} A^I_{xx} \\ A^I_{xy} \\ A^I_{yy} \end{Bmatrix}_{avg} = \begin{Bmatrix} 3.12 \\ 1.13 \\ 1.58 \end{Bmatrix} \quad \textcircled{5}\begin{Bmatrix} A^I_{xx} \\ A^I_{xy} \\ A^I_{yy} \end{Bmatrix}_{avg} = \begin{Bmatrix} 2.08 \\ 1.10 \\ 2.89 \end{Bmatrix} \quad \textcircled{6}\begin{Bmatrix} A^I_{xx} \\ A^I_{xy} \\ A^I_{yy} \end{Bmatrix}_{avg} = \begin{Bmatrix} 2.78 \\ 1.58 \\ 2.36 \end{Bmatrix}$$

$$\textcircled{7}\begin{Bmatrix} A^I_{xx} \\ A^I_{xy} \\ A^I_{yy} \end{Bmatrix}_{avg} = \begin{Bmatrix} 1.93 \\ 1.57 \\ 2.97 \end{Bmatrix} \quad \textcircled{8}\begin{Bmatrix} A^I_{xx} \\ A^I_{xy} \\ A^I_{yy} \end{Bmatrix}_{avg} = \begin{Bmatrix} 2.73 \\ 2.20 \\ 3.30 \end{Bmatrix} \quad \textcircled{9}\begin{Bmatrix} A^I_{xx} \\ A^I_{xy} \\ A^I_{yy} \end{Bmatrix}_{avg} = \begin{Bmatrix} 3.43 \\ 2.40 \\ 2.87 \end{Bmatrix} \quad \textcircled{10}\begin{Bmatrix} A^I_{xx} \\ A^I_{xy} \\ A^I_{yy} \end{Bmatrix}_{avg} = \begin{Bmatrix} 1.50 \\ 1.30 \\ 3.20 \end{Bmatrix} \quad \textcircled{11}\begin{Bmatrix} A^I_{xx} \\ A^I_{xy} \\ A^I_{yy} \end{Bmatrix}_{avg} = \begin{Bmatrix} 3.67 \\ 3.10 \\ 3.67 \end{Bmatrix}$$

Note:

Inelastic constants are lb/in $\times 10^7$ for one-inch thickness.
For clarity, only English units are shown.

Figure 2-31. Material Designations of Grouped Inelastic Material Properties at 366K (200F) for Use in Computer Program

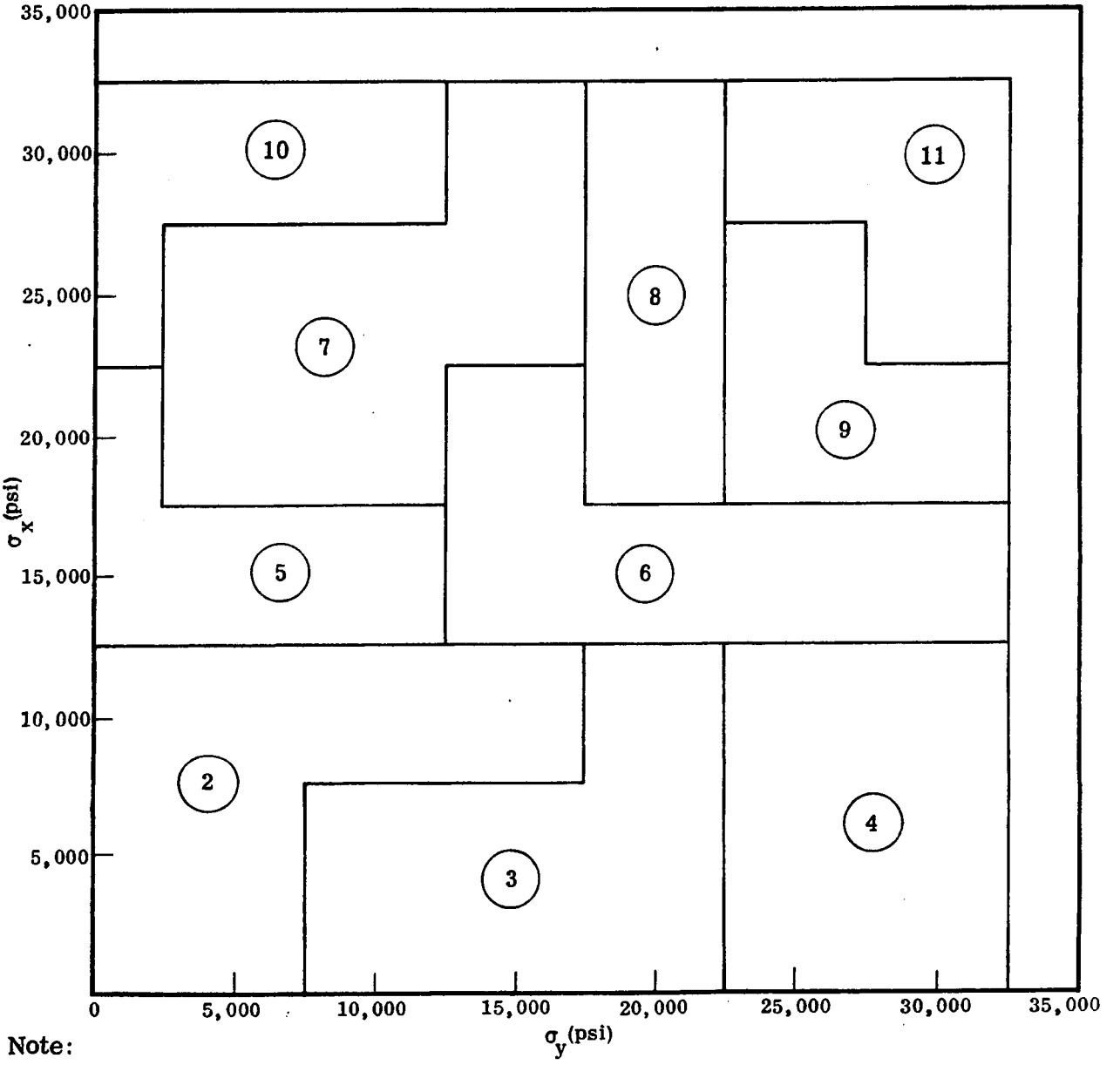

Note:
For clarity, only English Units are shown

Figure 2-32. Material Designations of Grouped Inelastic Material Properties with Respect to σ_x and σ_y at 366K (200F) for Use in Computer Program

$$A_{xx} = \frac{E_x t}{1-\nu_{xy}\nu_{yx}} = \frac{19.35 \times 10^6 \times 1}{1-0.265 \times 0.32}$$

$$= 2.1 \times 10^7 \text{ psi}$$

$$A_{yy} = \frac{E_y t}{1-\nu_{xy}\nu_{yx}} = \frac{23.4 \times 10^6 \times 1}{1-0.265 \times 0.32}$$

$$= 2.56 \times 10^7 \text{ psi}$$

$$A_{xy} = \nu_{yx} A_{11} = 0.32 \times 2.11 \times 10^7$$

$$= 0.67 \times 10^7 \text{ psi}$$

$$A_{66} = G_{xy}^{t} = 0.87 \times 10^7 \text{ psi}$$

for thickness = one inch (9)

Note: x, y Directions here correspond with that of the shear beam, which is opposite from that used for material properties in Section 2.5.1.

2.5.4 ELASTIC/INELASTIC BUCKLING ANALYSIS METHODS FOR SHEAR BEAM PANELS. The panels of the shear beam are very short panels loaded in general as shown in Figure 2-33. For compression buckling, the plastic buckling factors developed by Stowell (Reference 6) for metals are assumed to be appropriate for the web material. Accordingly, the equations are presented in Table 2-7, and correction curves for simply supported plates of Material B (±45° ST&A B/Al) are presented in Figures 2-34 and 2-35. The recommended procedure for the inelastic buckling analysis of the panel shown in Figure 2-33 is presented as follows (see Figures 2-36 and 2-37):

a. Find the bending buckling stress for the plate corresponding to $\sigma_{bc_{max}}$ by the equation

$$\frac{\sigma_{bc_{cr}}}{\eta_E} = k_b \frac{\pi^2 E_{bc_{max}}}{12(1-\nu_{xy}\nu_{yx})} \left(\frac{t}{a}\right)^2 \quad (10)$$

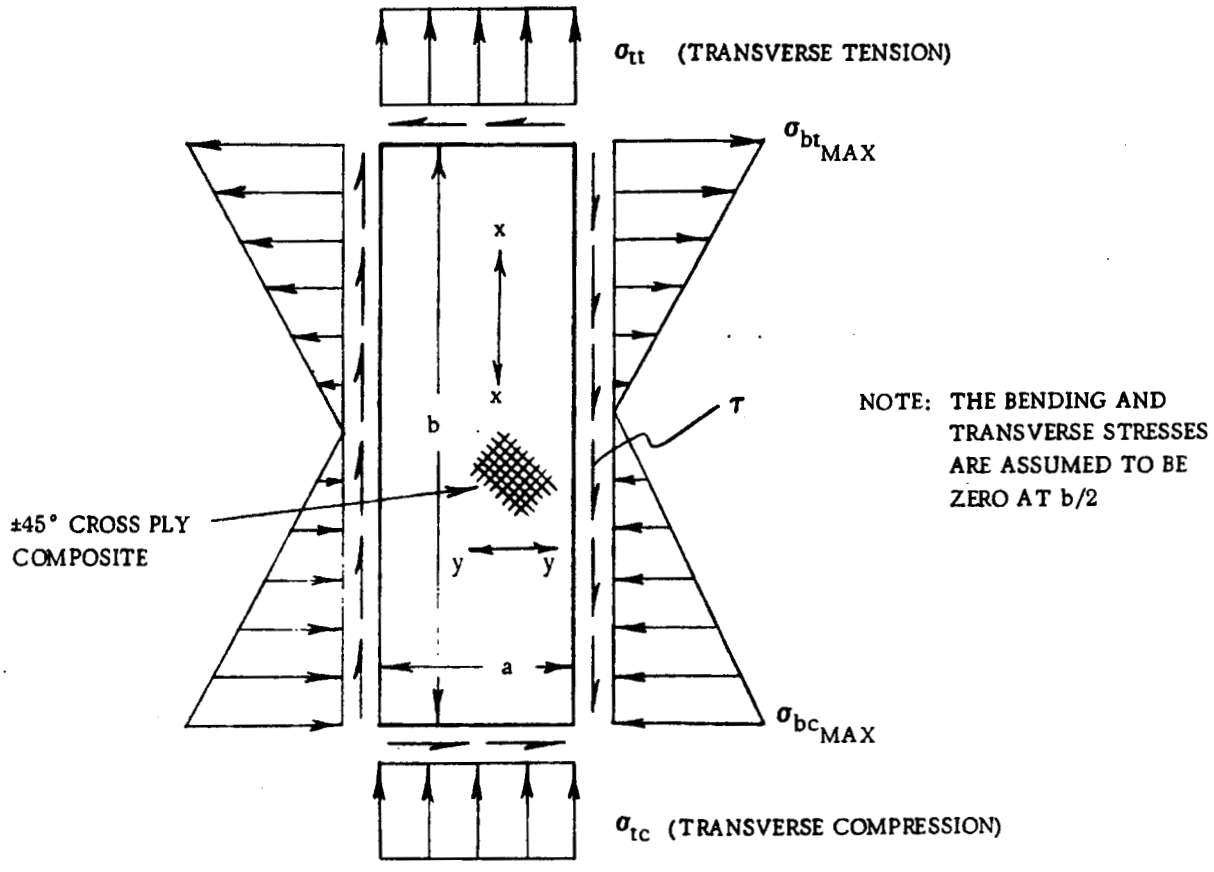

Figure 2-33. Critical Buckling Stress of Short Simply Supported Flat ±45° Composite Plate Under Combined Longitudinal Bending, Transverse Compression, and Shear

b. Find the buckling stress for the transverse compressive stress σ_{tc} that varies to zero at b/2 by the equation

$$\frac{\sigma_{tc_{cr}}}{\eta_C} = k_{tc} \frac{\pi^2 E_x}{12(1-\nu_{xy}\nu_{yx})} \left(\frac{t}{a}\right)^2 \tag{11}$$

c. Find the shear buckling stress by using Figures 2-38 through 2-43 or by the equations

$\theta > 1$

$$\tau_{cr}/\eta_s = \frac{1}{t}\left(\frac{2}{a}\right)^2 \left[D^I_{xx}(D^I_{yy})^3\right]^{1/4} \left(8.125 + \frac{5.04}{\theta}\right) \tag{12}$$

$\theta < 1$

$$\tau_{cr}/\eta_s = \frac{1}{t}\left(\frac{2}{a}\right)^2 \sqrt{D^I_{yy}(D^I_{xy} + 2D^I_{66})}\ \ 11.7 + 0.532\,\theta + 0.938\,\theta^2$$

$$\theta = \frac{\sqrt{D^I_{xx}\,D^I_{yy}}}{D^I_{xy} + 2D^I_{66}} \qquad (13)$$

$$\eta_s = G_{sec}/G \quad (\eta_s = 1.0 \text{ up to } \tau_{cr}/\eta_s = 56{,}000 \text{ psi})$$

d. Find the allowable shear stress τ_a with the panel simultaneously subjected to the compressive bending stress $\sigma_{bc_{max}}$ and the transverse compressive stress σ_{tc} by the following:

1. $R_b = \dfrac{\sigma_{bc_{max}}}{\sigma_{b_{cr}}}$ (Bending Stress Ratio)

2. $R_{tc} = \dfrac{\sigma_{tc}}{\sigma_{tc_{cr}}}$ (Transverse Stress Ratio)

3. Find $R_a = \tau_a/\tau_{cr}$ from the interaction curves shown in Figure 2-43 and

$$\tau_a = \tau_{cr} R_b$$

The stiffeners are to offer simple support to the panel so that the buckling analysis for simply supported plates is valid. Consequently, the stiffness of the stiffeners must be obtained by use of Figure 2-44, which was developed from information taken from Stein and Fralich (Reference 7) for plates in shear. D of the panel is the web bending stiffness $Et^3/12\,(1-\nu_{xy}\nu_{yx})$.

Table 2-7. Plasticity Factors (η) for Compressive Plate Buckling

Structure	η	Curve
Long flange, one unloaded edge simply supported and the other free	$\frac{E_{sec}}{E}$	A
Long flange, one unloaded edge clamped and the other free	$\frac{E_{sec}}{E}\left(0.428 + 0.572\sqrt{\frac{1}{4} + \frac{3}{4}\frac{E_{tan}}{E_{sec}}}\right)$	B
Long plates, both unloaded edges simply supported	$\frac{E_{sec}}{E}\left(\frac{1}{2} + \frac{1}{2}\sqrt{\frac{1}{4} + \frac{3}{4}\frac{E_{tan}}{E_{sec}}}\right)$	C
Long plate, both unloaded edges clamped	$\frac{E_{sec}}{E}\left(0.352 + 0.648\sqrt{\frac{1}{4} + \frac{3}{4}\frac{E_{tan}}{E_{sec}}}\right)$	D
Short plate loaded as a column $\left(\frac{L}{b} \ll 1\right)$	$\frac{1}{4}\frac{E_{sec}}{E} + \frac{3}{4}\frac{E_{tan}}{E}$	E
Square plate loaded as a column $\left(\frac{L}{b} = 1\right)$	$0.114\frac{E_{sec}}{E} + 0.886\frac{E_{tan}}{E}$	F
Long column $\left(\frac{L}{b} \gg 1\right)$	$\frac{E_{tan}}{E}$	G

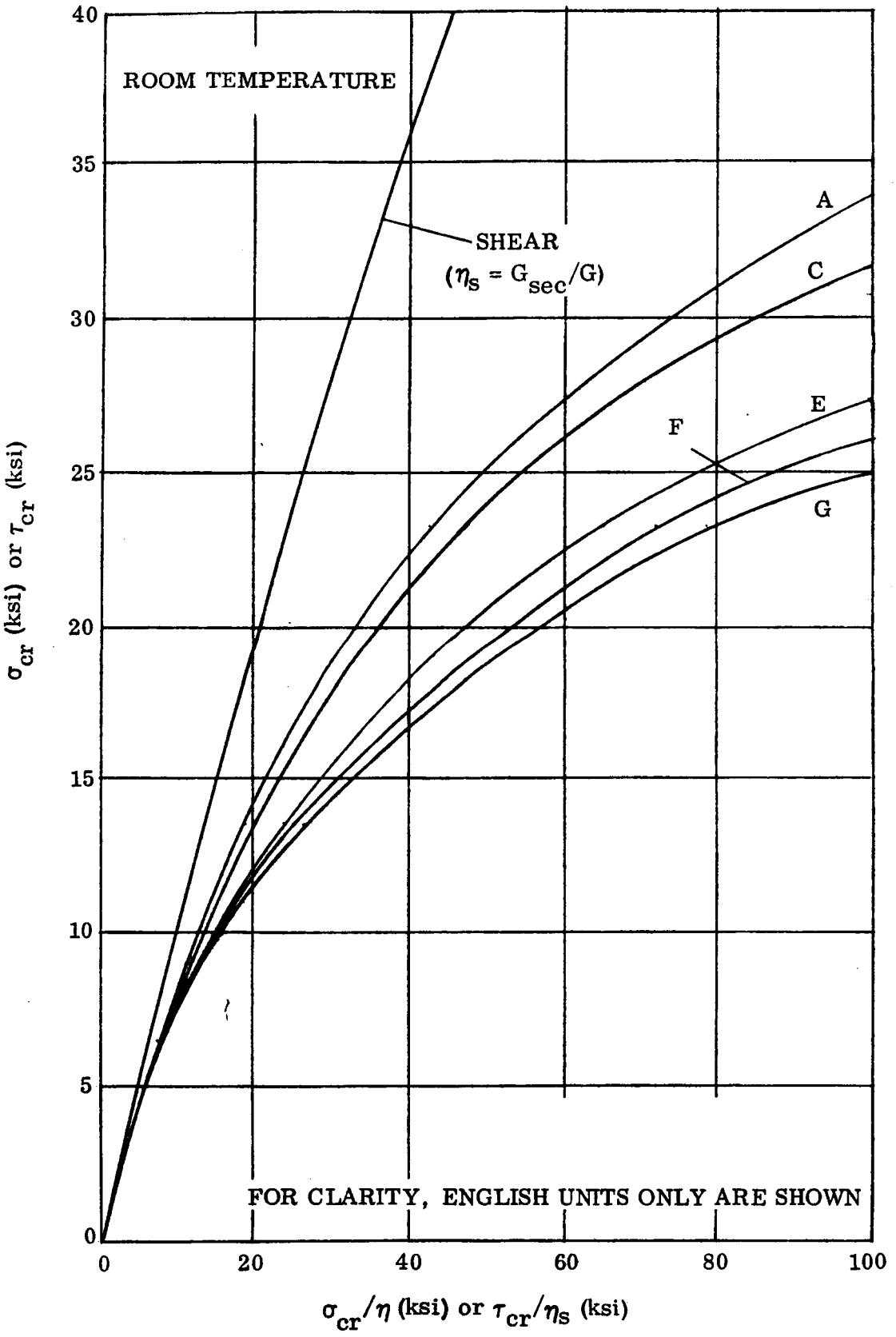

Figure 2-34. Flat Plate Plastic Buckling Correction Curves for Heat Treated ±45° B/Al

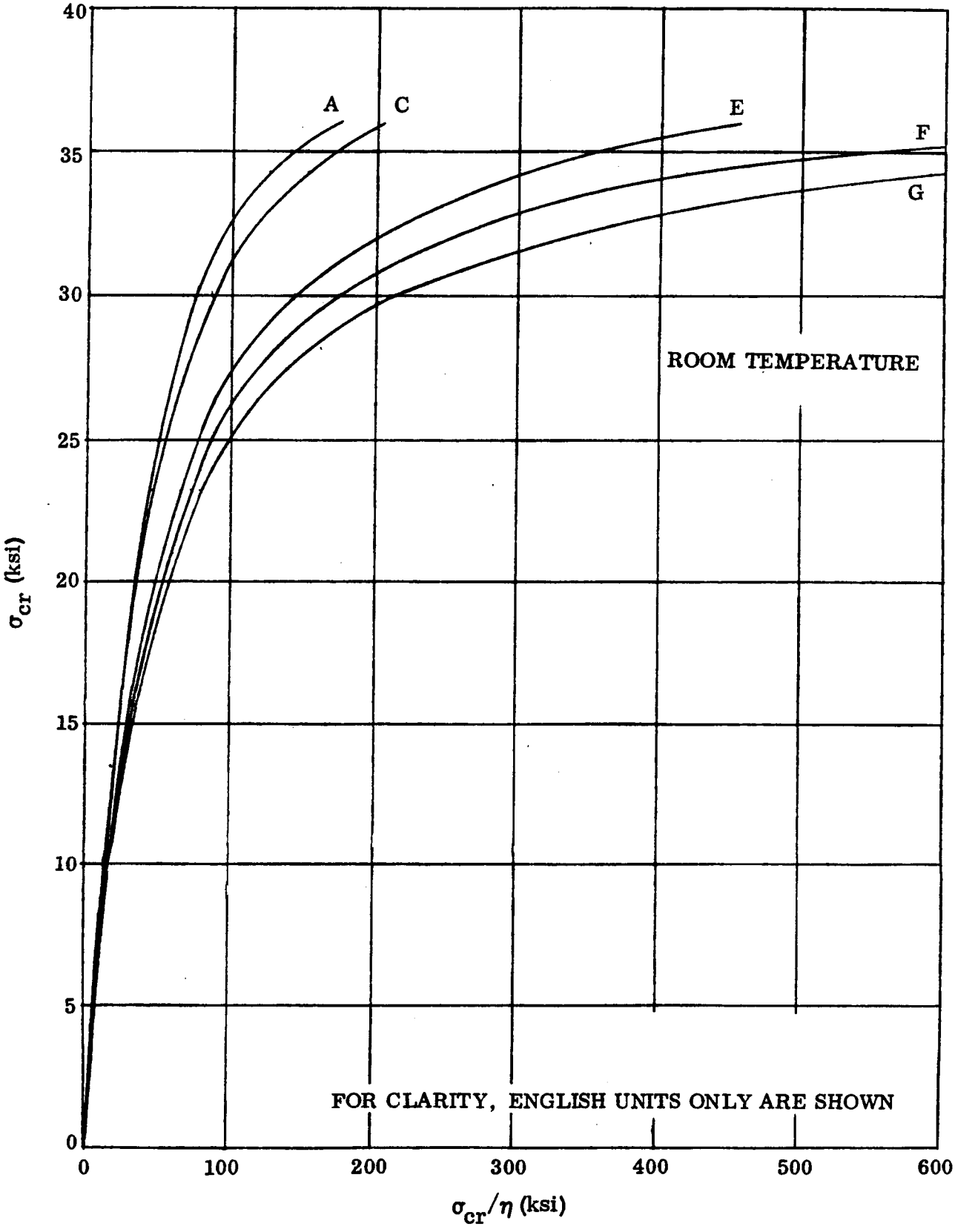

Figure 2-35. Flat Plate Plastic Buckling Correction Curves for Heat Treated ±45° B/Al

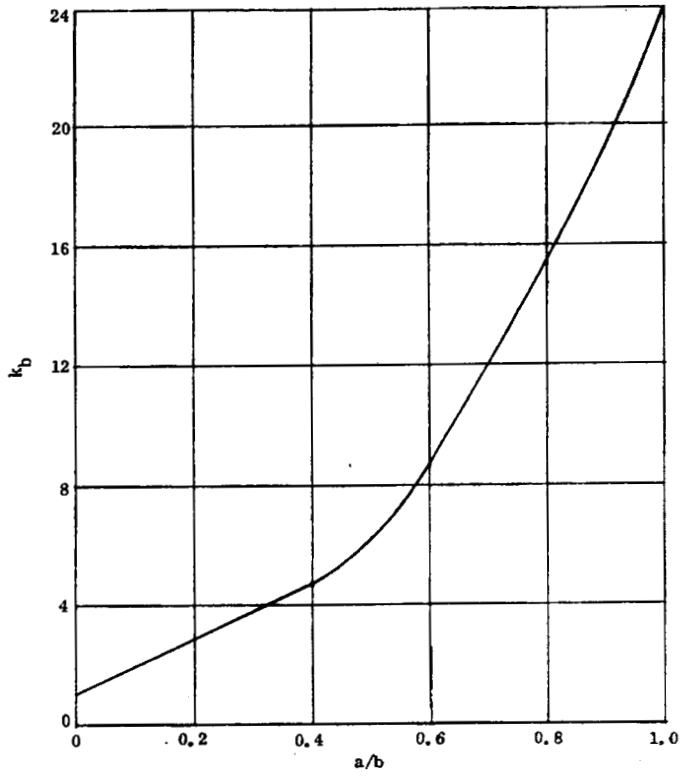

Figure 2-36. Buckling Coefficient for Bending of a Short Plate

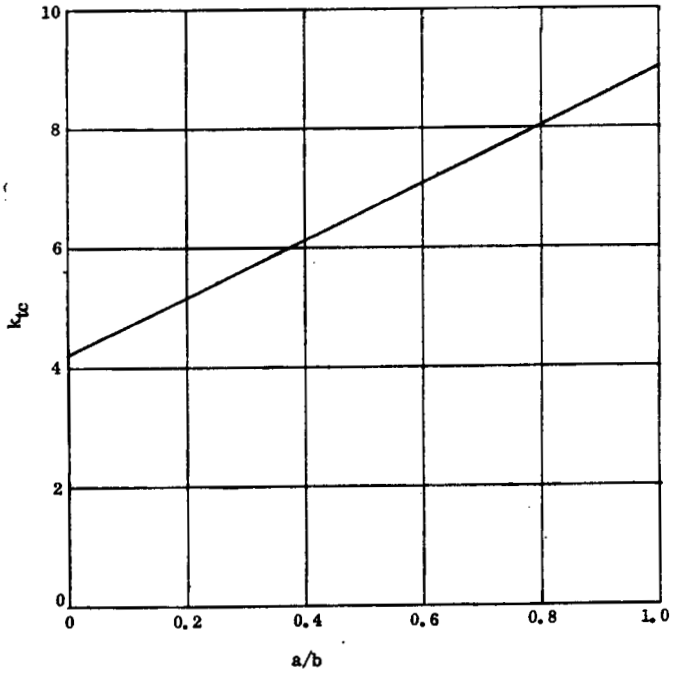

Figure 2-37. Buckling Coefficient for Varying Compression of a Long Plate

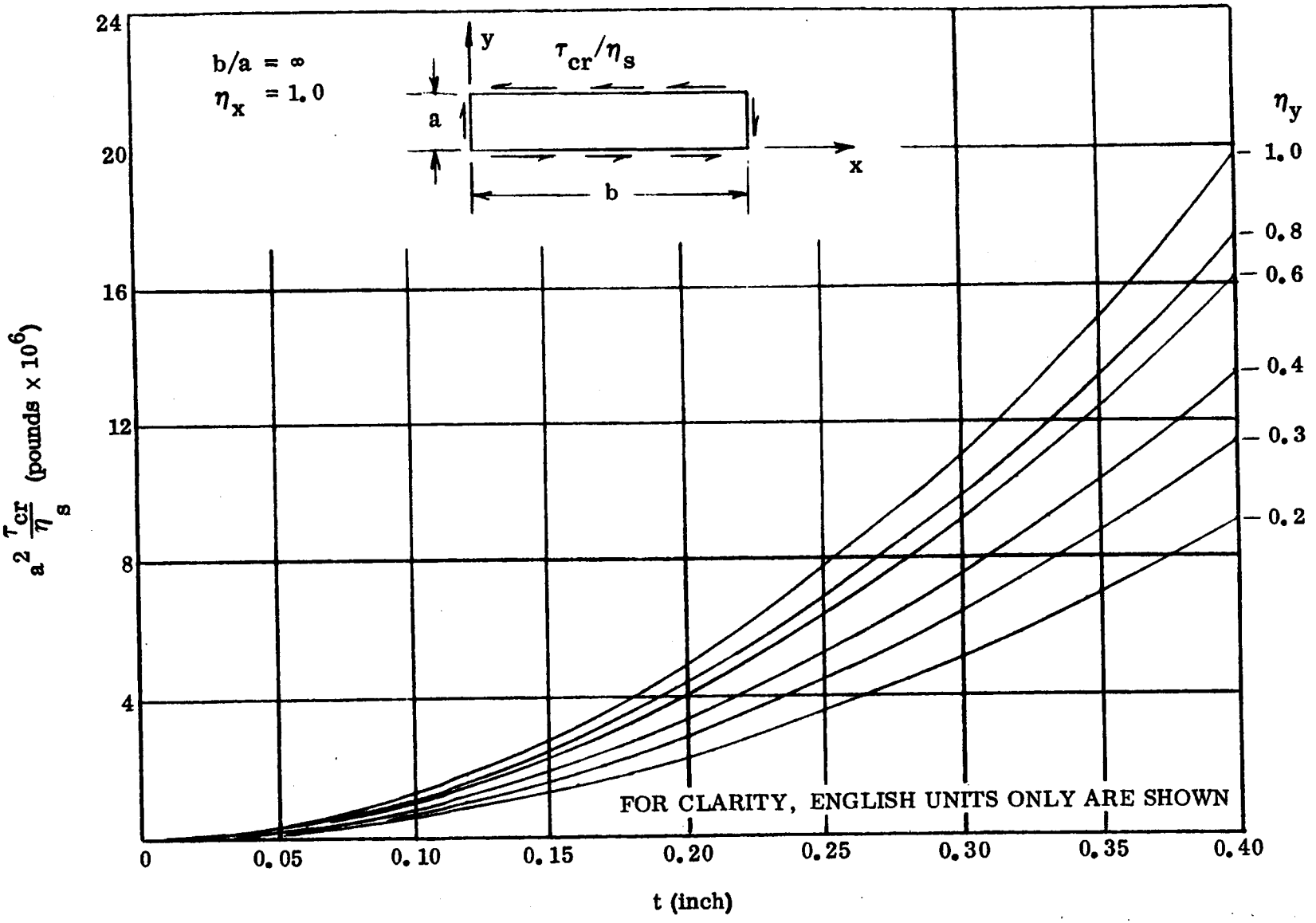

Figure 2-38. Shear Buckling of ±45° Heat Treated B/Al Long Flat Plates

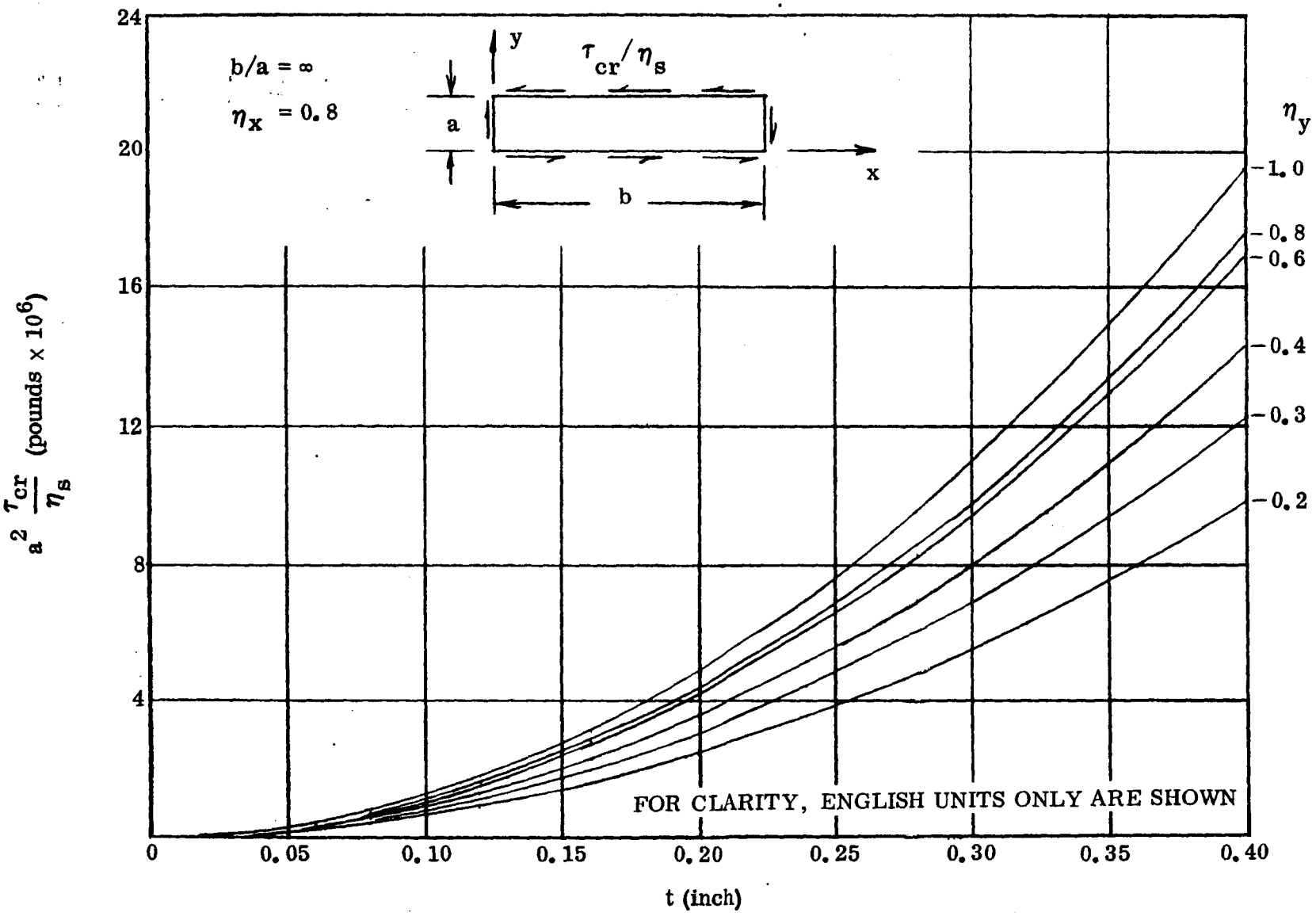

Figure 2-39. Shear Buckling of ±45° Heat Treated B/Al Long Flat Plates

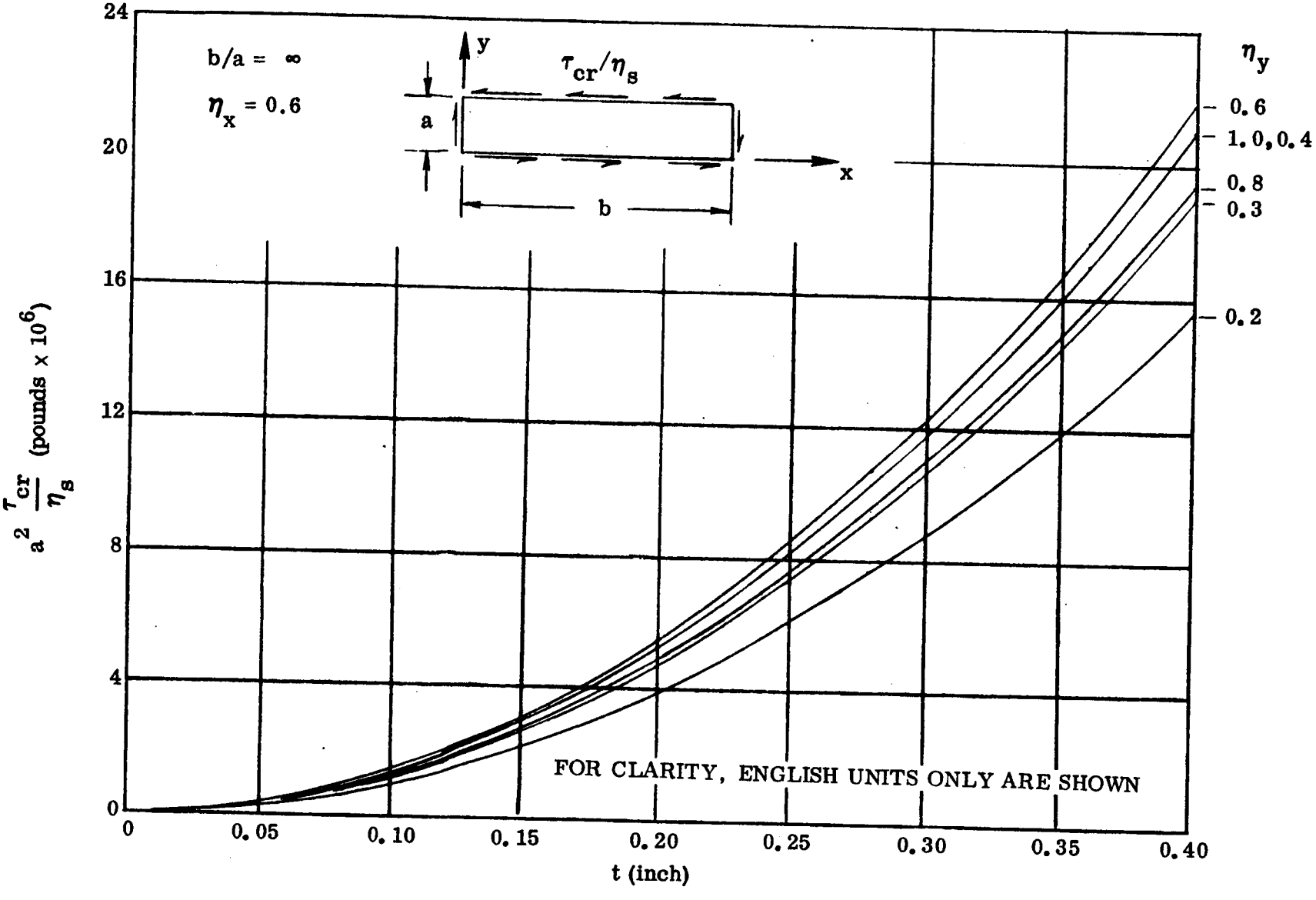

Figure 2-40. Shear Buckling of ±45° Heat Treated B/Al Long Flat Plates

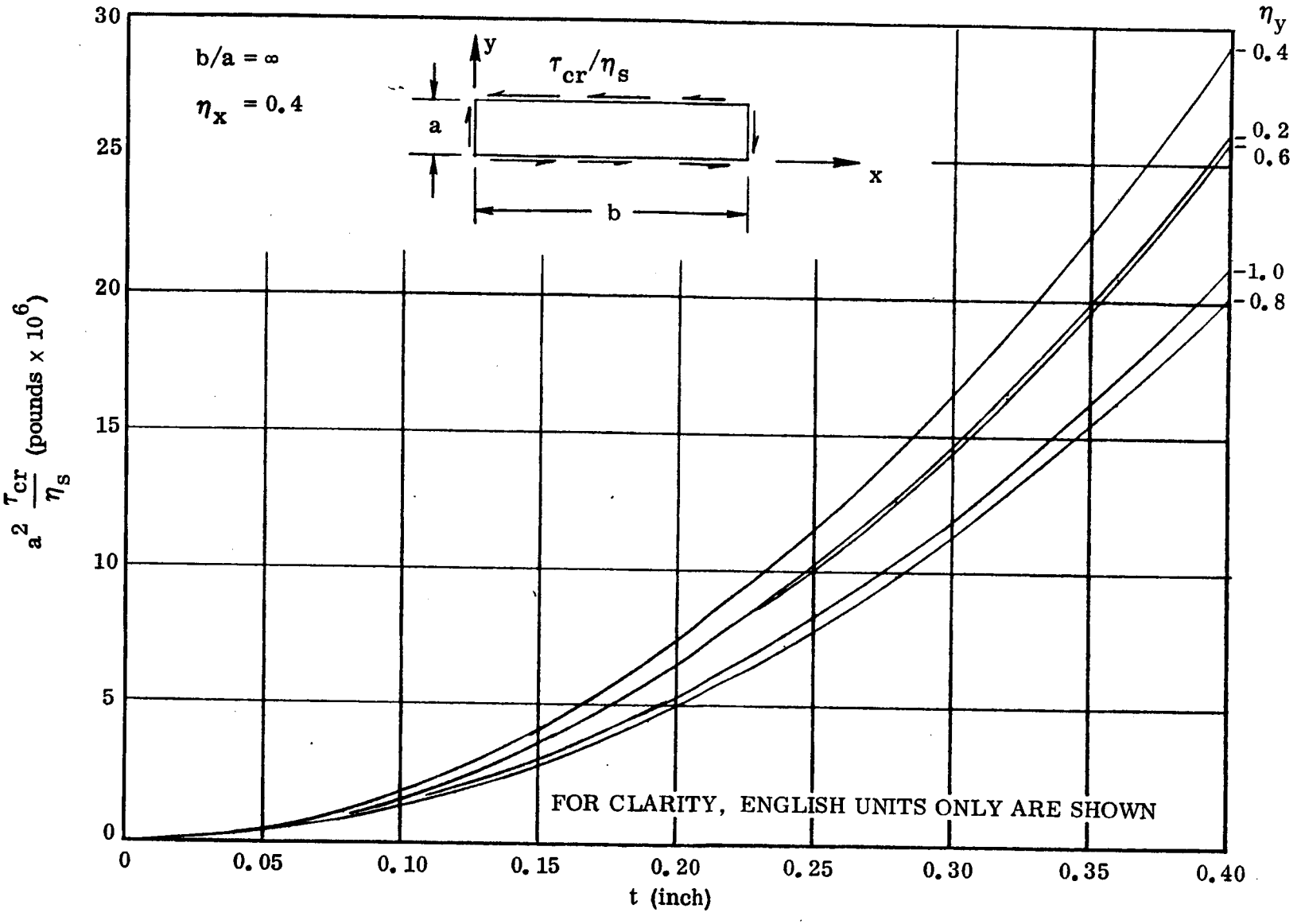

Figure 2-41. Shear Buckling of ±45° Heat Treated B/Al Long Flat Plates

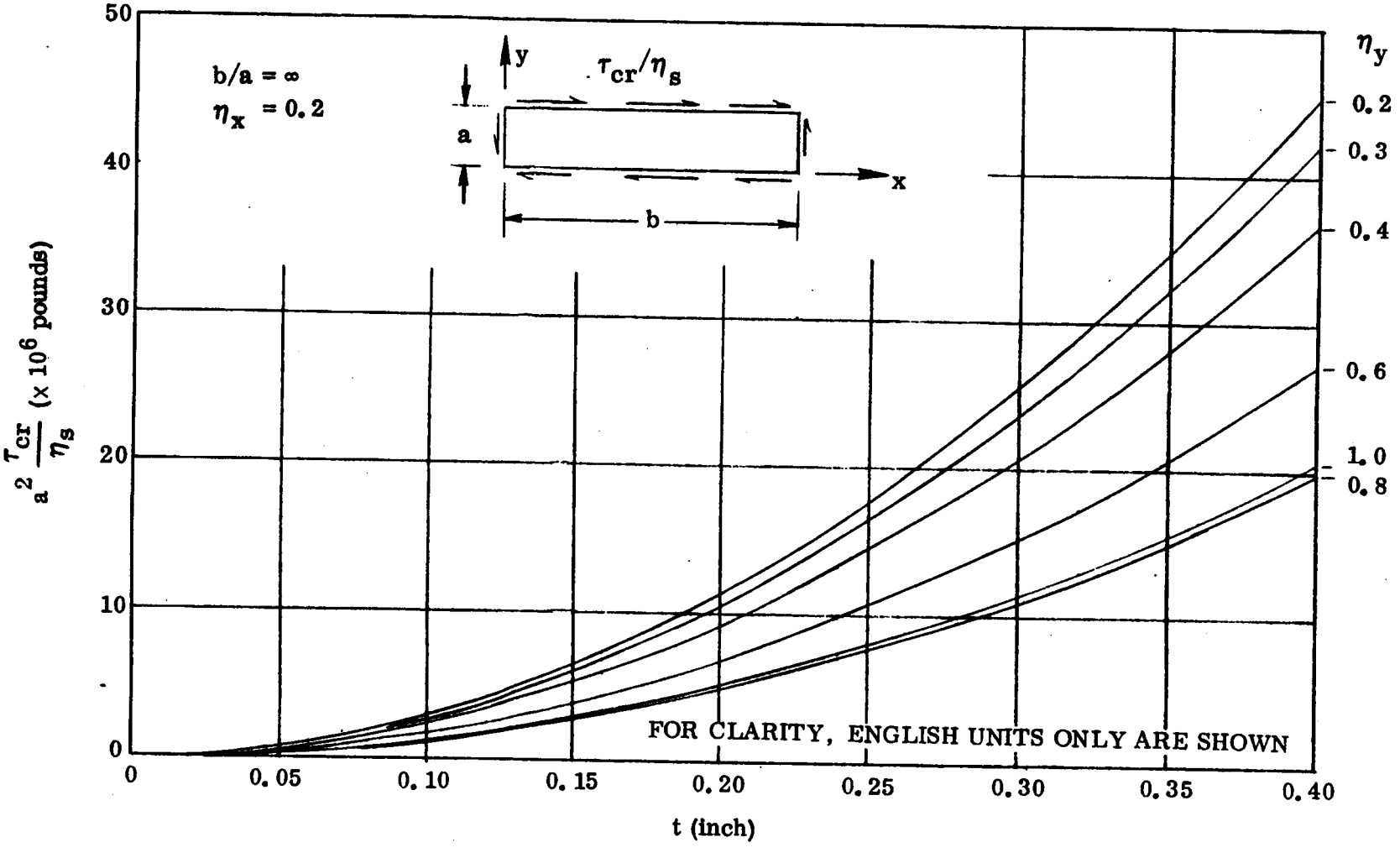

Figure 2-42. Shear Buckling of ±45° Heat Treated B/Al Long Flat Plates

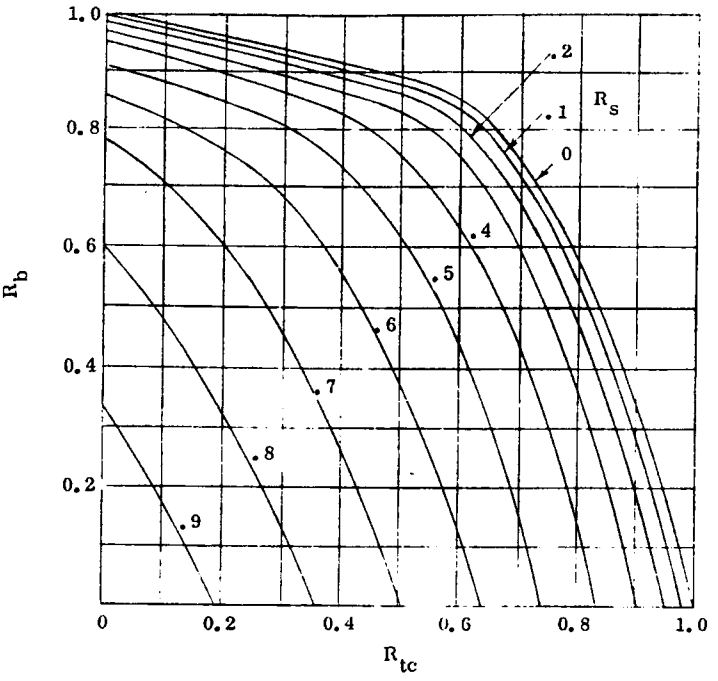

Figure 2-43. Interaction Curves

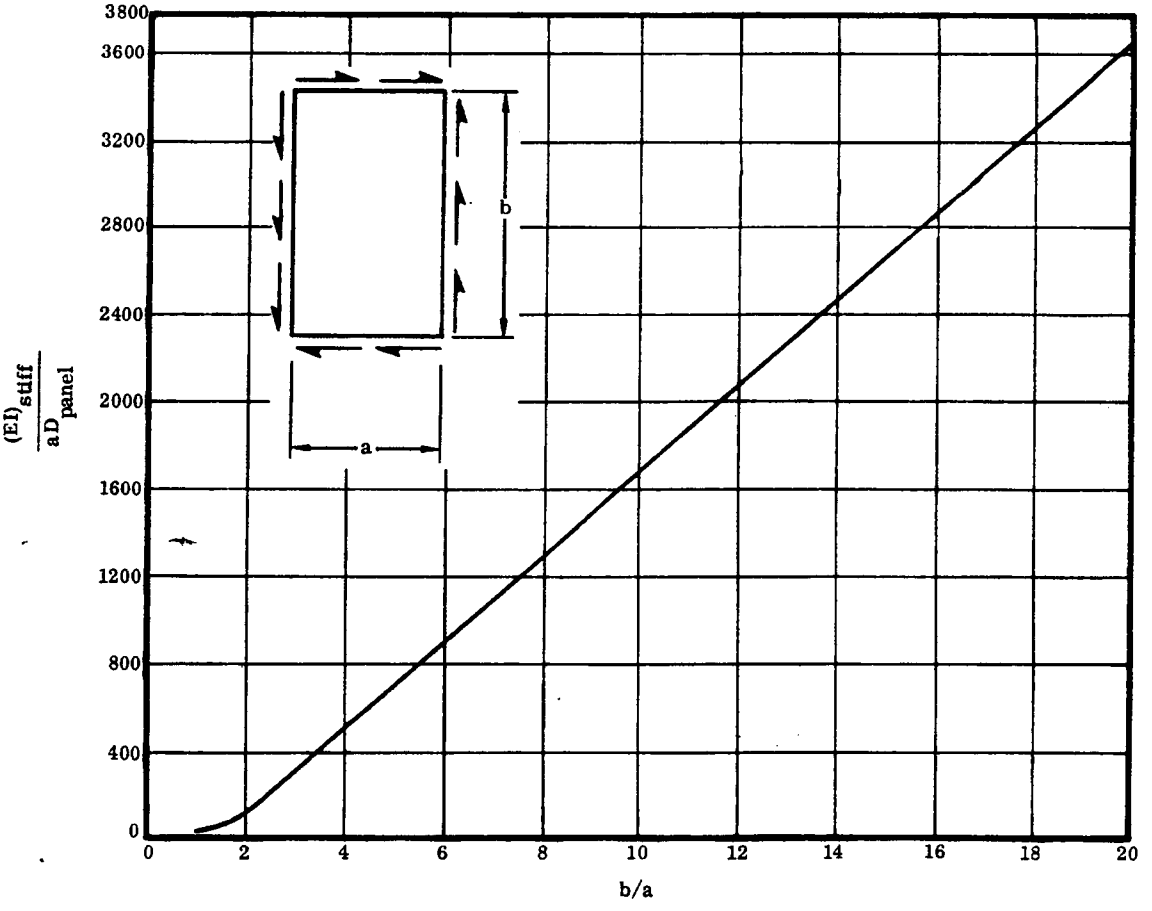

Figure 2-44. Required Edge Stiffener Properties for Simply Supported Isotropic Flat Plate in Shear

2.6 SUBCOMPONENT DESIGN AND ANALYSIS

The objective of this portion of the program was to investigate and verify structural joints and elements of the final shear beam design. Candidate joining methods, based on the present state of the art, were Con Braz joining, resistance spot welding, resistance spot joining, mechanical fasteners, adhesive bonding, and combinations of these techniques. These joining processes were investigated and the feasibility of each was established during joint screening tests. The most promising of these methods, based on joint strength, ease of fabrication, and applicability to full-scale design, were used in the design of the shear web beam. The subcomponent designs were developed to simulate components and critical joints in the full-scale beam design and to verify fabrication processes and joint properties. Candidate component test specimens were selected to represent fabrication or design areas of most significance to the success of the full-scale final design configuration. In all cases, the specimens failed at load levels in excess of those required for successful performance of the full-scale shear beam.

Five different types of shear beam subcomponents were designed to evaulate various techniques for joining elements of the boron/aluminum (B/Al) shear beam and to verify design assumptions and predicted strengths. The test specimens were sized in most cases to simulate sections of the full-scale component to establish a data point for both the shear-beam design and the larger scale component test specimen. The subcomponents designed were:

a. Web splice specimen.

b. Web-to-cap joint in unidirectional B/Al.

c. B/Al web-to-titanium cap joint.

d. Tension field ±45° B/Al panel.

e. Unidirectional B/Al tension-field panel

2.6.1 WEB SPLICE. The primary purpose of the web splice joint subcomponent test was to establish a splice-joint allowable that could be used to verify the joint strength used in the design of the shear web beam. The web splice test specimen was configured from a 5 mm (0.20 in.) thick web with 2.5 mm (0.10 in.) thick splice plates on both web faces. The web and splice material was ±45° crossply B/Al. Two types of joints were considered: spotwelded and mechanically fastened joints. The joint was sized to have sufficient shear load transfer capability to support shear flows of 5250 N/cm (3000 lb/in) predicted for the center bays of the full-scale shear beam. The design ultimate strength of this joint was 120,000 N (27,000 lb) or for equal distribution of load, 20,000 N (4500 lb) per double shear spotweld. With the spotwelds on 3.81 cm (1.5 in.) centers, this strength equates with the expected maximum ultimate shear flow of 5250 N/cm (3000 lb/in). It was expected that the bearing capability of

the B/Al would provide a joint of approximately equal strength with 1/4-inch mechanical fasteners. The joint strengths were based on the subelement test results for spotwelded and bolted joints. One of each specimen attachment type was thermally cycled 100 times through a temperature range of 77 to 366K (-320 to 200F) before testing. A typical spotwelded test specimen is shown in Figure 2-45.

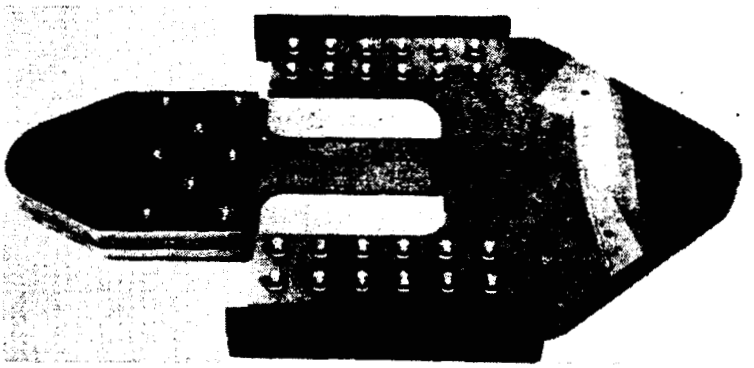

Figure 2-45. Web Splice Test Specimen and Fixture (122407B)

Tests of spotwelded and bolted ±45° ST&A B/Al splice joints were performed. The strain gage readings were not helpful in determining the load distribution in the spotwelds or bolts. They did, however, show that the shear stress was distributed parabolically over a section through the strain gages (1 and 2 or 3 and 4). The test results are shown in Table 2-8, where the bolts were 0.635 cm (1/4 in.) diameter and the center B/Al plate was 0.508 cm (0.200 in.) thick. The outer B/Al plates were 0.254 cm (0.100 in.) thick. Only average values, which are conservative, are reported in Table 2-8. Specimens 2 and 4 were thermally cycled 100 times through a temperature range of 77 to 366K (-320 to 200F) before testing. Test results indicated no adverse affects. Failed spotwelds are shown in Figure 2-46, and a typical bolted joint failure is shown in Figure 2-47.

Table 2-8. Shear Splice Test Results

Test	Type	P Newtons (pounds)	Average Double Shear Loading Fastener Newtons (pounds)	Average Bearing Stress N/cm^2 (lb/in^2)	Thermally Cycled 100 Times Before Testing
1	Spotweld	100,085 (22,500)	16,681 (3750)	—	No
2	Spotweld	115,653 (26,000)	19,274 (4333)	—	Yes
3	Bolted	232,641 (52,300)	38,775 (8717)	120,199 (174,340)	No
4	Bolted	239,313 (53,800)	39,881 (8967)	123,646 (179,340)	Yes

Figure 2-46. Failed Spotwelded Web Splice Test Specimen (125077B)

Figure 2-47. Failed Bolted Web Splice Test Specimen (125076B)

It is obvious that bolted splice joints provide the maximum shear strength available. However, in certain applications the spotwelds are satisfactory. Therefore, in the shear beam, one row of double shear spotwelds was used in the center section web splices, while the outer section utilized two rows of double shear spotwelds.

2.6.2 WEB-TO-CAP JOINT (ALL B/Al). This test specimen was configured to evaluate two full-scale joining techniques that were to be used in the web-to-cap joint shown in Figure 2-48. The first joint is the spotweld attachment between the ±45° crossply B/Al web and the unidirectional leg of the compression-beam cap. The second is the braze joints shown for the proposed attachment of the compression cap to its upstanding leg. Before the test specimen was fabricated, it was determined (from subelement tests) that the spotweld joint did not produce consistent joint strengths when there were considerable differences in gages of the elements being joined. Spotwelding for this application was therefore dropped and replaced with mechanical fasteners.

Further, in the course of subelement testing of the brazed joint, it was found that the Con Braz joining technique was not sufficiently developed to reliably join elements of the thick sections required for the beam cap. The subelement test results indicated that the joint shear strength was not sufficient to meet the required shear flow. It was decided that further braze-joint development in thick sections could not be accomplished in time to support the current program. The proposed test specimen was, therefore, abandoned in favor of an alternate approach. There was some concern earlier in the program that the braze and spotweld joining processes would not be readily adaptable to the heavier gages, and for this reason, a backup configuration utilizing a titanium element in the joint was included in the test program.

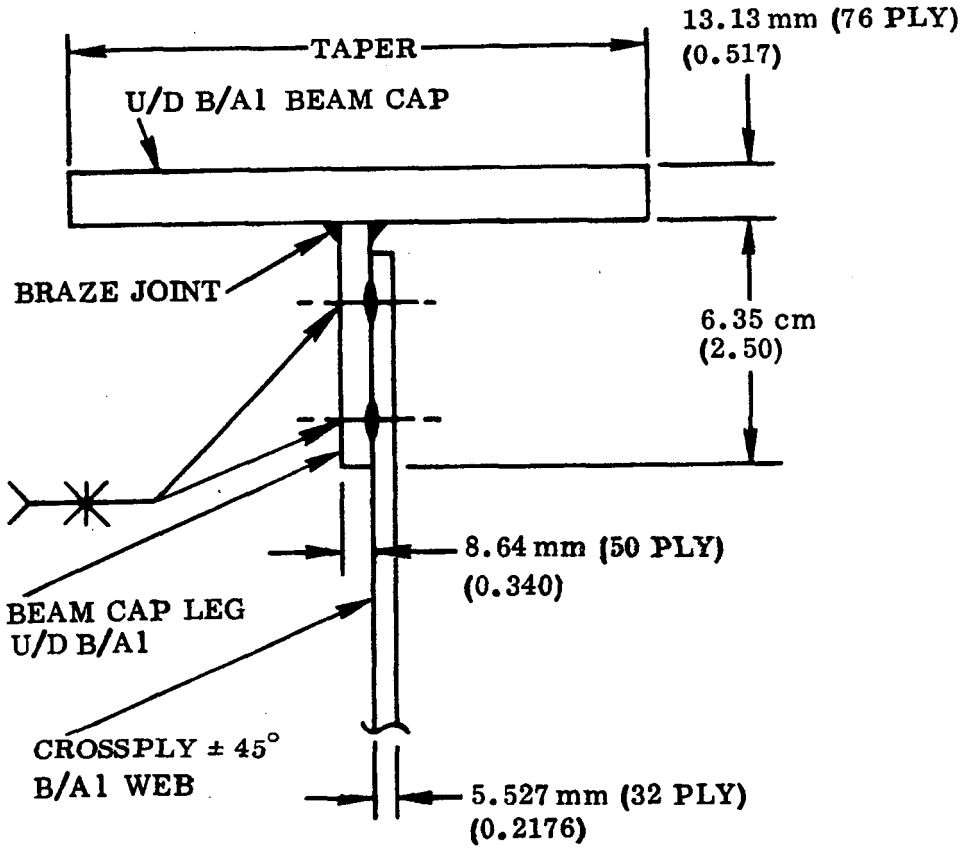

Figure 2-48. Shear Web Beam Compression Cap Cross-Section

2.6.3 WEB-TO-CAP-JOINT (B/Al TO TITANIUM). This specimen was configured to test a joint between the B/Al beam web and a titanium element from the beam cap, secured by a continuous spot-joining process. A cross-section of the joint is shown in Figure 2-49. The primary load in the joint is a shear load from the web to the beam cap. The maximum beam shear load in the region of the joint is 5250 N/cm (3000 lb/in) for the beam center bay and 10,500 N/cm (6000 lb/in) for the outer bay. This concept and the bolted joints were considered as alternate concepts to that discussed in the previous section.

Preliminary subelement test of resistance-spot-joined, single-lap-shear specimens indicated that adequate strength could be obtained to satisfy the requirements for a joint of this type. Three subcomponent test specimens were fabricated to simulate this joint.

A "picture-frame" fixture with two links was designed and fabricated for the purpose of testing in approximately pure shear the ±45° B/Al composite spot-joined to the titanium alloy. The fixture and specimen are shown in Figure 2-50. The links are provided to allow small geometric distortions without large stresses developing at the corners. This technique was quite successful and the shear flow distribution was approximately parabolic over the cross-section. Three tests were performed, and one

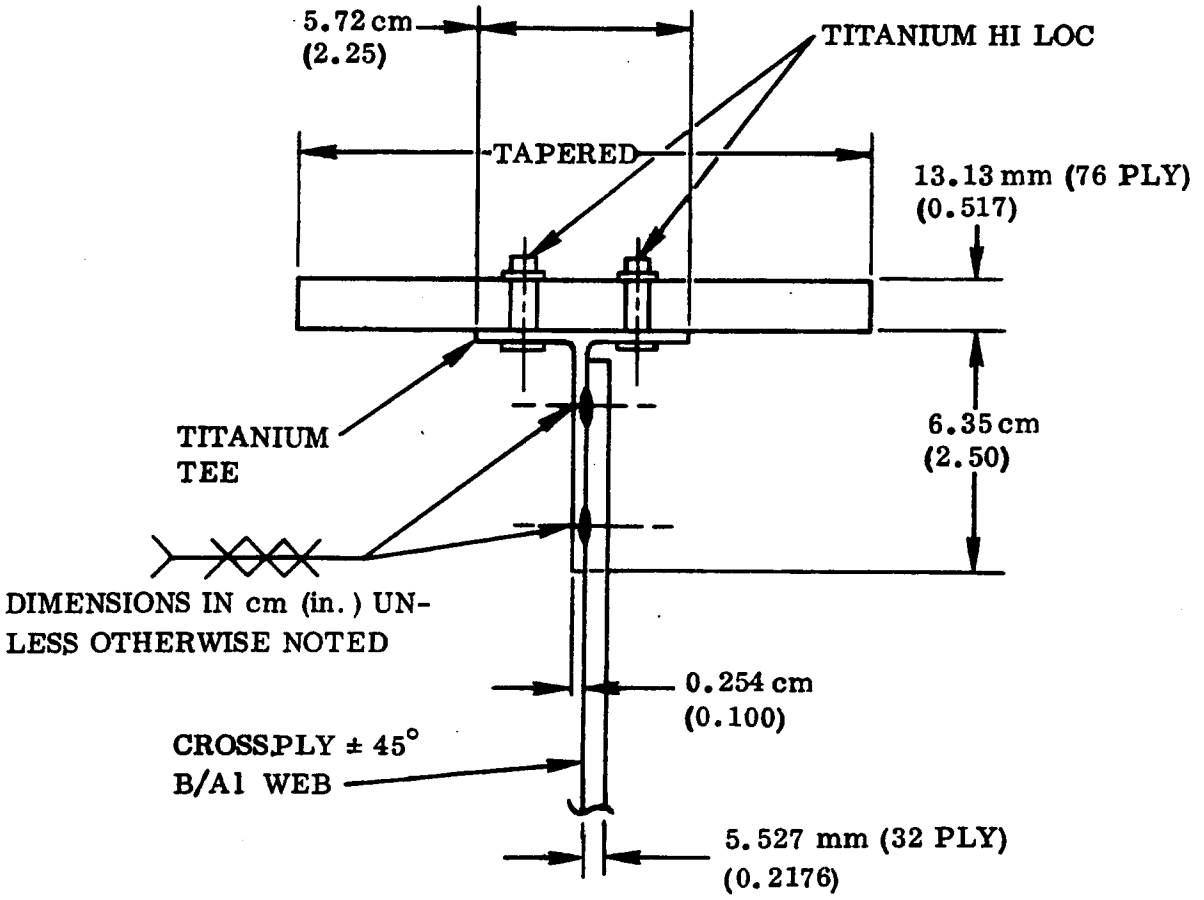

Figure 2-49. Shear Web Beam Compression Cap Cross-Section (Alternate Joint)

specimen was cycled 100 times from 77K (-320F) to 366K (200F) prior to testing. The fixture was loaded in tension as shown in Figure 2-50, and the test results are shown in Table 2-9.

Rosette strain gage readings were taken at locations shown in Figure 2-51, and corresponding plots of strains versus applied load for Test SSC 71-462-9C are shown in Figure 2-52.

The shear flows at the strain gage locations (A, B, C) are determined in Table 2-10. Since there are virtually no axial strains (Gages 2, 5, 8), the shear strain is found by the relation

$$\gamma = \epsilon_{tension} - \epsilon_{compression}$$

and, consequently, the shear flow is equal to

$$q = Gt\gamma$$

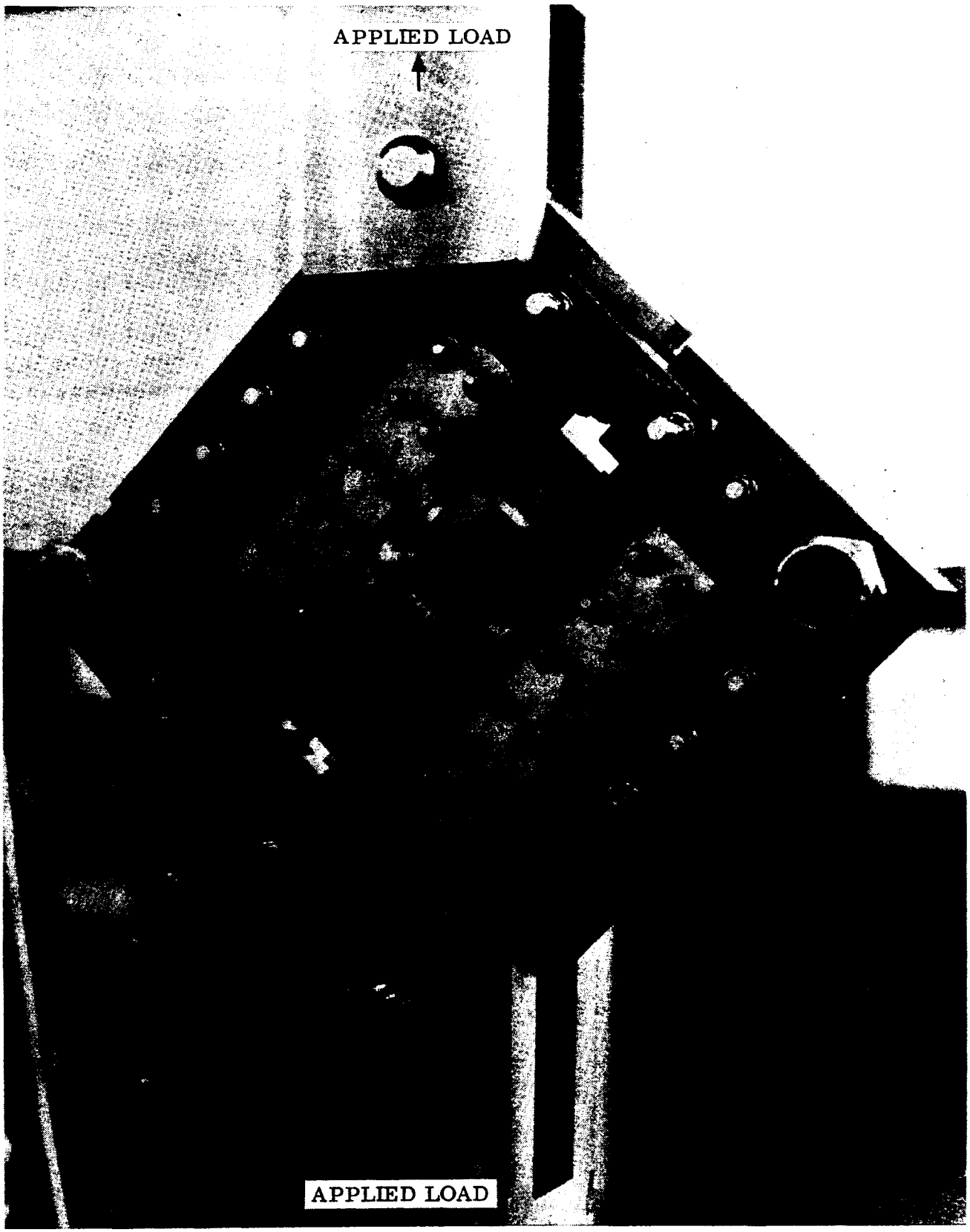

Figure 2-50. Picture Frame Shear Test — Tension (121589B) (Load applied as shown.)

Table 2-9. Spotjoined Material Test Results

Part Number	$t_{B/Al}$ cm (in.)	t_{Ti} cm (in.)	P N (lb)	q_{avg} N/cm (lb/in)	Thermally Cycled 100 Times Before Testing
SSC71-462-9A	0.467 (0.184)	0.272 (0.107)	114,319 (25,700)	4,972 (2,839)	No
SSC71-462-9B	0.467 (0.184)	0.272 (0.107)	126,996 (28,550)	5,523 (3,154)	Yes
SSC71-462-9C	0.467 (0.184)	0.272 (0.107)	151,239 (34,000)	6,578 (3,756)	No

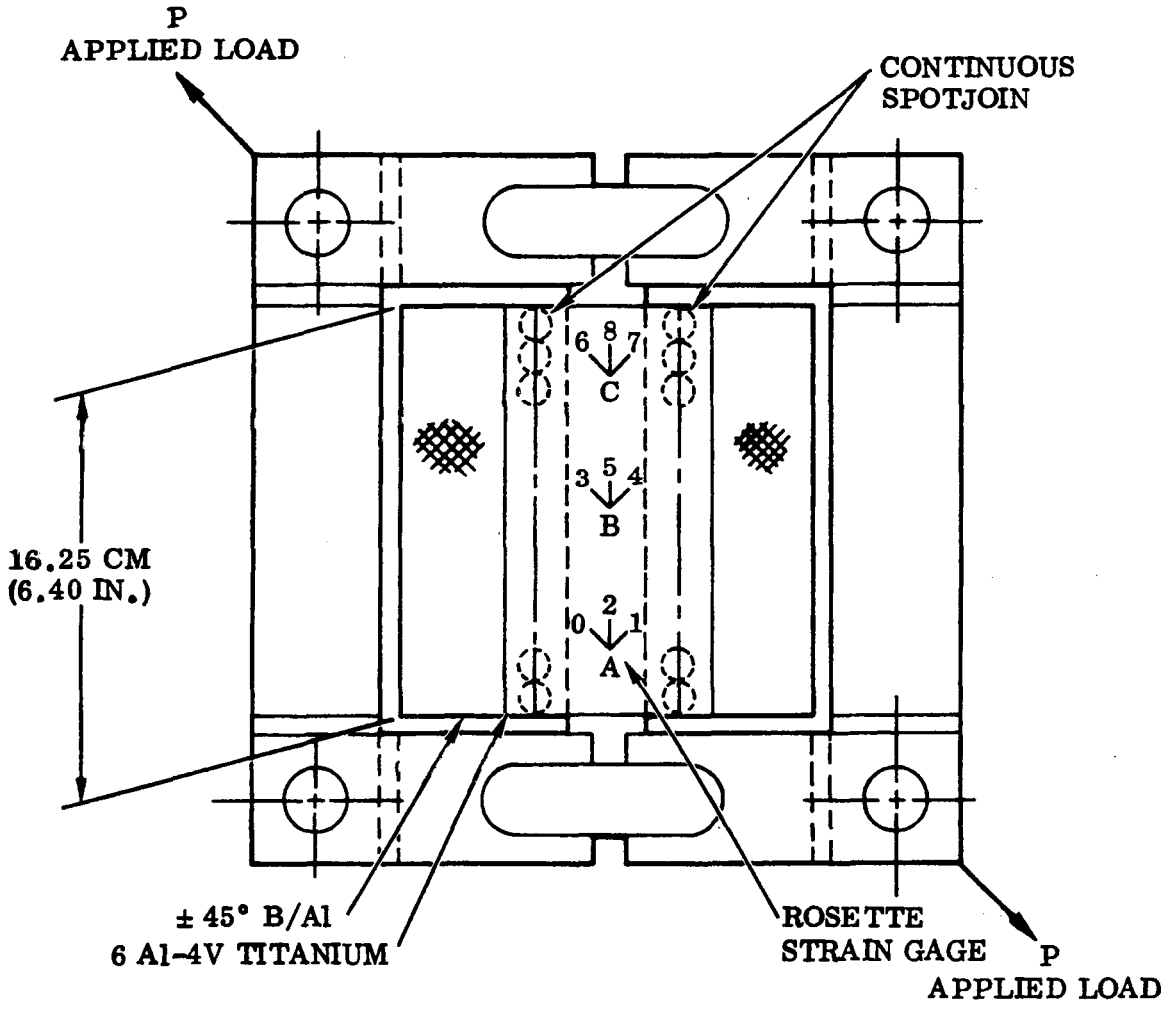

Figure 2-51. Rosette Strain Gages on Spotjoined Shear Test

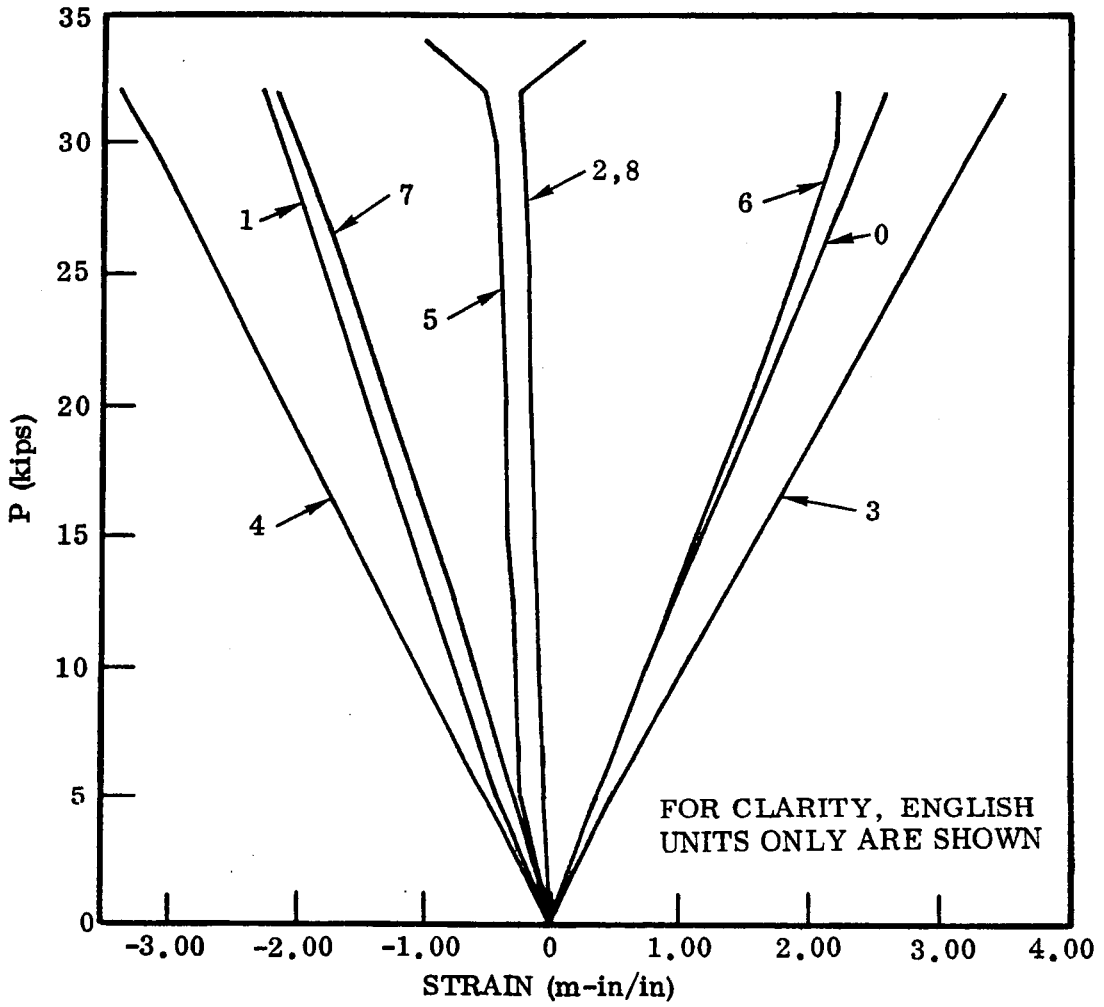

Figure 2-52. Load/Strain Curves for Test SSC71-462-9C

Table 2-10. Shear Flows at Strain Gage Locations

Test	Rosette	Compr Strain Gages 1, 4, or 7 cm/cm	Tensile Strain Gages 0, 3, or 6 cm/cm	γ Shear Strain radians	q Shear Flow N/cm(lb/in)	q_{avg} Shear Flow N/cm(lb/in)
SSCT1-462-9A	A	-0.00158	0.00141	0.00299	3474(1984)	
	B	-0.00285	0.00274	0.00559	6493(3708)	4488(2563)
	C	-0.00122	0.00179	0.00301	3497(1997)	
SSC71-462-9B	A	-0.00196	0.00220	0.00416	4833(2760)	
	B	-0.00314	0.00318	0.00632	7343(4193)	5348(3054)
	C	-0.00175	0.00158	0.00333	3868(2209)	
SSC71-462-9C	A	-0.00225	0.00263	0.00488	2232(3237)	
	B	-0.00336	0.00350	0.00686	3137(4550)	6250(3569)
	C	-0.00218	0.00222	0.00440	2013(2919)	

Since the rosette strain gages are located on the annealed 6Al-4V titanium sheet, the following corresponding properties were used:

$$G = 4.27 \text{ MN/cm}^2 \ (6.2 \times 10^6 \text{ psi})$$

$$t = 0.272 \text{ cm } (0.107 \text{ in.})$$

The average shear flow corresponding to the three rosette strain gage locations shown in Table 2-10 are in good agreement with those found by the use of external load and specimen geometry in Table 2-9. The maximum shear flows obtained in these tests exceeds those required in the shear beam, which are about 5250 N/cm (3000 lb/in) in the central region of the beam. Two rows of spotjoining are required in the outer regions of the shear beam where the maximum shear flow is about 10,500 N/cm (6000 lb/in). It is evident from the test results reported here that spotjoining has excellent potential.

2.6.4 B/Al TENSION FIELD PANEL. Two tension field test specimens utilizing ±45° and +45° STA B/Al were designed in conjunction with the corresponding "picture frame" test fixture. The shear frame technique (Reference 9) was modeled after the configurations successfully tested in graphite/epoxy by Convair/Fort Worth. One assembly includes the test specimen that tests a 0.254 cm (0.100 in.) thick ±45° crossply B/Al shear web for tension field strength. The other assembly includes a 0.152 cm (0.060 in.) thick unidirectional B/Al shear web for tension field testing. The two stiffener assemblies were fabricated from unidirectional B/Al. They were positioned to isolate the tension field panel from the fixture. They were sized to provide simple support to the panel and withstand secondary compressive loads. Both panels have an approximate aspect ratio of 2:1. Shear tabs were welded to the frame fittings and bolted to the webs of the stiffeners at each end. These tabs were intended for stiffener web shear load support and were found to be necessary during the Convair/Fort Worth shear frame test program.

Features incorporated in the fixture to reduce the local stress concentration were:

a. The corners of the test specimens were scarfed off sufficiently to prevent load introduction to the panel directly from the corner loading pin. Finite element analysis indicated that a 50 to 60% stress buildup occurs if the panel is loaded at the corner.

b. A series of titanium doublers was adhesively bonded to both faces of the B/Al test specimens. These doublers were varied in area coverage to provide a gradual transition in load carrying capability between the relatively massive steel frame and the test specimen web.

c. The cross-sectional area of the shear frame was sculptured to reduce the frame load carrying capability at the corners away from the load application. Stress concentration must be avoided in a shear frame test fixture at these corners.

Ideally, the applied tension loads impose pure shear upon the test specimen and the ±45° crossply is then capable of going into tension field after shear buckling occurs. However, the +45° B/Al must be oriented so that tension occurs in the fibers, and tension field can occur at the outset if required. These measures to ensure quality testing were successful since structural integrity was maintained at the corners, and web failure occurred within the isolated panel area; the +45° test specimen exceeded expectations. Rosette strain readings were recorded at the locations shown in Figure 2-53 up to the failure load. The gage orientations are shown in Figure 2-54.

2.6.4.1 Analysis of ±45° B/Al Test. During the entire test (Figure 2-55) the gages in the B-direction remained virtually unchanged. Consequently, the specimen was essentially loaded in pure shear. The tension (C-direction) and the compression (A-direction) strains are shown plotted against external loads in Figure 2-56. It is interesting to note that all strains were linear up to a load of 333,615 N (75,000 lb). It is presumed that slippage or local yielding was precipitated at that point, whereby a tension failure developed across a bolt hole at 369,200 N (83,000 lb), (Figure 2-57). It appears that the stress concentration effect at the hole was decisive. The average strains in the A and C directions were:

$$\epsilon_{A_{avg}} = -0.0017$$

$$\epsilon_{C_{avg}} = 0.00185$$

Since the B strains are zero, the shearing strain was

$$\gamma_{avg} = (\epsilon_C - \epsilon_A)$$

$$= 0.00355$$

The web material is heat treated ± 45° B/Al with an elastic shear modulus of

$$G = 8.0 \times 10^6 \text{ N/cm}^2 \ (11.6 \times 10^6 \text{ psi})$$

and a web thickness of

$$t = 0.282 \text{ cm } (0.111 \text{ in.})$$

The average computed elastic shear stress was

$$\tau/\eta_s = \gamma G = 28{,}391 \text{ N/cm}^2 \ (41{,}180 \text{ psi})$$

The inelastic shear stress from Figure 2-34 was found to be

$$\tau = 25{,}509 \text{ N/cm}^2 \ (37{,}000 \text{ psi})$$

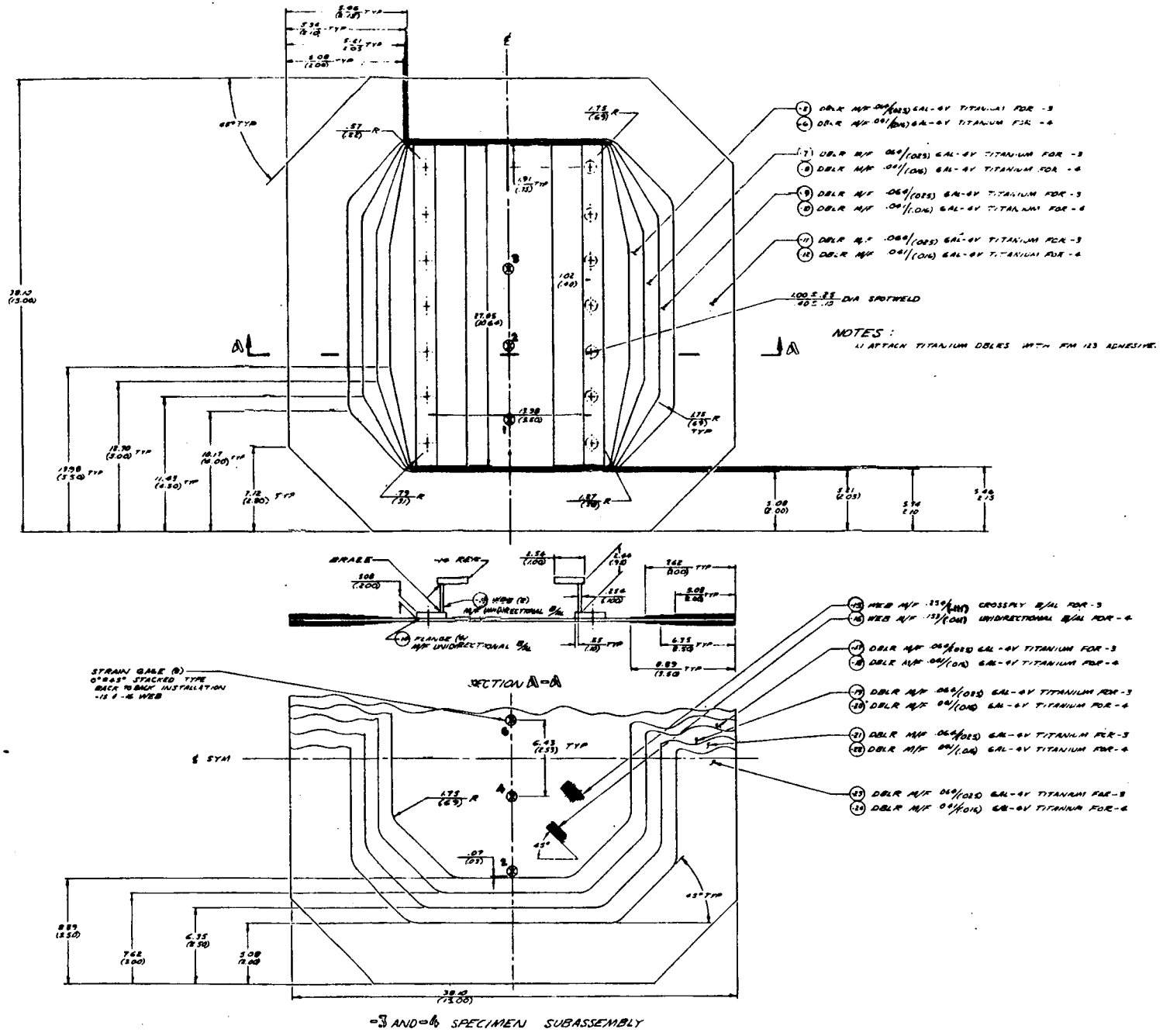

Figure 2-53. Crossply ±45° and +45° B/Al Tension Field Test Specimens

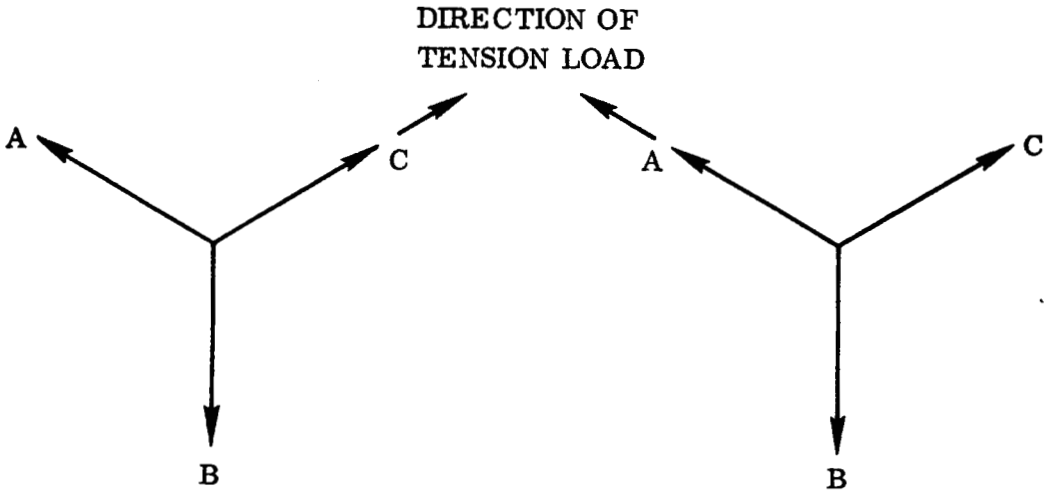

(a) ± 45° B/Al

(b) + 45° B/Al

Figure 2-54. Rosette Strain Gage Orientations in Test Specimens

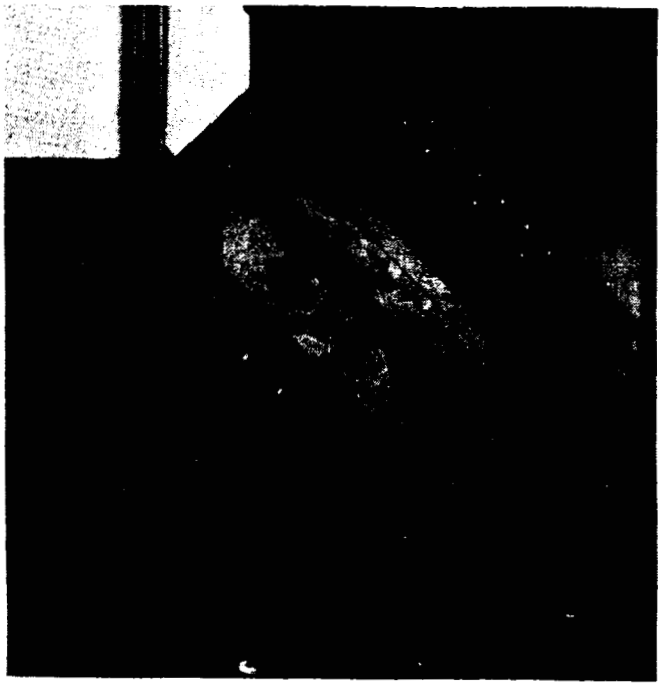

Figure 2-55. Tension Field Test in Progress (122589B)

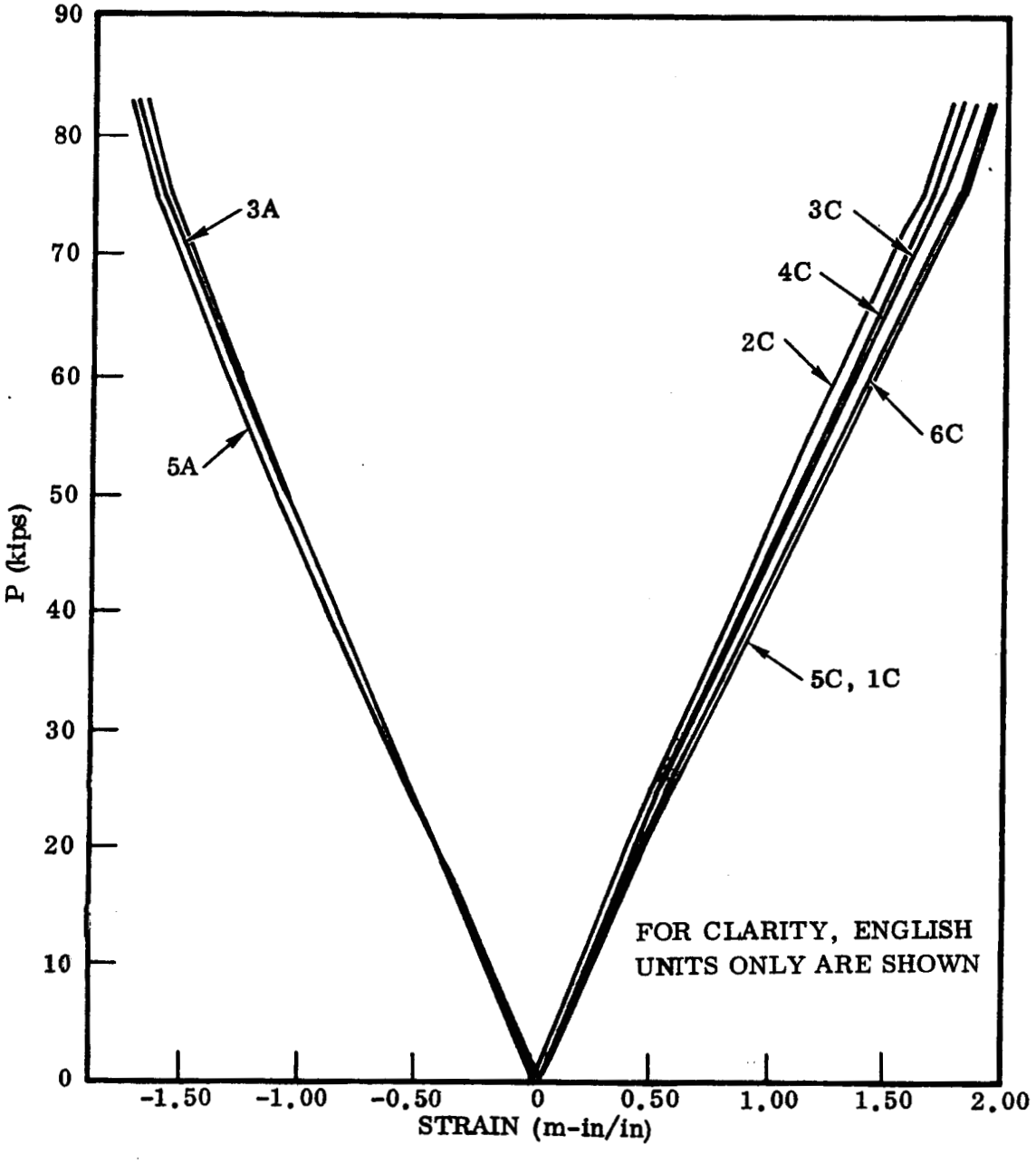

Figure 2-56. Strain Gage Readings Versus Applied Load for ±45° B/Al Tension Field Test

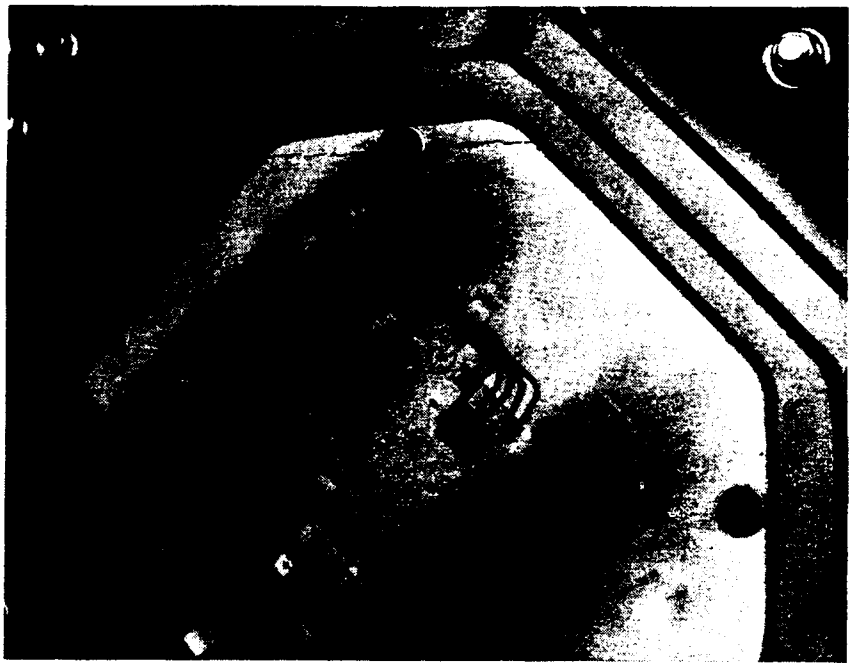

Figure 2-57. Tension Failure Across Bolt Hole (122588B)

The corresponding shear flow was

$$q = t\tau = 7192 \text{ N/cm } (4107 \text{ lb/in})$$

The average shear flow was also computed by use of the load P and the distance L between fittings, and was found to be

$$q = \frac{0.707P}{L} = \left(\frac{0.707 \times 83{,}000 \text{ lb}}{13 \text{ in.}}\right)$$

$$= 7907 \text{ N/cm } (4513 \text{ lb/in})$$

which is within reasonable agreement with that found by use of the strain gages. Theoretical buckling of the panel in shear is governed by Equation 12 or 13 in Reference 8, where inelastic solutions to these equations are plotted in Figures 3-25 through 3-29. Accordingly, from Figure 3-25 (Reference 8), with η_x and η_y equal to 1 and t = (0.111 in.)

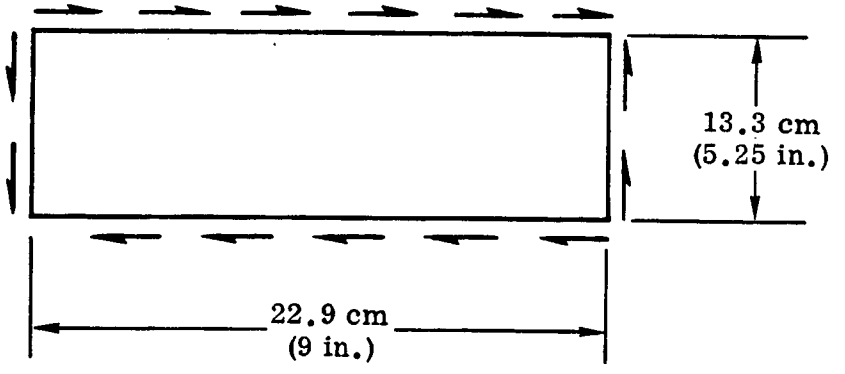

$$a^2 \tau_{cr}/\eta_s = 1.43 \times 10^6 \text{ lb}$$

$$\tau_{cr}/\eta_s = \frac{1.43 \times 10^6}{5.25^2}$$

$$= 35{,}714 \text{ N/cm}^2 \text{ (51,800 psi)}$$

The inelastic shear buckling stress (Figure 2-34) becomes

$$\tau_{cr} = 30{,}543 \text{ N/cm}^2 \text{ (44,300 psi)}$$

It is evident from the analysis that failure of the specimen was not in any way due to buckling of the panel, and that stress concentrations at the holes were the principal cause of failure.

2.6.4.2 Analysis of +45° B/Al Test. This test specimen buckled and then went considerably into tension field before failure occurred. The initial visible buckle, occurring at P = 186,824N (42,000 lb), can be seen in Figure 2-58. The ultimate tension field failure took place at P = 317,601N (71,400 lb) and is shown in Figures 2-59 and 2-60. The strain readings were not usable for P > 155,687N (35,000 lb). Up to the point of initial buckling, the gages in the B-direction remained virtually unchanged. Consequently, the specimen was essentailly loaded in pure shear, similar to the ±45° test.

The average shear flow may be calculated by use of the load P and distance L between fittings.

$$q = \frac{0.707P}{L}$$

$$L = 33 \text{ cm (13 in.)}$$

and the shear stress by

$$\tau = q/t$$

$$t = 0.155 \text{ cm (0.061 in.)}$$

2.6.4.3 Initial Visible Buckling

$$P = 186{,}824\text{N (42,000 lb)}$$

$$q = 4000 \text{ N/cm (2284 lb/in)}$$

$$\tau = 166{,}554 \text{ N/cm}^2 \text{ (37,443 psi)}$$

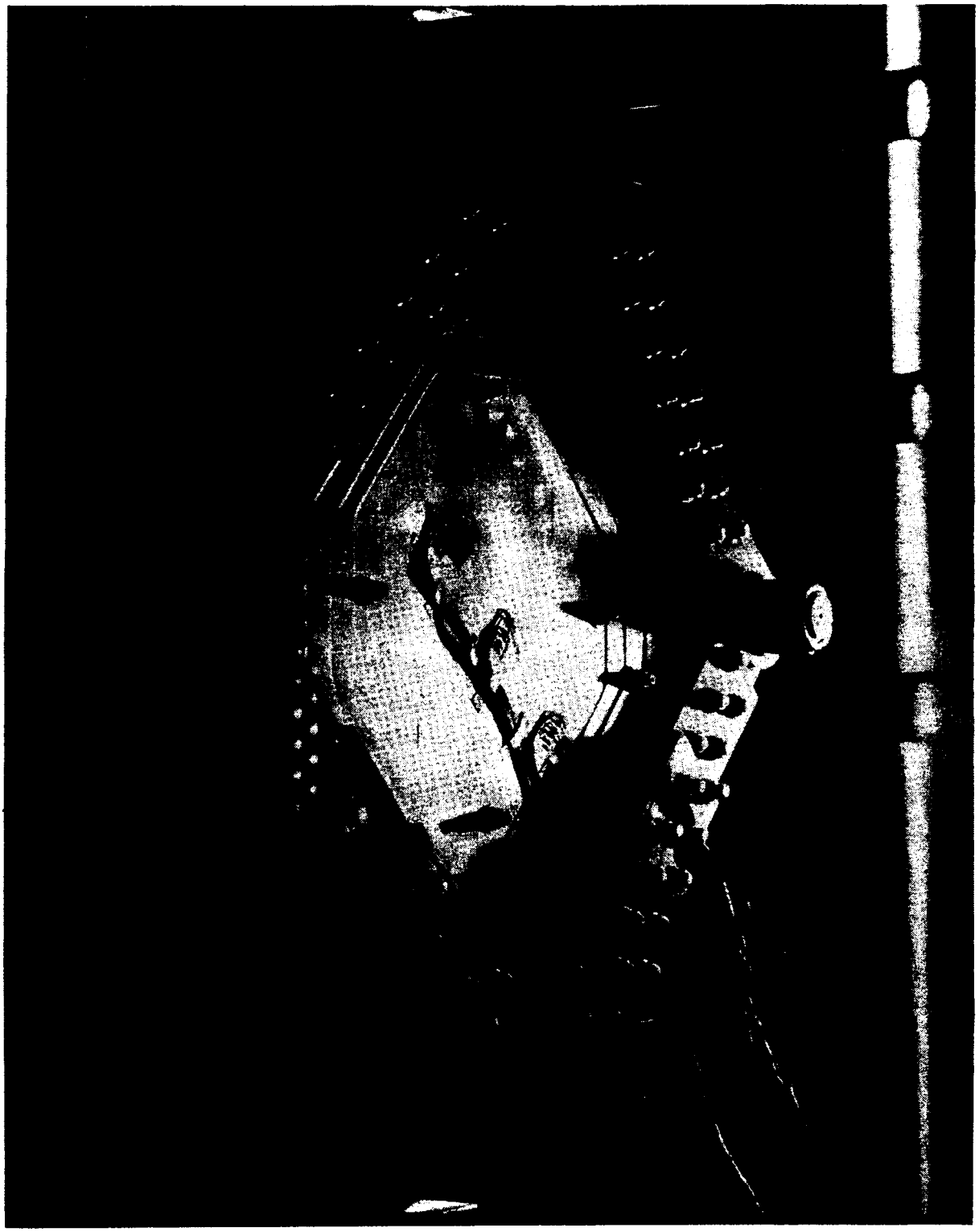

Figure 2-58. +45° B/Al Shear Test with Initial Buckle Visible (122760B)

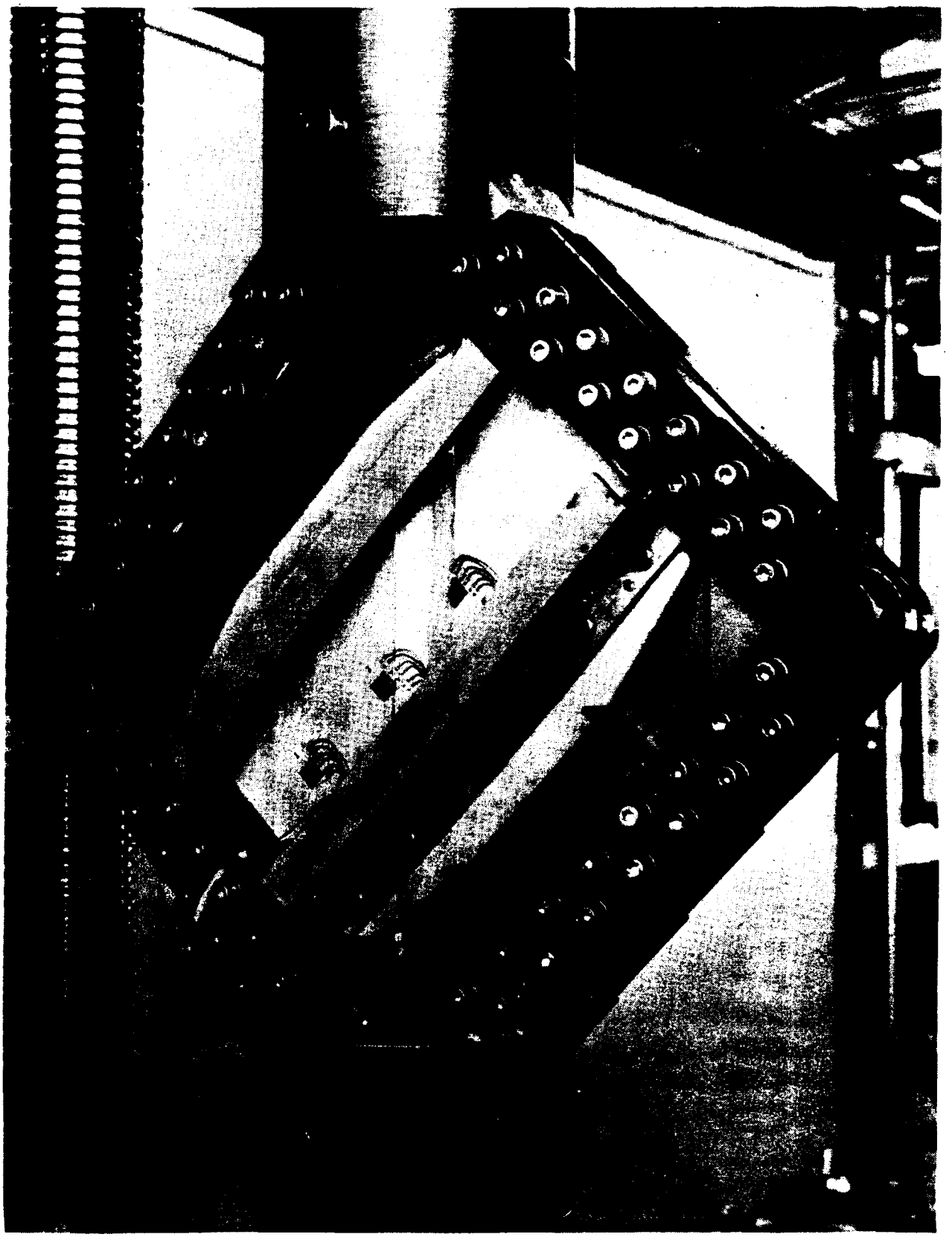

Figure 2-59. +45° B/Al Tension Field Failure (Front) (122761B)

Figure 2-60. +45° B/Al Tension Field Failure (Back) (122762B)

2.6.4.4 Tension Field Failure

$P = 317,601N$ (71,400 lb)

$q = 6800$ N/cm (3883 lb/in)

$\tau = 43,888$ N/cm^2 (63,656 psi)

Unlike the ±45° B/Al test, the stress concentrations at the holes appear to have little effect on the ultimate strength. Transverse flexure due to the deep buckle seemed to be the cause of initial fracture. Then secondary tensile failures occurred with cracks developing at the bolt holes as shown in Figure 2-60. Gage 3 had the least strain in the B-direction. Consequently, the readings of this gage, shown in Figure 2-61, are used in the determination of the shear modulus G. The shear stress and strain at P = 133,446N (30,000 lb) were used to determine G. The axial strains in the A- and C-directions are

$$\epsilon_A = 0.00096$$

$$\epsilon_C = -0.00093$$

and the shearing strain was

$$\gamma = \epsilon_A - \epsilon_C$$

$$= 0.00189$$

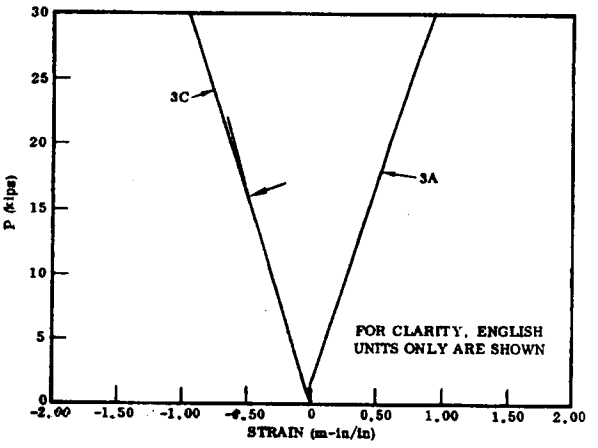

Figure 2-61. Strain Gage Readings 3A and 3C Versus Applied Load for +45° B/Al Tension Field Test

The shear stress is equal to

$$\tau = \frac{0.707P}{Lt}$$

$$= 18,443 \text{ N/cm}^2 \text{ (26,750 psi)}$$

and the shear modulus is

$$G = \tau/\gamma$$

$$= 9.75 \times 10^6 \text{ N/cm}^2 \text{ (14.15} \times 10^6 \text{ psi)}$$

From earlier testing of +45° B/Al material, the modulus of elasticity was found to average

$$E = 13.1 \times 10^6 \text{ N/cm}^2 \text{ (19} \times 10^6 \text{ psi)}$$

By use of the material property data available above and assuming Poisson's ratios $\nu_{xy} = \nu_{yx} = 0.3$, the elastic shear buckling allowable may be calculated. Equations for this purpose have been programmed on a digital computer and the solution obtained for this panel is

$$F_{s_{cr}} = 10,307 \text{ N/cm}^2 \text{ (14,950 psi)}$$

The corresponding applied load is

$$P_{cr} = 74,596\text{N (16,770 lb)}$$

By referring to Figure 2-61, it can be seen that the P/strain curve deviates from linear (shown by the arrow) in the neighborhood of P_{cr}, which implies that the theoretical buckling load has been approximately verified by the test.

The degree of tension field is governed by the ratio of τ/τ_{cr}, which is

$$\tau/\tau_{cr} = 4.2$$

This value is comparable to the performance of ductile metals such as aluminum and titanium in tension field beams.

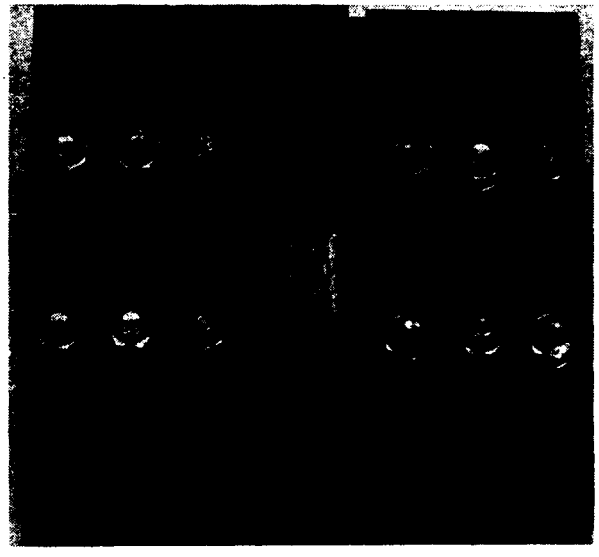

Figure 2-62. Iosipescu Shear Specimen in Fixture (119288B)

2.6.5 MATERIAL ALLOWABLES TEST. A test configuration was developed to measure the shear strength of the ±45° crossply heat-treated B/Al. This effort was initiated to establish realistic allowables for the shear beam design. The configuration developed (Figure 2-62) reflects the concepts outlined by Nicolae Iosipescu (Reference 9).

A total of four tests were run, and the average ultimate strength at failure was 345 MN/m^2 (50 ksi). A cursory examination of the fracture appearance indicated there was a mixed failure mode; however, it is felt that the 345 MN/m^2 strength may be taken as a minimum shear strength. The results of these test were used to establish the shear curve of Figure 2-34.

2.7 COMPONENT DESIGN AND ANALYSIS

The design of the shear beam component test article is shown in Figure 2-63. The test component, 0.96 by 1.0m (38 by 40 in.), is a representative segment of the full-scale mid-span portion of the thrust structure shear web beam. The component test specimen includes the following elements of the full-scale shear beam.

a. Crossply ±45° shear web 0.55 cm (0.217 in.) thick.

b. Tapered compression cap of unidirectional B/Al.

c. Vertical stiffeners of unidirectional B/Al.

d. Horizontal stiffener of unidirectional B/Al.

e. A typical web splice.

2.7.1 COMPONENT TEST SPECIMEN DESIGN. The test specimen is supported as a cantilever beam off of a test fixture designed and fabricated by NASA-MSFC. The framing members (all of which are 4340 steel except the compression cap) are pin connected at their intersections, thus minimizing secondary bending effects. The test specimen was designed for a 444.8 kN (100,000 lb) vertical force applied at the end of the cantilever beam. This is the equivalent of an average shear flow of 4540 N/cm (2600 lb/in) in the web. An 889.6 kN (200,000 lb) horizontal compression force is applied to the lower B/Al compression cap to simulate beam-cap loading. The beam cap was sized for a stress level of 620 MN/m^2 (90,000 psi). The load introduction fittings and beam attachment fittings were sized with a factor of safety of 1.4 on the applied load together with a safety factor of 2.0 on yield and 2.5 on ultimate.

The beam web was made of constant thickness ±45° B/Al, which differs from the full-scale beam that is tapered from the compression cap to the tension cap and has selectively placed 90° fibers in areas of high compressive stresses. The test article was not tapered for cost reasons; additional tooling would be required to provide the taper and no significant additional test data would be obtained.

The vertical stiffeners are on 12.7 cm (5 in.) spacings identical to the full-scale beam. They are, however, of constant section over the full length as opposed to the tapered stiffeners on the full-scale design. The stiffener section I is 68.720 cm^4 (1.651 in^4). The I required to enforce a nodal point in the panel is 45.161 cm^4 (1.085 in^4).

The horizontal stiffener was located 62.61 cm (24.65 in.) from the compression cap to provide an equivalent panel aspect ratio to that of the full-size beam. The cross-section is identical to the full-scale designs with a section I equal to 71.217 cm^4 (1.711 in^4).

The B/Al beam cap is 13.36 cm (5.25 in.) wide and tapered in thickness from 1.088 cm (0.428 in.) to 1.624 cm (0.639 in.) along its length to obtain the same stress levels as the full-scale design. The maximum stress in the full-scale design beam is 507 MN/m^2 (73,500 psi).

The assembly methods are identical to those used in the design of the full-scale beam. The compression beam cap consists of a unidirectional B/Al cap spliced to a 6Al-4V titanium tee with 0.635 cm (0.250 in.) diameter bolts. The titanium tee in turn is joined to the ±45° web with two rows of continuous spot joints. The web is provided with a typical splice joint, consisting of back-to-back 0.276 cm (0.1088 in.) 16 ply ±45° B/Al that was made integral with the vertical stiffener. The two web segments are spliced together with two rows of spotwelds.

All steel framing members, tension cap, load introduction fittings, and reaction fittings are assembled to the web with bolts.

The completed shear beam component is shown in Figure 2-64. A detailed description of the fabrication of the beam is presented in Volume II.

2.7.2 COMPONENT TEST SPECIMEN ANALYSIS. The component was modeled for the plane stress finite element computer program (P5543) to determine the internal loads. The model was laid out to provide output data that can be directly correlated with strain-gage test results (see Figure 2-65). Three loading sequences were used. They are:

a. Application of the 445 kN (100,000 lb) transverse load only.

b. Application of the 889.6 kN (200,000 lb) horizontal load only.

c. Application of the combined transverse and horizontal loads.

Plots of the stresses in the compression cap and corresponding web are shown in Figures 2-66, 2-67, and 2-68 for transverse, longitudinal and combined loadings.

Similar plots are shown in Figures 2-69 through 2-72 for the transverse post and corresponding web and web stresses at the fixed end of the beam. Horizontal and transverse beam deflections for the three loading cases are shown in Figure 2-73.

FOLDOUT FRAME

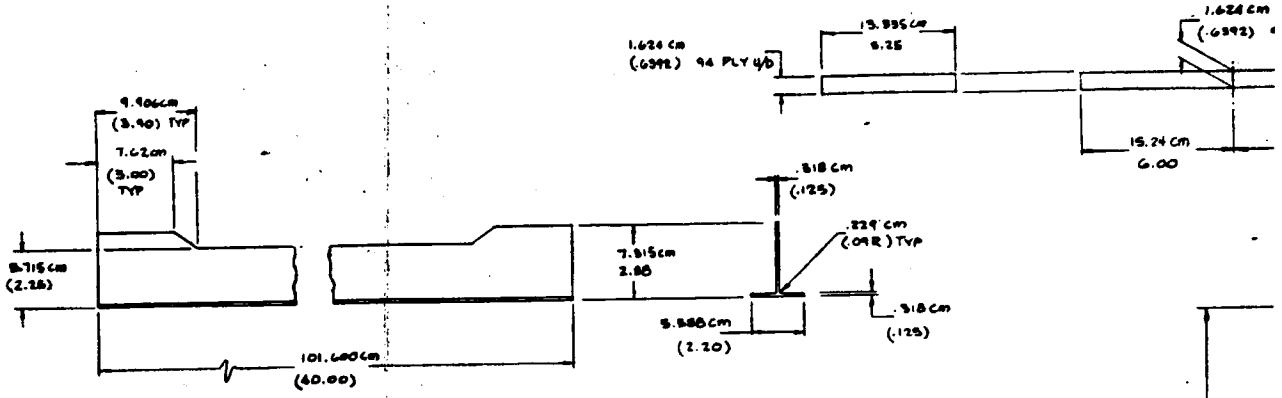

DETAIL -21 TEE

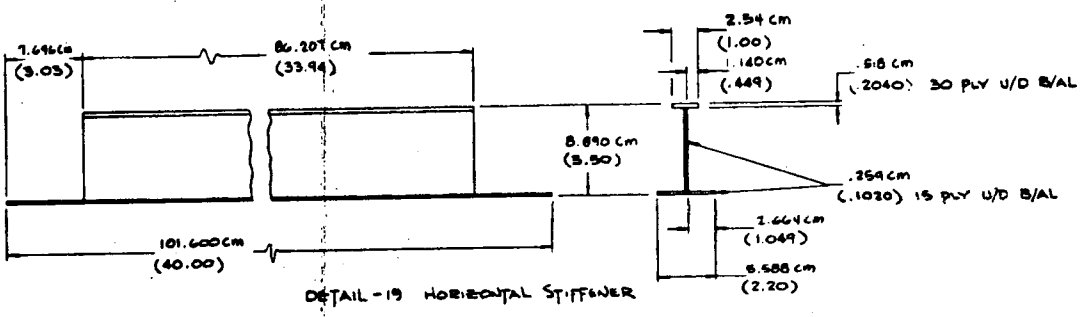

DETAIL -19 HORIZONTAL STIFFENER

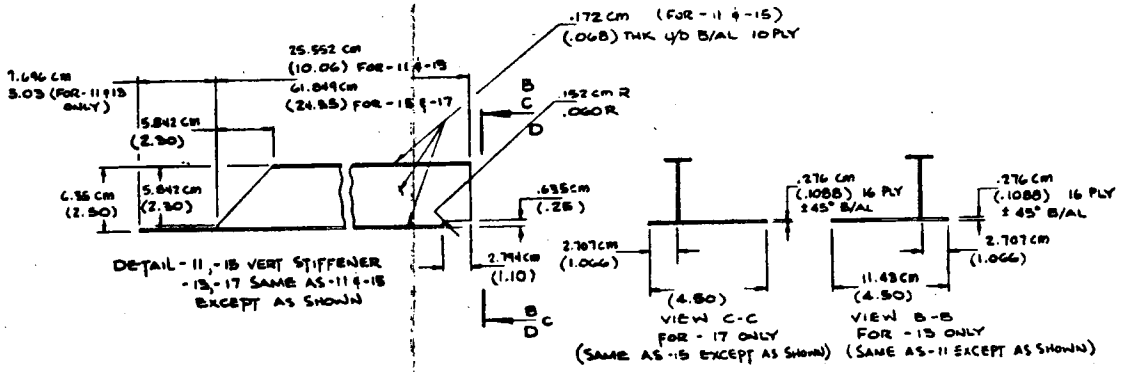

DETAIL -11, -15 VERT STIFFENER
-13, -17 SAME AS -11 & -15
EXCEPT AS SHOWN

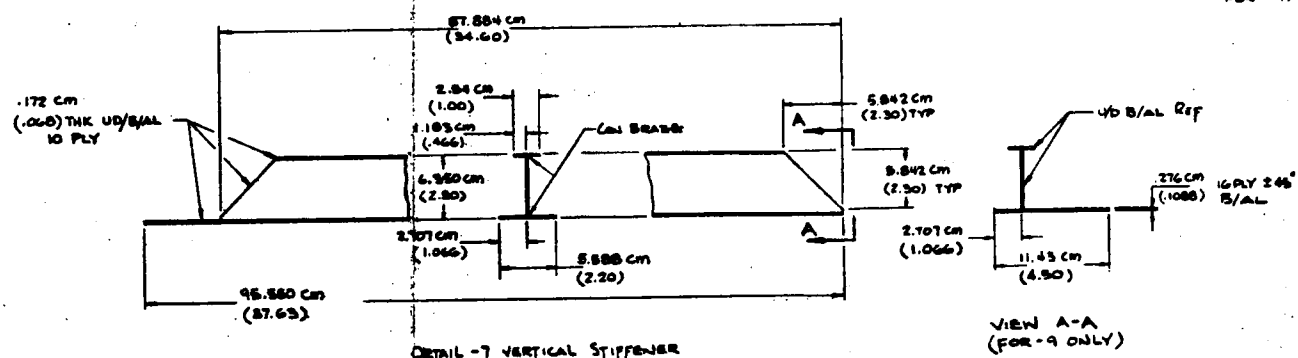

DETAIL -7 VERTICAL STIFFENER
DETAIL -9 VERTICAL STIFFENER (SAME AS -7 EXCEPT AS SHOWN IN VIEW A-A)

2-85/2-86 A

FOLDOUT FRAME 2

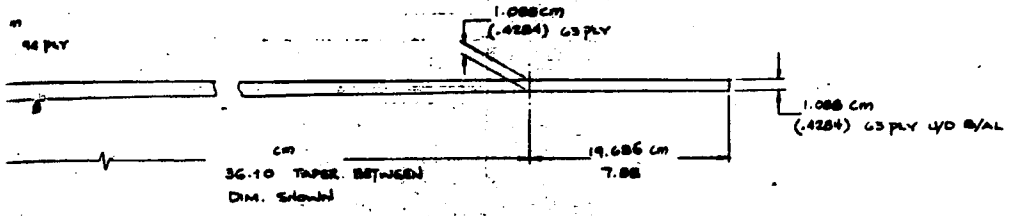

DETAIL - 27 BEAM CAP

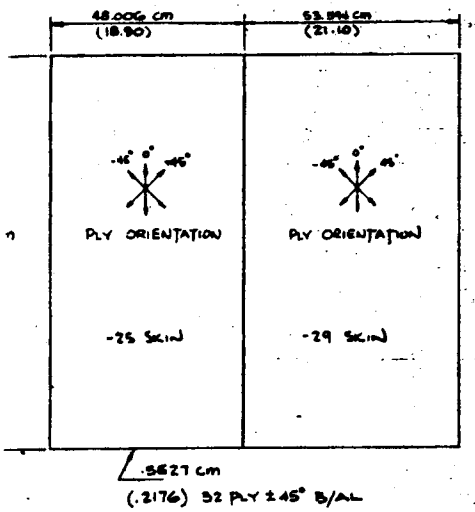

DETAIL - 25 SKIN
DETAIL - 29 SKIN

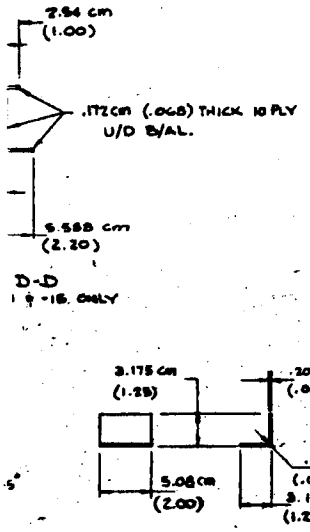

DETAIL - 23 CLIP

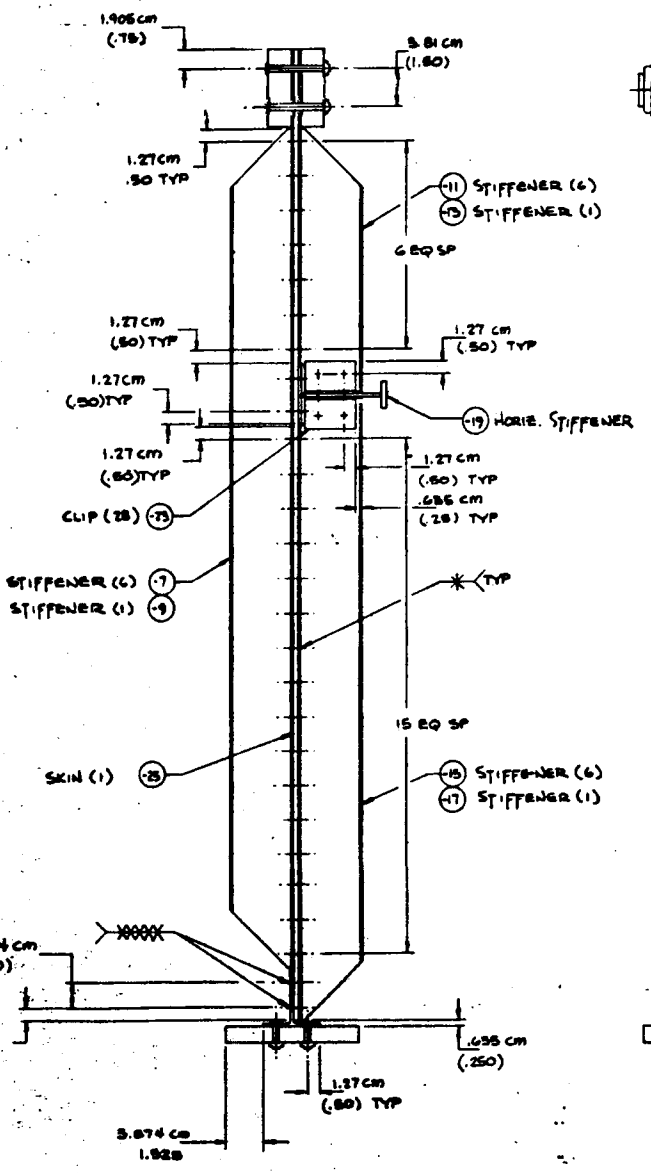

SECTION E-E

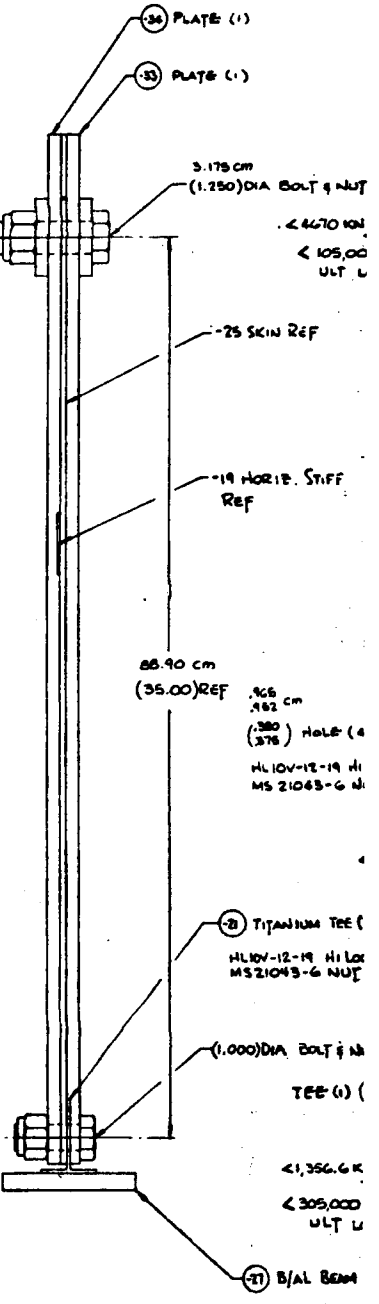

SECTION F-F

2-85 / 2-86 B

FOLDOUT FRAME 3

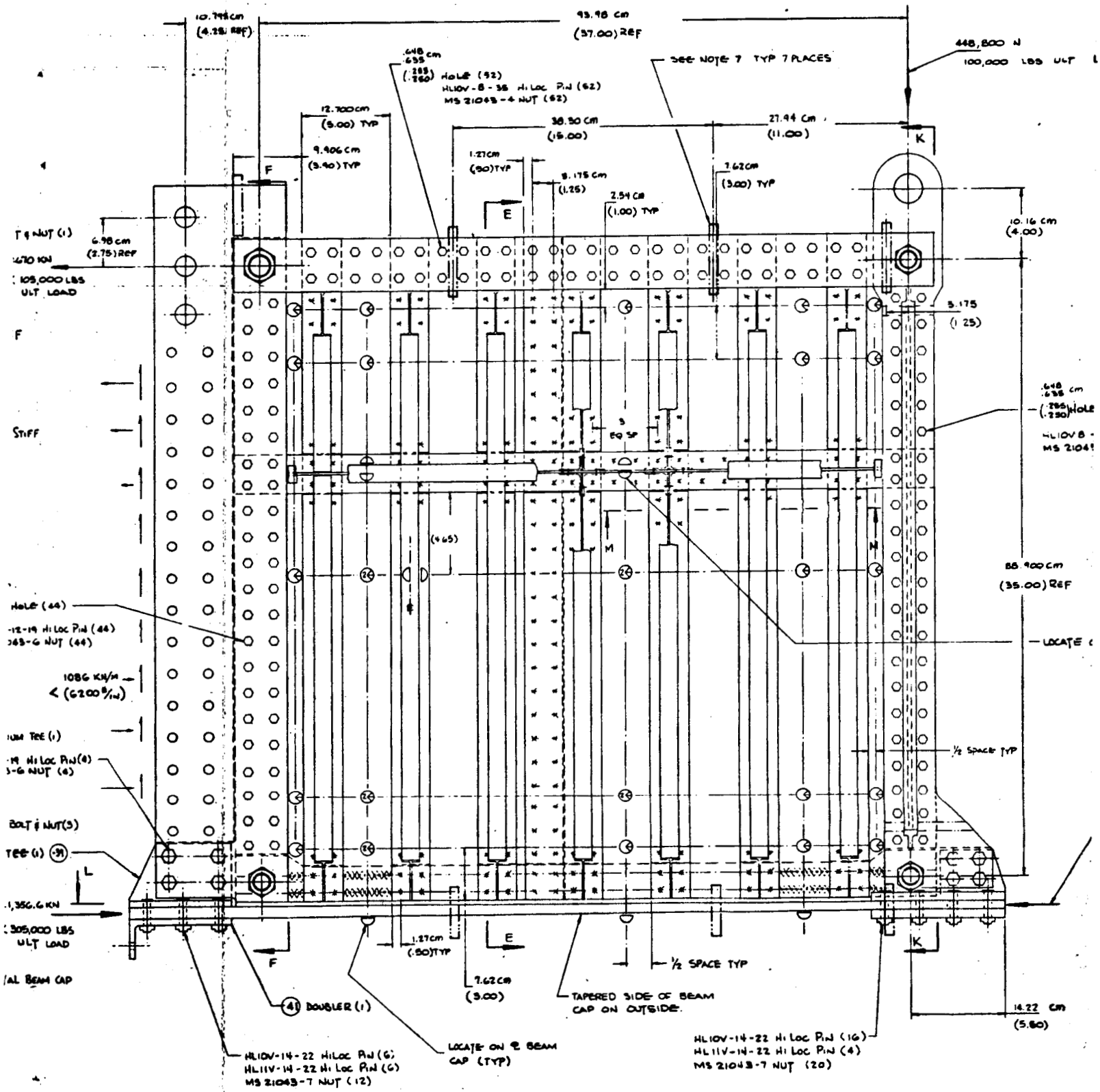

2-85 / 2-86 C

FOLDOUT FRAME 4

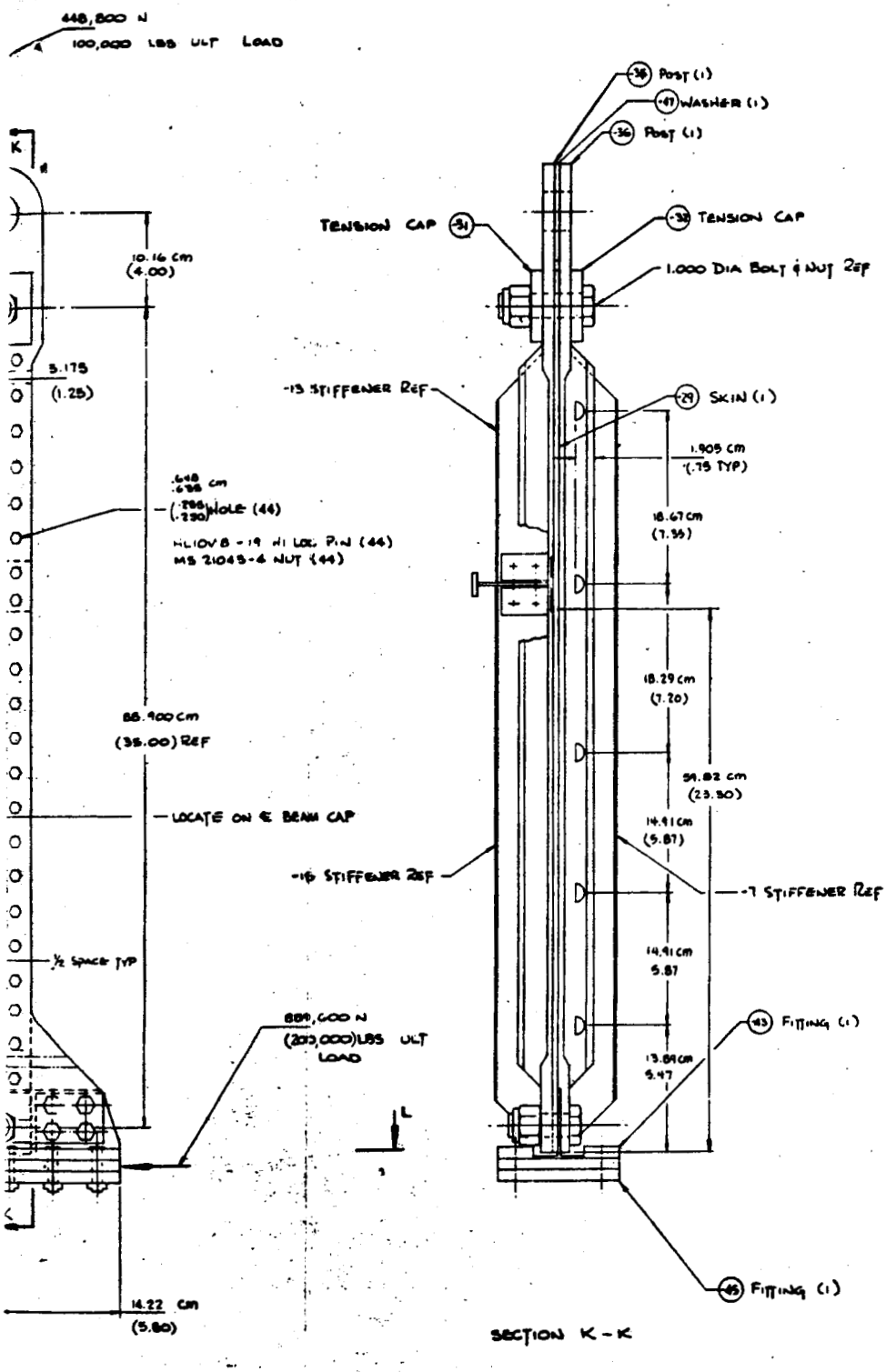

NOTES:

1. SYMBOL ⌓ DENOTES A SINGLE UNIAXIAL STRAIN GAGE
2. SYMBOL ⑳ DENOTES TWO ROSETTE STRAIN GAGES MOUNTED BACK TO BACK
3. SYMBOL ⊕ DENOTES A SINGLE ROSETTE STRAIN GAGE
4. LOADING SEQUENCE IS AS SPECIFIED BELOW:
   a. 4,448 KN (100,000 LBS) VERTICAL LOAD ONLY. RECORD STRAINS & REMOVE LOAD
   b. 8,896 KN (200,000 LBS) HORIZONTAL LOAD ONLY. RECORD STRAINS & REMOVE LOAD
   c. APPLY HORIZONTAL & VERTICAL LOAD IN A 2/1 RATIO TO FAILURE. RECORD STRAINS.
5. MEASURE VERTICAL DEFLECTION OF BEAM END FOR LOADING CONDITION 4a & 4c.
6. TOTAL QUANTITY OF STRAIN GAGES REQD: 7 UNIAXIAL & 18 ROSETTE STRAIN GAGES.
7. TEST RIG TO PROVIDE LATERAL RESTRAINT TO PREVENT TORSIONAL INSTABILITY. TYP(6) PLACES

Figure 2-63. B/Al Shear Beam Component Test Specimen

Figure 2-64. Frame Side of Completed B/Al Shear Beam Component and Test Fixture Assembly (129951B)

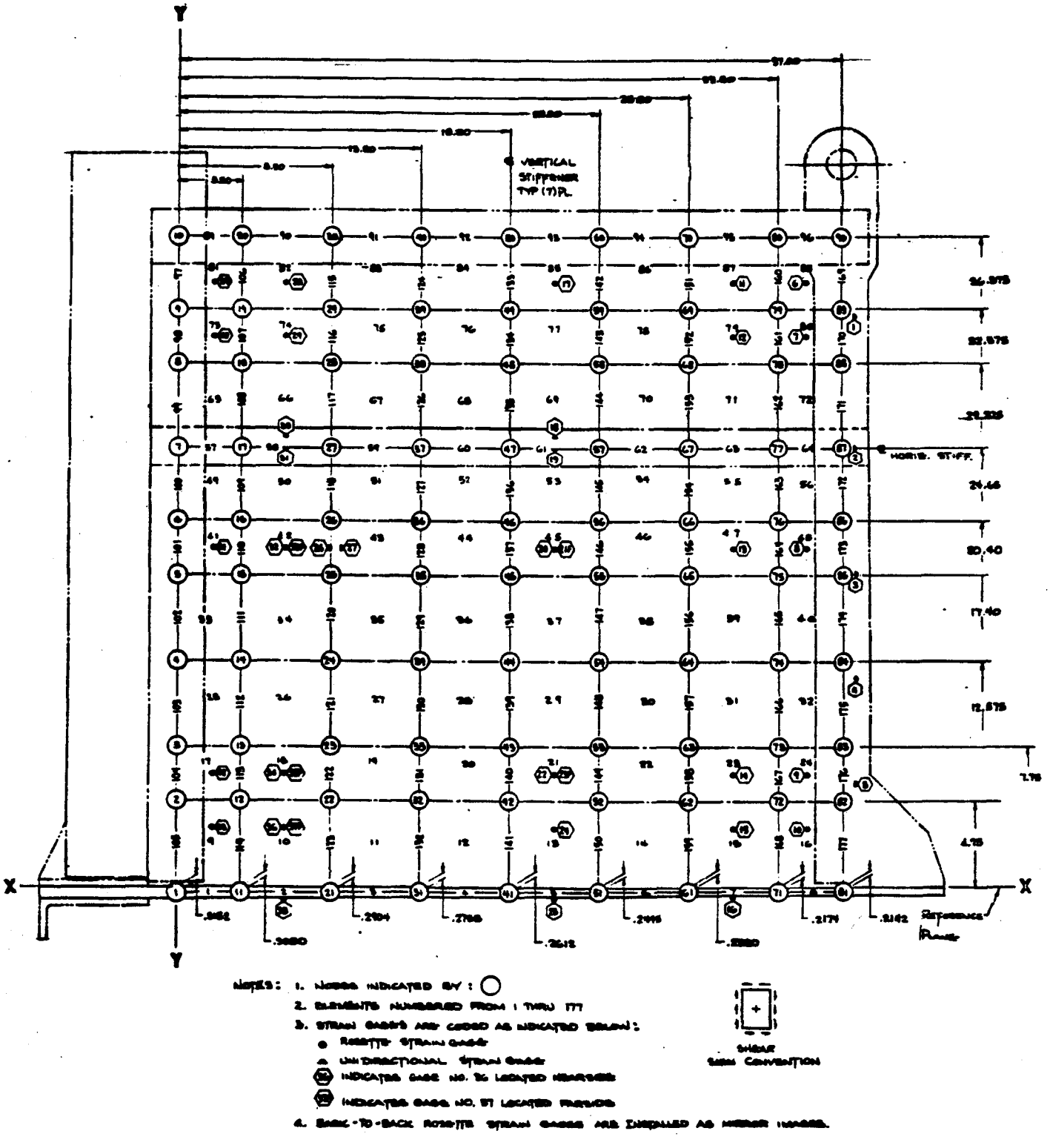

Figure 2-65. B/Al Shear Beam Computer Model Component Test Specimen

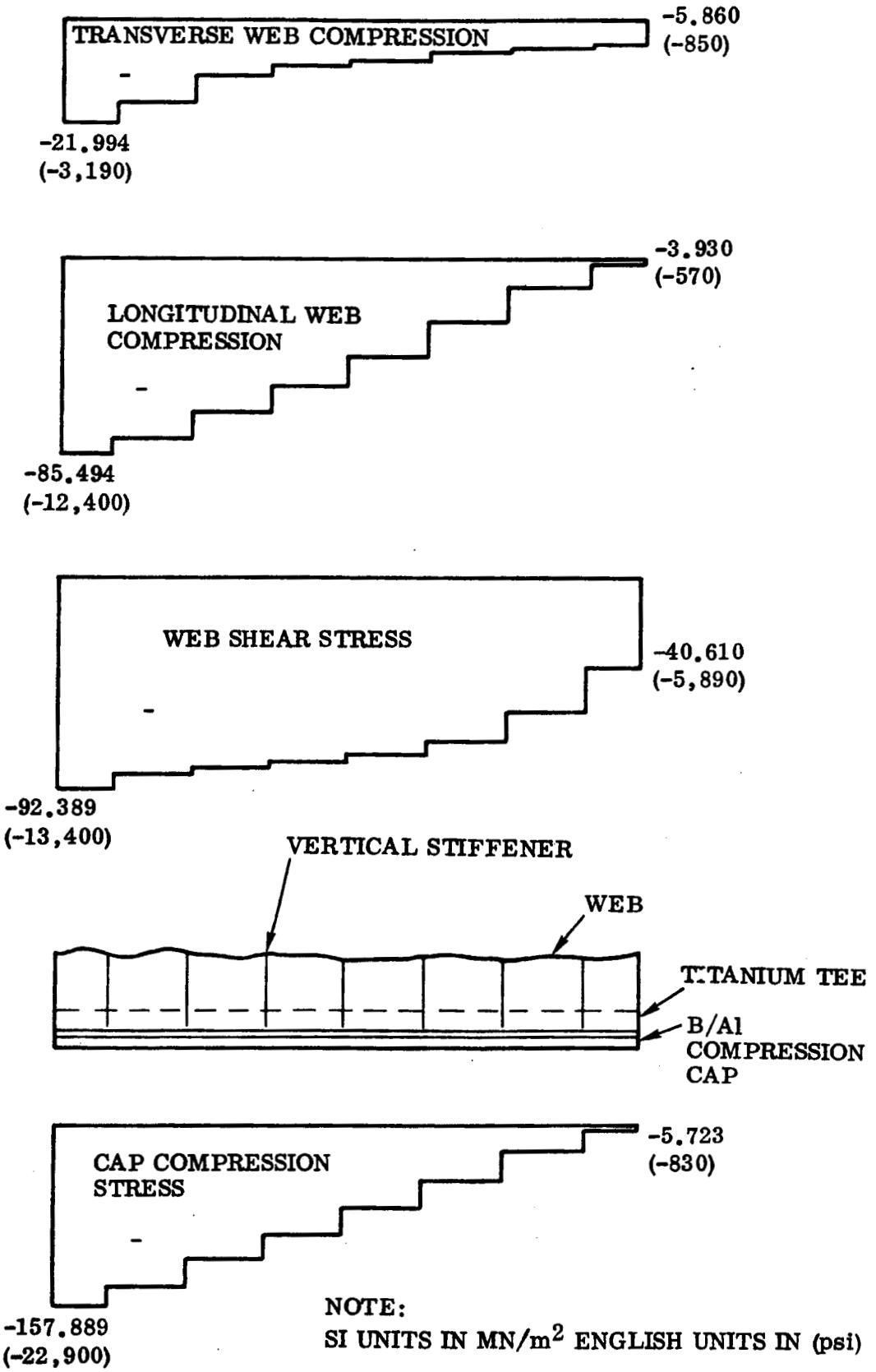

Figure 2-66. Stresses in Compression Cap and Corresponding Web — Transverse 689 MN (100 kips Only)

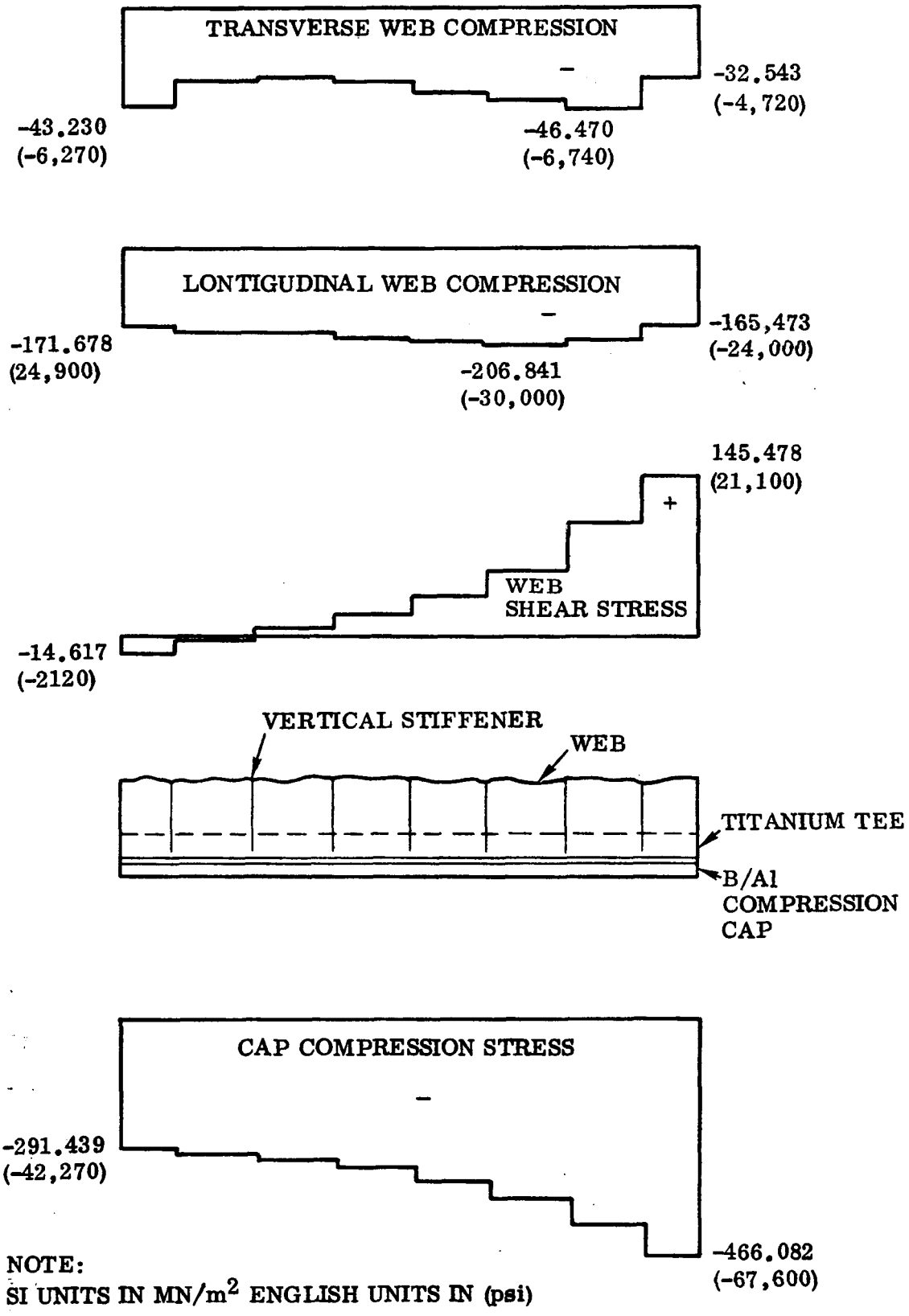

Figure 2-67. Stresses in Compression Cap and Corresponding Web — Longitudinal Load 1379 MN (200 kips)

NOTE:
SI UNITS IN MN/m^2 ENGLISH UNITS IN (psi)

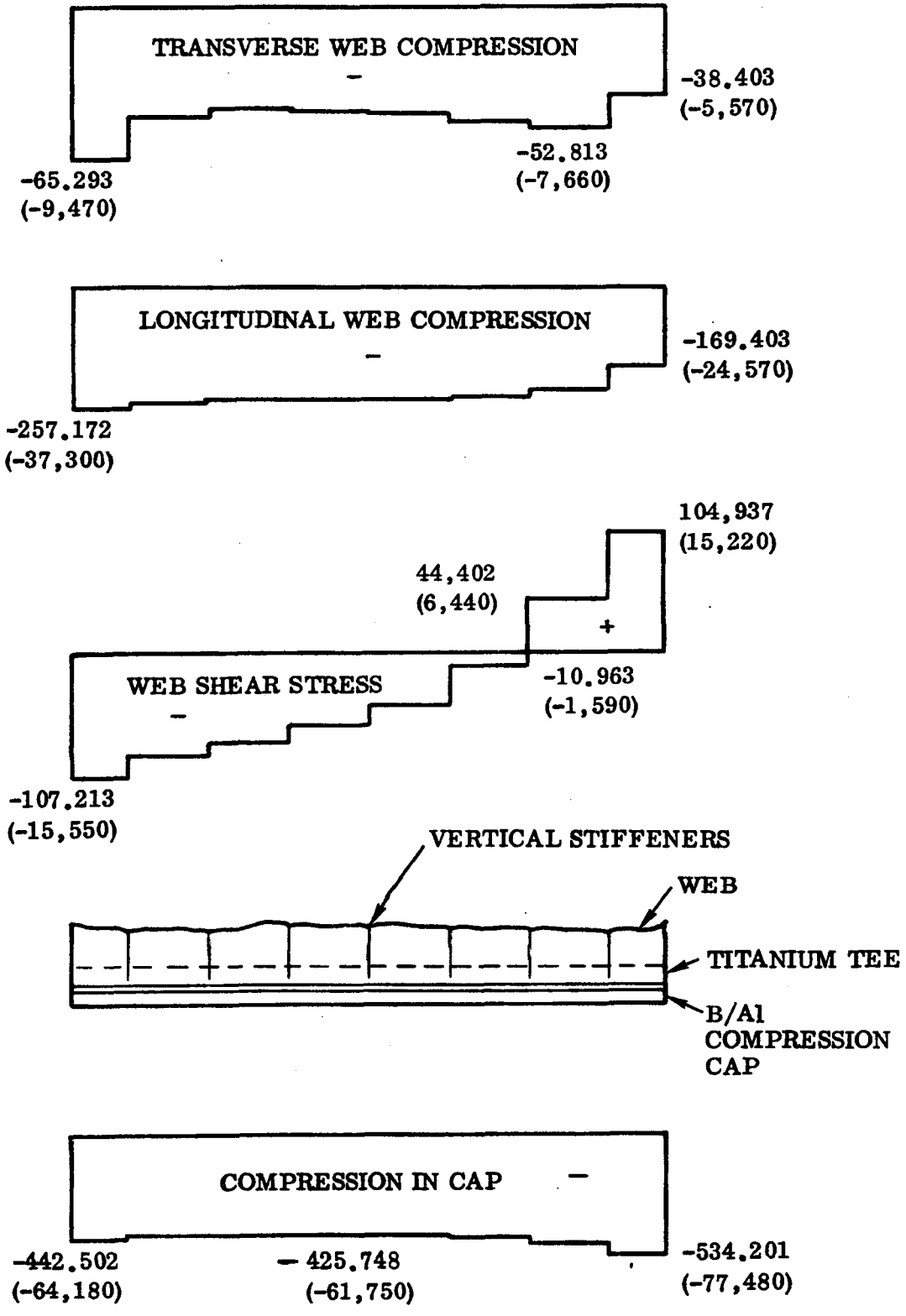

Figure 2-68. Stresses in Compression Cap and Corresponding Web — Combined Loading

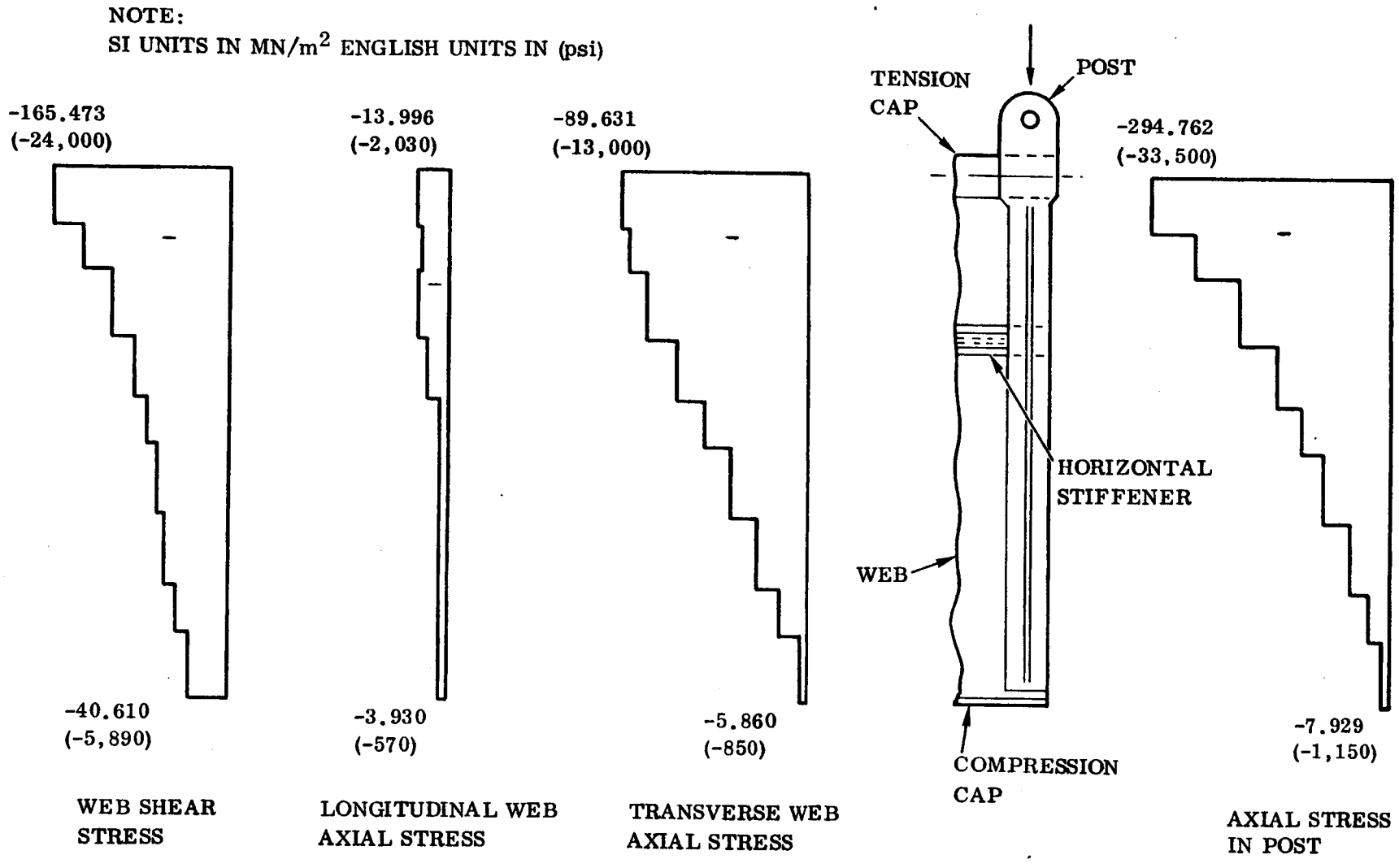

Figure 2-69. Stresses in Transverse Post and Corresponding Web —100 kips Transvers Load

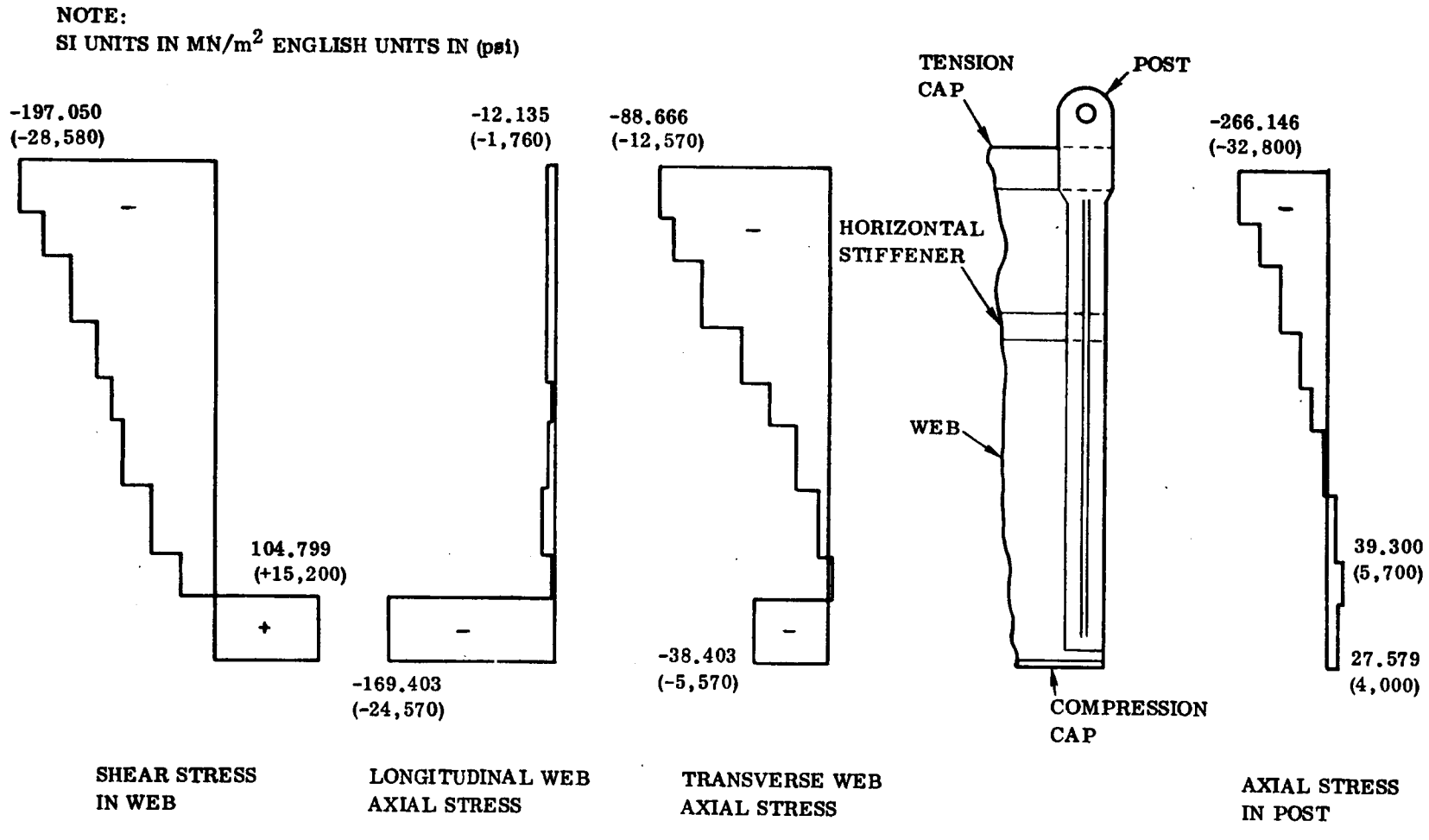

Figure 2-70. Stresses in Transverse Post and Corresponding Web — Combined Loading

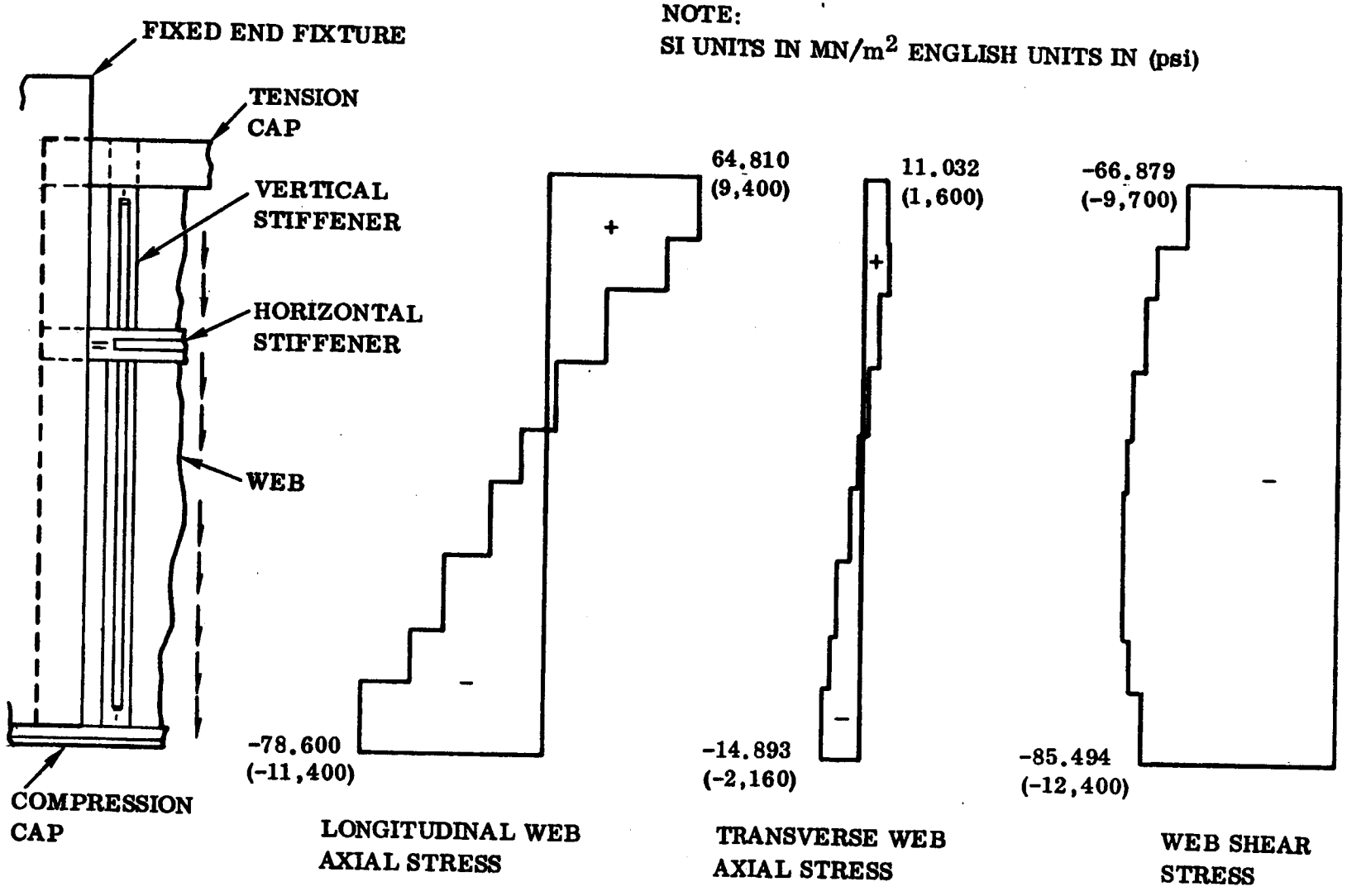

Figure 2-71. Stresses in Web at Fixed End of Beam — Transverse Loading 689 MN (100 kips Only)

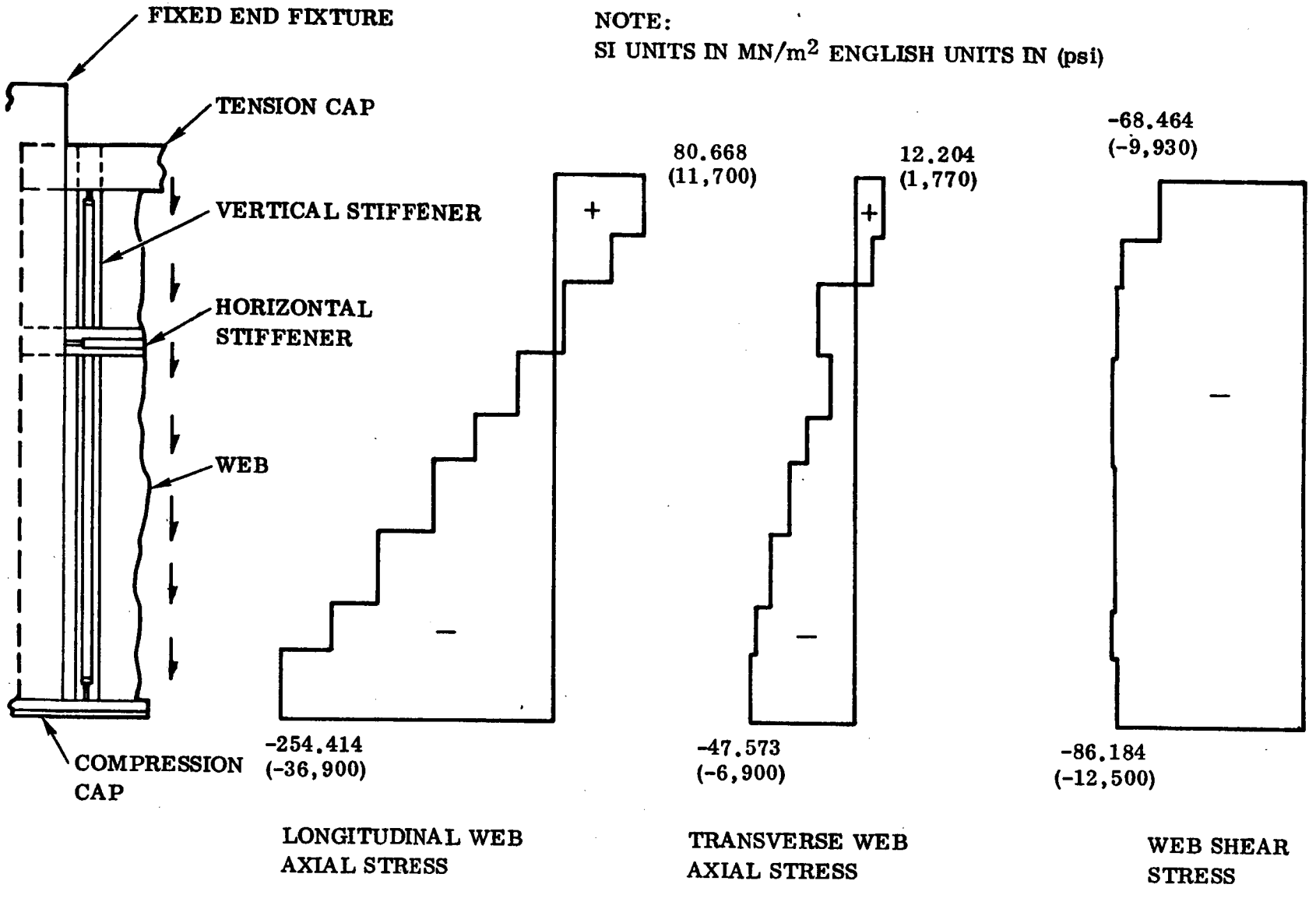

Figure 2-72. Stresses in Web at Fixed End of Beam — Combined Loading

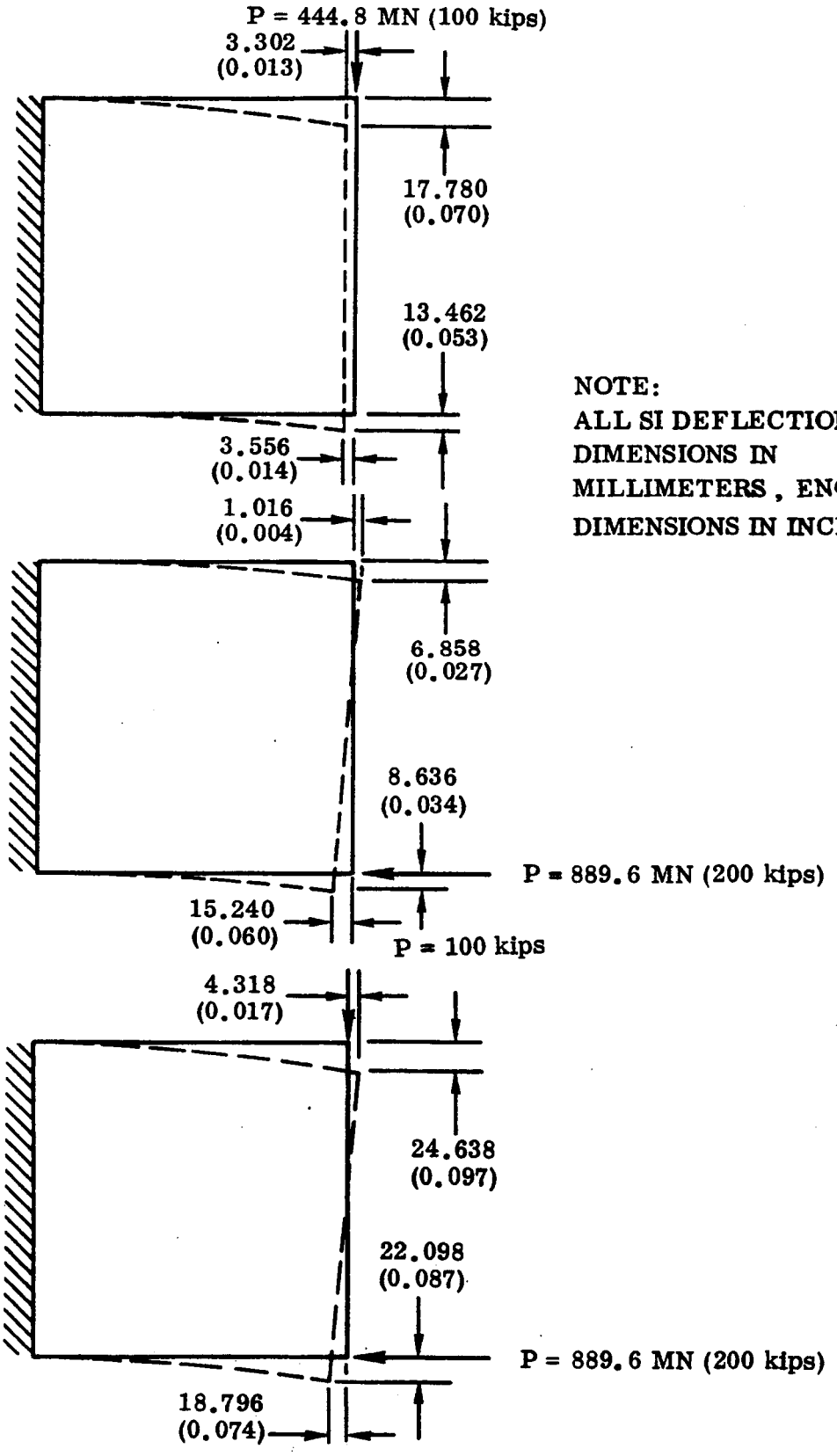

Figure 2-73. Beam Deflections

2.8 SHEAR BEAM TEST PLAN

The following procedure is to be used in testing the B/Al shear beam test article.

2.8.1 INSTALLATION

a. Install test specimen in test fixture similar to that as shown in Figure 2-74.

b. Ensure test beam is provided lateral support at points indicated to prevent torsional instability.

c. Install the 101 strain gages as shown in the approximate locations indicated in Figure 2-63.

d. Install deflection gage at the cantilever end of beam.

e. Hook up load cells for the horizontal and vertical loads.

2.8.2 PROCEDURE

a. The test of the cantilever beam is to be accomplished in four separate loading sequences, where the first three are at 75% of ultimate:

   1. Apply both the horizontal and vertical loads in a 2:1 ratio in increments of 44.48/22.24 kN (10,000/5,000 lb) to maximum loads of 667.2/333.6 kN (150,000/75,000 lb). Record strains and deflections at each increment. Remove load and proceed to substep 2.

   2. Apply only the vertical load in 22.24 kN (5,000 lb) increments to 333.6 kN (75,000 lb). Record strains and deflections. Remove the load and proceed to substep 3.

   3. Apply only the horizontal load in 22.24 kN (5,000 lb) increments to 667.2 kN (150,000 lb). Record strains and deflections at each increment. Remove the horizontal load and proceed to substep 4.

   4. Apply both the horizontal and vertical loads in a 2:1 ratio in increments of 44.48/22.24 kN (10,000/5,000 lb) to ultimate 889.6/444.8 kN (200,000/100,000 lb) and continue loading to failure. Record strains and deflections at each increment.

b. The maximum beam deflection with the applied vertical load (333.6 kN, 75,000 lb) is expected to be 0.1524 cm (0.060 in.).

c. The maximum lower beam cap strain with the applied horizontal load, case 3, at the strain gage located closest to the fixed end is less than 0.00141 m/m with the 667.2 kN (150,000 lb) applied load.

d. The maximum beam cap strain with the ultimate applied horizontal and vertical loads (case 4) at the strain gage located closest to the fixed end is less than 0.00268 m/m with the applied 445 and 890 kN (100,000 and 200,000 lb) load.

e. The maximum beam cap strain with the applied vertical load (case 2) at the strain gage located closest to the fixed end is less than 0.000597 m/m with the applied 333.6 kN (75,000 lb) load.

f. The ultimate load factor of safety is 1.4.

2.8.3 COMPONENT TEST SPECIMEN STRAIN GAGES. From the results of the linear finite element analyses, some of the more important strain gages have been analyzed and plotted as shown in Figures 2-75 through 2-89. The predicted strain readings are plotted versus applied load (loads). It is expected that the web materia response will be nonlinear, such that the plotted linear curves will bend down at the higher load levels. For strain gage locations refer to NASA MSFC drawing No. 31M03167, "Instrumentation Installation B/Al Shear Beam Component Test General Dynamics."

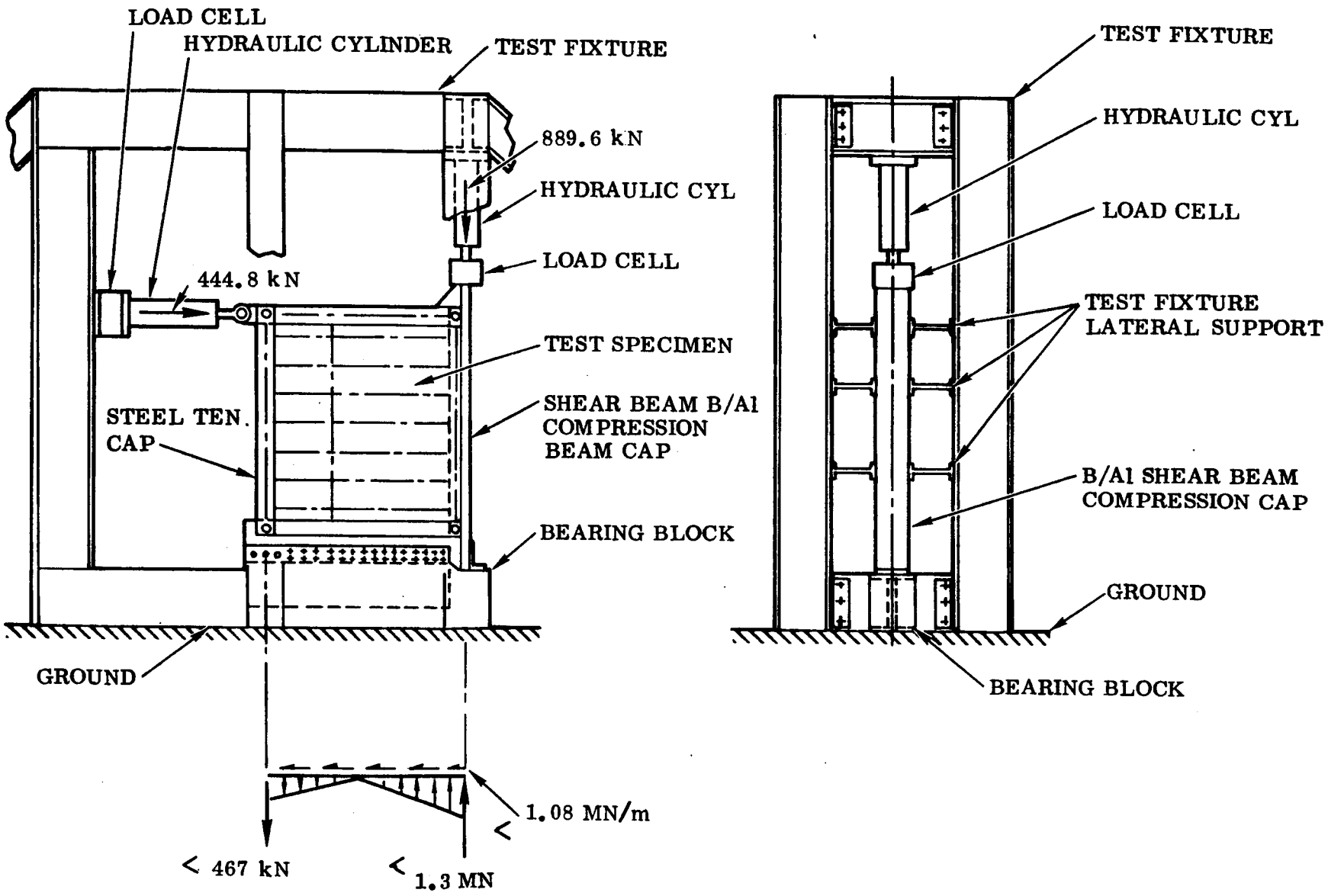

Figure 2-74. Test Rig, B/Al Shear Beam

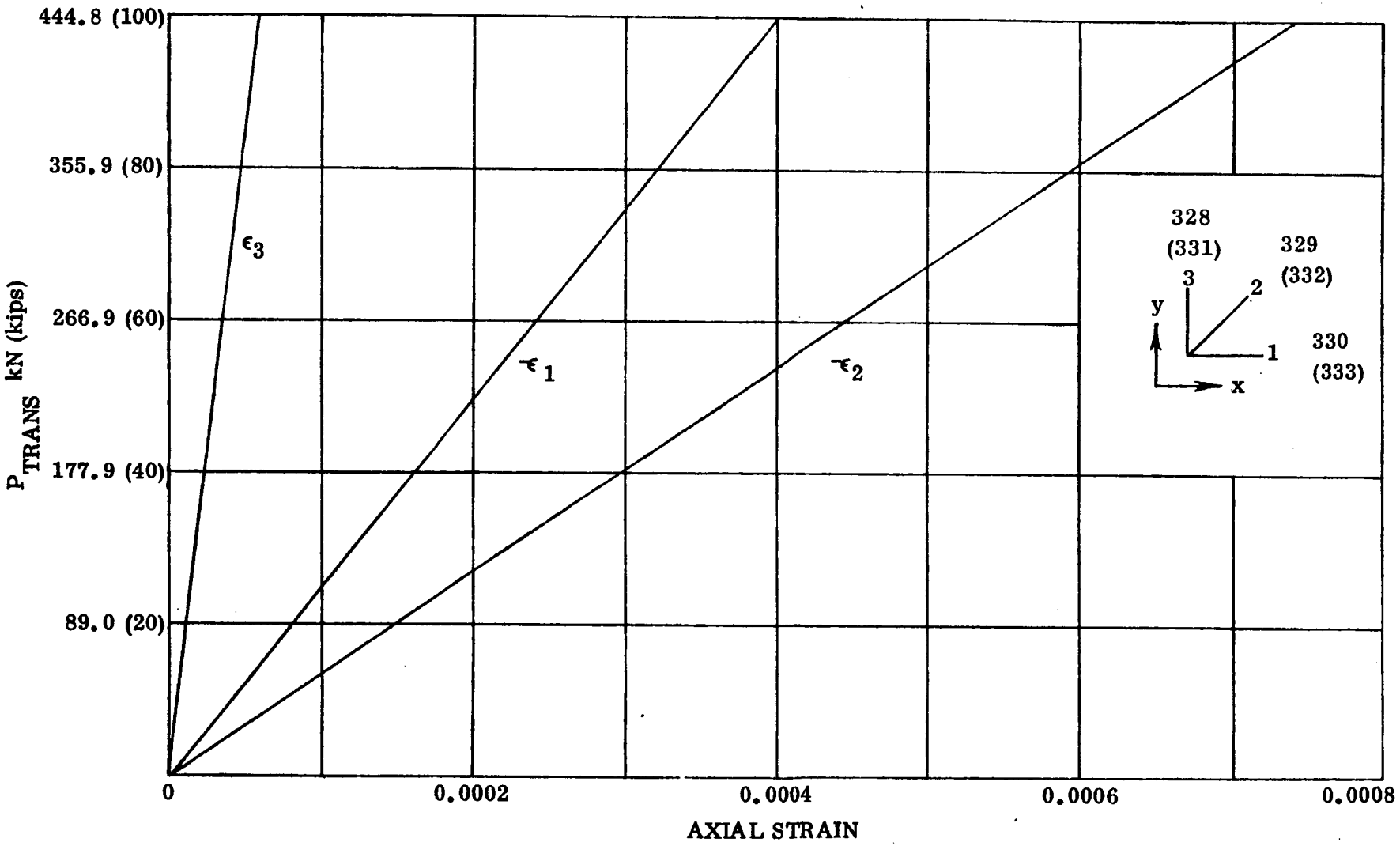

Figure 2-75. Predicted Rosette Numbers 330 through 333 Strains for Applied Transverse Load Only at End of Beam (Based on all Elastic Analysis)

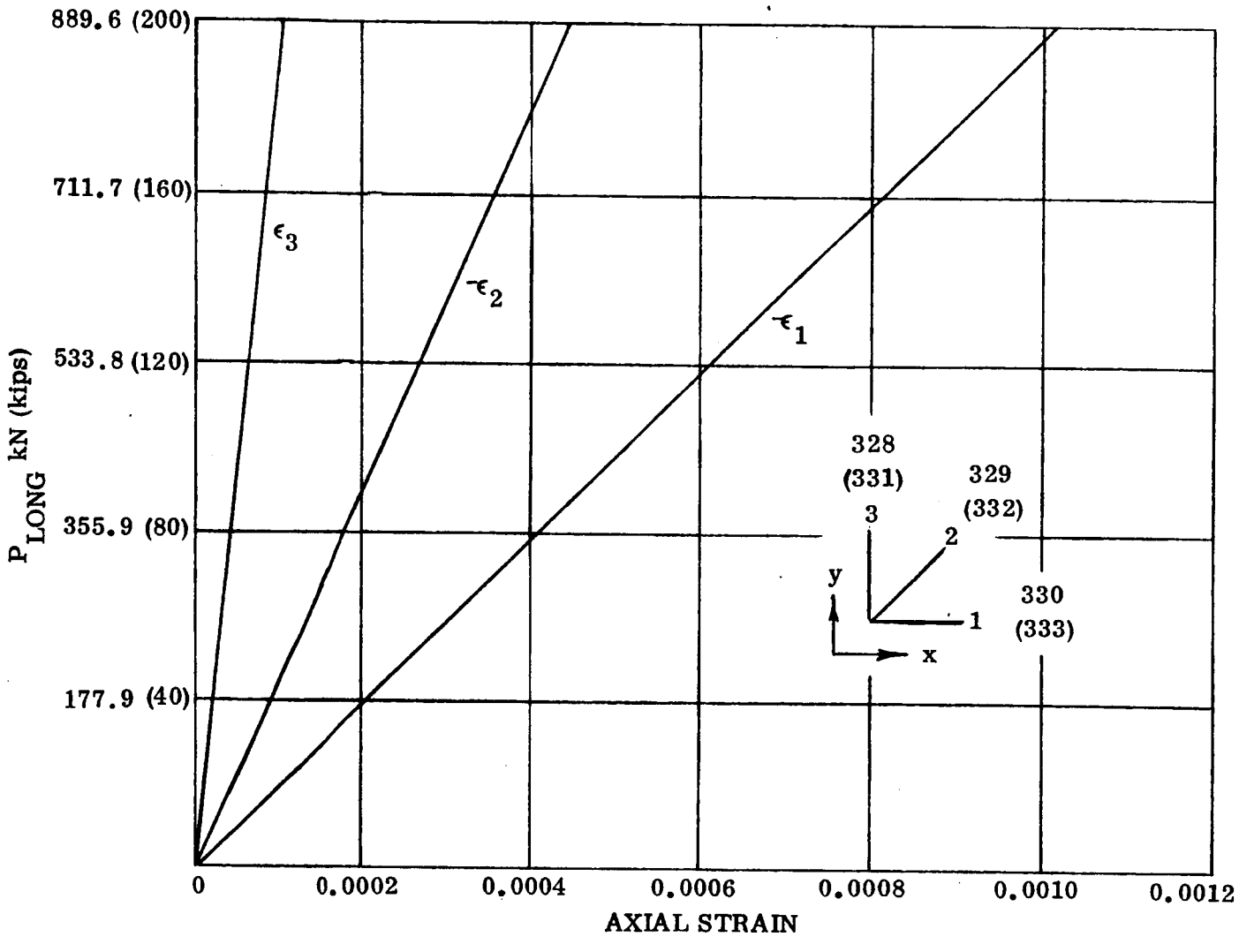

Figure 2-76. Predicted Rosette Numbers 330 through 333 Strains for Applied Longitudinal Load Only at End of Beam (Based on all Elastic Analysis)

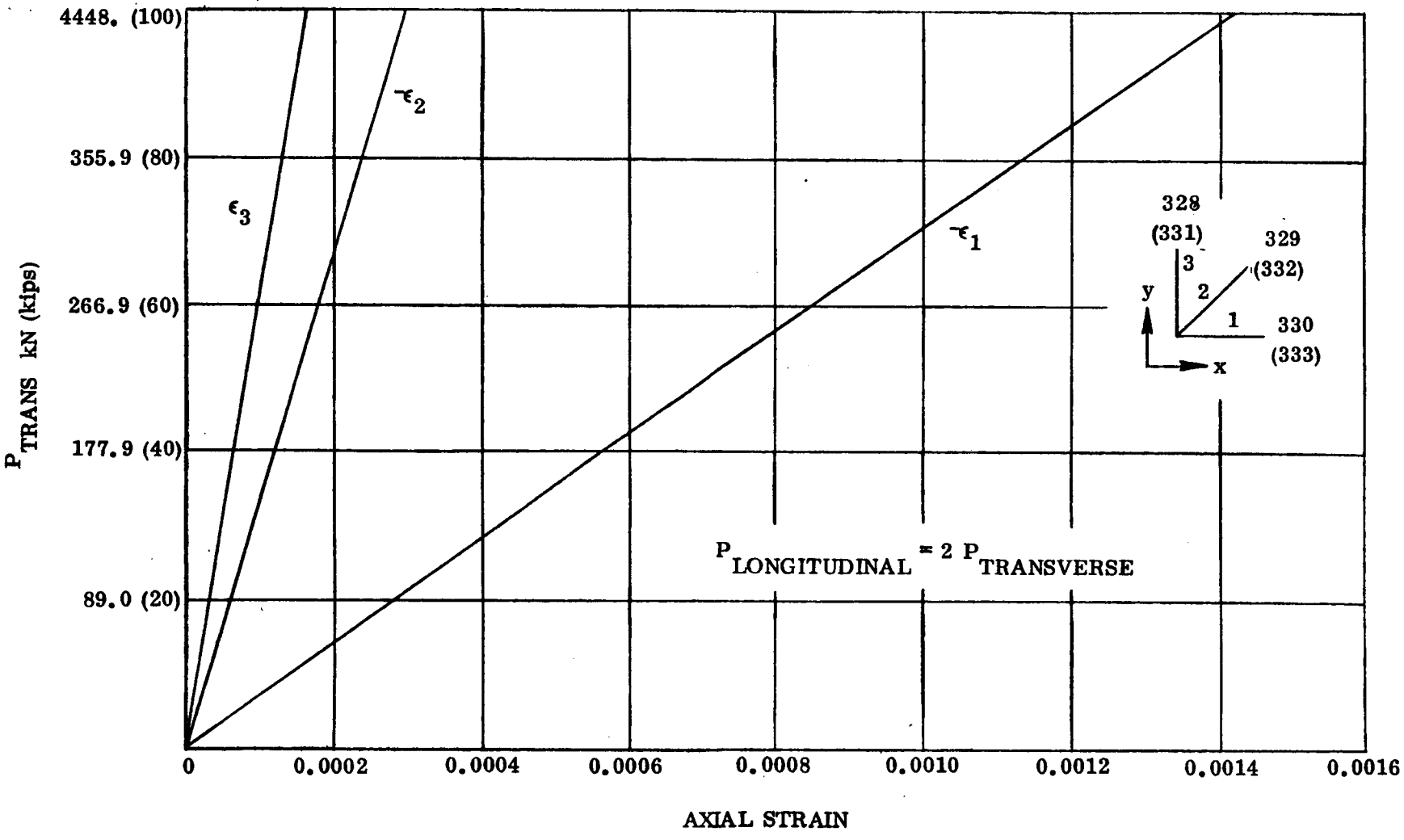

Figure 2-77. Predicted Rosette Numbers 330 through 333 Strains for Applied Longitudinal and Transverse Loads at End of Beam (Based on All Elastic Analysis)

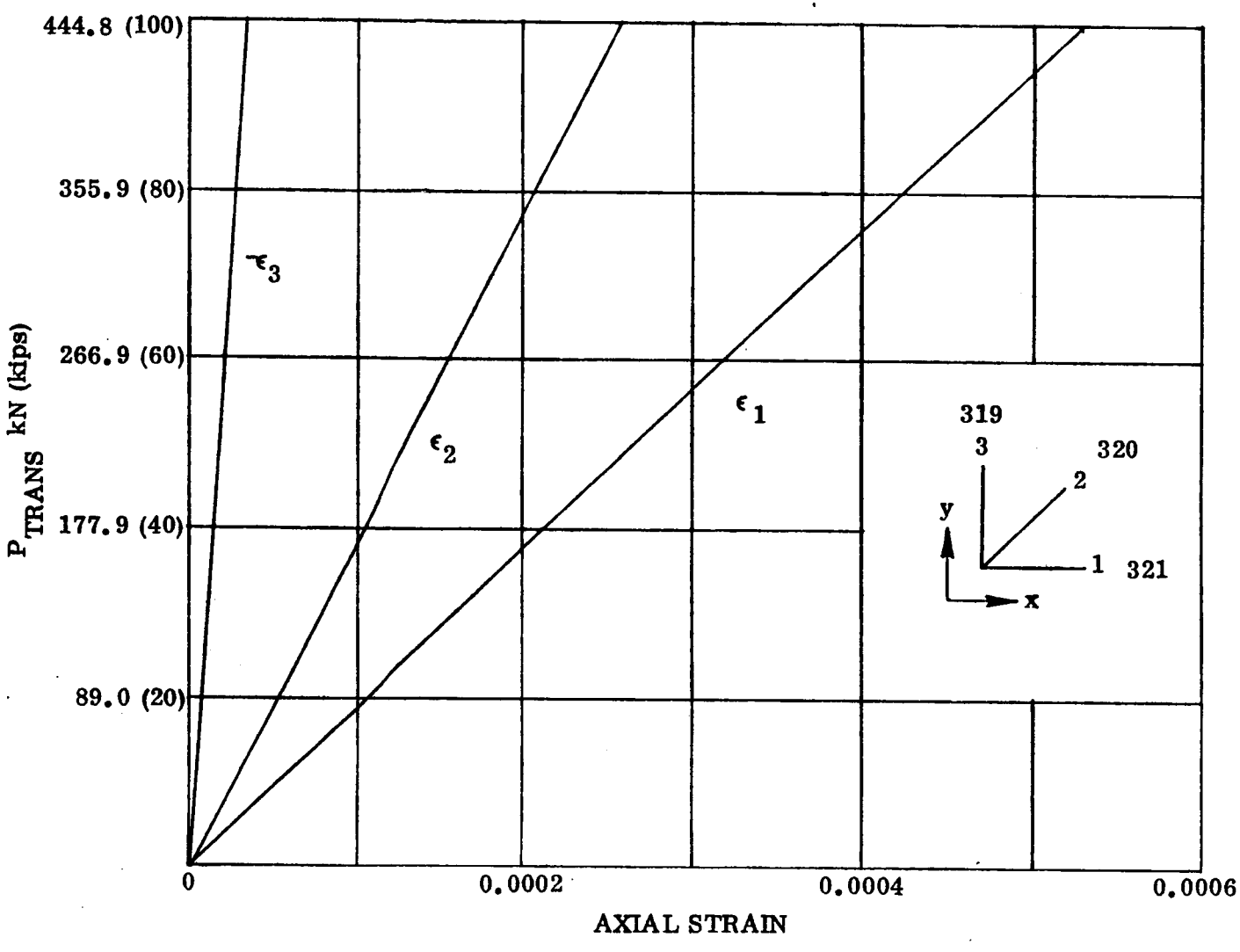

Figure 2-78. Predicted Rosette Numbers 319 through 321 Strains for Applied Transverse Load Only at End of Beam (Based on all Elastic Analysis)

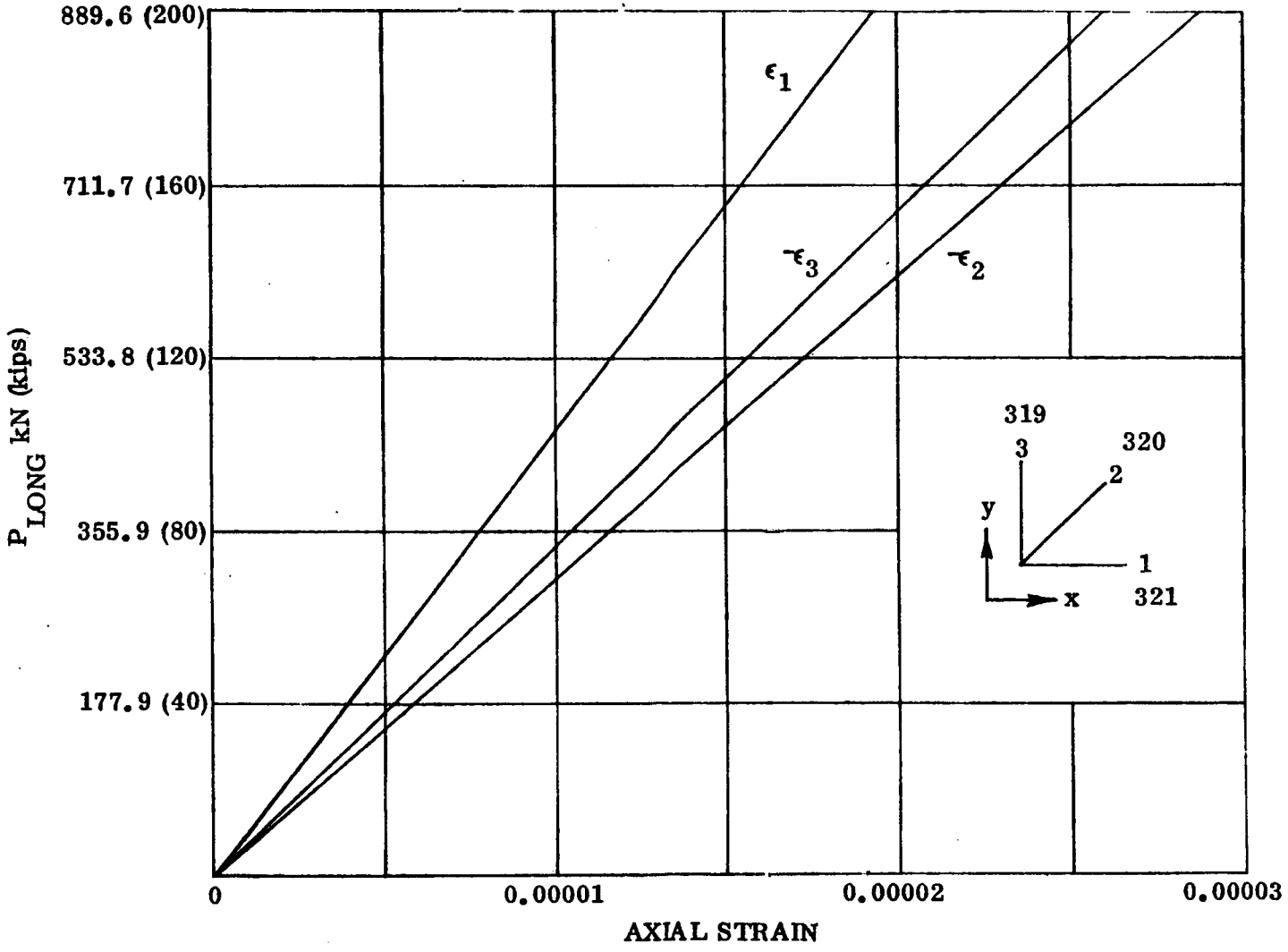

Figure 2-79. Predicted Rosette Number 319 through 321 Strains for Applied Longitudinal Load Only at End of Beam (Based on all Elastic Analysis)

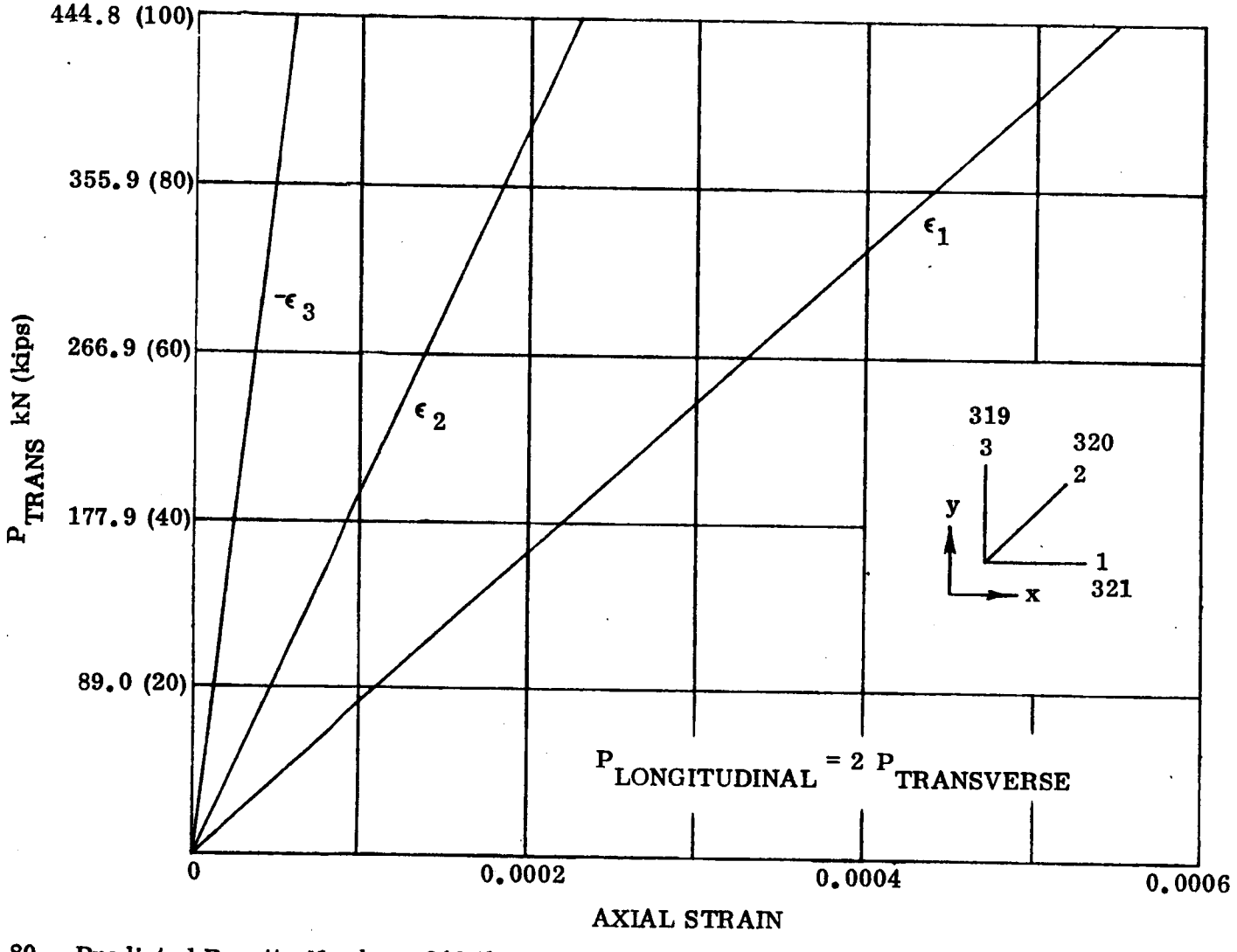

Figure 2-80. Predicted Rosette Numbers 319 through 321 Strains for Applied Longitudinal and Transverse Loads at End of Beam (Based on all Elastic Analysis)

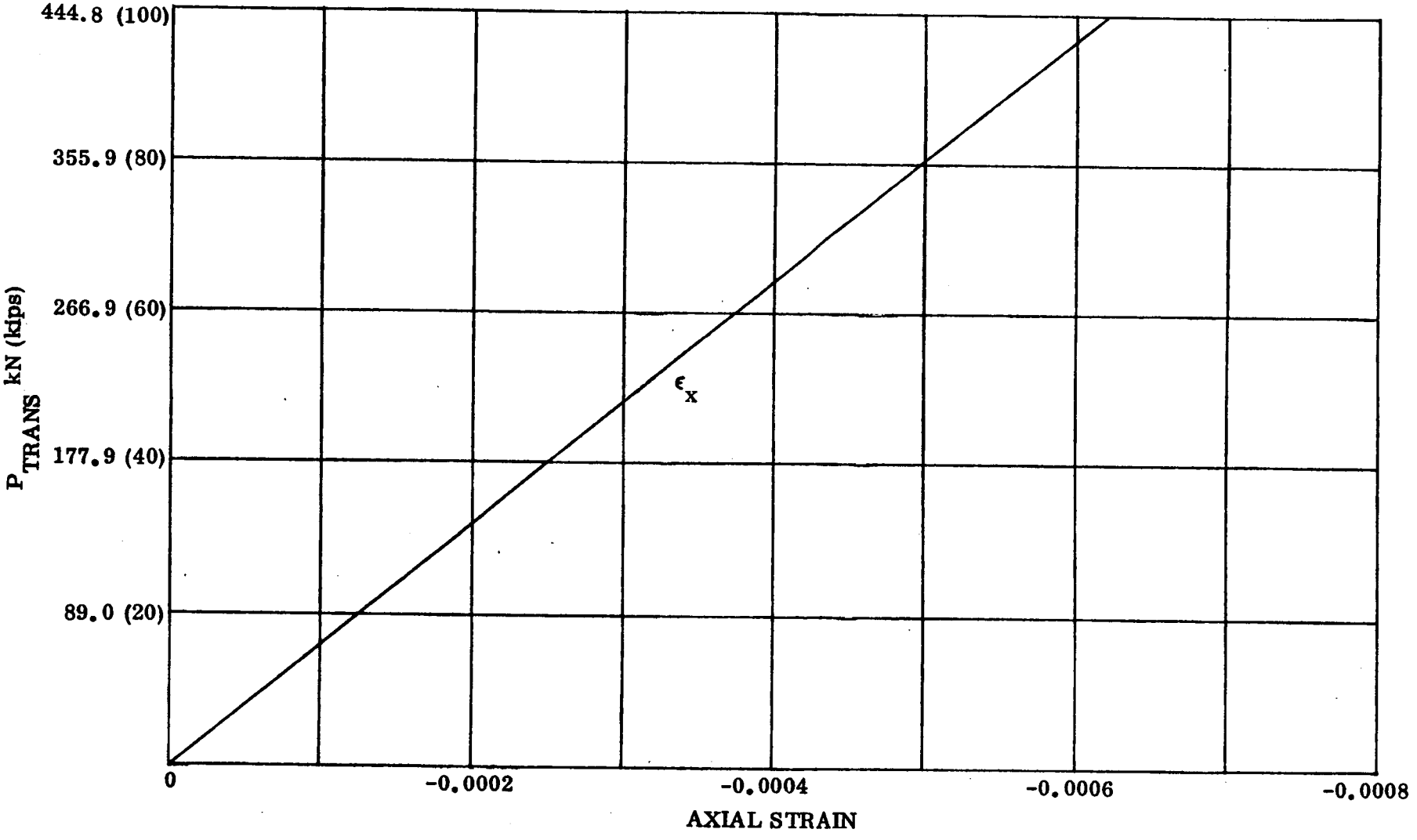

Figure 2-81. Predicted Strains for Gage Numbers 110 through 114 for Applied Transverse Load Only at End of Beam (Based on all Elastic Analysis)

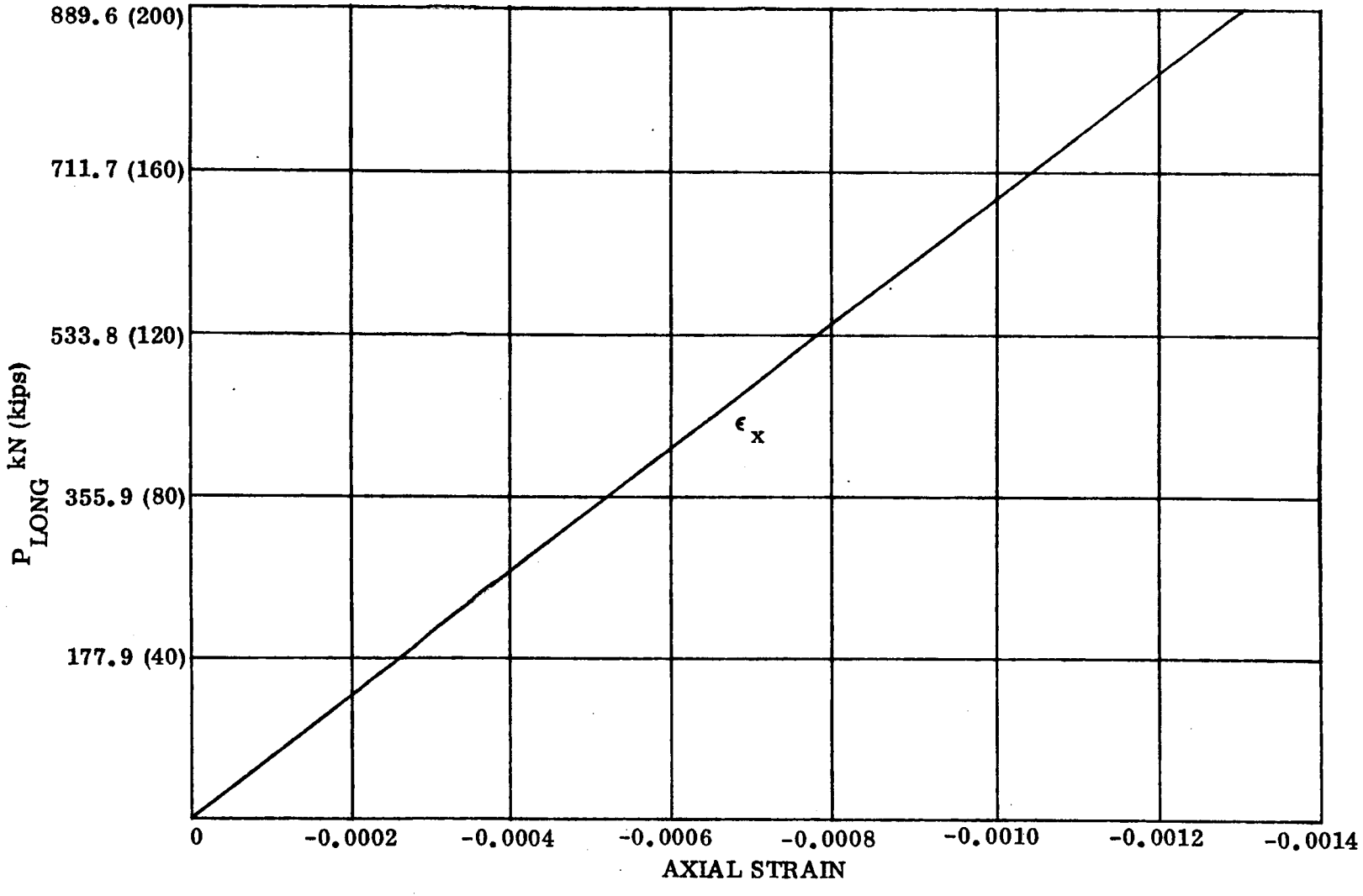

Figure 2-82. Predicted Strains for Gage Number 110 through 114 for Applied Horizontal Load Only at End of Beam (Based on all Elastic Analysis)

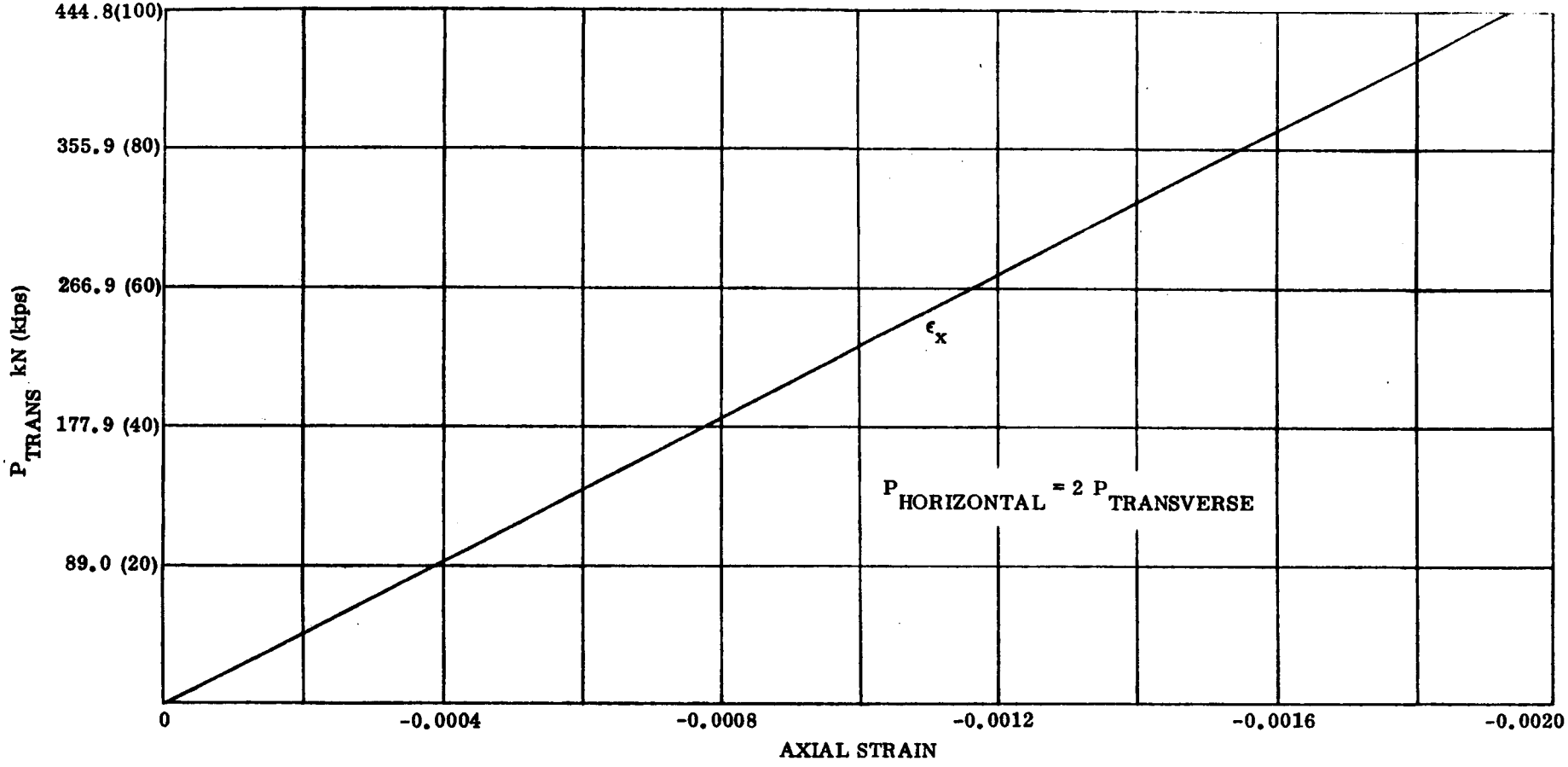

Figure 2-83. Predicted Strains for Gage Numbers 110 through 114 for Applied Horizontal and Transverse Loads at End of Beam (Based on All Elastic Analysis)

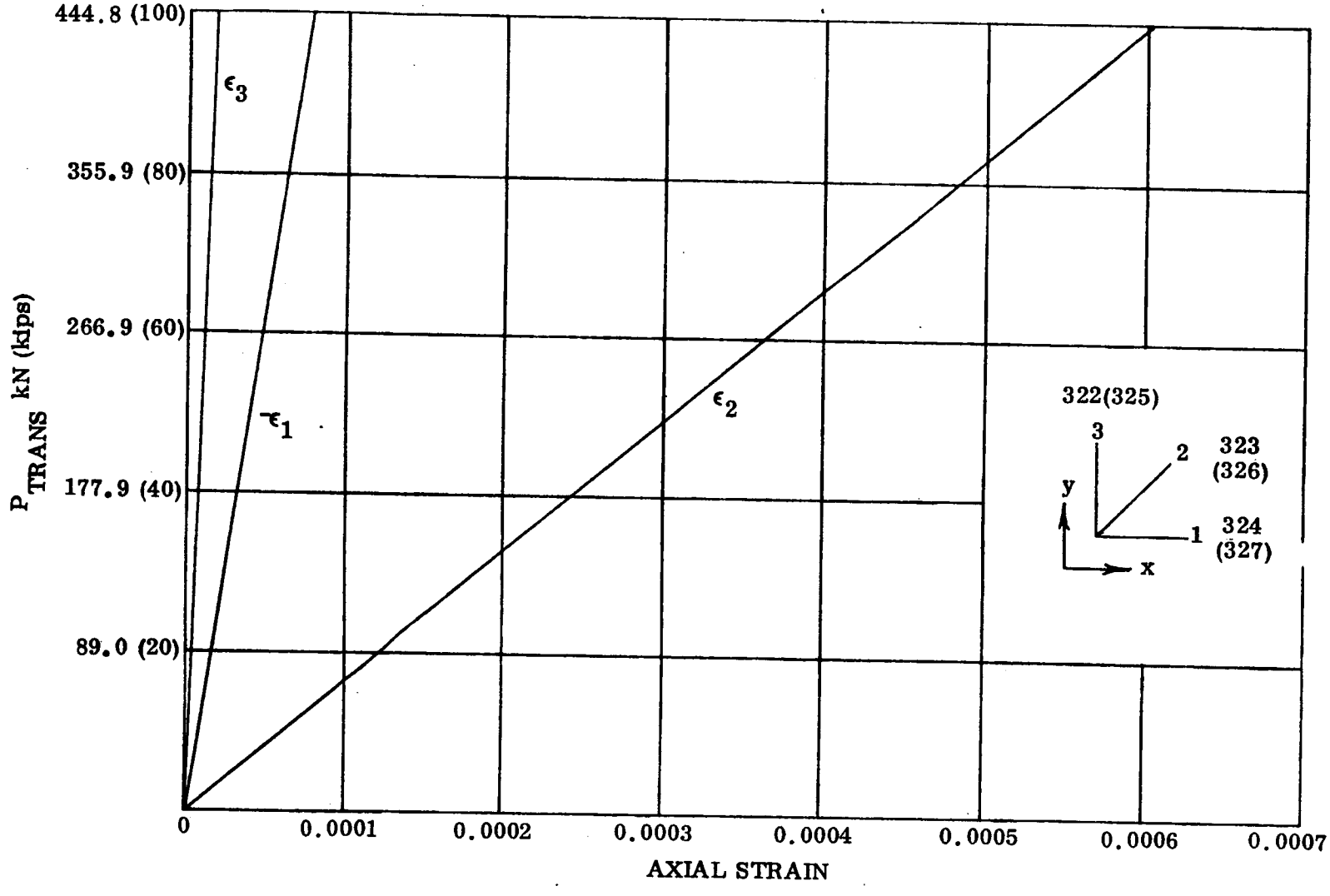

Figure 2-84. Predicted Rosette Numbers 322 through 327 Strains for Applied Transverse Load Only at End of Beam (Based on All Elastic Analysis)

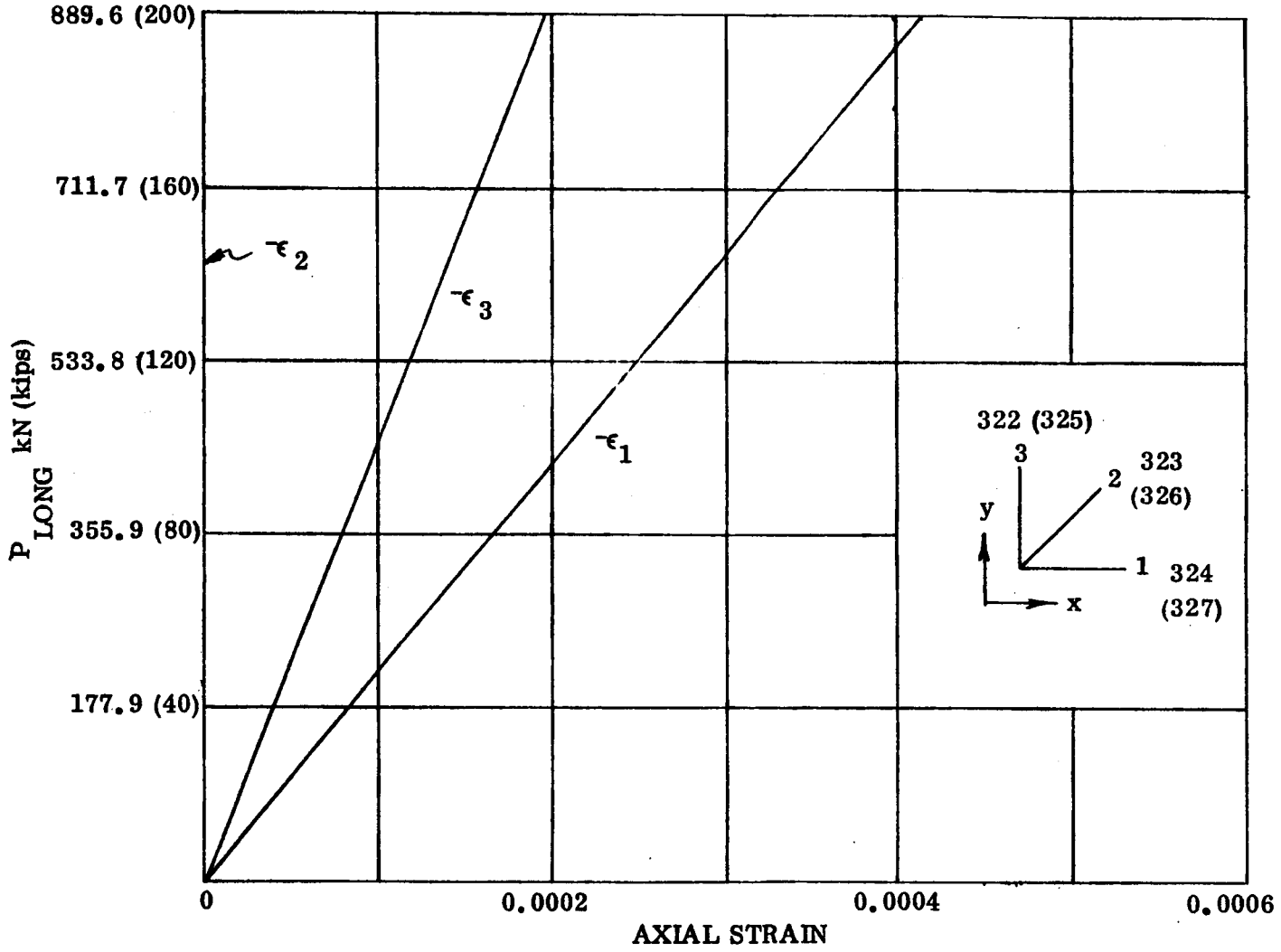

Figure 2-85. Predicted Rosette Numbers 322 through 327 Strains for Applied Longitudinal Load Only at End of Beam (Based on All Elastic Analysis)

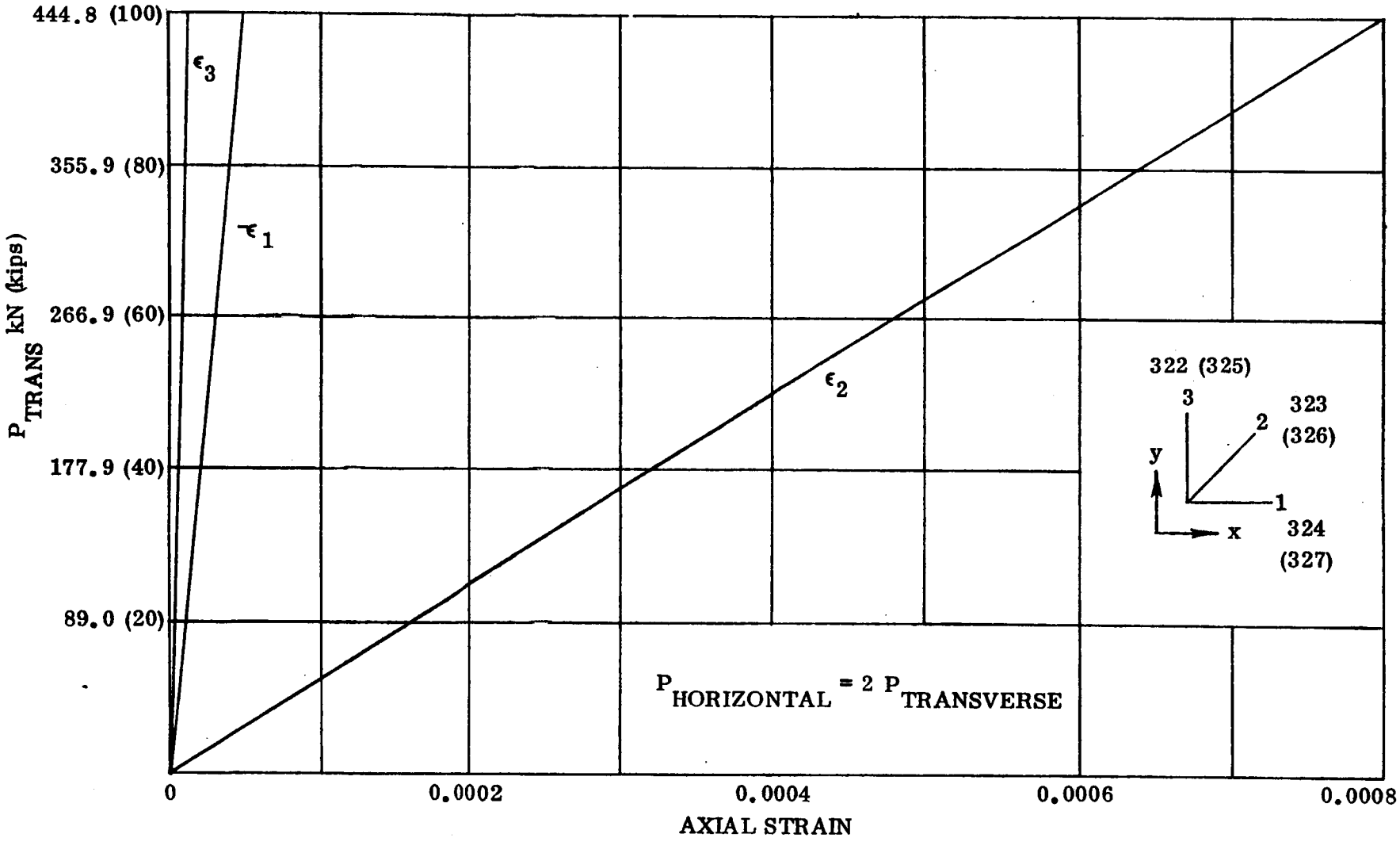

Figure 2-86. Predicted Rosette Numbers 322 through 327 Strains for Applied Longitudinal and Transverse Loads at End of Beam (Based on All Elastic Analysis)

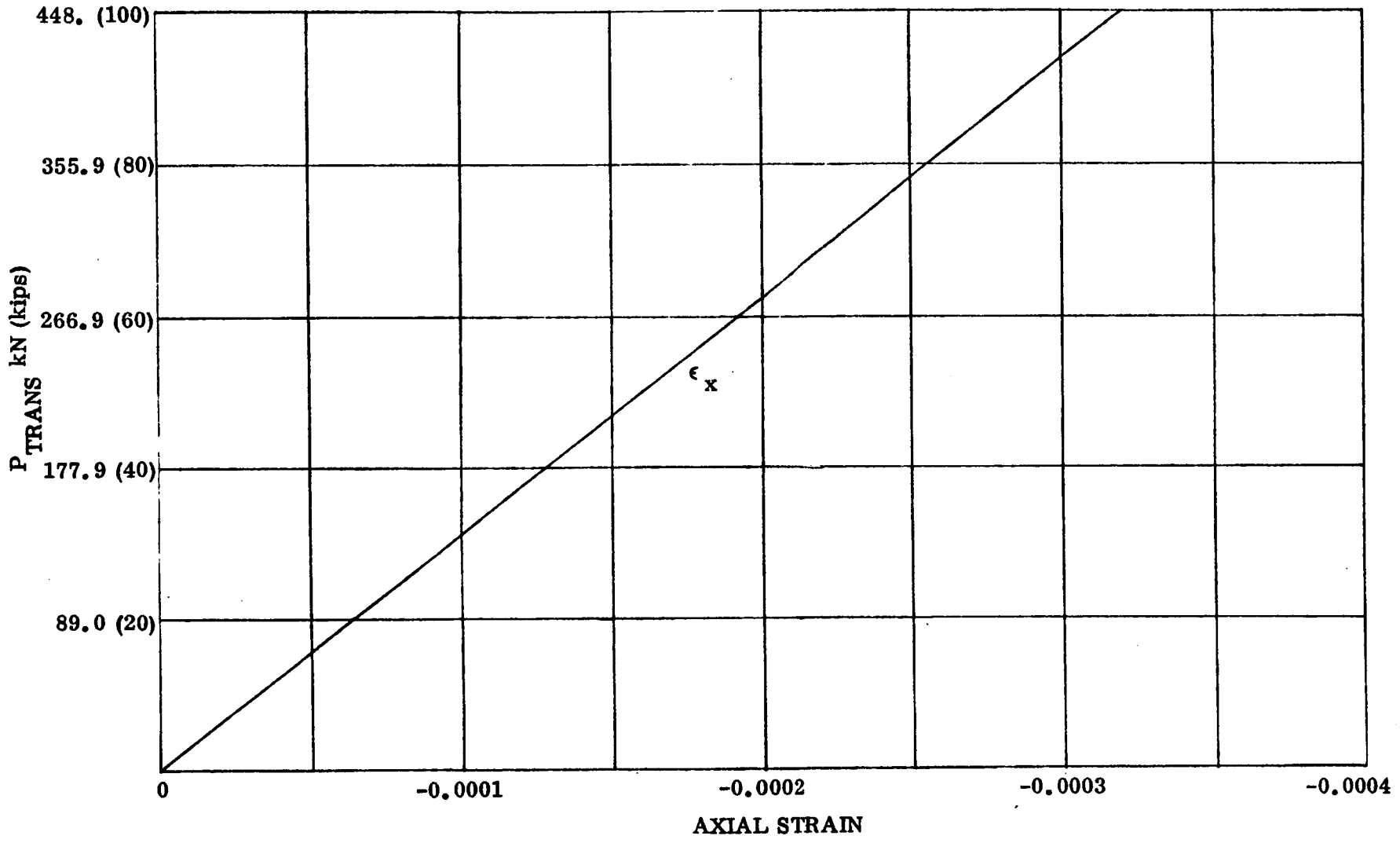

Figure 2-87. Predicted Strains for Gage Numbers 115 through 117 for Applied Transverse Load Only at End of Beam (Based on All Elastic Analysis)

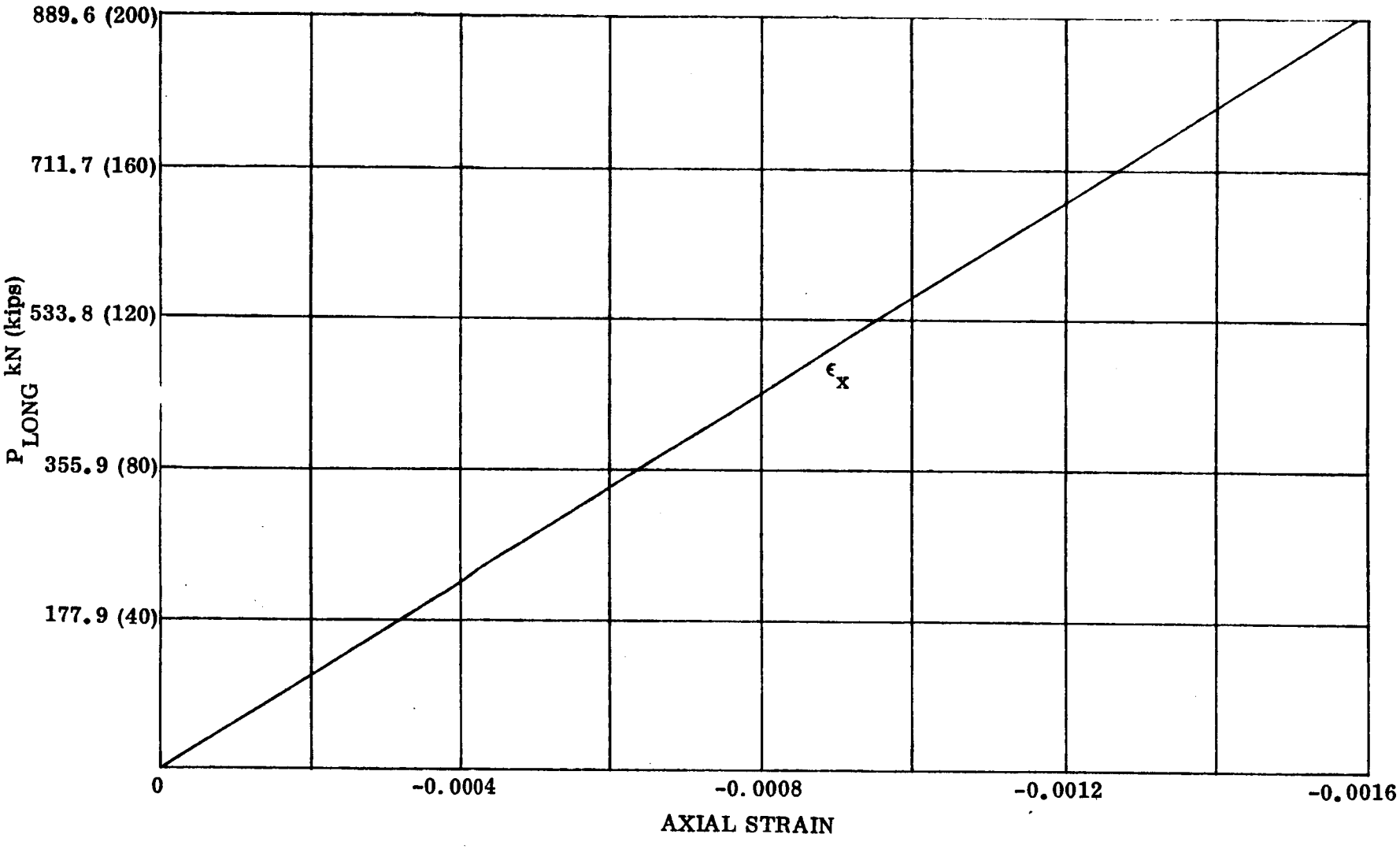

Figure 2-88. Predicted Strains for Gage Numbers 115 through 117 for Applied Longitudinal Load Only at End of Beam (Based on all Elastic Analysis)

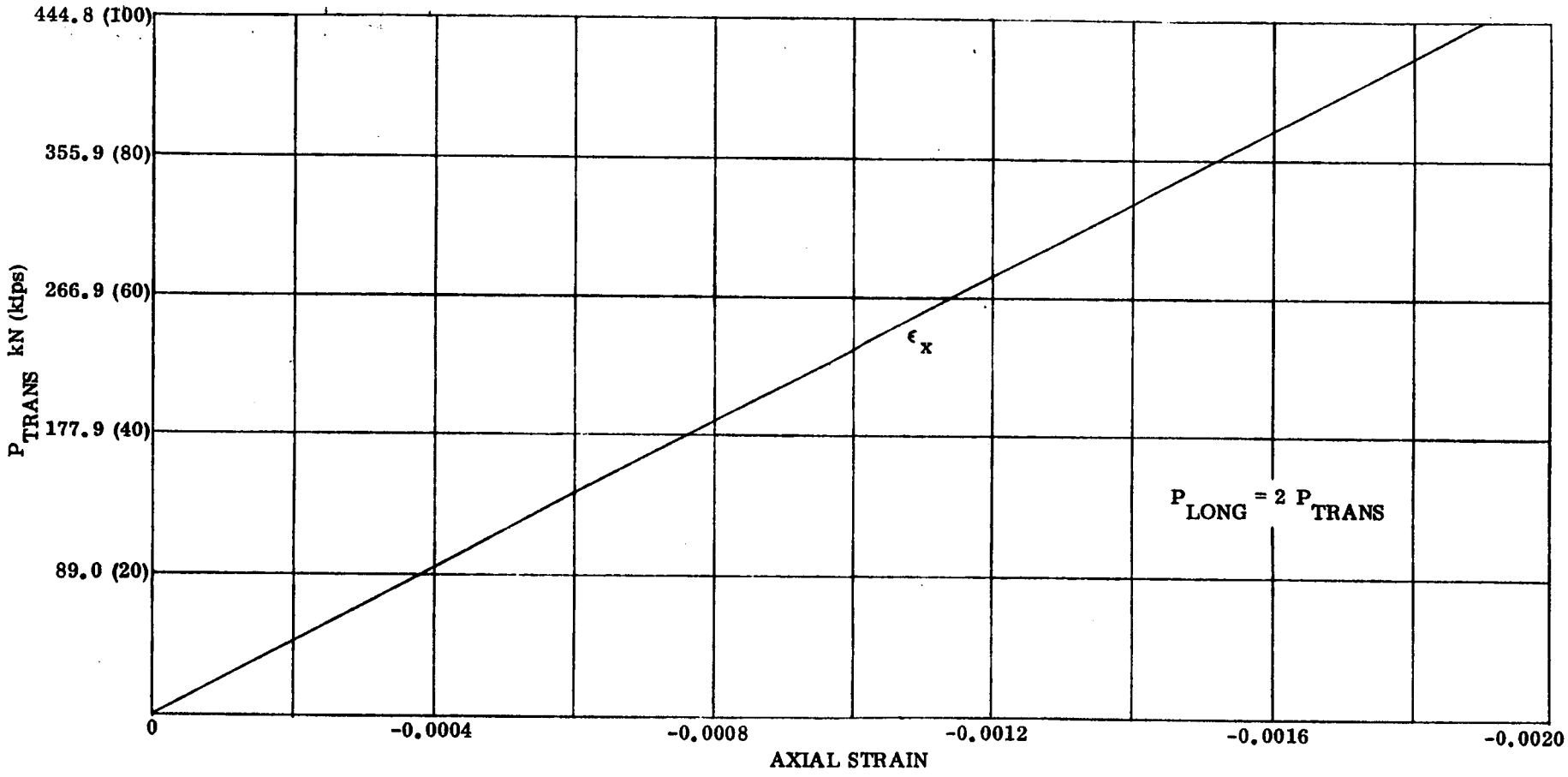

Figure 2-89. Predicted Strains for Gage Numbers 115 through 117 for Applied Horizontal and Transverse Loads at End of Beam (Based on All Elastic Analysis)

SECTION 3

TRUSS BEAM DESIGN AND ANALYSIS

3.1 TASK OBJECTIVE AND INTRODUCTION

The task objective for this phase of the program was to develop a boron/aluminum (B/Al) truss beam design for the reuseable Space Shuttle vehicle. The design requirements of the truss structure and the truss configuration are shown in Figure 3-1. The primary structural material used was B/Al with other optional materials used for fittings, splices, etc.

Although the truss is relatively straightforward in configuration, the member length, load magnitudes, and end moments at the lower truss joints presented a challenge to design in B/Al. Existing designs to date in composite materials utilize round tubular sections and open sections for compression members. These members are relatively small in cross section [2.54 to 5.08 cm (1 to 2 inch) diameter] and length and were fabricated into seamless tubing by an isostatic gas pressure bonding process. At the time of this design study, the large cross-sectional area and lengths of the truss structure were beyond the current state-of-the-art for B/Al fabrication utilizing this process. Brazed or bonded joints, which generally have sufficient strength to meet most

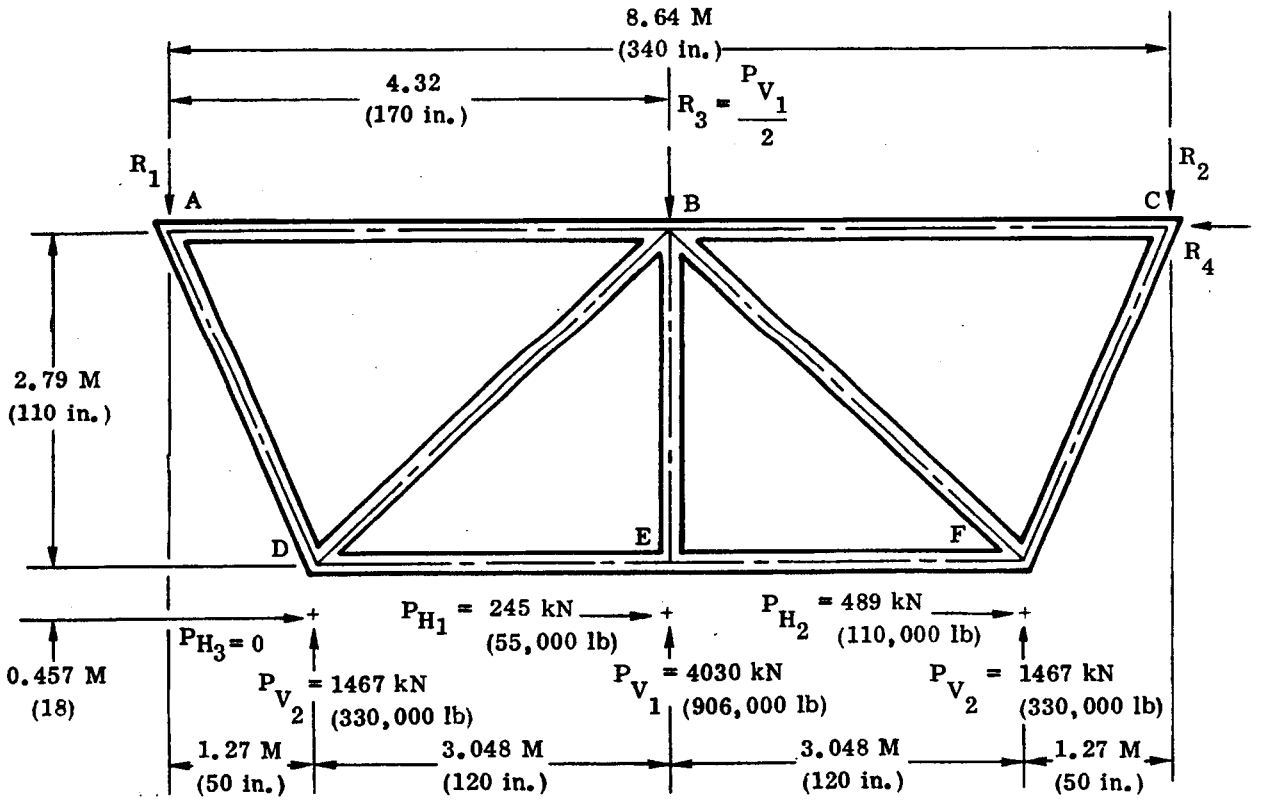

NOTE: ULTIMATE LOADS ARE SHOWN

Figure 3-1. Truss Configuration

design requirements, are impractical for large fittings. Only those cross-sectional areas and joints considered most feasible for the given loadings were considered. The shape had to lend itself to a simple and reliable joint that could be fabricated and inspected.

3.2 TRUSS DESIGN

Early in the design analysis of the truss beam, it was noted that four of the nine truss members did not require a compression load-carrying capability to comply with the design requirements. The truss complexity could be reduced by configuring these members for tension only. Since this was not realistic for a typical space shuttle structure, the design requirements were modified. A "rebound" condition was added that would result in compression loading conditions on all structural members. This consisted of:

$$P_{v_1} = -28,580 \text{ kN } (-63,000 \text{ lb})$$

$$P_{v_2} = -10,430 \text{ kN } (-23,000 \text{ lb})$$

$$P_{h_1} = 0$$

$$P_{h_2} = 0$$

$$P_{h_3} = 0$$

Based upon the revised loading conditions, the individual truss member axial loads and bending moments were determined. These loads are shown in Figures 3-2 and 3-3. The reactions at A, B, and C were determined from statics. The internal loads in the truss members were determined assuming that the member BE to the 245 kN (55,000 lb) side load application point is a rigid joint with members DE and EF pinned at E. Member CF was also assumed rigid to the 489 kN (110,000 lb) side load application point with members EF and BF pinned at Joint F. The bending moments at Points E and F and the relative stiffnesses of the attaching members were determined.

Numerous truss member configurations that could be fabricated from B/Al were examined. Truss member cross sections that could be built up by brazing, bonding, or mechanically fastening were considered. Seamless tubular members of circular cross sections normally used in efficient truss structures were not considered because tubular B/Al members of the size and length required were beyond the state-of-the-art at the time of the design study.

Joint design was an important factor in the selection of the optimum design. Open sections are generally desirable for attachment accessibility and inspection although they are not as efficient as a column member.

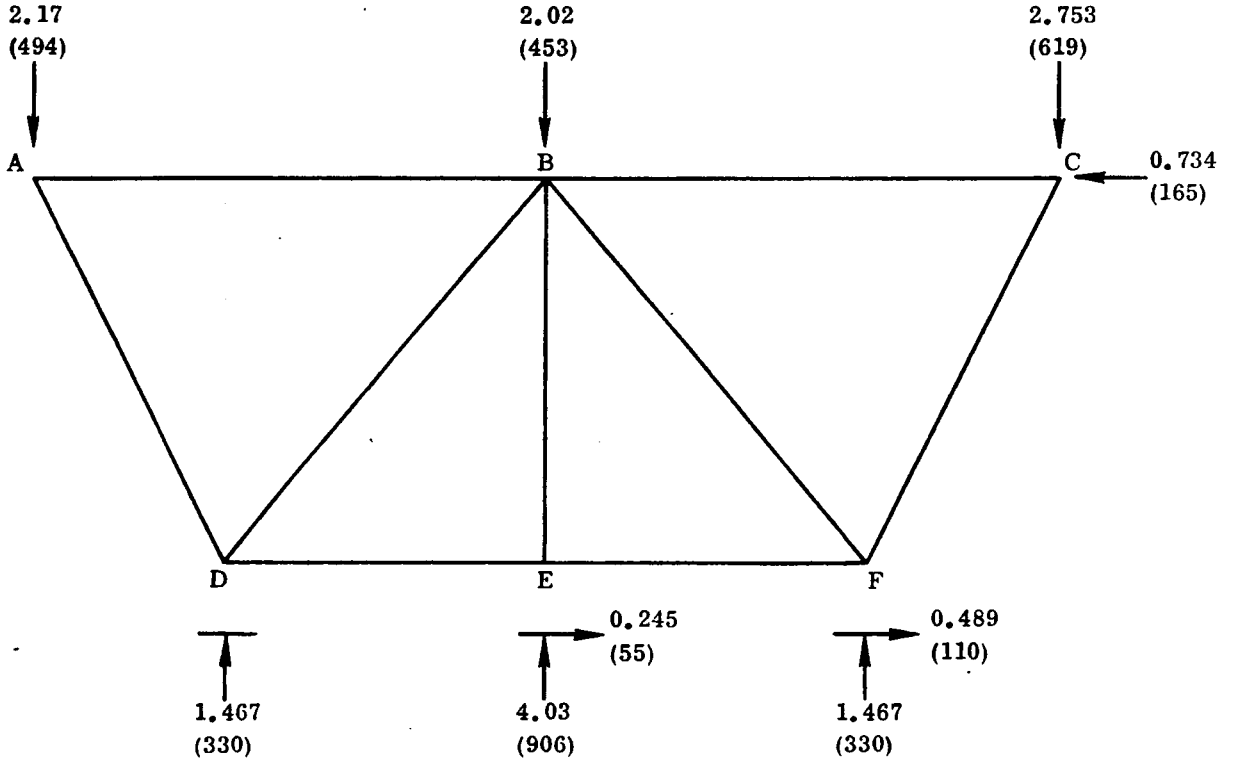

ALL LOADS IN MN (kips)

Figure 3-2. Truss External Loads

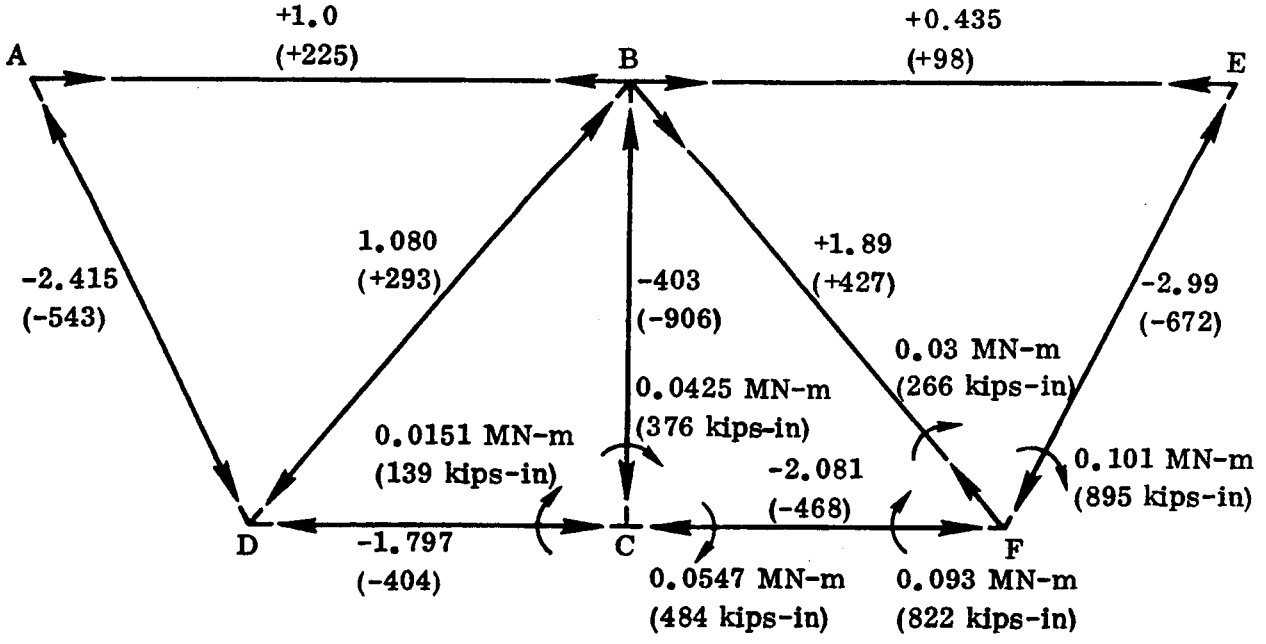

ALL LOADS IN MN (kips) UNLESS OTHERWISE NOTED

Figure 3-3. Internal Loads and Moments

Brazing and adhesive bonding were eliminated as prime joining methods for the following reasons:

a. The large loads in the truss result in high entry and exit peaking stresses at the bondline.

b. The thick sections required induce secondary local bending stresses that tend to peel the joint.

c. The thick sections require a long gradual taper for load entry and exit; this necessitates large end fittings.

d. Brazing or bonding of large surface areas are not reliable.

e. Joints cannot tolerate misalignment.

f. Consistent bond strength would be difficult to achieve and hard to prove.

g. The truss members are subjected to beam-column loading that tends to peel the joint.

Mechanical fasteners appeared to provide the greatest potential strength and reliability. To compensate for the low bearing strength and trans erse strength of B/Al when compared to conventional materials such as steel and titanium, the end fittings were selectively reinforced.

3.2.1 PRELIMINARY TRUSS DESIGNS. Two preliminary truss beam designs were configured for trade studies. These were a honeycomb stabilized and a square-tube truss.

3.2.1.1 Honeycomb Stabilized Truss Members. The honeycomb stabilized truss structure design is shown in Figure 3-4. Five of the nine members in the structure are highly loaded in compression. These members are the two outboard diagonal members, the center vertical member, and the two lower horizontal members. These members were configured from UD B/Al plate, stabilized by sandwiching an element of aluminum honeycomb (2.10×10^5 kg/m^3, 7.7 lb/ft^3, core density). The primary purpose of the honeycomb core was to preclude local crippling, thus increasing the column allowable or reducing the required material thickness for a given cross section. The two inboard diagonal members, which are primarily tension carrying, are Con Braz joined from UD B/Al plate into a cruciform section. The forward two horizontal members, also primarily tension carrying, are Con Braz joined into an H- or I-section. The tension member cross sections were selected because they lend themselves to a moment carrying and attachment fitting while having a sufficiently large I-section to meet the required "rebound" compressive load conditions. The allowable column strength was established for compression loading using the Euler equation. The local crippling stresses were established from the equation

FOLDOUT FRAME 1

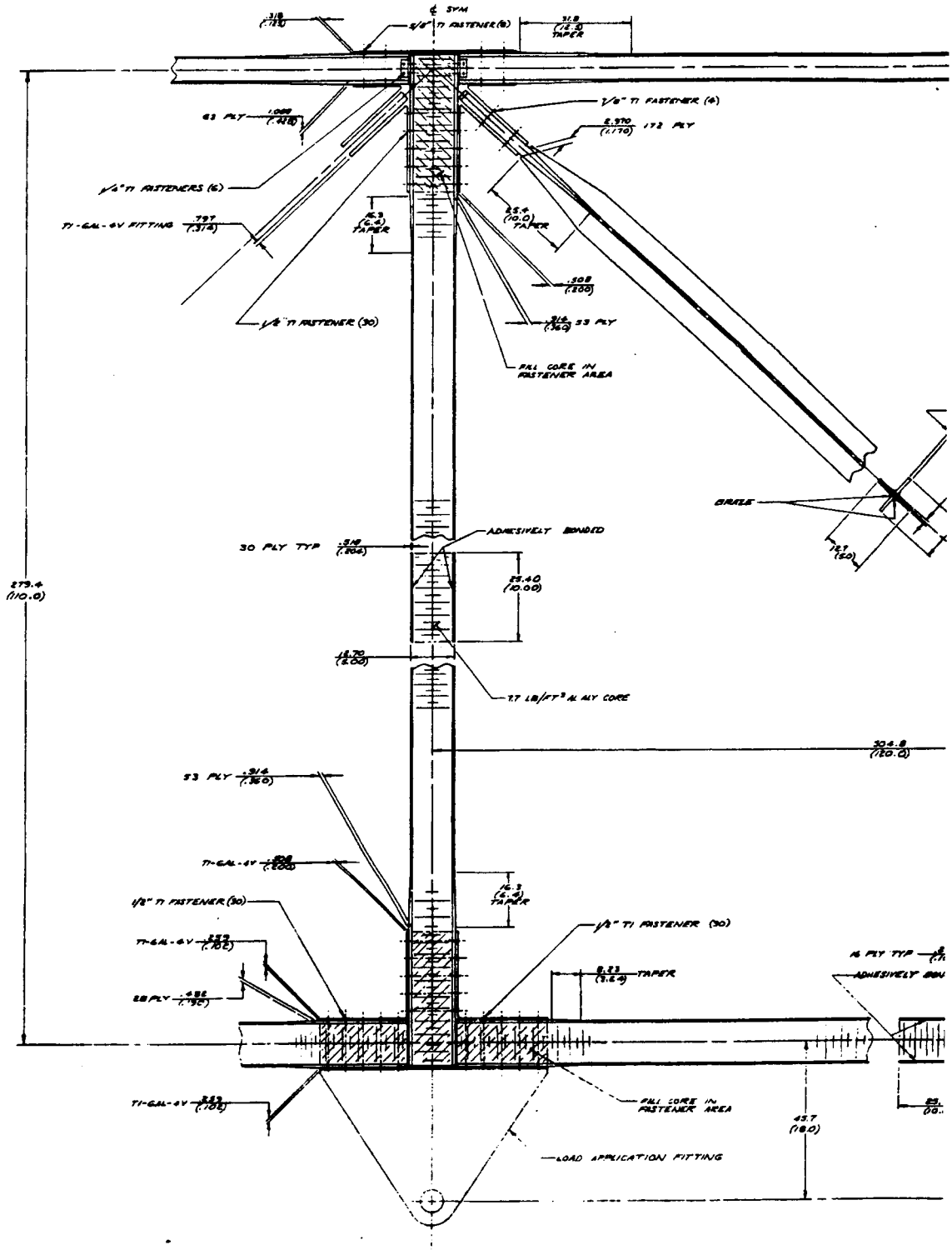

3-5/3-6 A

FOLDOUT FRAME 2

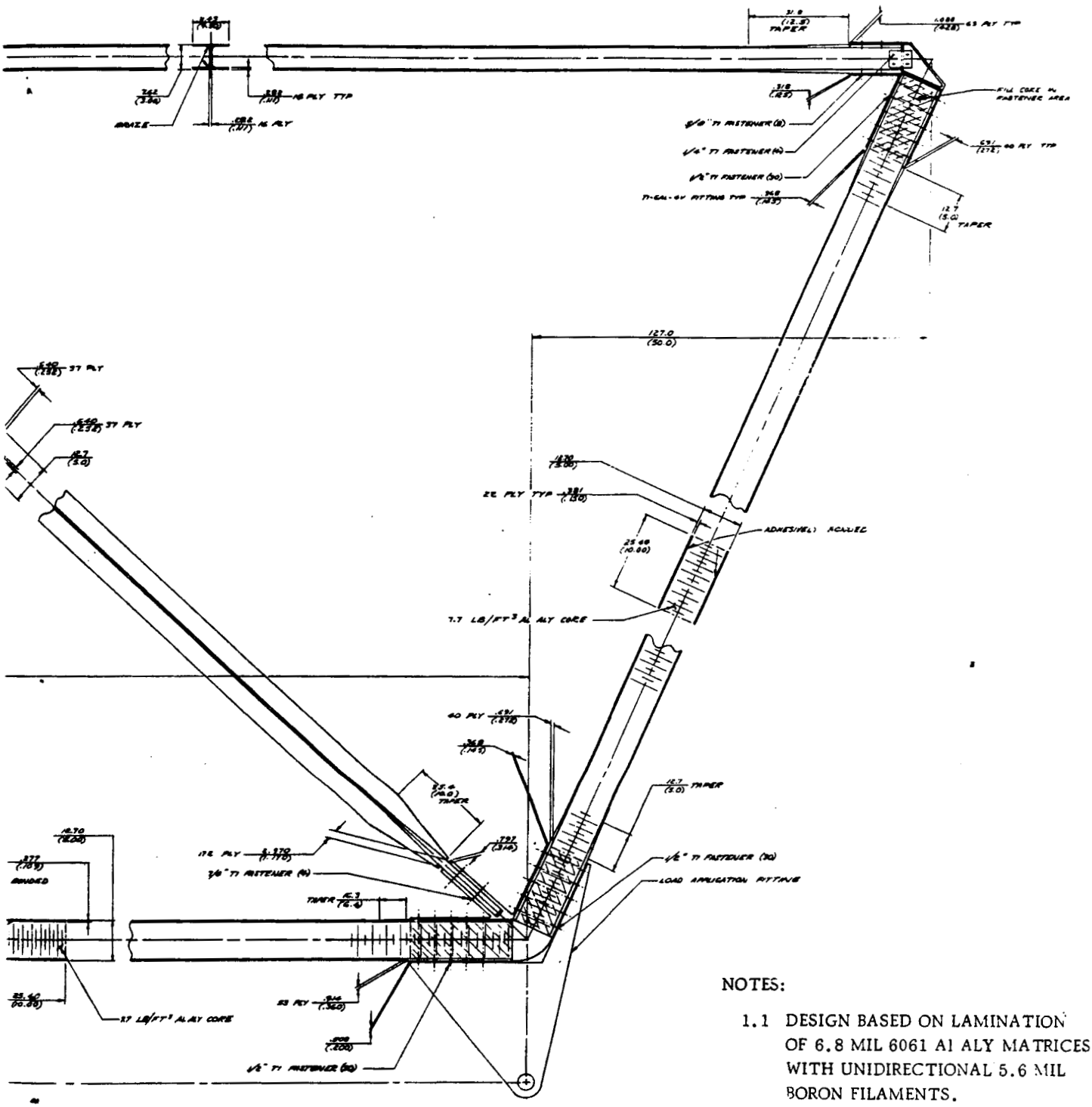

NOTES:

1.1 DESIGN BASED ON LAMINATION OF 6.8 MIL 6061 Al ALY MATRICES WITH UNIDIRECTIONAL 5.6 MIL BORON FILAMENTS.

1.2 DIMENSIONS IN CM (IN.)

Figure 3-4. Thrust Structure Truss Beam — B/Al Space Shuttle Application

B

$$F_{cr} = \left(\frac{t}{b}\right)^2 G_{xy} + \frac{\pi^2 E_{xx}}{12(1-\nu_{12}\nu_{21})}\left(\frac{t}{L}\right)^2$$

The end fittings are fabricated from 6Al-4V titanium alloy and spliced to the columns with titanium fasteners. The B/Al column ends were selectively increased in gage and reinforced to allow installation of sufficient numbers of fasteners to carry the load.

3.2.1.2 Square Tube Truss Members. The second preliminary truss design is shown in Figure 3-5. The design is similar to that discussed in Section 3.2.1.1 except the five highly loaded compression members are fabricated from UD B/Al plate, Con Braz joined into a square tube cross section. The members were sized for local crippling and as an Euler column. The tube ends are cut away on two sides for accessibility. They are provided with a laminated buildup of material on the other two sides for attachments. The laminar buildup is required to compensate for the low bearing strength, as compared to conventional materials such as steel and titanium, of the UD B/Al. The truss members are attached to the corner fittings with titanium mechanical fasteners. The corner fittings are machined from titanium alloy.

3.2.2 TRUSS BEAM PRELIMINARY DESIGN SUMMARY. A weight summary of the two truss concepts is shown in Table 3-1. These two concepts were the result of an examination of several truss member configurations that could be fabricated from UD B/Al. The primary difference in the weights of the two concepts is the weights of the five highly loaded compression members and end attachment. The square tube concept requires a thicker wall gage for local stability than the honeycomb concept; however, the thinner gages used in the honeycomb concept are more than offset by the core material, adhesive, and end joint potting material required. The added complexity of the design, fabrication difficulties, inspectability, and increased weight precluded serious consideration of the honeycomb concept.

Table 3-1. Summary of Truss Beam Weights (Tradeoff Study)

	Honeycomb Stabilized Truss		Square Tube Truss	
	kg	lb	kg	lb
Member (1)	65.2	143.7	24.7	54.4
Member (2)	43.3	95.4	43.3	95.4
Member (3)	108.9	240.0	39.7	87.6
Member (4)	93.3	205.6	27.8	61.2
Member (5)	45.4	100.2	45.4	100.2
"C" Gusset	12.5	27.6	12.5	27.6
"B" Gusset	18.0	39.6	18.0	39.6
"F" Gusset	39.9	88.0	39.9	88.0
"E" Gusset	24.1	53.2	24.1	53.2
Fasteners	37.6	82.8	16.8	37.1
Total	488.1	1076.1	292.2	644.3

3.3 FINAL DESIGN TRUSS BEAM

The final design truss beam is shown in Figure 3-6. The truss members are sized to the loads shown in Figure 3-2. Truss members 1, 3, and 4 are rectangular in cross section, 11.43 cm (4.5 in.) deep and 15.24 cm (6 in.) wide. The section properties are shown in Table 3-2. The elements of the cross section are fabricated from UD B/Al plate, Con Braz joined at the corners to form the cross section. The elements are tapered in thickness where required along the length and tailored to the combined bending and compression load. The members are flared out at the ends and increased in thickness to provide bolt attachment to the corner fittings. Titanium doublers are diffusion bonded to end members to increase the bearing area and transverse strength of the UD B/Al and prevent splitting under the high bearing loads.

Truss members 2 and 5 are primarily tension members. However, they are sized to be capable of reacting the "rebound" compression loads indicated in Figure 3-2 and the combined tension-bending loads indicated. Truss members 1, 3, and 4 are subjected to large compression and bending loads and are sized as a beam column. Because the members are comparatively long and slender, the secondary bending moments due to the axial loads are of considerable proportion. The maximum bending moment occurs at the right end and decreases to a minimum at the left end. The beam member cross section was therefore tapered to the combined loads.

Table 3-2. Truss Beam Section Properties

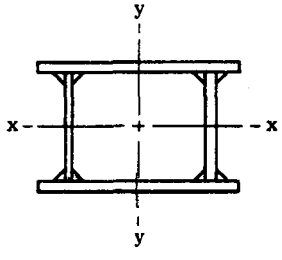

Member 1, 3, and 4

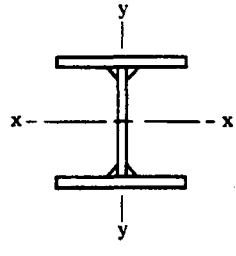

Member 2 & 5

	Left End of Member							Right End of Member						
	Area	I_{x-x}	I_{y-y}	P_{xx}	P_{yy}	$\bar{x}$	$\bar{y}$	Area	I_{xx}	I_{yy}	P_{xx}	P_{yy}	$\bar{x}$	$\bar{y}$
Member	cm^2 (in^2)	$cm^4 \times 10^{-2}$ (in^4)	$cm^4 \times 10^{-2}$ (in^4)	cm (in.)	cm (in.)	cm (in.)	cm (in.)	cm^2 (in^2)	$cm^4 \times 10^{-2}$ (in^4)	$cm^4 \times 10^{-2}$ (in^4)	cm (in.)	cm (in.)	cm (in.)	cm (in.)
1	48.587	8.682	15.119	4.227	5.578	7.62	5.72	48.587	8.682	15.119	4.227	5.578	7.62	5.72
	7.531	20.859	36.323	1.664	2.196	3.00	2.25	7.531	20.859	36.323	1.664	2.196	3.00	2.25
2	14.664	2.709	1.119	4.298	2.824	6.35	5.59	28.942	5.549	2.202	4.379	2.819	6.35	5.59
	2.273	6.509	2.688	1.692	1.112	2.50	2.20	4.486	13.331	5.290	1.724	1.110	2.50	2.20
3	48.587	8.682	15.119	4.227	5.578	7.62	5.72	48.587	8.682	15.119	4.227	5.578	7.62	5.72
	7.531	20.859	36.323	1.664	2.196	3.00	2.25	7.531	20.859	36.323	1.664	2.196	3.00	2.25
4	34.606	6.649	10.616	4.384	5.540	7.62	5.59	39.639	7.060	12.555	4.219	5.629	7.62	5.59
	5.364	15.974	25.505	1.726	2.181	3.00	2.20	6.144	16.962	30.163	1.661	2.216	3.00	2.20
5	9.155	1.875	0.696	4.526	2.756	5.72	5.23	9.155	1.875	0.696	4.526	2.756	5.72	5.23
	1.419	4.503	1.671	1.782	1.085	2.25	2.06	1.419	4.503	1.671	1.782	1.085	2.25	2.06

FOLDOUT FRAME 1

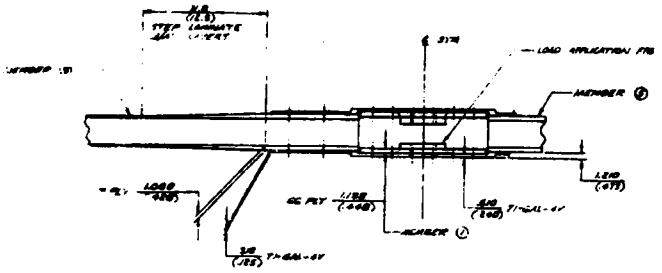

VIEW A-A

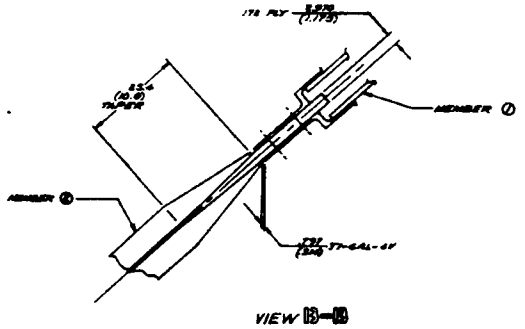

VIEW B-B

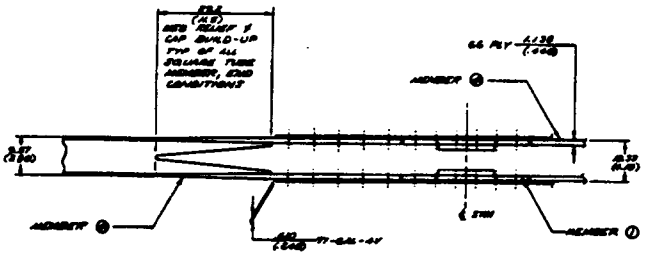

VIEW C-C

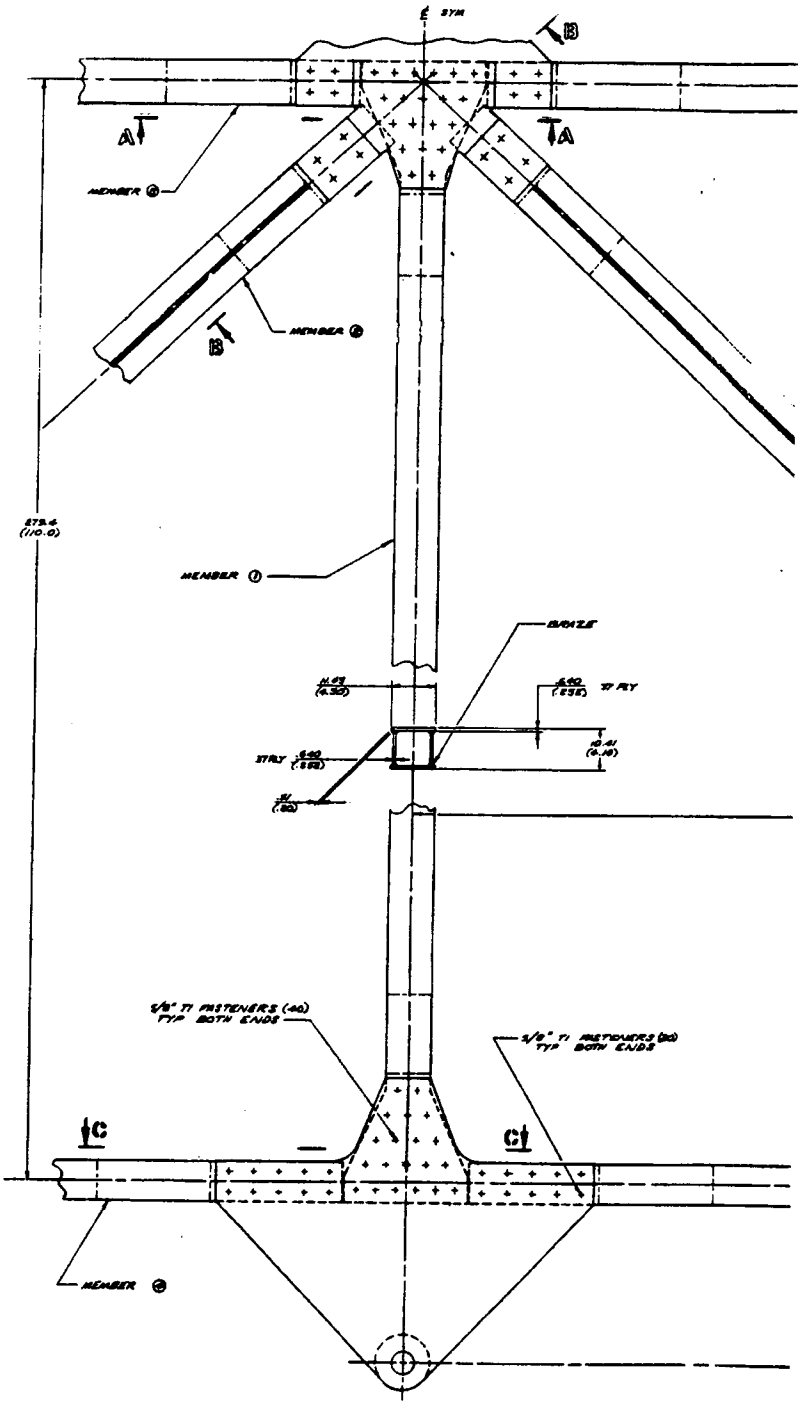

3-9/3-10 A

FOLDOUT FRAME 2

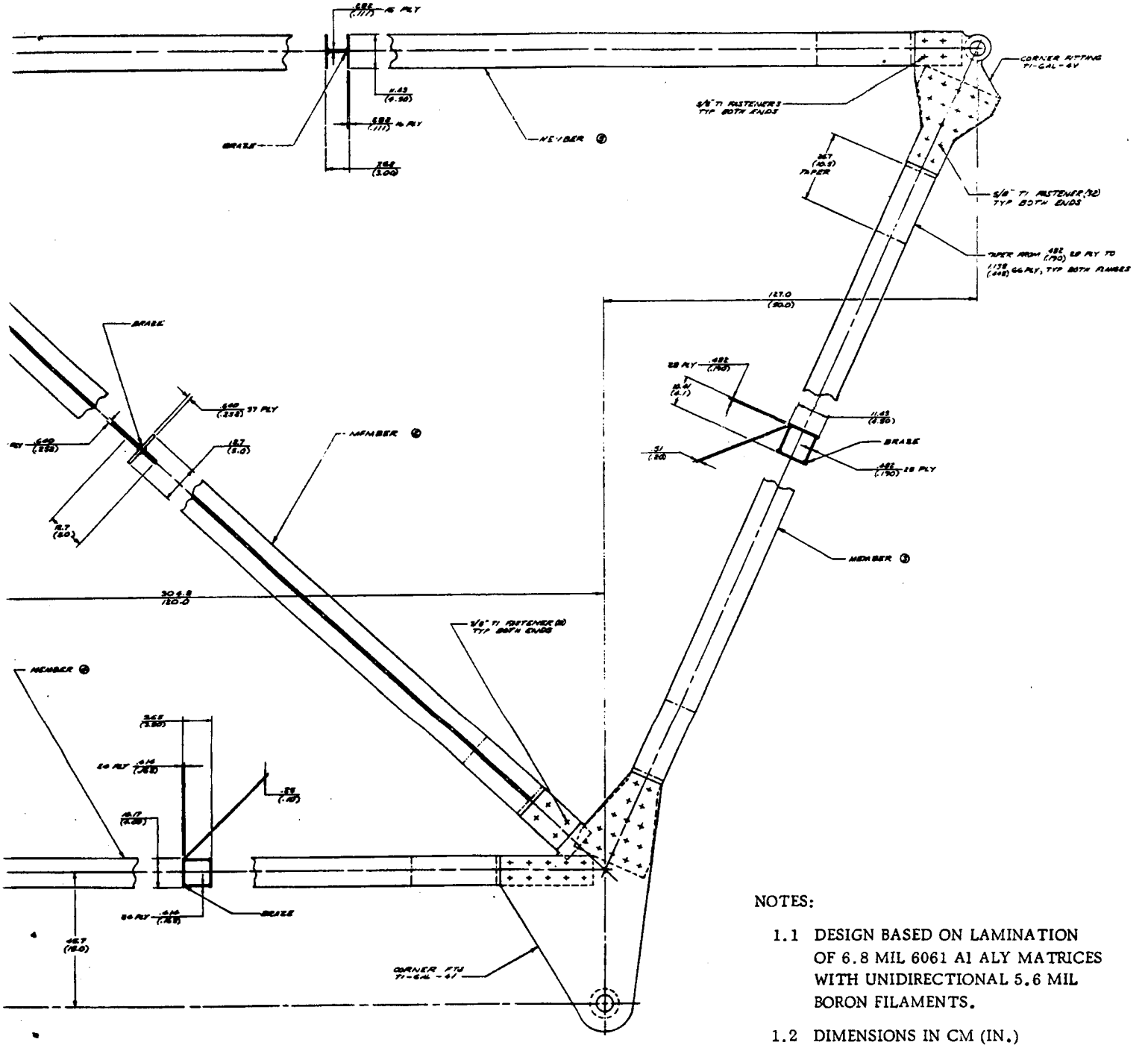

NOTES:

1.1 DESIGN BASED ON LAMINATION OF 6.8 MIL 6061 A1 ALY MATRICES WITH UNIDIRECTIONAL 5.6 MIL BORON FILAMENTS.

1.2 DIMENSIONS IN CM (IN.)

Figure 3-5. Thrust Structure Truss Beam — B/Al Space Shuttle, Square-Tube Configuration

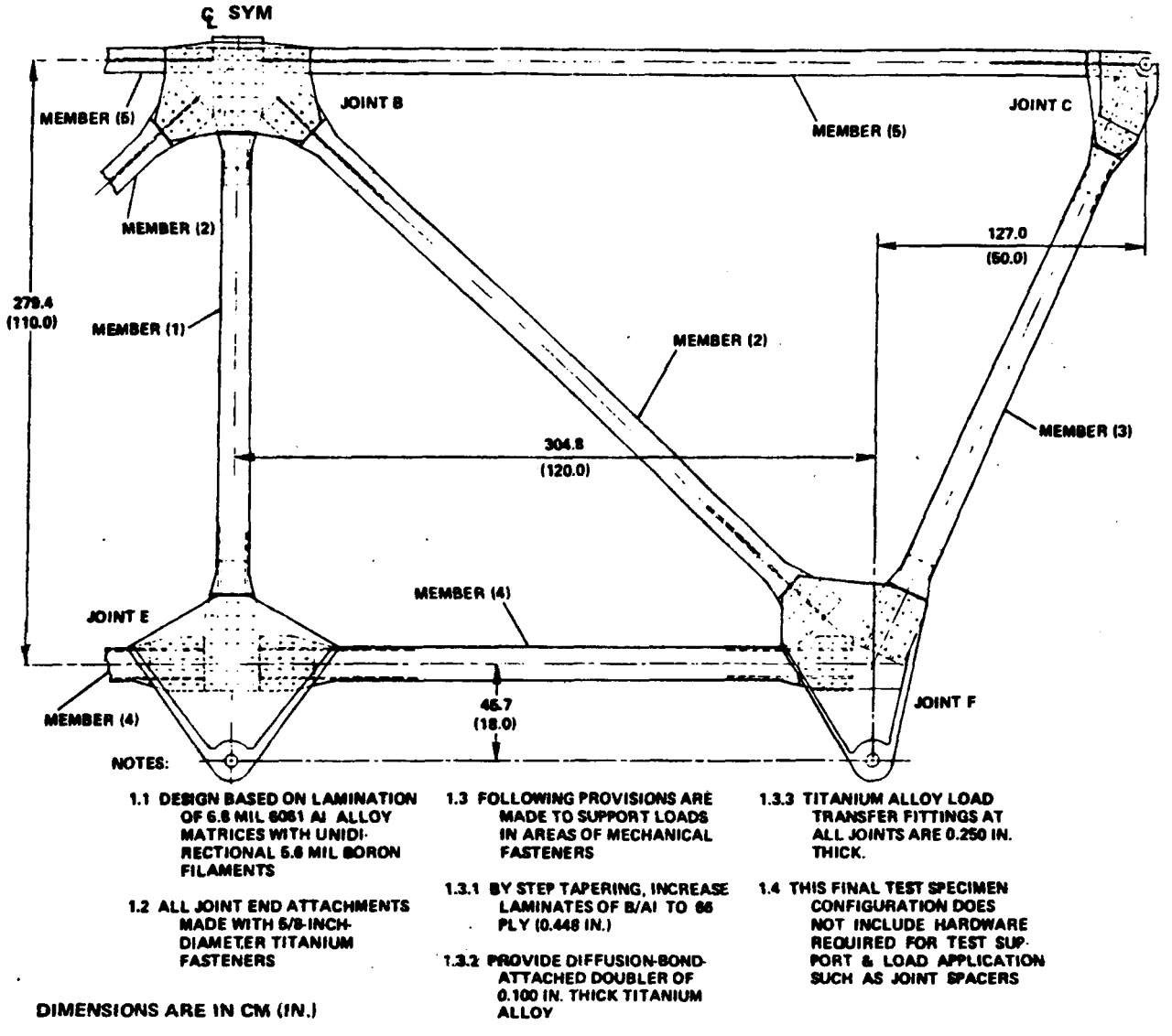

Figure 3-6. Thrust Structure Truss Beam, B/Al Space Shuttle Square-Tube Configuration

The end fittings are essentially two machined gusset plates mounted back-to-back to the truss member ends. The gussets are bolted to the truss members with 1.58 cm (5/8 in.) diameter titanium bolts. A removable nut plate rail assembly provides internal access to the tubular member for fastener attachment.

The estimated weight of the final detail designed truss-beam configuration is 511 kg (1128 lb). A breakdown of the total beam weight is shown in Table 3-3.

The total weight given for the final design of the truss beam is considerably higher than that predicted in the predesign. A majority of this weight difference is due to the load introduction details of the end members. This weight penalty would be applicable to either of the two initial candidate designs; therefore, the selection of the tubular member truss is still valid.

Table 3-3. Summary of Truss-Beam Weight

Item	Unit Weight kg	Unit Weight lb	No. of Units	Total Weight kg	Total Weight lb
Member (1)	49.3	108.6	(1)	49.3	108.6
Member (2)	24.5	56.2	(2)	51.0	112.4
Member (3)	44.7	98.5	(2)	89.4	197.0
Member (4)	42.9	94.6	(2)	85.8	189.2
Member (5)	15.1	33.4	(2)	30.3	66.8
Nutplate Rails			(10)	2.1	4.7
Fasteners			480 each	62.6	137.9
"C" Gusset	5.9	12.9	(4)	23.4	51.6
"B" Gusset	8.4	18.5	(2)	16.8	37.0
"F" Gusset	15.7	34.7	(4)	63.0	138.8
"E" Gusset	19.1	42.1	(2)	38.2	84.2
			Total	511.8	1128.2

Since the time that the study was initially performed, a new process has been developed by which large B/Al tubes may be made with integral titanium end fittings (Figure 3-7). The end fittings and the tubes are joined by diffusion bonding during the tube fabrication process and form a high-strength unit. This concept would permit the use of round B/Al tubes that could be assembled by bolted joints or be welded directly into the truss. It is recommended that in any future truss design, consideration be given to this new development.

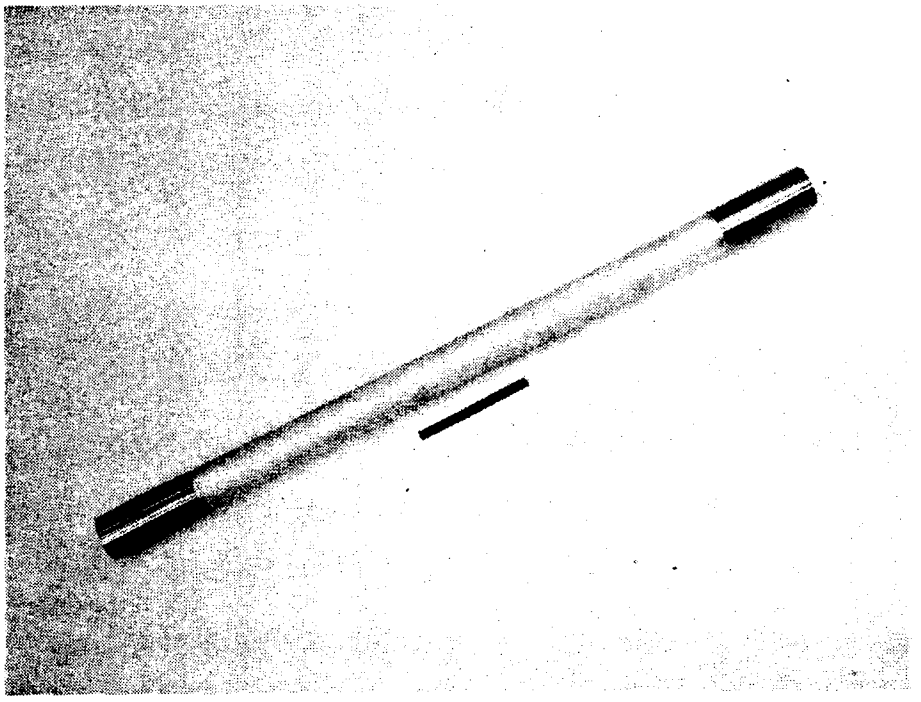

Figure 3-7. B/Al Tube with Diffusion Bonded Titanium End Fittings (128667-B)

3.4 FINAL TRUSS BEAM ANALYSIS

The final truss beam members were analyzed as a beam column. The maximum moment is given by the equation

$$M_{max} = \frac{M_2}{\sin \frac{L}{J}} \qquad \text{where} \qquad J = \sqrt{\frac{EI}{P}}$$

For truss members 1, 2, and 3 the maximum moment occurs near the two-third point along the beam column. The maximum moment in member 4 occurs at the right fitting attachment. The maximum moments are:

	M_{max}		X	
Member	cm-Newtons	inch-lb	meters	inches
1	719.68	637,000	1.384	54.5
2	406.73	360,000	2.794	110.0
3	1434.85	1,270,000	1.633	64.3
4	928.70	822,000	2.499	98.4
5	0	0		

The column strength was determined using the Johnston Euler equation in the form:

$$F_c = F_{cc}\left(1 - \frac{F_{cc}\frac{L'}{\rho}}{4\pi^2 E_c}\right)$$

where

F_c = column strength

F_{cc} = crippling stress — weighted average for the total cross section

L' = $L/\sqrt{C}$ effective column length

ρ = radius of gyration of cross section

The crippling stresses are determined using Figure 3-8, which is plotted in nondimensional form. The material properties used are shown in Volume II. The column allowables are shown in Table 3-4.

Failure under the combined bending and compression was determined by the stress ratio method $\frac{f_c}{F_c} = \frac{f_b}{F_b} = 1$ with the results shown in Table 3-4.

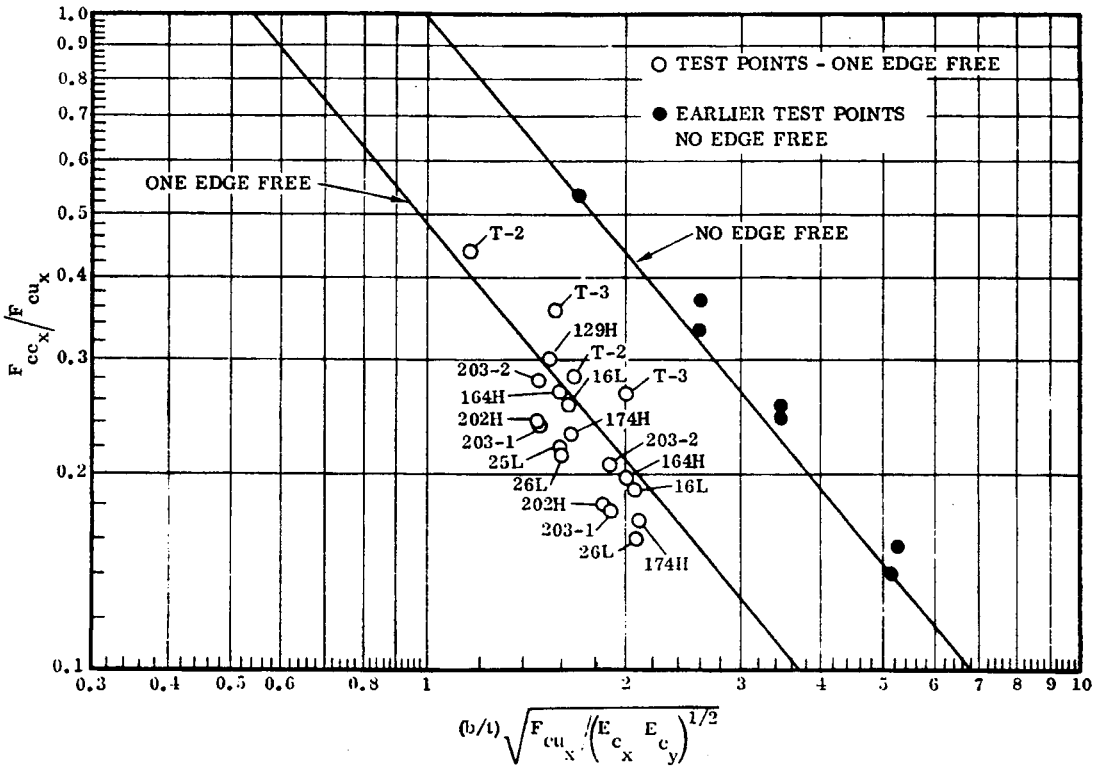

Figure 3-8. Crippling Curves for 50 v/o UD B/6061 Al

Table 3-4. Column Allowables for Final Truss Beam

Member	F_{cc} MN/m^2 (psi)	F_c MN/m^2 (psi)	f_c MN/m^2 (psi)	R_c	f_b MN/m^2 (psi)	F_b MN/m^2 (psi)	R_b	M.S.
1	1341.1 (194,500)	1189.4 (172,500)	827.4 (120,000)	0.697	363.4 (52,700)	1551.4 (225,000)	0.234	+0.07
2	1216.9 (176,500)	792.9 (115,000)	1020.0 (14,800)	0.126	687.4 (99,700)	1551.4 (225,000)	0.44	+0.77
3	1341.0 (194,500)	1151.5 (167,000)	595.0 (86,300)	0.516	724.0 (105,000)	1551.4 (225,000)	0.467	+0.02
4	1172.1 (170,000)	999.8 (145,000)	511.6 (74,200)	0.365	566.8 (82,200)	1551.4 (225,000)	0.365	+0.14 *
	1075.6 (156,000)	937.7 (136,000)	586.1 (85,000)	0.624	392.3 (56,900)	1551.4 (225,000)	0.253	+0.14 **
5	381.3 (55,300)	300.6 (43,600)	85.8 (12,450)	2.5	—	—	—	2.5

F_{cc} = Crippling stress

F_c = Allowable column stress

f_c = Compressive column stress

R_c = Stress ratio in compression

f_b = Maximum bending stress including secondary bending

F_b = Bending modulus of rupture

R_b = Stress ratio in bending

$$M.S. = \left(\frac{1}{R_c + R_b}\right) - 1$$

* Right end

** Left end

The attachments of the gusset plates to the truss members are made with 1.585 cm (5/8 inch) diameter 6Al-6V-2Sn titanium heat treated bolts with an allowable single shear strength equal to 147 kN (33,150 lb).

To prevent splitting of the unidirectional B/Al members under the transverse bolt loads, a titanium plate is diffusion bonded to the B/Al end interface. The bearing loads of the composite-titanium end are taken in proportion to the moduli of the materials. The allowable bearing load is 162 kN (36,500 lb). The truss members introduce a direct compression or tension load and torques into the gusset plates. One-half the load is taken by each gusset plate, and a fitting factor of 1.15 was used. The joint was analyzed as bolt groups (see Figure 3-9) and the maximum bolt loads were determined. The joint strengths of each of the members are shown in Table 3-5.

Table 3-5. Truss Structure Joint Strength

Joint	Member	Max. Bolt Load kN (lb)	M.S.
A & C	3	95.19 (21,400)	+0.40
	5	62.50 (14,050)	+1.12
B	1	88.96 (20,000)	+0.42
	2	109.20 (24,550)	+0.22
	5	62.50 (14,050)	+1.12
D & F	2	132.11 (29,700)	+0.003
	3	129.00 (29,000)	+0.025
	4	100.53 (22,600)	+0.32
E	1	90.74 (20,400)	+0.46
	4	99.19 (22,300)	+0.34

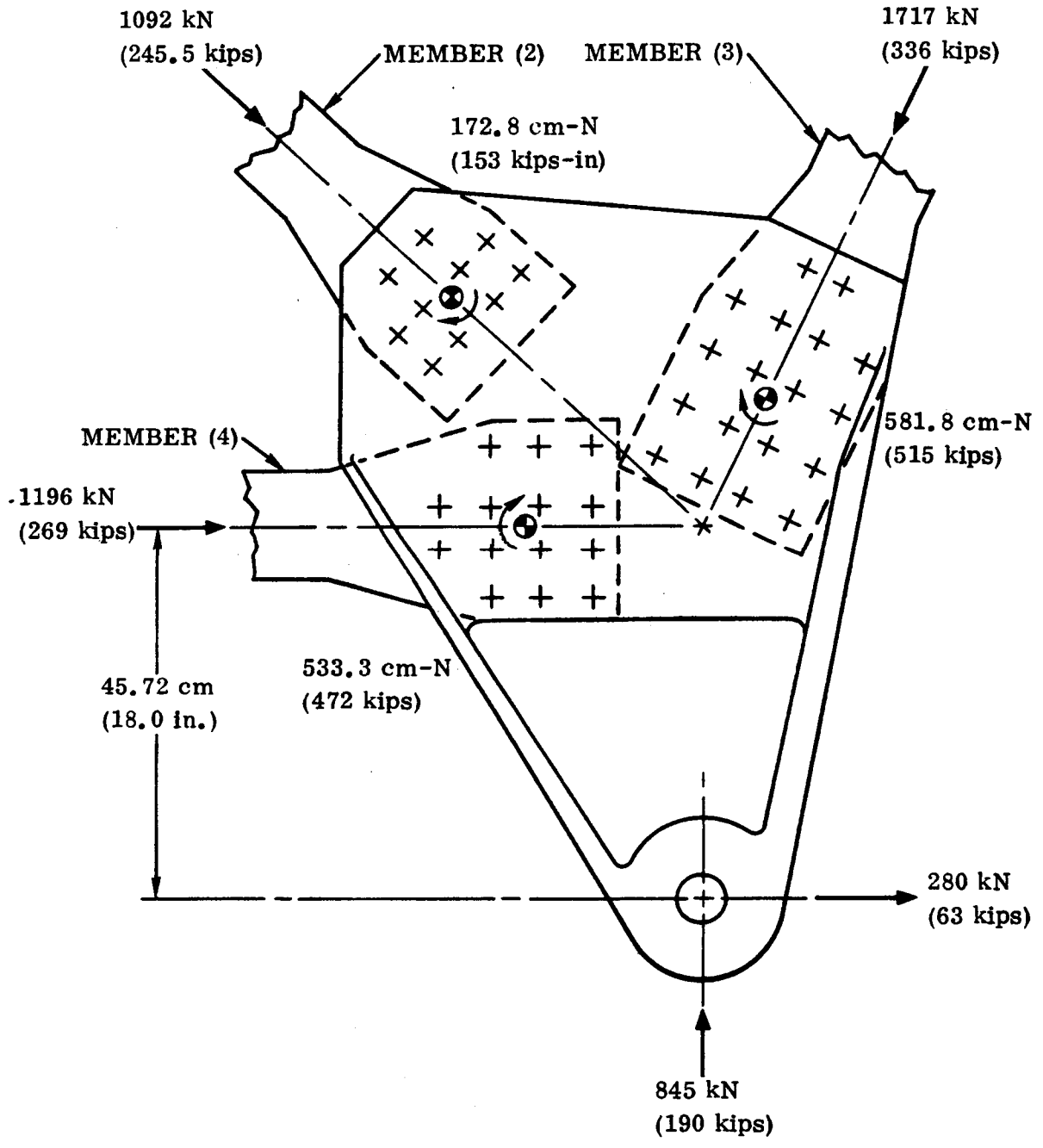

Figure 3-9. Joint "F" Fitting Attachment

SECTION 4

CONCENTRATED LOAD COMPRESSION PANEL

4.1 INTRODUCTION

A compression panel capable of 589K (600F) service was designed. The basic design problem was to receive the 3.2 MN (800,000 pound) concentrated axial compression load at the lower edge of the panel and to distribute this load across the full section of the panel so that the distributed reactant forces across the top (forward) edge of the panel did not exceed 15,300 N/m (8670 lb/in), a factor of 1.3 over the average loading. Thus, a high degree of shear stiffness was required, and stiffness criteria rather than buckling strength controlled the design. The design temperature of 589K (600F) was another major consideration since certain material properties suffer significant degradation at this temperature.

4.2 DESIGN

The compression panel (Figure 4-1) is 3m (120 in.) square, and has a 3.59 MN (800,000 lb) concentrated load that must be sheared out over its length. As a first step in the design study, an evaluation was made comparing stringer- and honeycomb-stiffened panels. The stringer-stiffened skin panel was judged to be superior because it has greater joining flexibility, greater adaptability to tailoring, and was more amenable to conventional inspection techniques.

The final structure was, therefore, configured to a skin-stringer frame design from ±45° crossply B/Al skin having a variable thickness and tailored to the shear flow requirements. An Omega-shaped hat section was selected for the stringer cross section. It most closely approximates the optimum shape for stability under column loading. It reduces the width of the unsupported skin between stiffeners and lends itself to fabrication by Con Clad forming. The stringers are fabricated from unidirectional B/Al sheet and tapered in a cross-sectional area to the load requirements.

The thrust post was configured primarily from unidirectional B/Al. Like the stringer and skin elements, its cross-sectional area is tailored to the load path requirements. This fitting is approximately 82.5 by 160 cm (33 by 64 in.). Its elements may be fabricated into the desired configuration by either the Con Braz process, diffusion-bonding process, or by joining with secondary structural elements.

Frames (see Figure 4-1) provide general stability for the panel. These frames have unidirectional B/Al T-sections for caps and a truss-type web fabricated from titanium. The two are assembled by the spot-joining process.

4.2.1 THRUST FITTING. Several cross-sectional shapes for the thrust fitting were considered. An I-section shape at first seemed the logical solution to the problem of high column loading plus bending due to the offset load point. The three flat elements were to be joined by the Con Braz joining process. The I-section appeared less appropriate when the requirement limiting peaking of the load at the forward edge of the compression panel was taken into account. This necessitated transferring the load from the thrust fitting into the panel web as rapidly as possible, and required a more substantial shear path at the lower end of the thrust fitting/panel web interface close to the load introduction point, than the I-section could give. Consequently, the shape became a compound channel/angle section providing a broad flange interface with the panel web with two stub uprights for column stability. The four shear paths from the uprights feel a shear stress of 36.70 MN/m^2 (5300 psi) maximum, while the full section area 0.0037 m^2 (13.5 in^2) carries 415.0 MN/m^2 (60,000 psi) column stress. The centroid of the section, not including the panel web, lies 3.18 cm (1.25 in.) from the face of the panel web and the 3.55 MN (800,000 pound) load is assumed to act at this point. A load introduction fitting will distribute this load across the area of the section. Since the rate of shear transfer from the thrust fitting into the panel web is intentionally rapid, the fitting cross section dwindles along its 2.3m (7.5 ft) length from the maximum of 93.0 cm^2 (15.5 in^2) to 15.0 cm^2 (2.5 in^2). Material thickness for the fitting varies from 1.27 cm (0.50 in.) to 0.304 cm (0.12 in.).

4.2.2 PANEL WEB. The panel web should logically consist of a single piece, or at least two half-panels spliced down the center. However, due to the dimensional limitations of available composite production facilities, the web design is a fabricated build-up of six separate sheets, each approximately 0.915m x 3.025m x 0.635 cm (3 ft x 10 ft x 1/4 in.), joined edge-to-edge. Splice strips are added at each joint, and the stiffeners are located so that they also contribute to shear splicing. The longitudinal stiffeners and the lateral frame stiffeners effectively divide the panel web into 64 subpanels. The various thicknesses of these subpanels are optimized to give the required overall shear stiffness pattern required by the top-edge peak-load limitation.

4.2.3 STIFFENERS. Significant advantages exist in the choice of a hat section for stiffeners. 1) The stiffeners are subject to high axial loads. The flat elements of the hat section with no edges free are characteristically stable compared to open section shapes. 2) The symmetrical shape is far less likely to develop induced transverse bending due to axial loading than are asymmetric shapes. This is an important consideration where transverse properties are lower than longitudinal properties.

The hat section stiffeners for this panel have a cross section area of 6.46 cm^2 (1.0 in^2) maximum. Two methods of manufacture are available for the stiffeners. Both are relatively low cost methods and start with flat UD B/Al sheet. In the first method, the shapes are hot formed on equipment using heated dies. The second is the Con Clad process that utilizes thin sheet steel bonded to the surface of the B/Al to permit cold forming. Either process can produce hat section stiffeners suitable for this panel.

FOLDOUT FRAME 1

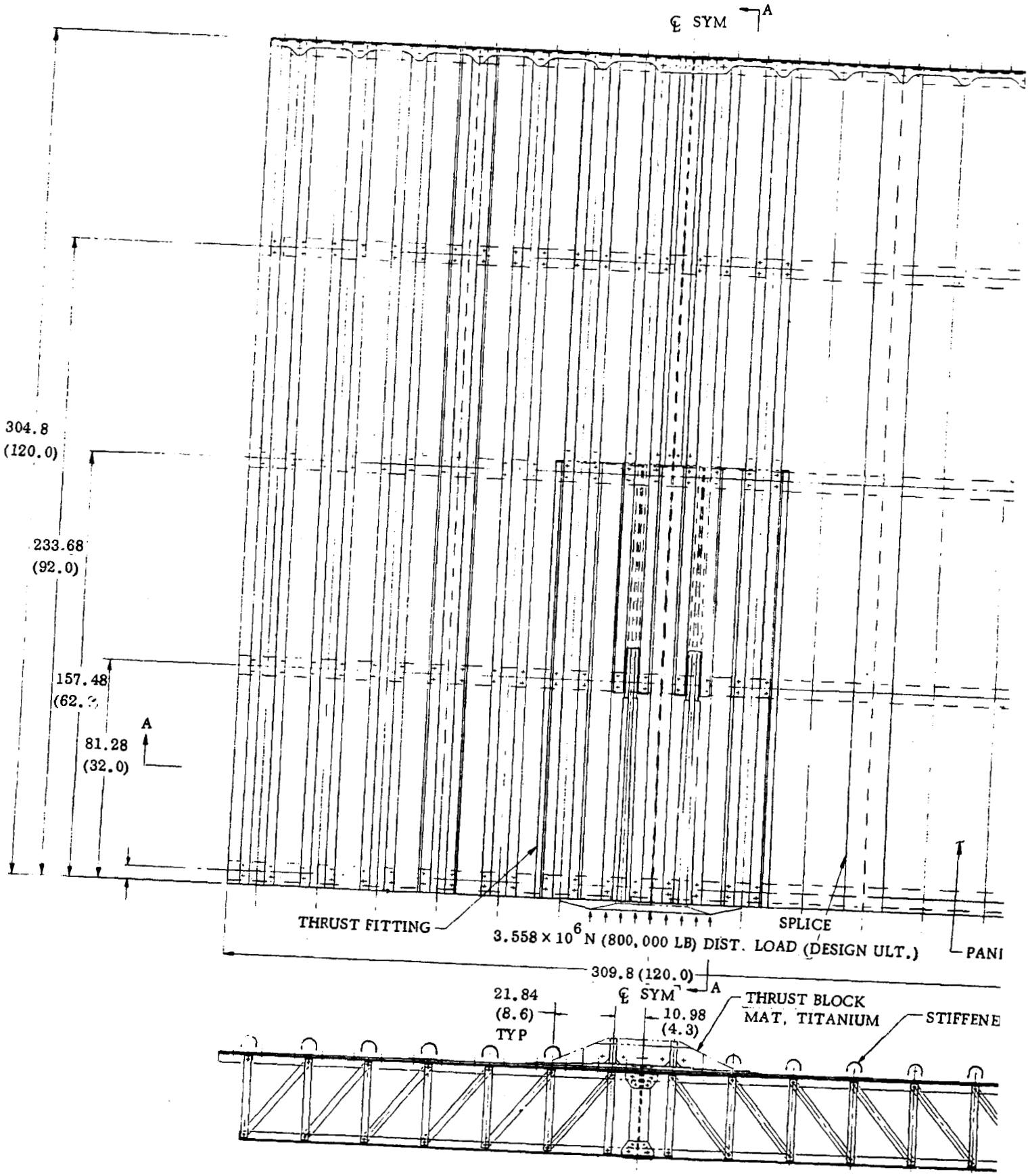

4-3/4-4 A

Figure 4-

FOLDOUT FRAME 2

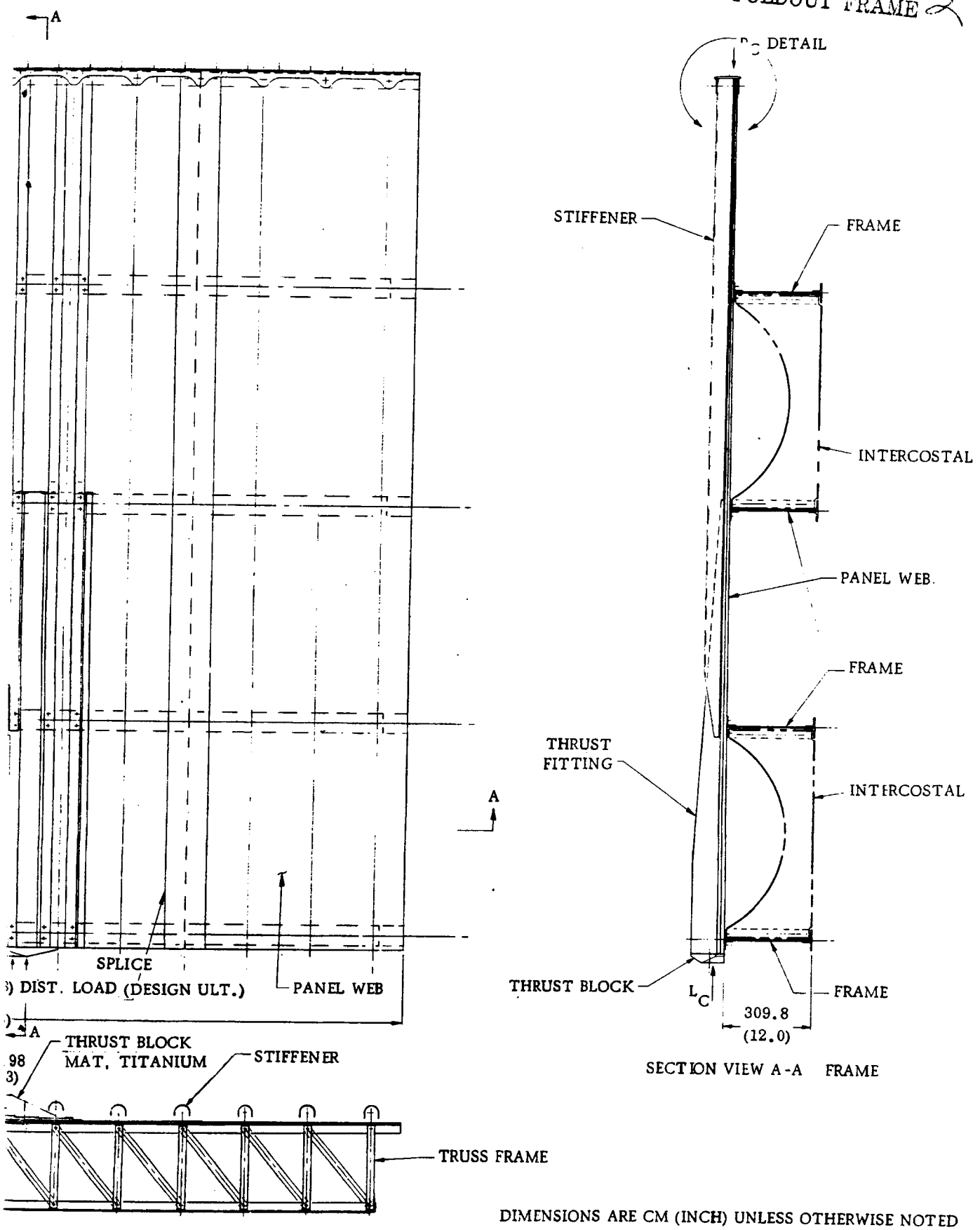

DIMENSIONS ARE CM (INCH) UNLESS OTHERWISE NOTED

Figure 4-1. B/Al Composite Compression Panel Assembly

The weight of the boron/aluminum compression panel has been calculated to be 256 kg (565 lb). This represents a weight savings of approximately 17% from an all titanium structure. The final weight summary is shown below.

	Weight Summary kg	(lb)
Shear Web	122.40	277.0
Stiffeners	34.40	78.0
Frames	47.00	106.0
Thrust Fitting	28.60	65.0
Upper Edge Closure	6.20	14.0
Splices	6.20	14.0
Thrust Block	4.55	10.0
Fasteners	0.45	1.0
Total	256.0	565.0

4.3 STRUCTURAL ANALYSIS

Structural analysis for this study made use of a finite element model that simulated the structural flexibilities and boundary conditions for calculation of internal load distribution. The model is shown in Figure 4-2. The model represents a half-structure 304.8 x 152.4 cm (120 x 60 in.) having stringers at equal 21.84 cm (8.58 in.) spaces with half-panels at each side 10.81 cm (4.29 in.). The length is divided into four bays by five frames at 76.2 cm (30 in.) spacing. Detail structure is simulated by bar elements (stringers and frames) and by rectangular or triangular elements (webs). The frame element simulates only the flange adjacent to the panel.

For internal load analysis the structure was divided into a basic grid of nodes forming 19 x 7.62 cm (7.5 x 3 in.) rectangles. The area adjacent to the centerline and load-introduction structure was further subdivided to form a grid with half the vertical spacing of the basic grid. Triangle panels provide the transition between the two areas of different grid sizes. The left side of the model (the structure centerline) is constrained against lateral (X) movement because of symmetry. The right side is allowed to move, as is the bottom. The top side, which must provide a relatively uniform load transfer to the vehicle structure, is reacted by a simulated structure of titanium, two bays long, with the top constrained against longitudinal (Y) movement.

The load introduction structure at the bottom centerline is simulated with a set of bar elements and web elements that overlay the basic structure and cover an area 30.48 cm (12 in.) wide (in the half-structure) by 152.4 cm (60 in.) long. The design loading

3.558 MN (800,000 pounds) ultimate, is applied 1.779 MN (400,000 pounds) to each side. It is applied to the model as centered 10.89 cm (4.29 in.) from the centerline side in three increments: 0.296; 1.186; and 0.296 MN (66,667; 266,667; and 66,667 pounds) at X = 0, 27.66, and 32.72 cm (X = 0, 10.89, and 12.88 in.) respectively.

The structure is also loaded by the effects of thermal expansion, which is calculated for a uniform temperature of 589K (600F).

4.3.1 FINITE ELEMENT MODEL. The plane stress program P5543 utilizes the structural model previously discussed and analyzes its elements with the equations associated with a two-degree-of-freedom network to define member stresses at element centroids and deflections at nodes. Bar loads for stringers and frame flange are uniaxial and the axial load output is representative of the loading midway between node points. The adjacent panel shears modify the axial stringer load at the node points. The panel segments are plates subject to biaxial in-plane loading and shear. The webs are analyzed as simply supported panels between stringers and are strength checked for stress interaction.

The programmed model assigns five separate material call numbers to identify materials with a group of elements. These five call numbers can be made by any combination of materials and a solution can be obtained for internal load distribution. The material groups are:

No. 1 – Panel Webs
No. 2 – Panel Stringers
No. 3 – Support Structure (webs and stringers)
No. 4 – Applied Load Post
No. 5 – Applied Load Webs

The web materials can be either isotropic or anisotropic. The "bar" materials must be isotropic material.

4.3.2 WEB ANALYSIS. For web analysis, the structure's plate is divided into a gridwork of rectangular plates. The computer PLNST analysis determines in-plane loading of axial loads and shears. For isotropic materials the principal stresses are also output. For orthotropic webs the principal stresses are not significant and the stresses in the laminate (construction) axes are output on computer cards in the format usable in laminate analysis P5127.

Panel strength is determined by P5127 computer analysis of the laminate using the natural axis strength allowables of the various lamina. Failure of fibers in any orientation is considered ultimate strength for the laminate. The loading is calculated as acting from centerline to centerline of stringers. Figure 4-3 summarizes the web strength margins of safety.

FOLDOUT FRAME

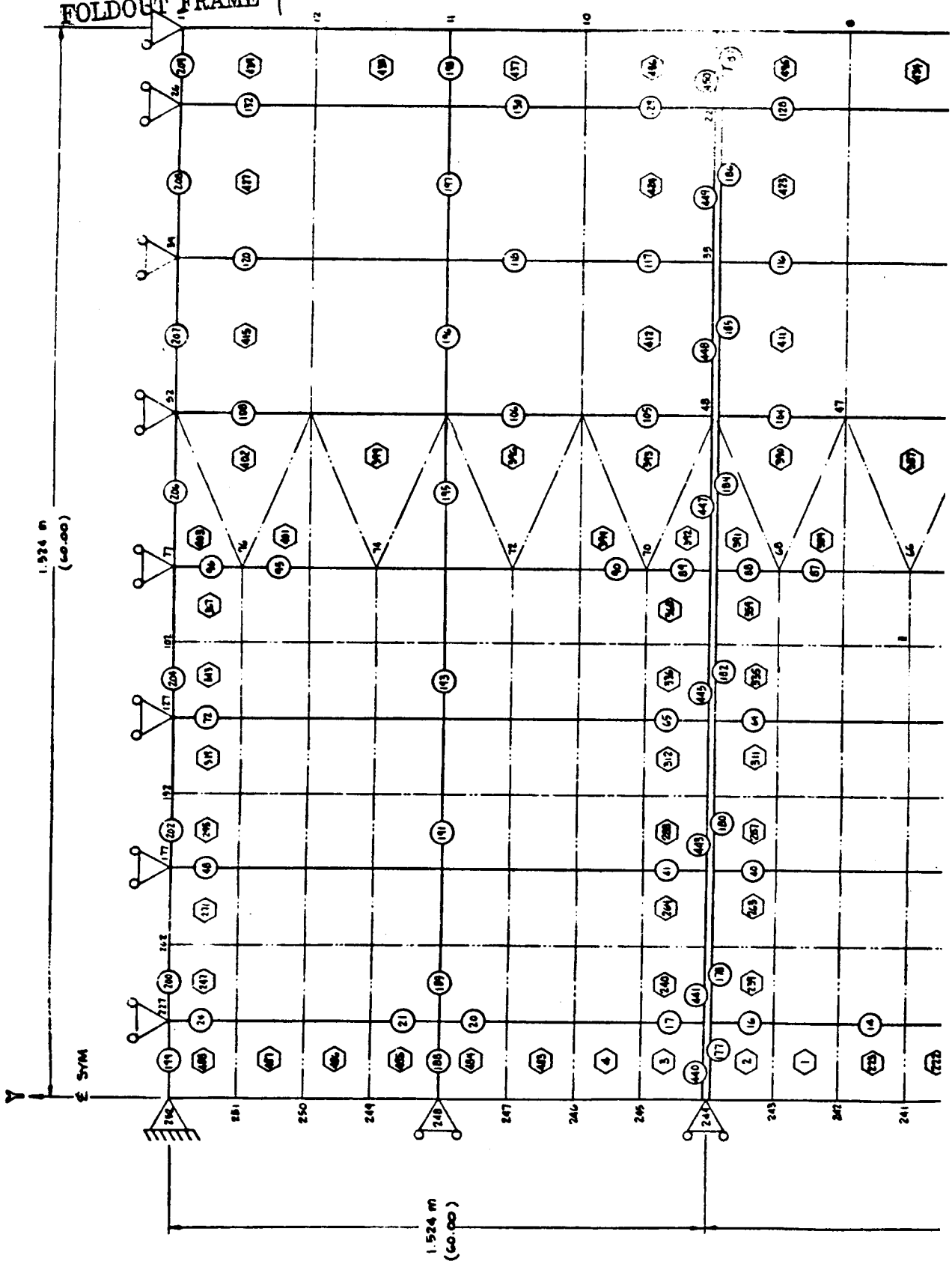

4-7/4-8 A

FOLDOUT FRAME

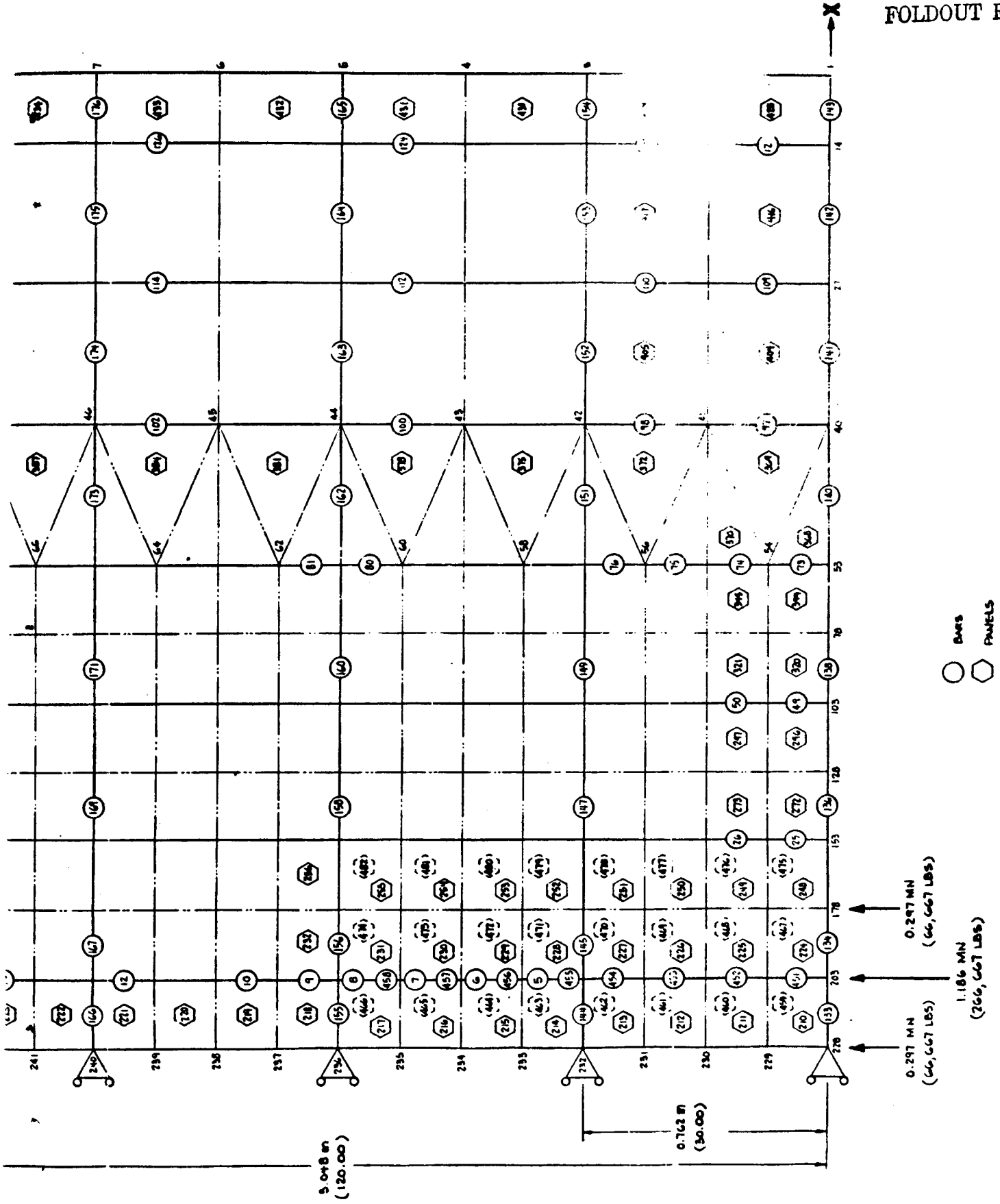

Figure 4-2. Structural Model of Compression Panel

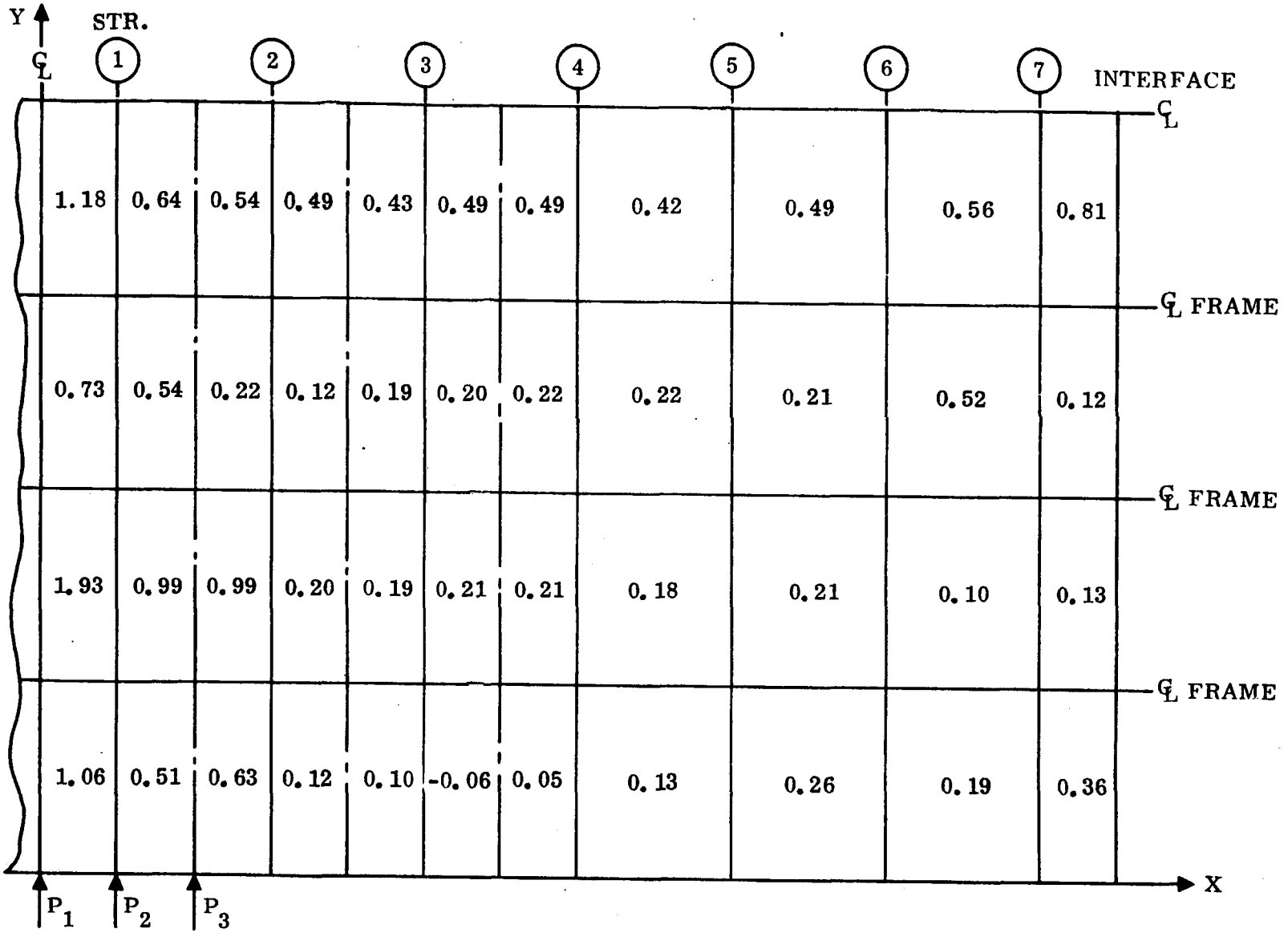

Figure 4-3. Web Plane Strength Margin of Safety at 589K (600F)

A panel buckling analysis was incorporated into the P5543 program to determine the load interaction buckling margins of the panel webs. Each element loading intensity was considered active over the full panel size; i.e., the model evaluated a 12.7 by 76.2 cm (5 by 30 in.) panel simply supported between stringers and frames whereas the full panel is simulated by two or more elements. The criterion used for panel buckling is the biaxial buckling equation from Reference 10, Equation 4.3.2.7, biaxial compression,

$$N_{x_{cr}} = \frac{\pi^2}{b^2}\left[\frac{D_{11}m^4\left(\frac{b}{a}\right)^4 + 2(D_{12}+2D_{66})m^2n^2\left(\frac{b}{a}\right)^2 + D_{22}n^4}{m^2\left(\frac{b}{a}\right)^2 + \phi\, n^2}\right]$$

where

$$\phi = \frac{N_y}{N_x}$$

for orthotropic materials, or the shear buckling equation for orthotropic plates (Reference 10, 4.3.2.13),

$$N_{xy_{cr}} = \left(\frac{2}{b}\right)^2 (D_{11}D_{22}^3)^{1/4}\left(8.125 + \frac{5.05}{\theta}\right)$$

where

$$\theta = \frac{(D_{11}D_{22})^{1/2}}{D_{12}+2D_{66}} > 1 \qquad \frac{a}{b} = \alpha$$

or (Reference 10, 4.3.2.14),

$$N_{xy_{cr}} = \left(\frac{2}{b}\right)^2 \left[D_{22}(D_{12}+D_{66})\right]^{1/2}(11.7 + .532\,\theta + .938\,\theta^2)$$

where

$$\theta = \frac{(D_{11}D_{22})^{1/2}}{D_{12}+2D_{66}} < 1$$

The interaction buckling strength margin of safety was calculated using strength ratios in the relation

$$M.S. = \frac{2}{R_c + \sqrt{R_c^2 + 4R_s}} - 1$$

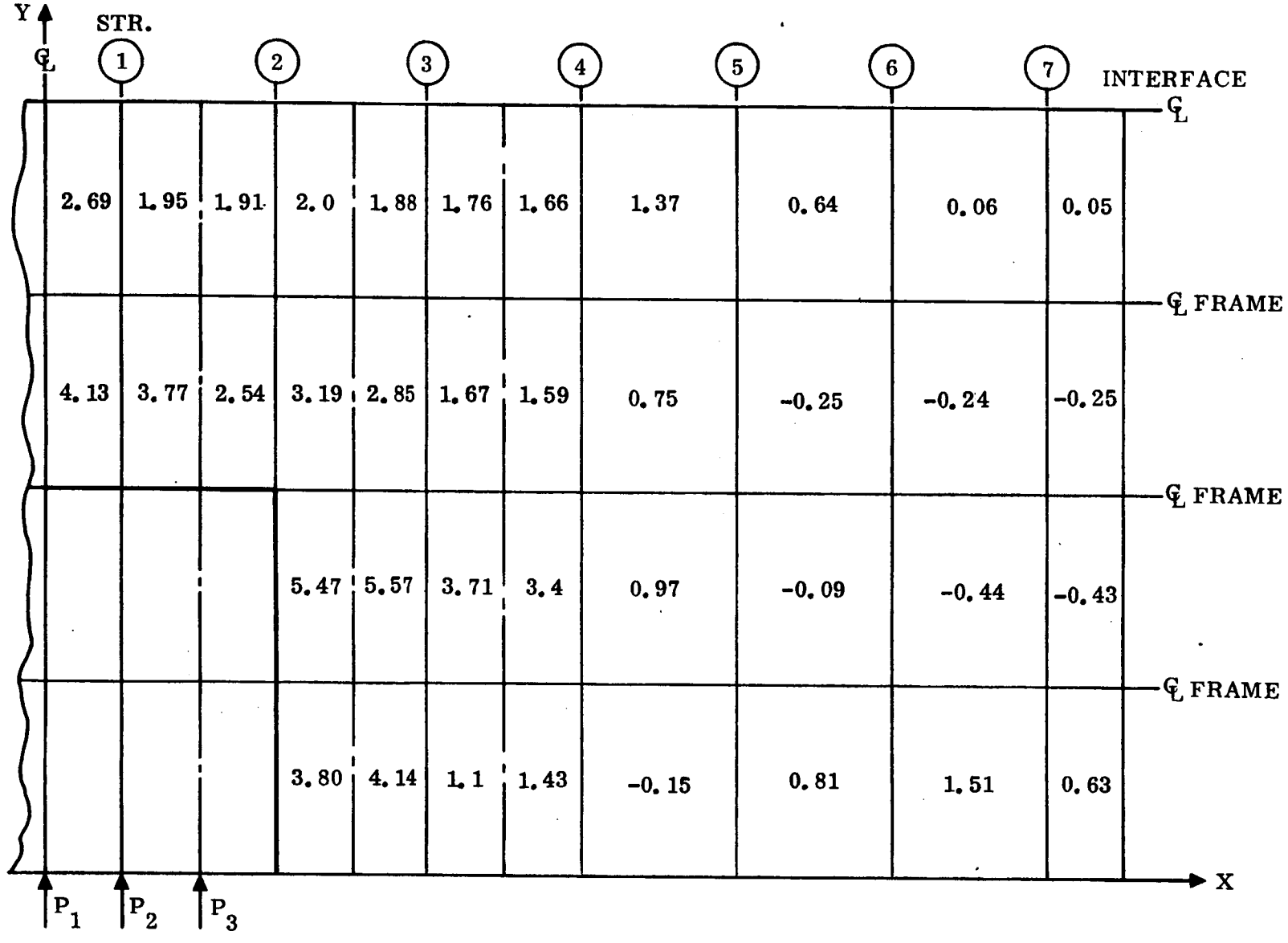

Figure 4-4. Web Buckling Margins of Safety at 589K (600F)

The computer analysis of the buckling, summarized in Figure 4-4, shows some large margins but the efficiency is considered satisfactory since considerations of shear stiffness and load distribution may be more significant than the margin of safety for buckling. Figure 4-5 shows the possible gage reduction factor based on a margin of safety and the thickness sensitivity of t^3.

4.3.3 STRINGER ANALYSIS. The stringer analysis considers two basic failure modes, local crippling of stringer elements and column stability.

Local crippling of the stringer elements is based on b/t for each element, one edge free or all edges simply supported, using nondimensional crippling curves available for the material. These curves equate $F_{cc}/F_{tu_{11}}$ against

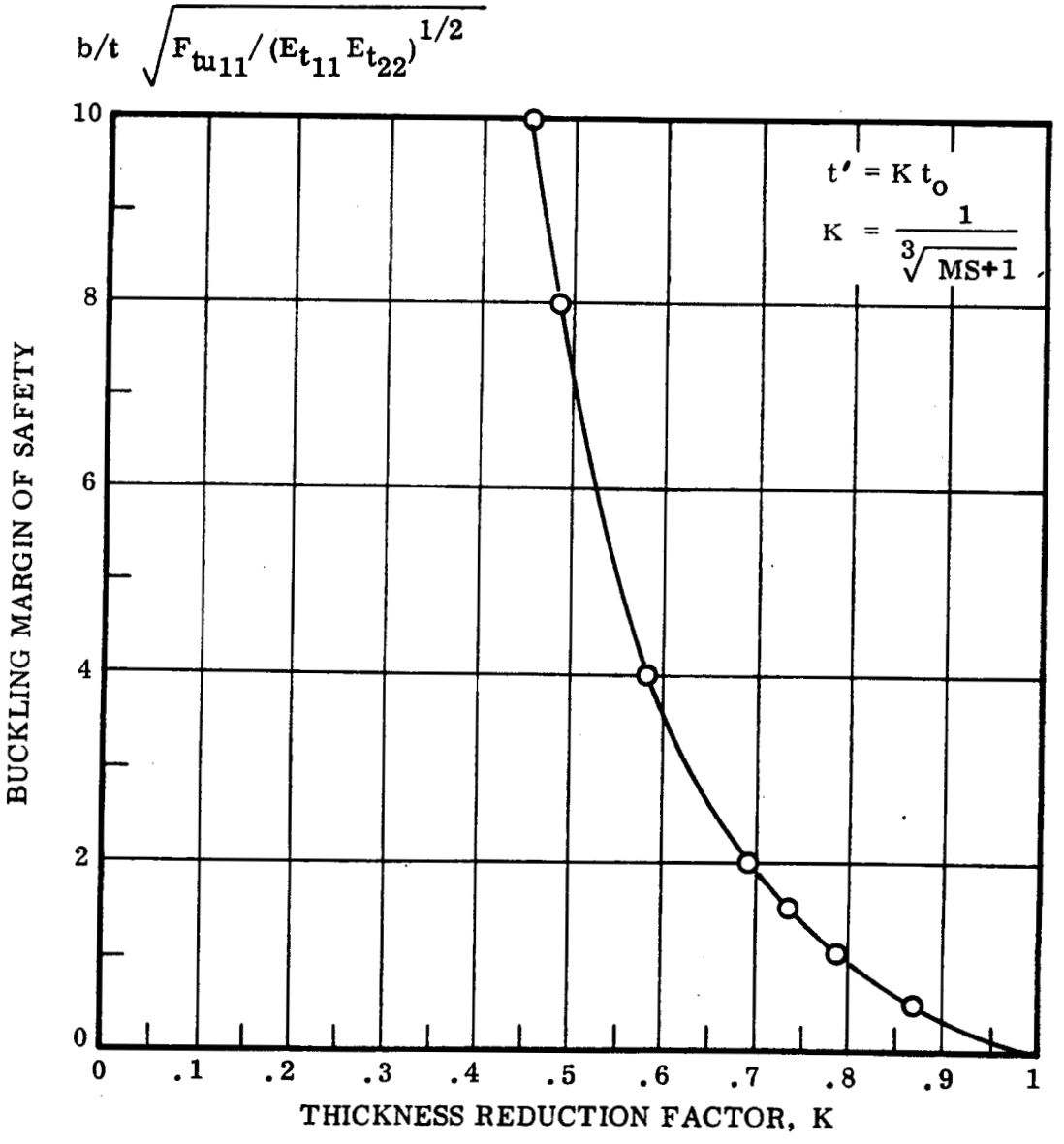

Figure 4-5. Web Gage Reduction Factor Based on t^3 Efficiency

The b/t is determined for thicknesses that are multiples of the basic lay-up so that the axial stiffnesses do not vary. In general the thickness is kept constant and any section area variation is produced by varying the height of the stringer.

Column stability is checked for pin-ended columns of web and stringer supported by the frames. The stability check is for the Euler column with an appropriate crippling cutoff using the Johnson parabolic cutoff criteria. The column load consists of the stringer axial load and the effective web axial load (between stringers). The webs have been checked for load interaction stability and are considered unbuckled. Areas are adjusted for compatibility stiffness. Table 4-1 summarizes the stringer loads.

4.3.4 FRAMES. The plate stringer structure is supported by deep frames at 30-inch spacings. The deep frames are assumed to provide plane stiffness by the adjacent flange area only. The frame stiffness enforces column inflection at the frames. The flange area is for an EI requirement of

$$EI = \frac{N_x b^4}{4 L \pi^2}$$

where

N_x = 1.516 MN/m (8660 lb/in)

b = 304.8 cm (120 inches)

L = 76.2 cm (30 inches)

EI = 4.958 MN/m^2 (1.728 x 10^9 lb-in^2)

The trade study used a constant one-square-inch flange area for the stabilizing frames, which requires a frame depth of

$$h = \left(\frac{17.28 \times 10^8 \times 2}{1}\right)^{1/2} = 5.86 \times 10^4 / (E)^{1/2} \text{ inches.}$$

4.3.5 CONCLUSION. The ability of the panel design to meet the design objectives is summarized in Figures 4-6 and 4-7. These figures show the shear flow distribution across the panel at various heights and the running load intensity across the top of the panel. The requirement to keep the maximum load intensity below 1.3 average has been achieved.

Table 4-1. Summary of Stringer Axial Loads (P_y)

Str. No.	1	2	3	4	5	6	7
Y \ X→	4.28	12.86	21.43	30.00	38.57	47.14	55.71
3.75		6,058	4,363	2,721			
7.50	-	-	-	-	1,536	1,101	538
11.25		-721	3,159	2,872			
18.75		-5,048	-1,462	-793			
22.50	-	-	-	-	-827	-876	-1,392
26.25		-6,732	-5,817	-5,454			
33.75	-9,708	-12,144	-9,411	-7,611			
37.50	-	-	-	-	-5,095	-4,255	-4,102
41.25	-12,954	-12,772	-10,984	-11,388			
48.75	-16,072	-15,429	-12,659	-14,645			
52.50	-	-	-	-	-12,082	-9,793	-8,453
56.25	-26,839	-19,951	-14,536	-16,725			
63.75	-70,563	-36,474	-19,862	-21,012			
67.50	-	-	-	-	-18,062	-14,738	-12,362
71.25	-69,089	-36,032	-22,375	-23,161			
78.75	-61,899	-34,484	-23,981	-24,948			
82.50	-	-	-	-	-22,577	-19,335	-17,589
86.25	-54,759	-32,976	-25,053	-26,056			
93.75	-47,511	-32,417	-28,150	-25,447			
97.50	-	-	-	-	-23,023	-20,348	-19,766
101.25	-41,56	-31,647	-28,394	-26,052			
108.75	-37,366	-30,858	-28,139	-26,215			
112.50	-	-	-	-	-24,811	-24,029	-23,484
116.25	-32,601	-29,669	-27,615	-25,894			

Note: For clarity only English units are shown (dimensions in inches, loads in pounds)

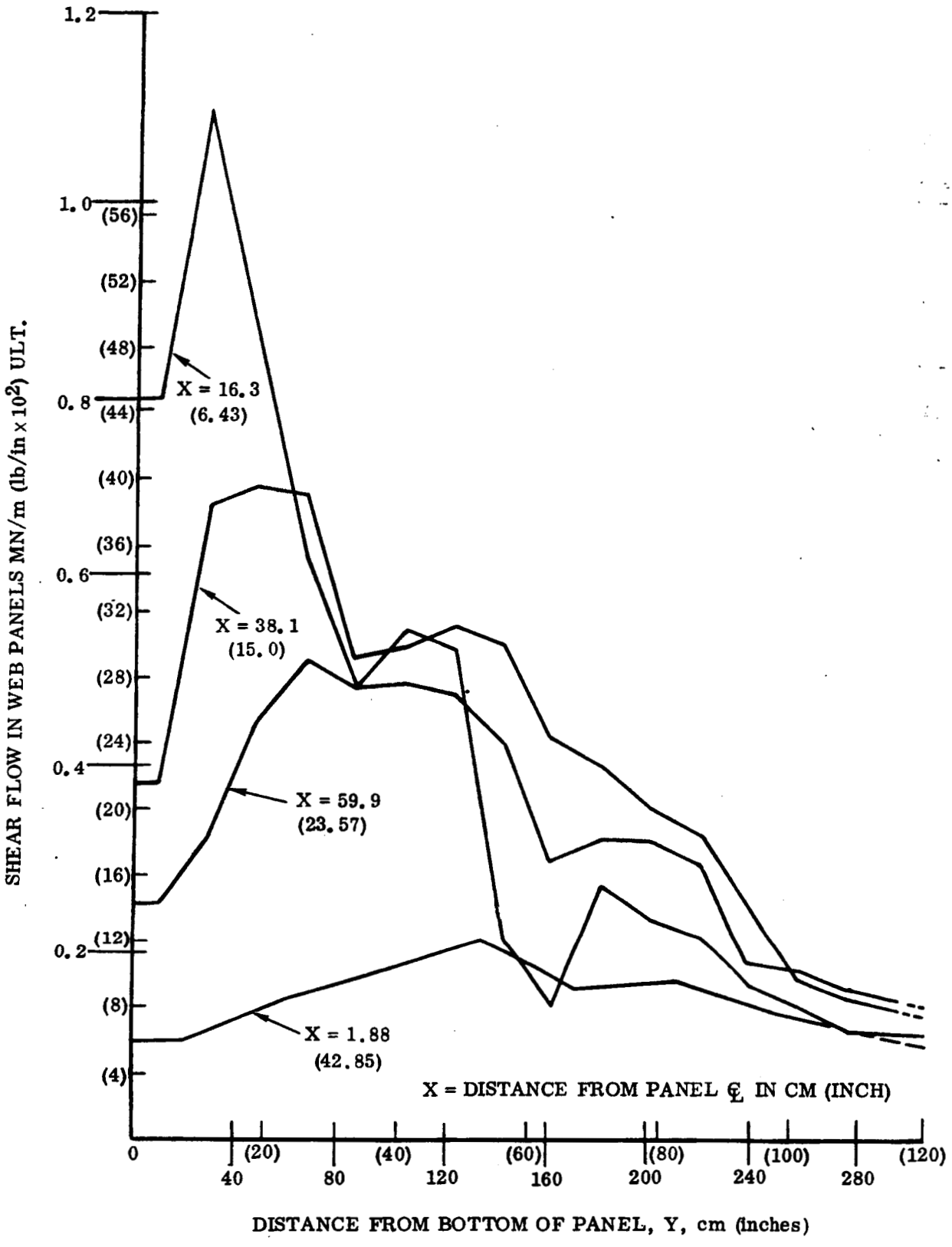

Figure 4-6. Shear Flow Distribution Curves by Distance from Panel Centerline at 589K (600F)

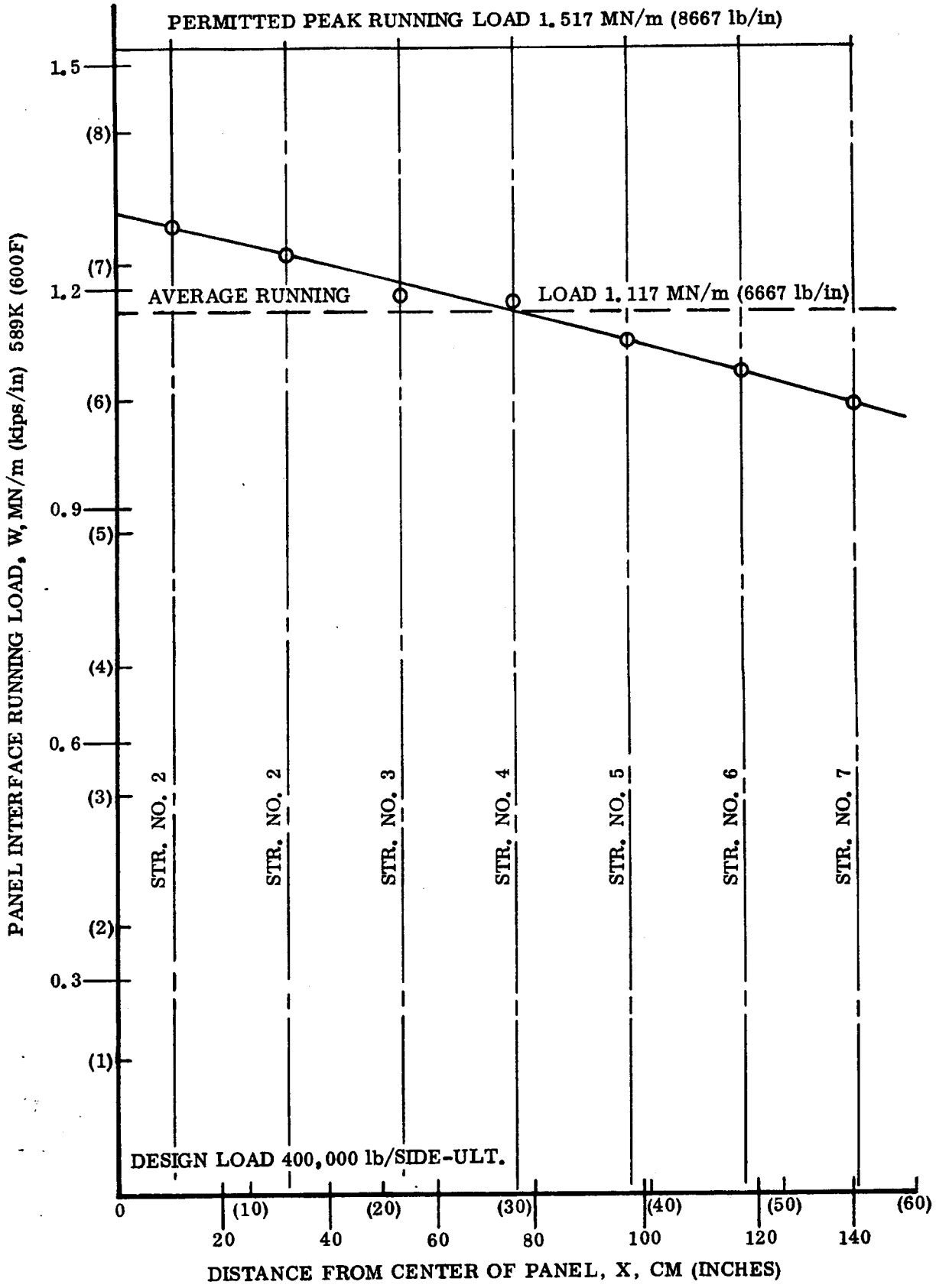

Figure 4-7. Plot of Interface Load Versus Distance from Center of Panel and Applied Load

SECTION 5

UNIFORMLY LOADED COMPRESSION PANEL

5.1 INTRODUCTION

The task objective was to design and fabricate a uniformly loaded boron/aluminum (B/Al) compression panel using fabrication processes and techniques directly applicable to a full-scale, space shuttle structure.

5.2 DESIGN CRITERIA

The uniformly loaded compression panel was designed and analyzed to the criteria given in Table 5-1.

Table 5-1. Panel Design Criteria

Load	P_{ult} 1.26 MN/m (7200 lb/in)
Material	5.6 mil boron/6061 aluminum
Temperature	589K (600F)
Safety factors	1.1 yield, 1.4 ultimate
Panel supports	
Edges	Simple support
Ends	Simply supported
Frames	Optional

5.3 PANEL DESIGN

The uniformly loaded compression panel (Figure 5-1) was designed to withstand a uniformly applied compression load of 1.26 MN/m (7200 lb/in). The panel simulates a section of space shuttle booster thrust structure with frames spaced at 101.6 cm (40 in.). A two-bay panel is then 203.2 cm (80 in.) long. The test panel has a frame in the center and when tested will require simple support at the ends. (See Appendix A for detail drawings of the compression panel.)

5.3.1 PANEL SKIN. For the given loading conditions a unidirectional skin could have been used; however, the actual flight conditions would include shear strains in addition to the compression load. Since the magnitude of these shear strains was unknown, and to make the panel as realistic as possible, a skin/ply orientation was chosen that possesses more shear capability than a completely unidirectional orientation. A $[\pm 45/0_3]_S$ orientation was therefore chosen for the skin. A single piece of skin 73.6 by 200 cm (29 by 79 in.) was used for the panel so that no splices were required.

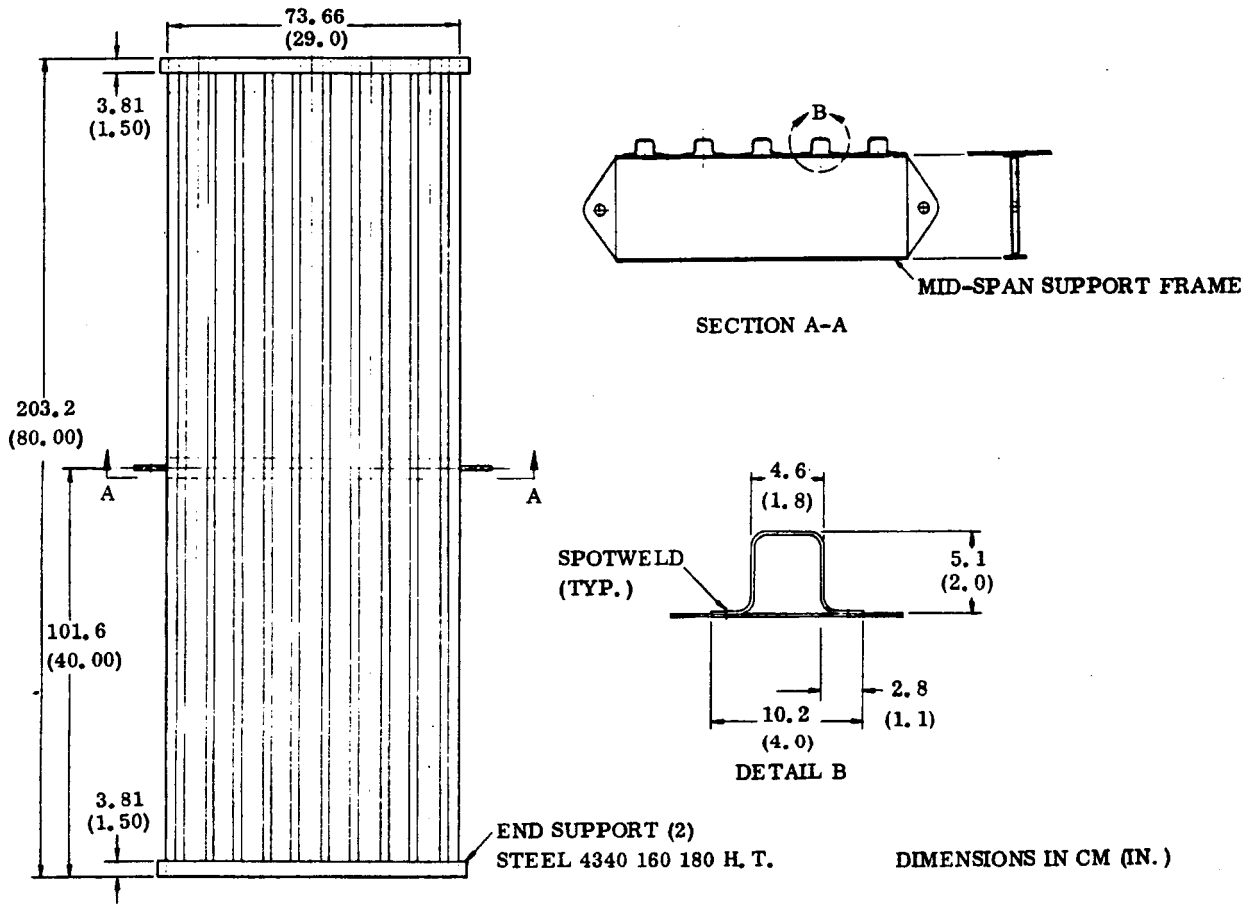

Figure 5-1. Hat-Section-Stiffened Compression Panel

5.3.2 PANEL STIFFENERS. The primary load path for the panel consisted of five B/Al hat-section stiffeners. The stiffeners were constant thickness [0_{14}] B/Al with cross section as shown in Figure 5-2.

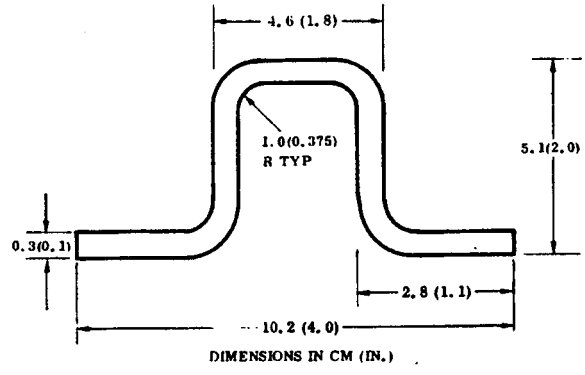

Figure 5-2. B/Al Stiffener Cross Section

The stringers are attached to the skin by spot welding. Mechanical fasteners were also considered but were to be used only in the event that the spotwelding failed to produce the needed strength.

Subelement and subcomponent testing (Section 5.5) proved that spot welds had adequate strength at the test temperature; therefore, it was not necessary to use mechanical fasteners.

5.3.3 LOAD INTRODUCTION BLOCKS. The load introduction fittings at each end of the panel are made from steel blocks, slotted to receive the ends of the skin and stringers (Figure 5-3). The slots are then filled with foaming polyimide during bonding of the end plates to the panel. This method had been used on numerous high-temperature crippling specimens and compression panels, and was a simple, convenient method of load introduction for high temperature testing.

The knife edge supports required for testing may be bolted to the flat end plates as necessary.

5.3.4 PANEL FRAME MEMBER. The center frame of the panel consists of a built-up titanium I-section frame (Figure 5-4). Legs were provided at each end of the frame for attachment to the testing machine. The frame was sized to ensure simple support at the center of the panel. This sizing included the calculation of the minimum spring rate of the support struts (see Section 5.6). The frame is attached to the panel by steel locks bolts. Both Number 6 and Number 8 sizes were used.

5.3.5 COMPLETED COMPRESSION PANEL. Figure 5-5 is a photograph of the completed B/Al compression panel. A detailed description of the fabrication of the component test specimen is presented in Volume II.

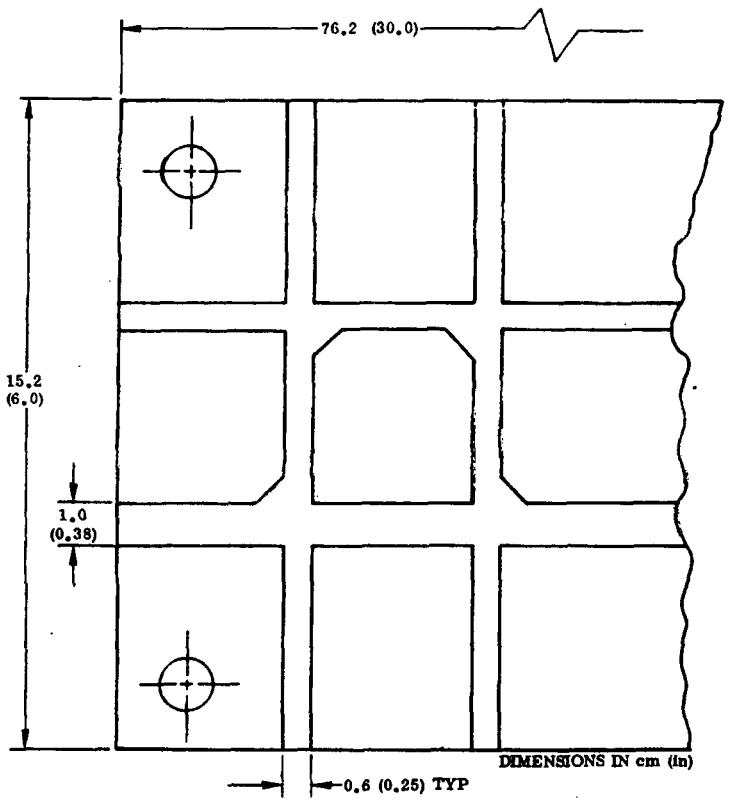

Figure 5-3. Steel End Fitting

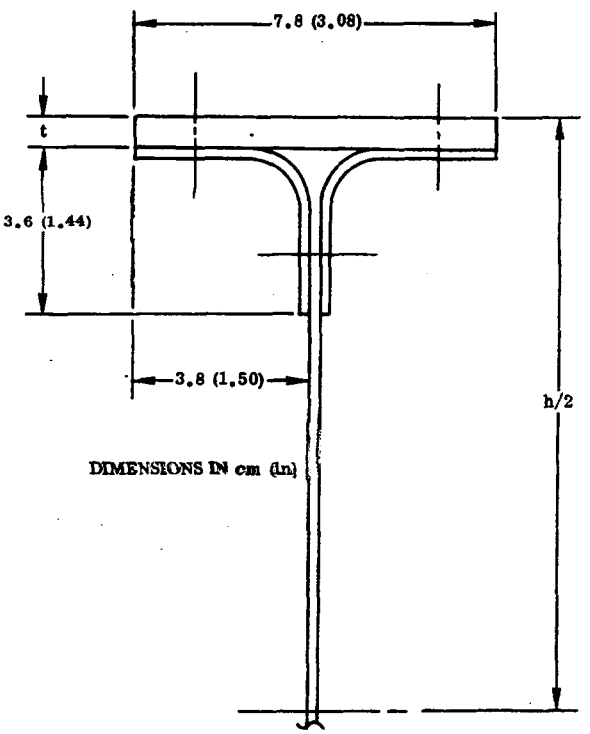

Figure 5-4. Titanium Frame Detail

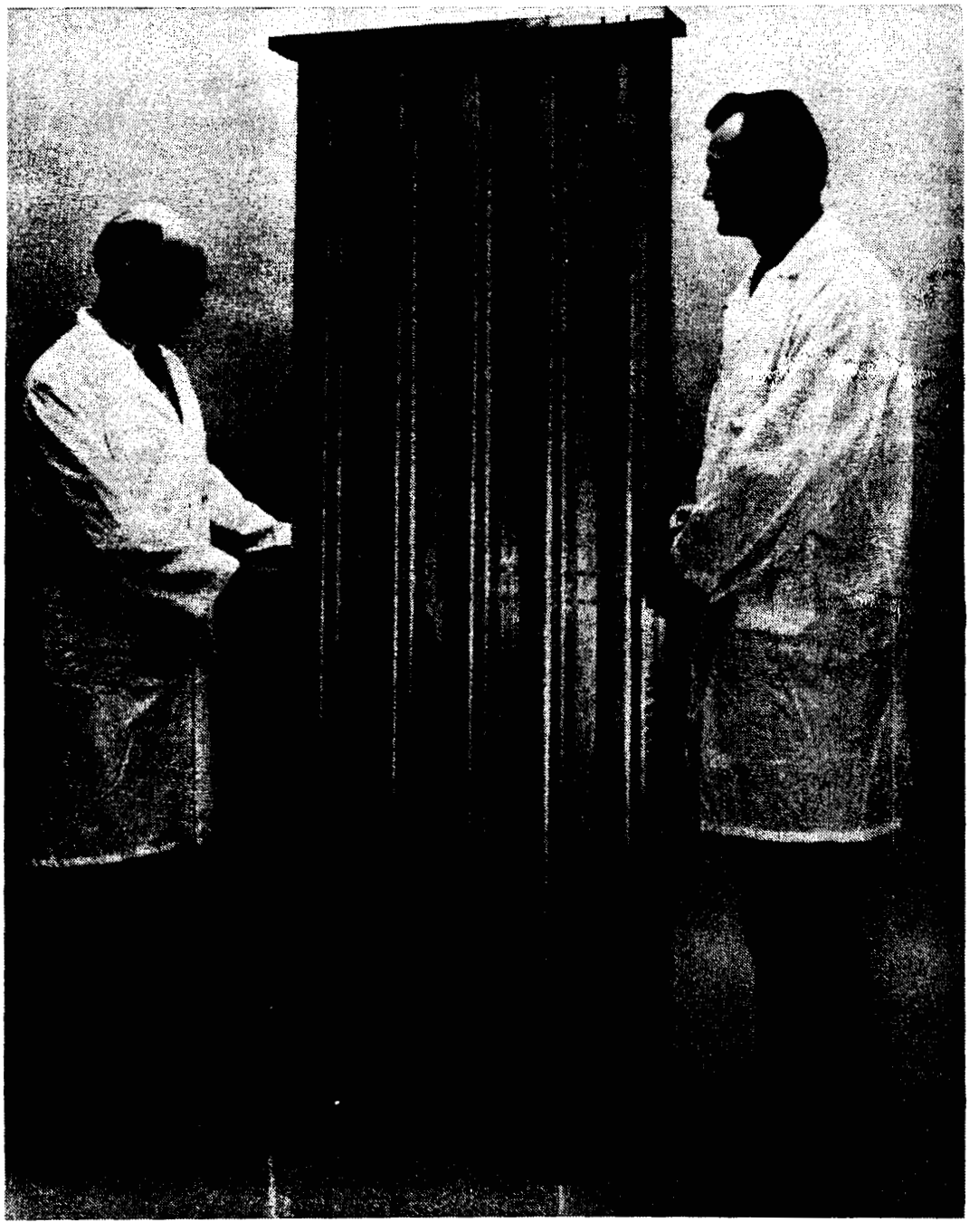

Figure 5-5. Stringer Side of Completed B/Al Compression Panel (133438B)

5.4 COMPRESSION PANEL ANALYSIS.

The compression panel analysis was made for a centrally loaded panel using the basic analysis procedure for conventional sheet stiffener construction given in Reference 11. For this method each stiffener together with an effective width of sheet is treated as a column using the Johnson 2.0 parabola equation in the form

$$F_c = F_{cc} - \frac{F_{cc}^2 (L'/\rho)^2}{4\pi^2 E_c}$$

where

F_c = Short column strength

F_{cc} = Stiffener weighted average crippling stress

L' = Effective column length ($L/\sqrt{c}$ where c is the end fixity coefficient)

ρ = Radius of gyration of cross section

E_c = Modulus of elasticity in compression

The procedure for determining the critical stress end load is:

a. Determine the slenderness ratio (L'/ρ) for the stiffener alone about the centroidal axis parallel to the sheet.

b. Compute the crippling stress (F_{cc}) of the stiffener cross section.

c. With F_{cc} and L'/ρ from (a) and (b) above, compute the allowable column stress F_{co} using the Johnson 2.0 parabolic short-column buckling equation

$$F_{co} = F_{cc} - \frac{F_{cc}^2 (L'/\rho)^2}{4\pi^2 E_{c_{11}}}$$

d. Determine the effective width of sheet acting with the stiffener at a stiffener stress F_{co} from (c). The effective width for a sheet stiffener combination or different materials is given by

$$\frac{2W_e}{t} = \frac{1.7 E_s \text{ (sheet)}}{\sqrt{E_s \text{ (stiff)}}} \sqrt{\frac{1}{F_{co}}}$$ (Reference 12)

For the hat section stiffener, an effective width of $2 W_e$ acts at each flange.

e. Compute ρ for the stiffener plus effective sheet and hence L'/ρ.

f. Recompute the critical column stress using L'/ρ from step (e).

g. Repeat steps (d), (e) and (f) until satisfactory convergence of F_{co} is obtained.

h. The critical load, P_c, is given by

$$P_c = F_{co} [A_{st} + t_s \Sigma W_e]$$

This procedure is applicable only to a centrally loaded column and hence, to avoid eccentricity of loading in the proposed test where pinned-end conditions are simulated, the end fixtures should apply the load at the centroid of the effective section at failure; i.e., at the centroid of the effective section computed for the final iteration for F_{co}.

5.4.1 CRIPPLING ANALYSIS. The crippling analysis of the unidirectional B/Al stringer was based on the method presented in Reference 11. In this method, the hat section stiffener is subdivided into elements as shown.

The crippling widths (b_i) are given by

$$b_2 = W_2 + W_3/2 \quad \text{(one edge free)}$$

$$b_5 = W_5 + \frac{(W_4 + W_6)}{2} \quad \text{(no edge free)}$$

$$b_8 = W_8 + W_7 \quad \text{(no edge free)}$$

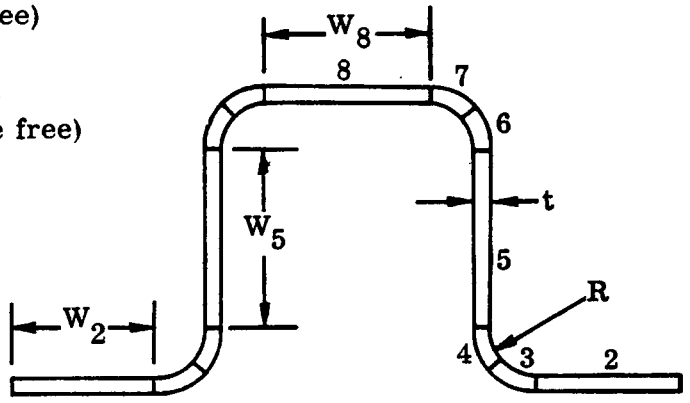

and where

$$F_{cc_3} = F_{cc_2}$$

$$F_{cc_4} = F_{cc_6} = F_{cc_5}$$

$$F_{cc_7} = F_{cc_8}$$

The crippling analysis is made using Figures 5-6 and 5-7. The overall crippling stress is a weighted average value, i.e.,

$$F_{cc} = \frac{\Sigma F_{cc_i}}{\Sigma A_i}$$

By this process the crippling strength of the hat section stiffener at 589K (600F) was calculated to be 458.8 MN/m^2 (66,500 psi).

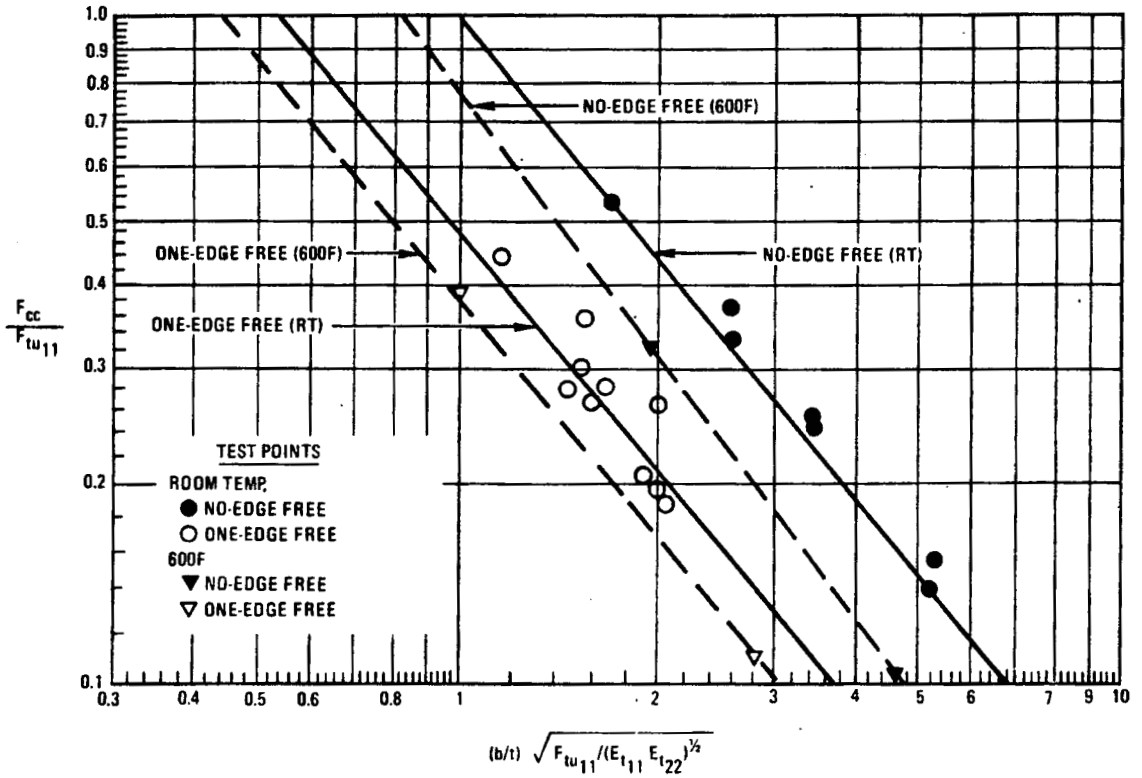

Figure 5-6. Nondimensional Crippling Curves for UD B/Al Composites

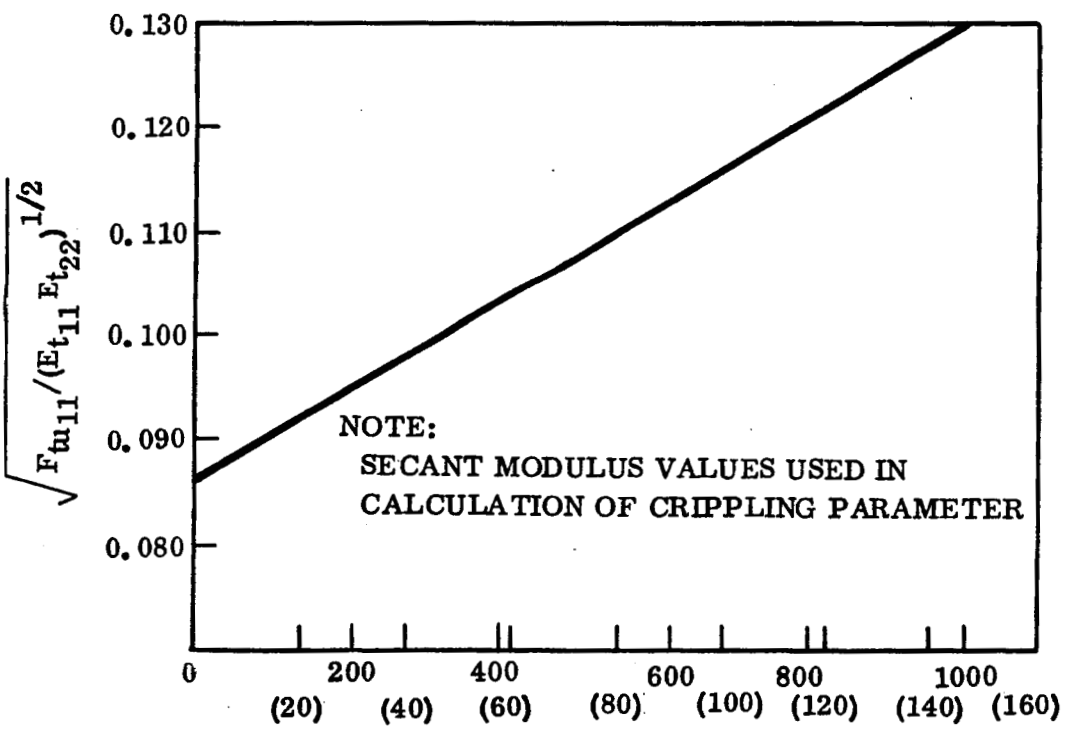

Figure 5-7. Element Crippling Parameter vs Element Stress for UD B/Al at 589K (600F)

5.4.2 SECTION PROPERTIES. The initial approximation for the critical column stress was based on the section properties of the stiffener only; i.e., the contribution of the sheet was neglected.

Item	A	y	Ay	Ay^2	I_o
1	0.1380	0.1156	0.01595	0.00814	—
2	0.0632	0.0526	0.00332	0.00017	—
3	0.0632	0.2813	0.01778	0.0050	—
4	0.2017	1.068	0.21542	0.2300	0.019
5	0.0632	1.6915	0.1069	0.1808	—
6	0.0632	1.9202	0.12136	0.2330	—
7	0.0818	2.0204	0.16527	0.3339	—
Total	0.6743		0.646	0.9847	

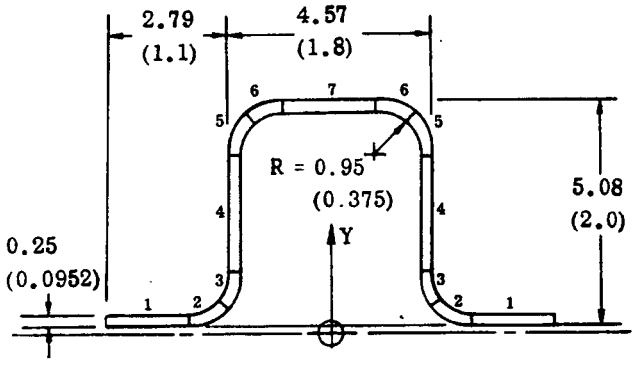

DIMENSIONS IN CM (IN.)

$$\bar{y} = \frac{\Sigma Ay}{\Sigma A} = 2.42 \text{ cm } (0.958 \text{ in.})$$

$$I_{NN} = \Sigma Ay^2 + \Sigma I_o - \Sigma Ay \cdot \bar{y} = 16.02 \ \mu m^4 \ (0.385 \text{ in}^4)$$

$$\rho = (I/A)^{1/2} = 1.45 \ (0.571)$$

$$L/\rho = 70.07$$

5.4.3 COLUMN ANALYSIS

Stiffener Only (No Sheet)

Short Column Stress:

$$F_{co} = F_{cc}\left(1 - \frac{F_{cc}\,(L'/\rho)^2}{4\pi^2 E}\right)$$

$$= 293.7 \text{ MN/m}^2 \ (42{,}606 \text{ psi})$$

Effective width of sheet at above stress

$$\frac{2W_e}{t} = \frac{1.7\,E_s \text{ (sheet)}}{\sqrt{E_s \text{ (stiff)}}} \sqrt{\frac{1}{F_{co}}}$$

where $2W_e$ is the effective width acting at each flange of the hat section.

Total effective width

$= 10.43$ cm (4.017 in.)

Section properties for stringer plus 10.43 cm (4.017 in.) of sheet.

$\bar{y} = 1.76$ cm (0.692 in.)

$I_{NN} = \Sigma Ay^2 + \Sigma I_o - \Sigma Ay \cdot \bar{y} = 22.91\ \mu m^4$ (0.5506 in^4)

$\rho = 1.94$ (0.762)

$\frac{L'}{\rho} = 52.466$

Stiffener Plus 10.43 cm (4.17 in.) Effective Sheet

$$F_{co} = F_{cc}\left(1 - \frac{F_{cc}\,(L'/\rho)^2}{4\pi^2 E}\right)$$

$= 366.24$ MN/m^2 (53,125 psi)

Effective width of sheet at above stress

$= 9.14$ cm (3.60 in.)

Section properties with 9.14 cm (3.6 in.) effective sheet

$\bar{y} = \frac{\Sigma Ay}{\Sigma A} = 1.8$ cm (0.712 in.)

$t = \Sigma Ay^2 + \Sigma I_o - \Sigma Ay \cdot \bar{y} = 22.4\ \mu m^4$ (0.5382 in^4)

$\rho = (I/A)^{1/2} = 1.94$ cm (0.7653 in.)

$L'/\rho = 52.27$

Short Column Stress

$F_{co} = 366.94$ MN/m^2 (53,227 psi)

Previous approximation, $F_{co} = 366.24$ MN/m^2 (53,125 psi)

Hence F_{co} has converged sufficiently

$$F_{co} = 366.94 \text{ MN/m}^2 \text{ (53,227 psi)}$$

Allowable column load

$$P_{co} = F_{co} (A_{stiff.} + t\Sigma W_e)$$

$$= 53,227 \times 0.9191$$

$$= 217 \text{ KN (48,920 lb)}$$

Ultimate design load

$$= 7200 \times 5.8$$

$$= 185 \text{ KN (41,760 lb)}$$

$$\text{M.S.} = \frac{48,920}{41,760} - 1 = +0.17$$

5.5 SUBCOMPONENT DESIGN AND ANALYSIS

Two subcomponents of the compression panel were designed and tested to verify the structural integrity of the elements. The first of these was a stringer compression specimen that was intended to be a 46 cm (18 in.) long, flat ended, crippling specimen for testing at 589K (600F). A testing error damaged this specimen. It was subsequently repaired and retested as a 33 cm (13 in.) long combination skin-stringer crippling specimen.

A second stringer-only crippling specimen was then made and tested to verify the predicted stringer crippling strength.

5.5.1 SKIN-STRINGER CRIPPLING SPECIMEN. The skin-stringer crippling specimen (Figure 5-8) consisted of a 30 cm (12 in.) long section of stringer spotwelded to a $[\pm 45/0_3]_s$ skin that duplicated the construction of the full-size panel. The ends of the specimen were potted into steel load introduction blocks with a foaming polyimide adhesive, the end plates being held flat and parallel with each other. The total length of the specimen was 33 cm (13 in.) This type of crippling specimen had been used on other test programs with good results.

5.5.2 SKIN-STRINGER CRIPPLING TEST. The configuration of the specimen enabled the effects of skin buckling to be determined and enabled an evaluation of the spotwelds under the influence of the buckled skin. The total length of the specimen provided an

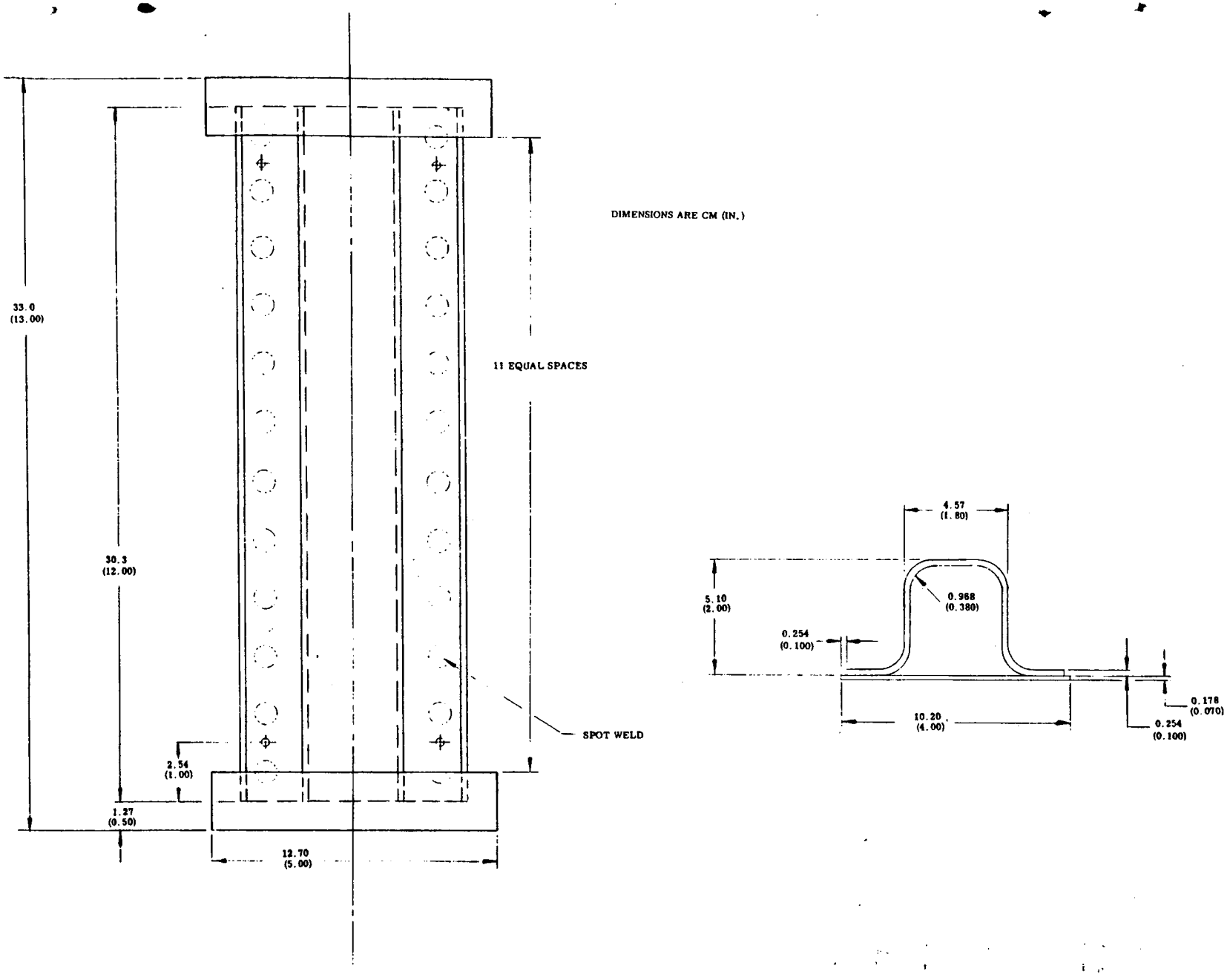

Figure 5-8. Skin Stringer Crippling Specimen

L'/ρ of 10. This is below the L'/ρ of 12 considered a minimum bound in crippling tests. The 33 cm (13 in.) length, however, was the longest length achievable using the rebuilt specimen.

Six strain gages were applied to the specimen. These were intended primarily to achieve uniform load introduction when placed in the test machine. Figure 5-9 shows the strain gage locations. The specimen was placed directly between the platens of an 896 kN (200,000 lb) Tinius Olson universal testing machine. Stainless steel foil shims were utilized to achieve uniform strain distribution. All shimming was accomplished at room temperature.

The specimen was heated by means of two quartz lamp banks arranged on opposite sides of the specimen. The specimen temperature was monitored using four thermocouples attached to the specimen as shown in Figure 5-10.

The specimen was heated until the center thermocouples on both sides read 589 ±5K (600 ±10F). This temperature was held for about 15 minutes prior to application of load. The load was applied in increments of 22.4 kN (5000 lb) with strain measurements taken at each load increment. A continuous load deflection plot was recorded during the test.

The specimen failed at a load of 445 kN (100,000 lb) after sustaining this load for several minutes (during which time the operator was preparing to switch the test machine to a higher load range).

Failure occurred at the center of the specimen. The skin buckled away from the stringer in a narrow area with the buckle occurring primarily between spot welds.

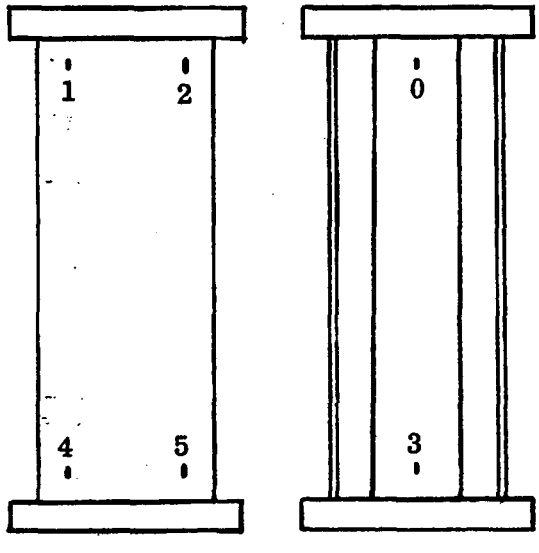

Figure 5-9. Strain Gage Locations

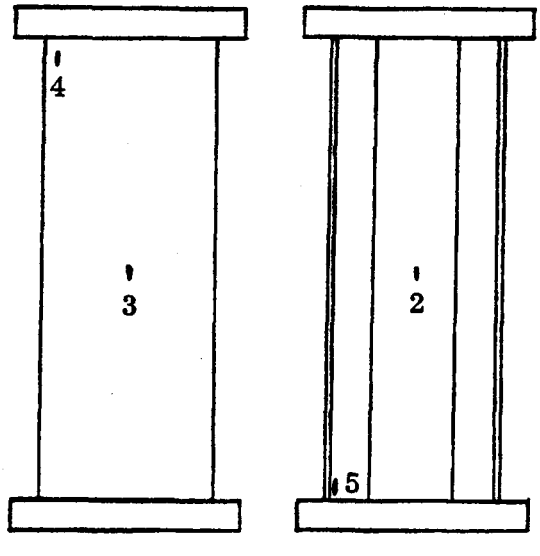

Figure 5-10. Thermocouple Locations

Figure 5-11 shows the failure on the skin side of the specimen. The damage is seen to be localized between spot welds. The stringer suffered a crimping failure along a narrow band around the entire perimeter of the section as seen in Figure 5-12. The damage was severe but localized, and the two ends of the specimen remained joined together.

Figure 5-13 shows the shear offset which occurred at failure.

Figure 5-14 is a stress-strain curve of the crippling test. The change in values at 517 MN/m^2 (75,000 psi) is the point at which the skin flanges of the stringer began to buckle. This is somewhat higher than the 458.8 MN/m^2 (66,500 psi) predicted for the stringer. This difference was due primarily to the stabilizing influence of the skin.

The spotwelds proved to be more than adequate in providing a joint between the skin and stringer.

The test substantiated the basic stringer section design and the method of skin-to-stringer attachment and indicates that local crippling will not be a probable failure mode for the component panel.

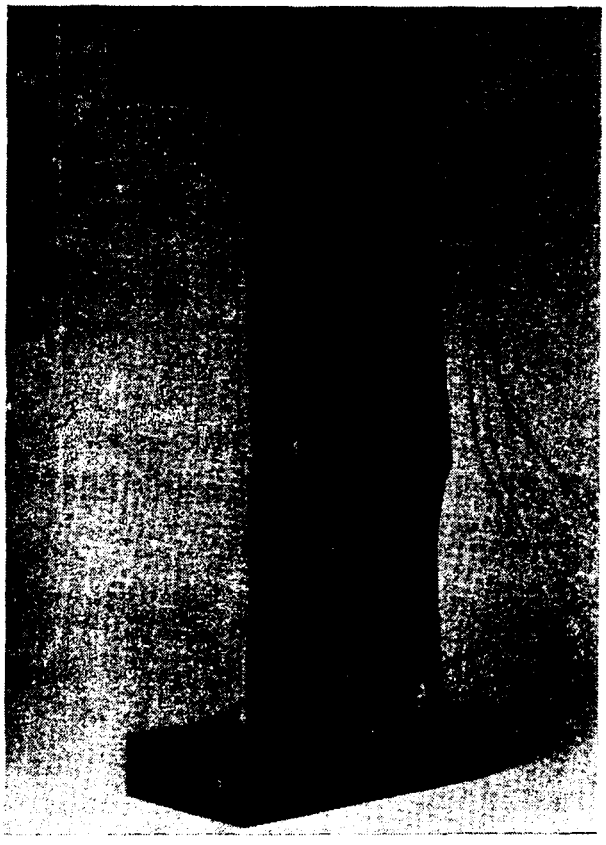

Figure 5-11. Rear Side of Failed Subcomponent (131340B)

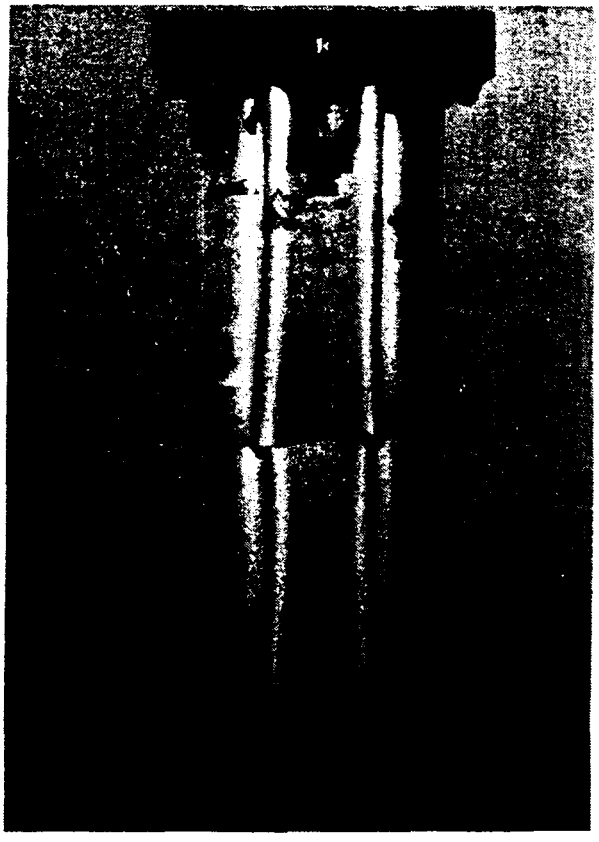

Figure 5-12. Front Side of Failed Subcomponent (131339B)

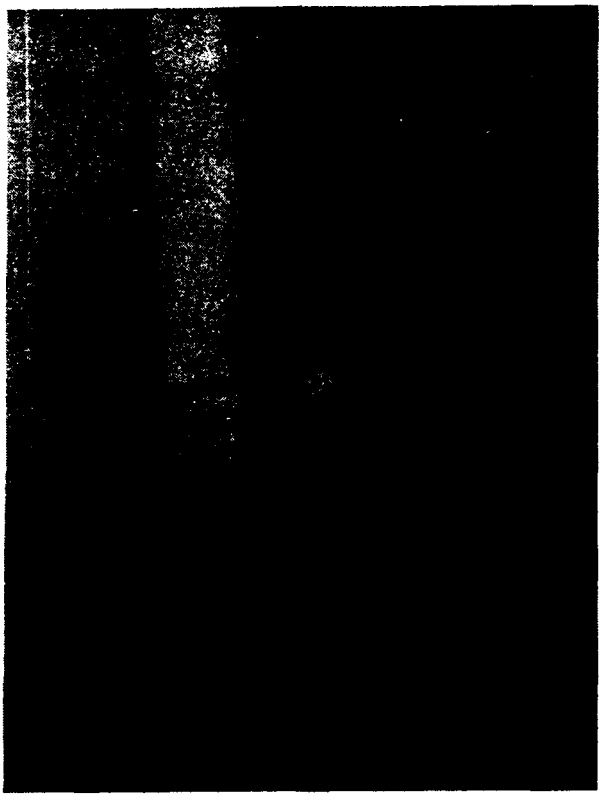

Figure 5-13. Close-up View of Failed Subcomponent (131341B)

5.5.3 STRINGER CRIPPLING TEST. A second stringer crippling specimen was fabricated from a surplus panel stiffener. This specimen was made using the same steel end block used in the previous test specimen, but without the panel skin. The length of this specimen was 35.56 cm (14 in.), which provided an L'/ρ of 12.5 that is ideal for a crippling specimen and is chosen whenever possible. The specimen was tested in a manner identical to the first specimen and failed at a load of 240 kN (54,000 lb) equivalent to a stress of 496.9 MN/m^2 (72,090 psi). This compares favorably with the predicted crippling stress of 458.8 MN/m (66,500 psi).

Figures 5-15 through 5-18 show the appearance of the specimen after testing. The failure mode depicted is typical of thick section of B/Al tested in compression at 589K (600F). The failure is a shear crimping and is similar to the shear crimping failure of a sandwich panel under edgewise compression. The failure is precipitated by a low shear modulus and low shear strength of the core in a sandwich panel, and the matrix in a composite.

5.6 TEST PLAN FOR BORON/ALUMINUM COMPRESSION PANEL

5.6.1 TEST SETUP

5.6.1.1 Test Loading. Limit load for the panel is 6.634×10^5N (149,143 lb). Ultimate load for the panel is 9.288×10^5N (208,800 lb). The test machine capacity shall be at least 1.334×10^6N (300,000 lb).

5.6.1.2 Test Temperature. The panel shall be tested at a stabilized temperature of 588.7K (600F). Maximum temperature variation shall be +8.3K, -14K (+15F, -25F).

5.6.1.3 End Support. The panel was designed to be tested simply supported at the two ends. The panel is supplied with flat plates at each end to which the simple support devices shall be attached.

The load axis of the panel is denoted by markings on the steel plate at each end (Figure 5-19). The simple support devices shall be located such that the end loads are introduced within 0.038 cm (0.015 in.) of this axis. The steel end plate may be drilled as required to permit attachment of the simple support fittings.

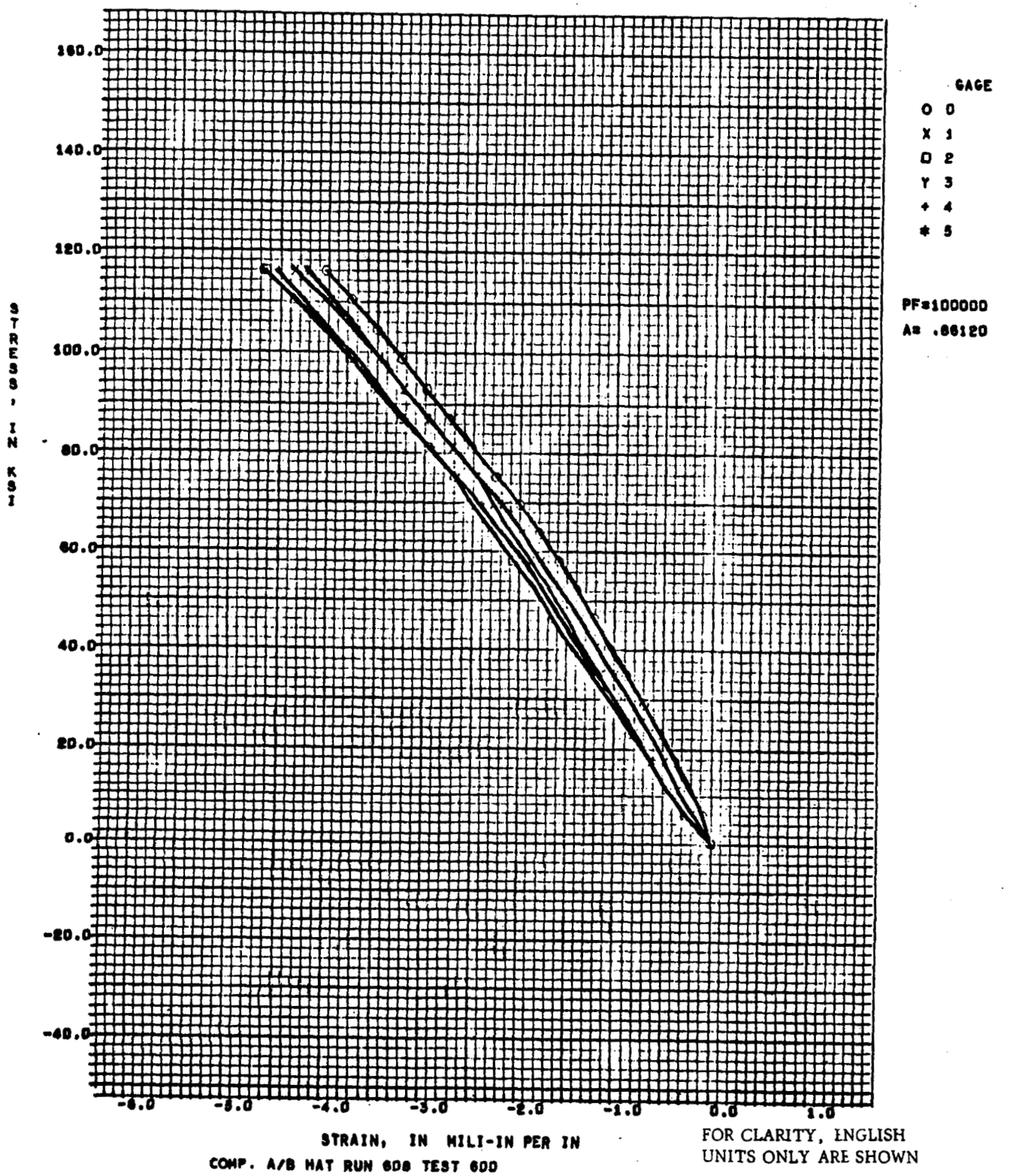

Figure 5-14. Stress-Strain Curve for Crippling Specimen

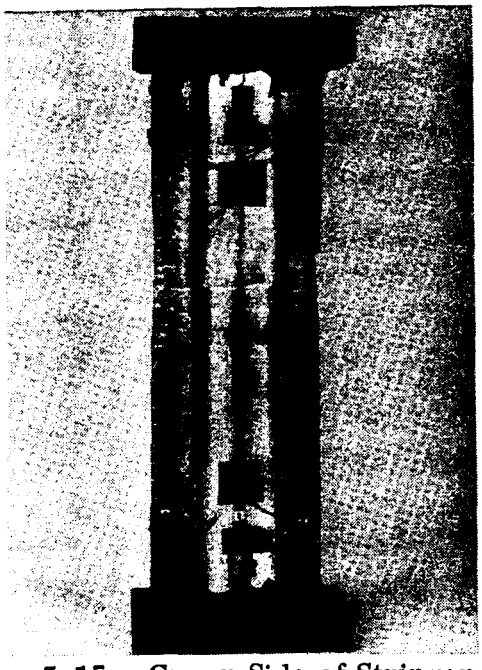

Figure 5-15. Crown Side of Stringer Crippling Specimen Showing Strain Gages and Location of Failure (133425B)

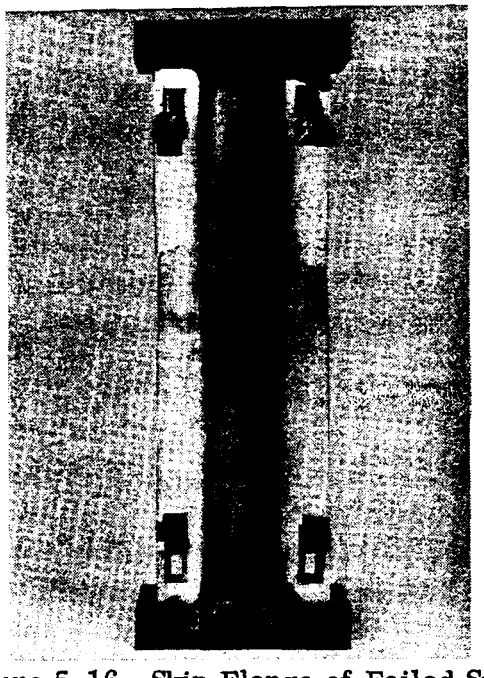

Figure 5-16. Skin Flange of Failed Specimen. Failure of flanges occurred prior to crimping of channel section (133426B)

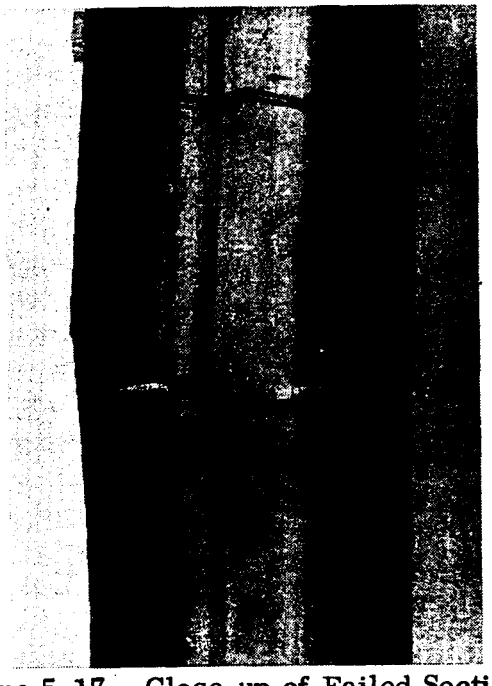

Figure 5-17. Close-up of Failed Section Showing Crimping Failure (133428B)

Figure 5-18. Close-up of Interior of Hat Section After Failure (133427B)

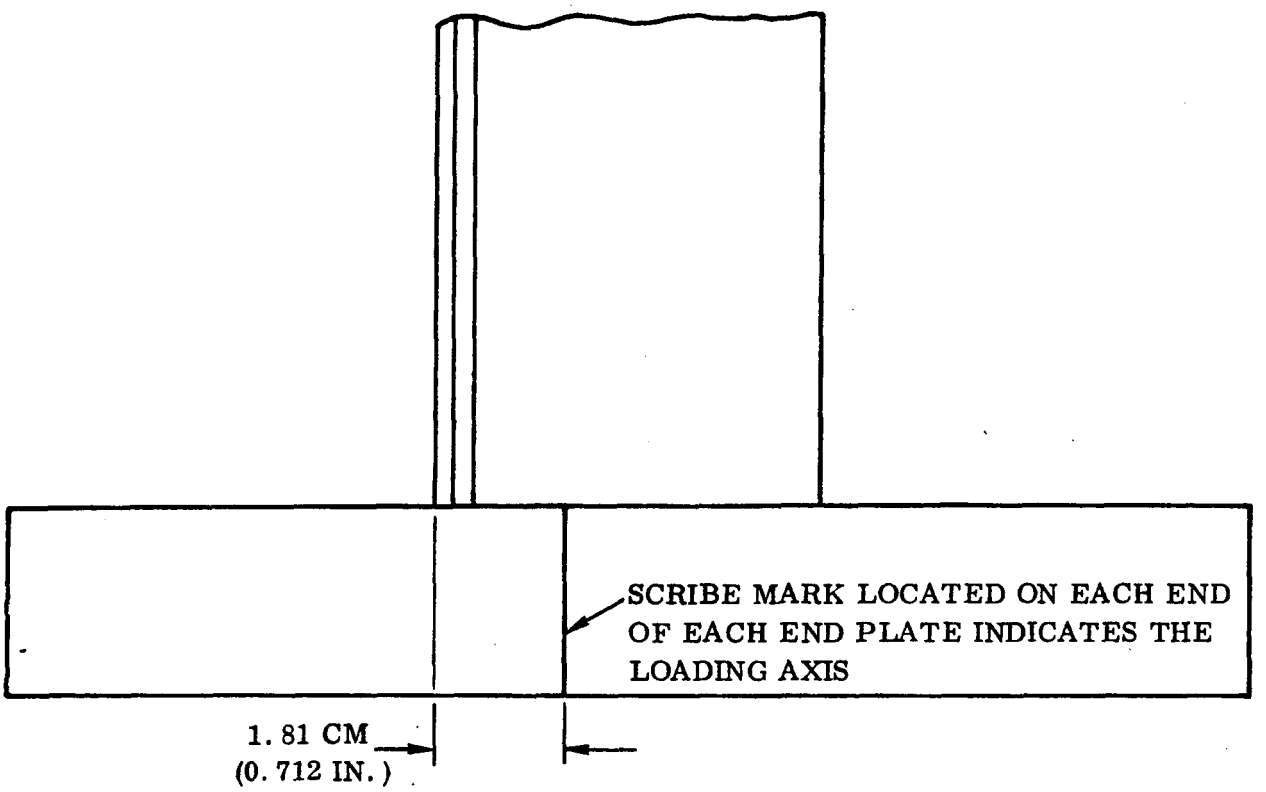

Figure 5-19. Load Application Point

The requirement for simple support may be met by means of members of differing radii, one of which is attached to the end plates at each end. The requirements of simple support and the maintenance of the design column length can be met by a device with a geometry as shown in Figure 5-20.

5.6.1.4 Frame Support. The center frame of the panel shall be provided with two supports each of which provide a minimum spring rate of 8.756×10^6 N/m (50,000 lb/in), normal to the plane of the panel relative to the baseplates or machine plattens.

5.6.1.5 Edge Supports. The split tubing edge supports supplied with the panel shall be installed along each free skin edge such that the gaps between the ends of each tube and the adjacent structure (frame or end block) shall be approximately equal. The clamp bolts shall be tightened sufficiently to lightly clamp the tubes to the skin. Excessive tightening should be avoided.

5.6.1.6 Instrumentation. The panel shall be provided with strain gages, thermocouples, and deflection measurements as indicated in Figures 5-21 and 5-22. A thermocouple shall be provided for each strain gage location for a total of 48 thermocouples.

Each group of three gages in the 200 series (i.e., 201, 202, 203) represents a rosette and is considered one location.

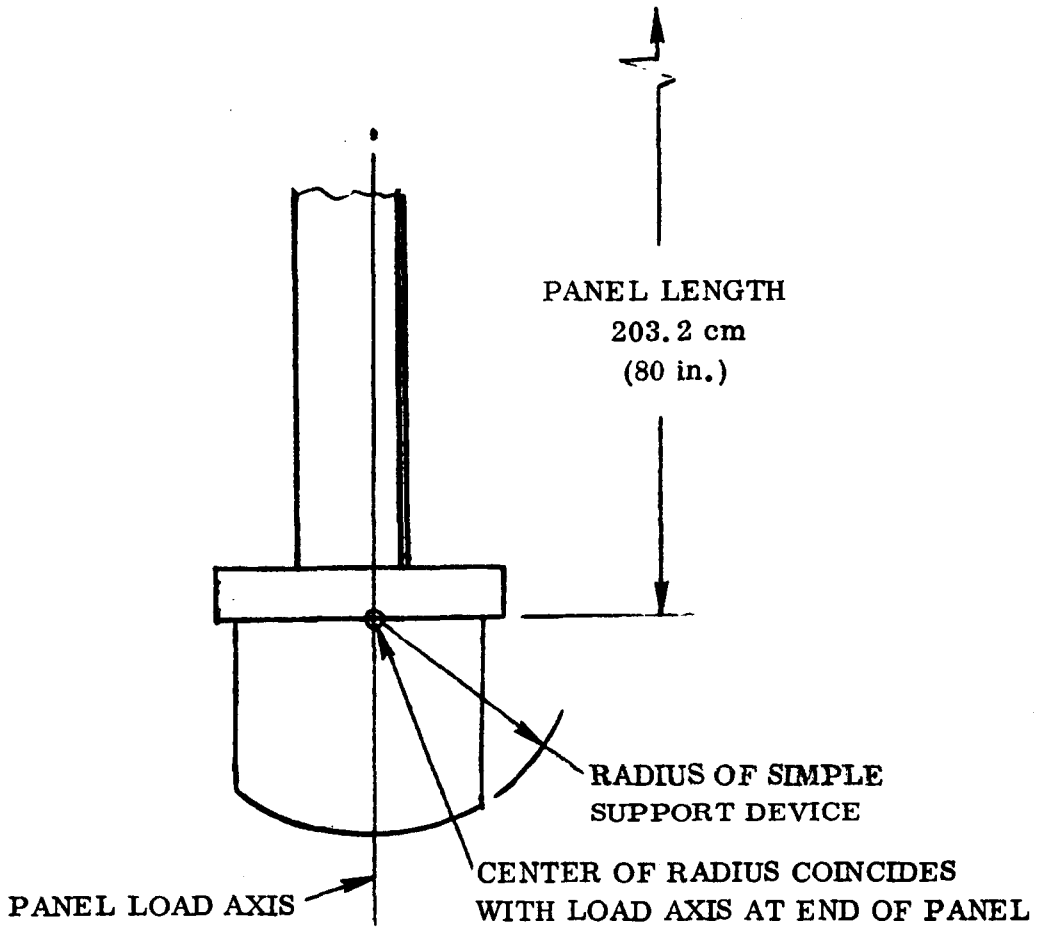

Figure 5-20. Simple Support End Load Introduction

In addition, it is recommended that 20 additional thermocouples be placed as indicated in Figure 5-21 to monitor temperatures near the end of the panel. Deflection measurements are to be placed as indicated in Figure 5-22.

5.6.2 INSTALLATION

1. Install panel in test fixture, attach frame support links, end fittings, and split tubes.
2. Connect the strain gages, thermocouples and deflectometers.
3. Perform continuity checks and calibration of all instrumentation.

5.6.3 PROCEDURE

5.6.3.1 Room Temperature 40% Limit Load Test.

1. Apply approximately 890N (200 lb) to panel and visually verify that it is centered and that the end plate makes uniform contact with the load introduction devices.
2. Apply 10%, 20%, 30%, and 40% and 10% limit loads and record data at each step.
3. Review data to verify that the load introduction across the panel width is uniform. If required, make adjustments and rerun step 2.

5.6.3.2 No Load 589K (600F) Test

1. Apply approximately 890N (200 lb) to panel. Maintain this load during the application of heat.
2. Start applying heat to specimen. Raise temperature gradually and monitor thermocouple data frequently. Watch for thermocouples indicating higher-than-average readings.
3. Raise specimen temperature to 588.7K (600F) and record all thermocouple data. Verify that all panel temperatures are within desired tolerance band.

5.6.3.3 Structural Test at Temperature

1. Verify that all instrumentation is operative.
2. Apply approximately 890N (200 lb) to panel and maintain this load while panel is heated.
3. Raise specimen temperature to test temperature, 588.7K.
4. Apply compressive loads to specimen at 10% LL steps (Table 5-2) recording data at each step. Continue loading to 110% LL. Reduce load to 10% LL and record data at this level. Caution: Record data as quickly as possible at each load level and do not dwell at a load level any longer than necessary. This procedure is to avoid creep effects at the elevated temperatures.
5. Apply compressive loads to specimen in 10% LL steps (Table 5-2) recording data at 10% LL steps. Continue loading to 140% LL. If no failure occurs at this load level, continue loading until failure. Observe caution of step 4.
6. Photograph failed panel.

Table 5-2. Compression Panel Test Loads

Percent Limit Load (% LL)	Load (MN)	Load (pounds)	Percent Limit Load (% LL)	Load (MN)	Load (pounds)
10	0.06634	14,914	* 100	0.6634	149,140
20	0.13268	29,830	† 110	0.7297	164,050
30	0.199	47,740	120	0.7961	178,970
40	0.2654	59,660	130	0.8624	193,890
50	0.3317	74,570	‡ 140	0.9288	208,800
60	0.398	89,486	150	0.9951	223,700
70	0.4644	104,400	160	1.061	238,600
80	0.5307	119,310	170	1.1278	253,500
90	0.597	134,230			

* Limit; † No Yield; ‡ Ultimate

FOLDOUT FRAME

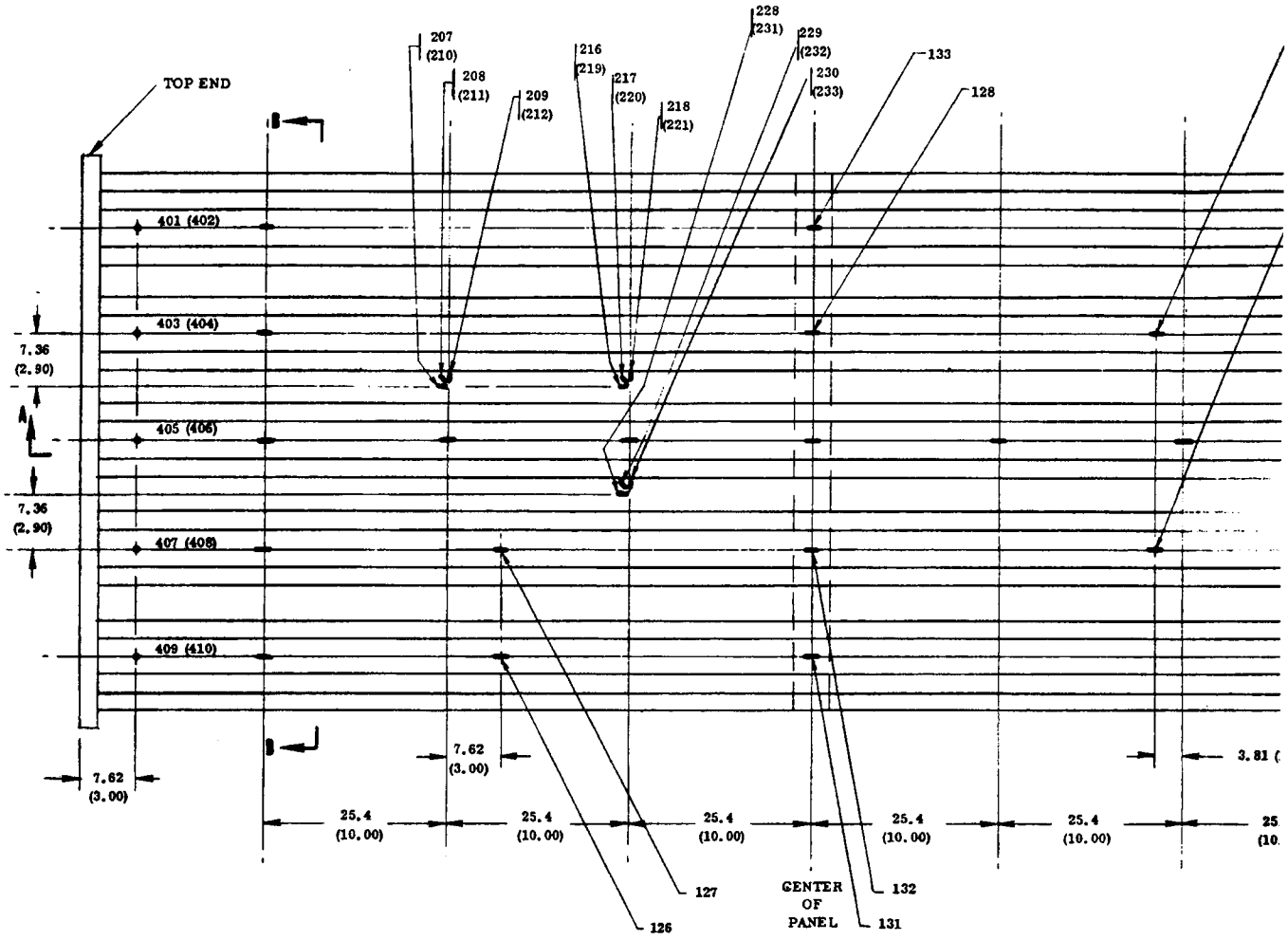

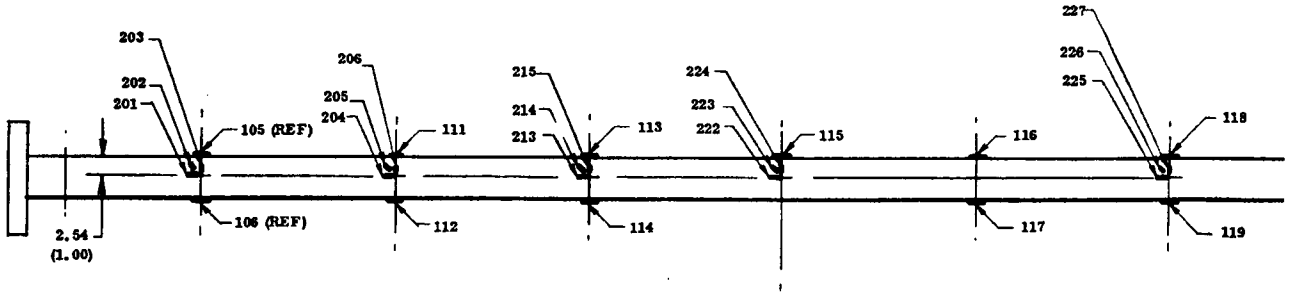

SECTION
A-A
CENTER STRINGER

● THERMOCOUPLE, FRONT & B

▬ STRAIN GAGE AND THERMOC

ROSETTE GAGE AND THERMO

5-21 A

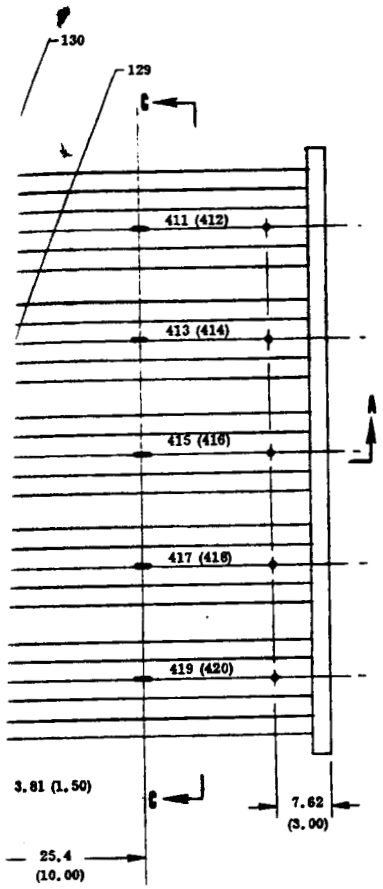

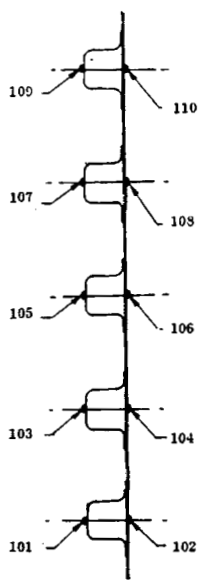

SECTION B-B

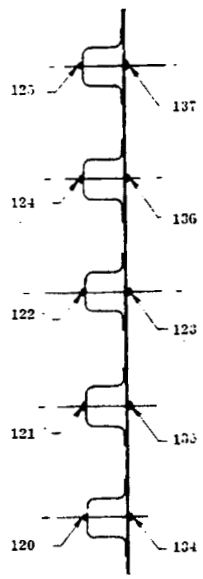

SECTION C-C

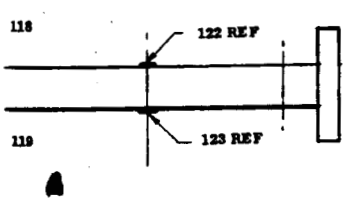

DIMENSIONS IN CM (IN.)

RONT & BACK SIDE

HERMOCOUPLE

) THERMOCOUPLE

Figure 5-21. Compression Panel Strain Gage and Thermocouple Instrumentation

FOLDOUT FRAME

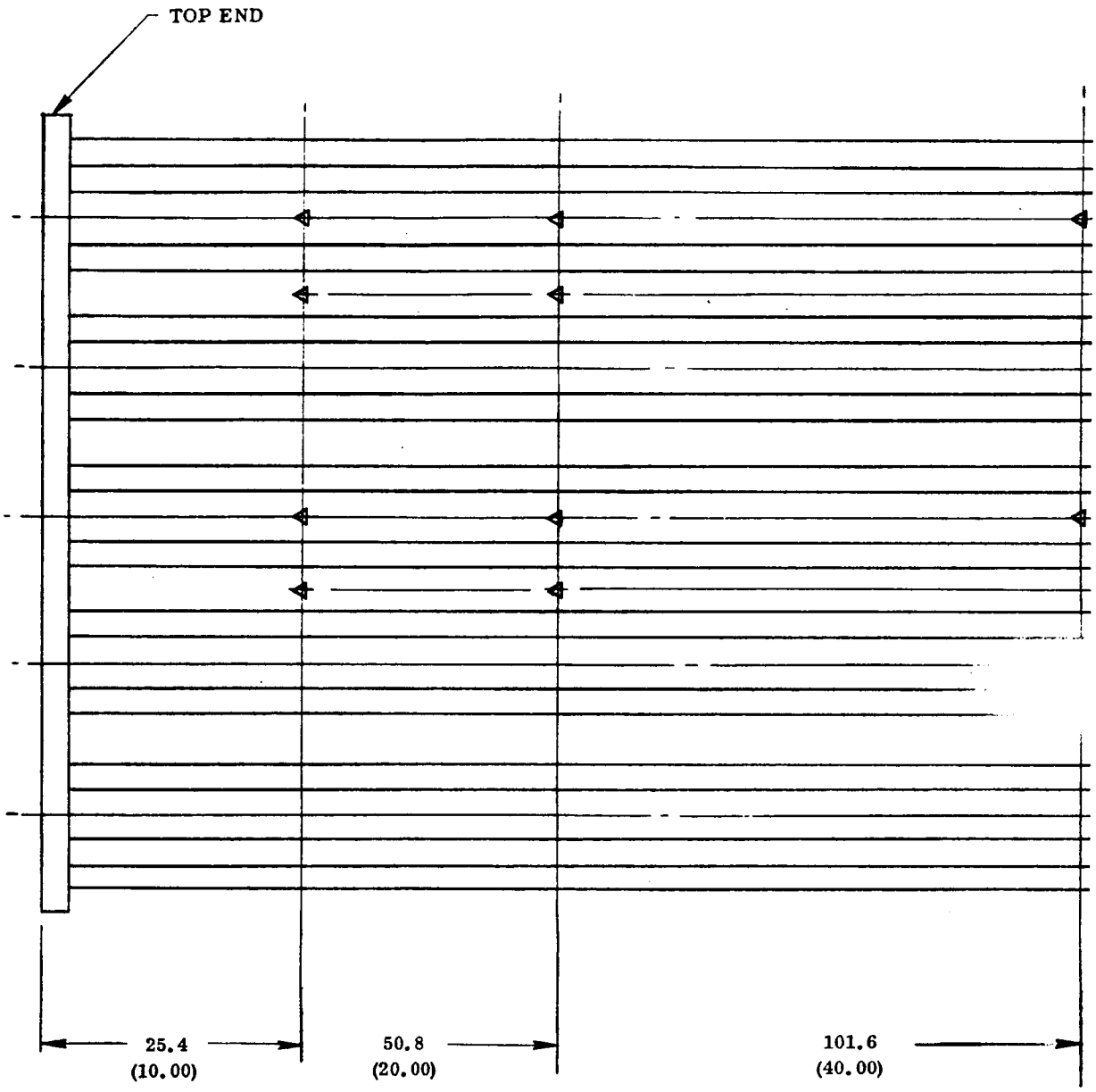

FOLDOUT FRAME 2

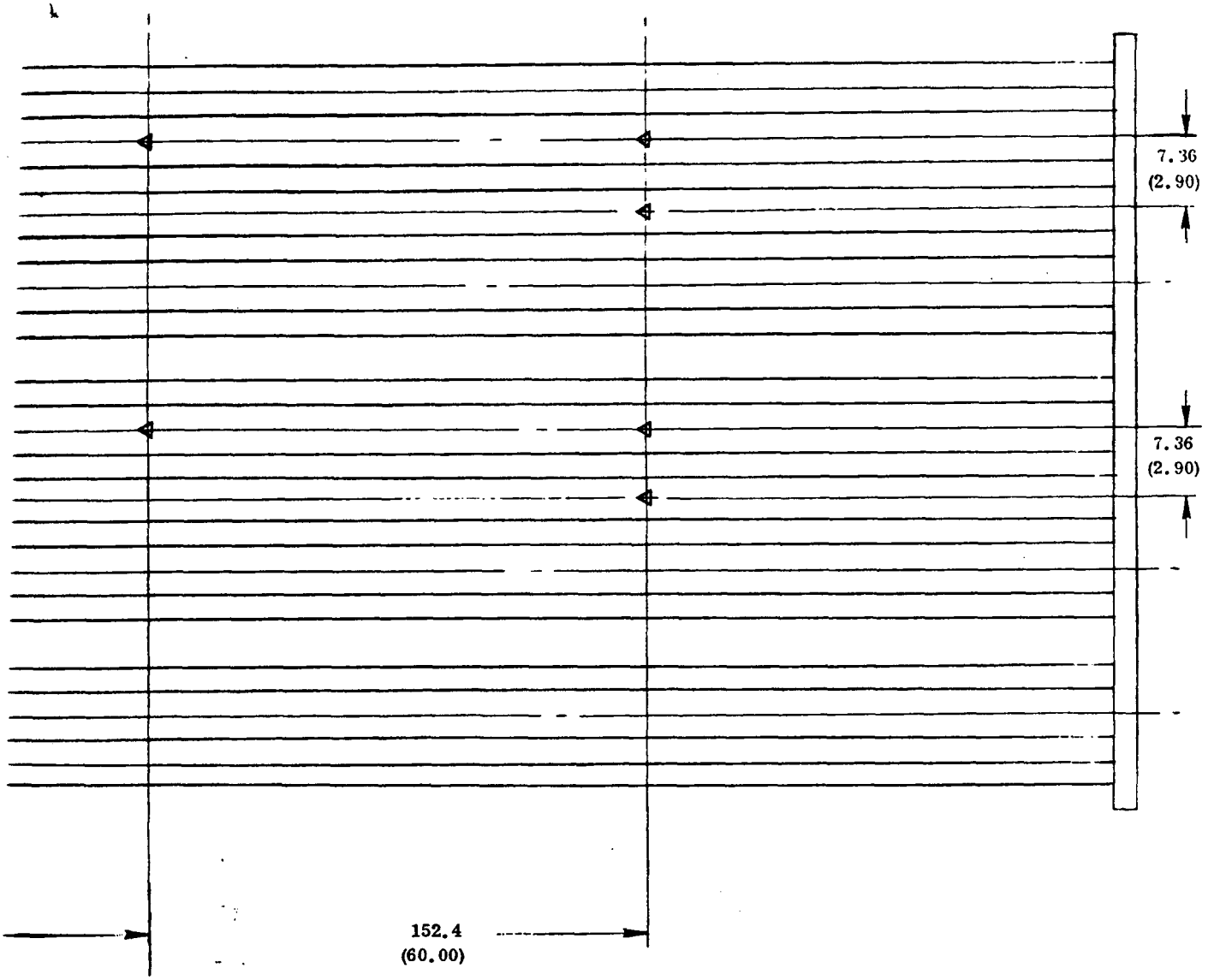

△ DEFLECTOMETER LOCATION

DIMENSIONS IN CM (IN.)

5-22-13

Figure 5-22. Compression Panel Deflection Measurements

SECTION 6

CONCLUSIONS AND RECOMMENDATIONS

Based on the work performed on this program and presented in Volumes I and II, the following conclusions and recommendations are made.

6.1 DESIGN AND ANALYSIS

1. Four large, heavily loaded, structural segments of the space shuttle booster section were designed utilizing boron/aluminum (B/Al). The adequacy of these designs was then proved by analysis. The successful design and analyses of these large, complex structures increases the confidence level in the use of this advanced composite material.

2. Subelements representative of sections of the booster structure were successfully designed, analyzed, fabricated and structurally tested thus demonstrating the adequacy of the design and analysis of B/Al structures.

3. Compression flight hardware structures made from B/Al may now be designed with a high degree of confidence for usage up to 589K (600F). This is due to the advancement of the state-of-the-art of crippling analysis methods for unidirectional B/Al, that was accomplished at Convair Aerospace prior to and during the present program.

4. It is recommended that crippling analysis methods be developed for B/Al crossply materials, to be used primarily in skins and joints.

5. The nonlinear behavior of B/Al crossply material made it necessary to use some nonlinear analytical methods for the shear beam web. Biaxial stress-strain data was not available; consequently, it became necessary to use secant moduli and Poisson's ratio data from uniaxial stress-strain curves to approximate them.

6. It is recommended that biaxial stress-strain and stress-Poisson ratio curves be generated for crossply B/Al composites for use in future flight hardware design and analysis tasks.

6.2 MATERIAL PROPERTY TESTING

1. Mechanical properties were determined on unidirectional and crossplied B/Al at room and elevated temperatures. Typical longitudinal tensile strengths of 1289 MN/m^2 (216 ksi) were obtained.

2. A statistical analysis was performed on the mechanical property data to provide design allowables. Additional testing is required to provide a large data base and increase confidence levels.

3. The effects of heat treatments on the mechanical properties of B/Al were determined. Maximum improvements in strength and modulus were obtained with a solution treat plus cryogenic soak plus aging treatment.

4. A test program was performed to determine the susceptibility of B/Al to corrosion and to evaluate a number of corrosion protection systems for use in low- and high-temperature environments. Both acrylic and polyurethane coating systems provided adequate corrosion protection at moderately elevated temperatures [366K (200F)]. A chromic acid anodizing process provided the best protection at high temperatures [589K (600F)]; however, additional testing at high temperatures is recommended.

5. Quality assurance (nondestructive and mechanical property testing) indicated that the B/Al material received on this program [64 panels weighing in excess of 137 kg (300 lb)] was consistently of high quality. All material was received on schedule.

6.3 PROCESS DEVELOPMENT

6.3.1 MACHINING

The use of a diamond disc cutoff saw to machine large, thick B/Al sections was demonstrated. The saw was used to trim sections over 1.5 cm (0.6 in.) thick, with the cut surface sufficiently smooth to permit subsequent fabrication without further machining. The average wheel loss was 2×10^{-5} m/m for B/Al material in the as-received condition; however, wheel loss doubled for heat treated material.

The rotary ultrasonic machine was found to be satisfactory for drilling thick B/Al over 0.3 cm (0.1 in.) thick, heat treated B/Al, and B/Al joined to conventional materials such as steel and titanium. Hole punching techniques followed by reaming with a diamond-plated twist drill produced excellent quality holes in B/Al under 0.3 cm (0.1 in.) thick.

Additional development of the hole punching process could result in an increase in the material thicknesses that can be processed by this technique.

6.3.2 CON BRAZ JOINING. The method and applicability of Con Braz joining was demonstrated on the program. Over 24.5 m (80 ft) of I-sections were successfully Con Braz joined using a semi-automated joining module. While brazing alloys for applications up to 393K (250F) are available, additional work must be performed to develop alloys suitable for 589K (600F) application. Additional work must also be performed to develop proper joining techniques for thick gage [1.3 cm (0.5 in.) thick and greater] B/Al. Thermal cycling Con Braz joined structures (B/Al to B/Al and B/Al to Ti) between 77K (-320F) and 366K (200F) has no detrimental effect on joint properties.

6.3.3 RESISTANCE WELDING AND RESISTANCE JOINING. Resistance welding and resistance joining proved satisfactory for joining multiple sheets of B/Al and Ti in thicknesses up to 1.5 cm (0.6 in.). Joint efficiencies from 60 to 100% were obtained at room temperature; these values were not affected by thermal cycling. Over 50% of joint strength was retained at 589K (600F).

6.3.4 PLATING. Both electroless and electrolytic brush plating were successfully incorporated into B/Al fabrication. The electroless process yielded slightly higher joint strengths, while the brush plating was more convenient for in situ plating where immersing in a bath was undesirable.

6.3.5 CON CLAD FORMING. Room temperature forming of B/Al sheets up to 2m (80 in.) in length and 0.3 cm (0.1 in.) in thickness was performed on standard shop brake presses when mild carbon steel was clad to the composite surface prior to forming. This cladding may impart some residual tensile stresses into the composite panel. Further investigations to determine the extent of these residual stresses are recommended to permit even greater utilization of this forming process.

6.4 COMPONENT FABRICATION

Two selected components utilizing the processes examined on this program were fabricated.

6.4.1 SHEAR BEAM COMPONENT. A 1 by 0.96m (40 by 38 in.) shear resistant shear web beam was fabricated and shipped to NASA-MSFC for testing at room temperature.

6.4.1.1 Shear Beam Elements. The shear beam consisted of 21 vertical and horizontal I-section stiffeners fabricated by Con Braz joining. The heat treated web was spliced together by resistance welding. A compression cap that tapered in thickness was attached to the web with mechanical fasteners and by resistance joining. The stiffeners were attached to the web by resistance welding and tied to each other (at intersection joints) with mechanical fasteners.

6.4.1.2 Shear Beam Cost and Weight. The final weight of the shear beam component was 35.4 kg (78 lb), and the total cost, excluding tooling, was $66,700 or $1880/kg ($855/lb). Tooling costs amounted to $11,000; therefore, the cost of the shear beam, including nonrecurring items was $78,000, or $2060/kg ($940/lb).

6.4.2 COMPRESSION PANEL COMPONENT. A 2 by 0.75m (80 by 29 in.) compression panel was fabricated and shipped to NASA-MSFC for testing at 589K (600F).

6.4.2.1 Compression Panel Elements. The compression panel consisted of a single crossplied skin with five Con Clad formed stringers running the full 2m (80 in.) length. The stringers were resistance welded to the panel. A titanium frame was mechanically fastened to the rear of the panel 1m (40 in.) from each end.

6.4.2.2 Compression Panel Cost and Weight. The final weight of the compression panel was 20.2 kg (44.4 lb), and the total cost, excluding tooling was $30,400, or $1510/kg ($690/lb). Tooling costs amounted to $4400; therefore the cost of the compression panel, including nonrecurring items was $34,800 or $1740/kg ($790/lb).

6.4.3 B/Al STRUCTURES. This program demonstrated that B/Al structures can be designed and fabricated for representative structural assemblies having high load intensities. The fabrication can be accomplished with todays technology and existing shop equipment and personnel. Using sheet metal fabrication techniques, these composite structures can be fabricated at a reasonable cost.

SECTION 7

REFERENCES

1. Schaefer, W. H., Christian, J. L., et al, Evaluation of the Structural Behavior of Filament Reinforced Metal Matrix Composites, AFML-TR-69-36, January 1969.

2. Schaefer, W. H., Aluminum-Boron F-106 Engine Access Door Design and Test Evaluation, Convair Aerospace Division Report GDC-ERR-1514, August 1970.

3. Schaefer, W. H., Wennhold, W., et al, Composite Fuselage Development, Convair-San Diego report to General Dynamics, Fort Worth, for Air Force Contract F33615-70-C-1494, 1969.

4. Christian, J. L., Development and Evaluation of Advanced Metal Matrix Composite Materials, Convair Aerospace Division Report GDC-ERR-1571, December 1970.

5. Kuhn, P., A Summary of Diagonal Tension Field, NACA TN 2661, May 1952.

6. Stowell, E. Z., A Unified Theory of Plastic Buckling of Columns and Plates, NACA TN 1556, April 1948.

7. Stein, M. and Fralich, R., Critical Shear Stress of Infinitely Long, Simply Supported Plate with Transverse Stiffeners, NACA TN 1851, April 1949.

8. Miller, M. F., Christian, J. L., et al, Design, Manufacture, Development, Test, and Evaluation of Boron/Aluminum Structural Components for Space Shuttle, NAS8-27738, Quarterly Report No. 2, January 1972.

9. Iosipescu, Nicolae, ASTM Journal of Materials, Vol. 2, No. 1, March 1967.

10. Advanced Composites Design Guide, Air Force Materials Laboratory, November 1971.

11. NASA Structures Manual, Marshal Space Flight Center.

12. E. E. Spier, Crippling Analysis of Boron/Aluminum Composites in Compression Structure, AFMC.

APPENDIX A

DESIGN DRAWINGS

FOLDOUT FRAME -1

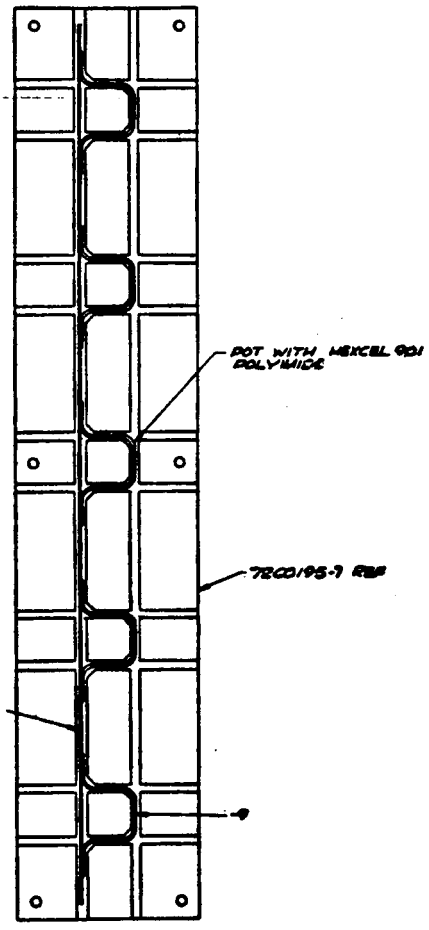

SECT. B-B

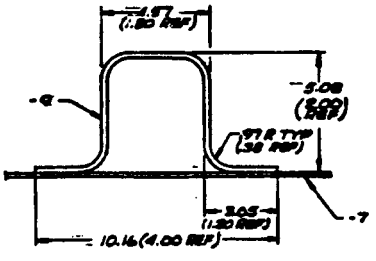

SECT. A-A
ROTATED 90° COUNTERCLOCKWISE
SCALE: 1/1

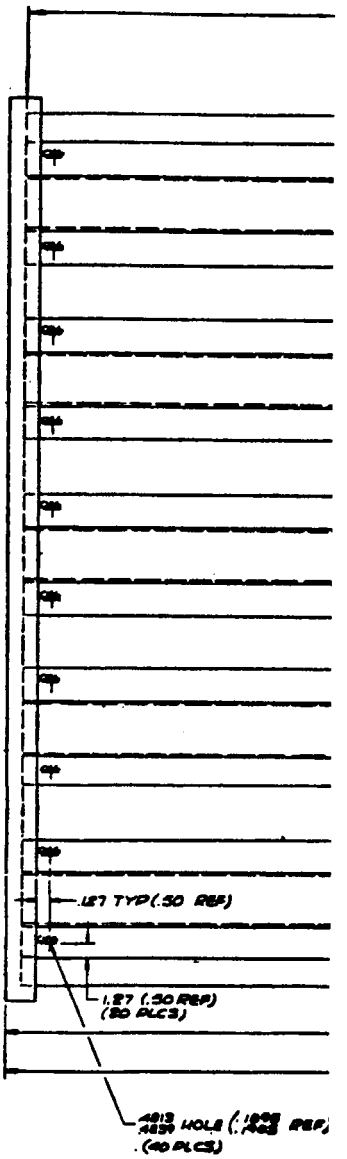

A-1 / A-2 -A

FOLDOUT FRAME - 2

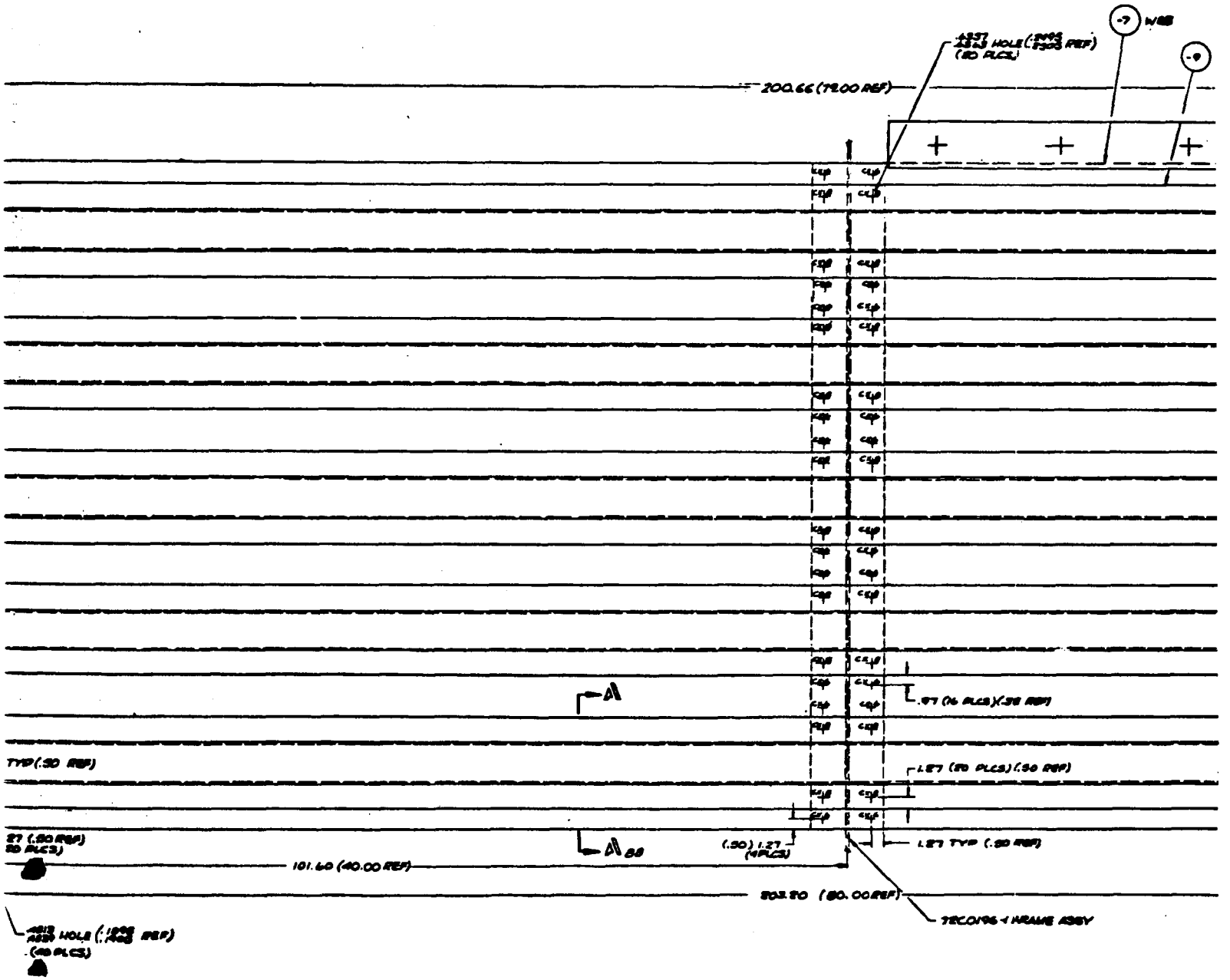

FOLDOUT FRAME -3

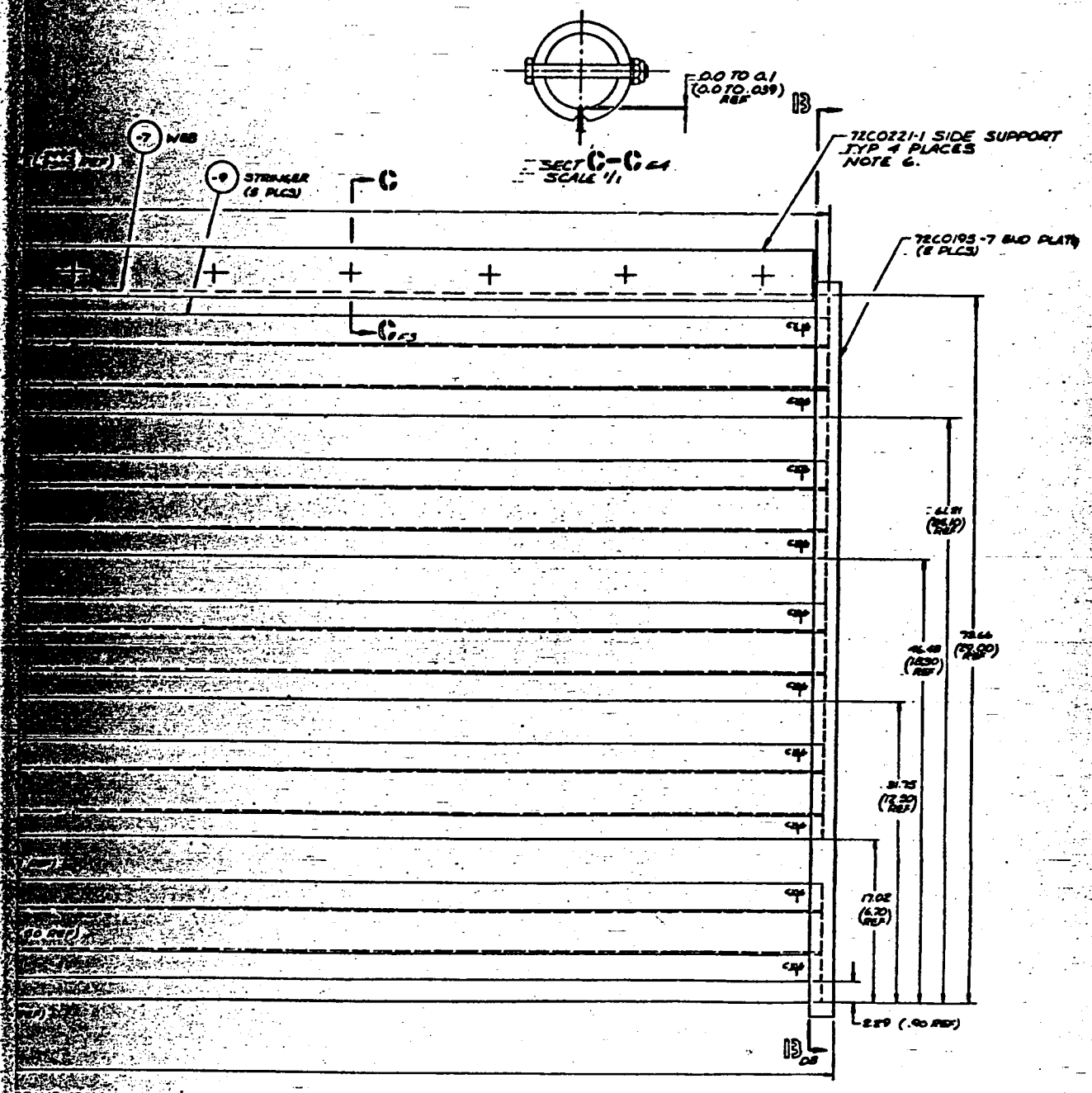

A-1/A-2 -C

REVISIONS					
ZONE	LTR	DESCRIPTION		DATE	APPROVED
G3	A	ADD SIDE SUPPORTS		6-173	

FOLDOUT FRAME - 4

SIDE SUPPORT

-7 END PLATE

NOTES:

1. IMPRESSION MARKING OF PARTS NOT PERMITTED.
2. BREAK SHARP EDGES, .015.
3. CK6 = NAS1466 PIN & NAS1080-6 COLLAR.
4. CK8 = NAS1468 PIN & NAS1080-8 COLLAR.
5. ALL DIMENSIONS ARE IN CENTIMETERS.
6. APPROXIMATLY CENTER THE 72C0221 SIDE SUPPORTS BETWEEN THE PANEL ENDS AND THE FRAME CAP

-1	UNIT OF MEAS	ITEM OR FIND NO.	CODE IDENT NO.	PART OR IDENTIFYING NUMBER	NOMENCLATURE OR DESCRIPTION	ZONE	NO.	NOTE TEXT (STOCK SIZE, MATERIAL, SPECIFICATION, TYPE (TEMPER, ETC.), HEAT TREAT)
20				NAS1493-8	COLLAR			
40				NAS1493-6	COLLAR			
20				NAS1466-9	PIN			
20				NAS1466-5	PIN			
20				NAS1468-7	PIN			
4				72C0221-1	SIDE SUPPORT	F	3	
1				72C0196-1	FRAME ASSY	B	5	
2				72C0195-7	END PLATE	F	3	
5				-9	STRINGER	G	4	M [0₁₀]. BORON ALUMINUM
1				-7	WEB	G	4	M [0/±45], BORON ALUMINUM
4				-1	ASSY	D	5	E

REQUIREMENTS FOR ASSEMBLY/INSTALLATION

NOTE SYMBOL: E—END ITEM; G—GENERAL NOTE; L—LIGHT; M—MATERIAL; R—REFERENCE DESIGNATION; S—STOCK NO.; U—USAGE DATA

PARTS LIST

UNLESS OTHERWISE SPECIFIED

ALL MACHINED SURFACES √

SEE 0-76914 FOR ABBREVIATION, CODE AND SYMBOL REQUIREMENTS

SEE 0-76902 FOR STANDARD MANUFACTURING AND INSTALLATION REQUIREMENTS

ASSOCIATED LIST REQUIRED SEE DOCUMENT SAME NUMBER PREFIXED UL ☐ FOR USAGE LIST

UNLESS OTHERWISE SPECIFIED DIMENSIONS ARE IN INCHES

TOLERANCES .X ±.1 .XX ±.03 .XXX ±.010 ANGULAR PER 0-76902

CHECK

STRESS

GR ENGR

SUBMIT

CONTRACT NO.

SECURITY CLASSIFICATION

CONVAIR AEROSPACE DIVISION OF GENERAL DYNAMICS SAN DIEGO, CALIFORNIA

COMPRESSION PANEL - BORON ALUMINUM

SIZE J | CODE IDENT 14170 | DRAWING NO. 72C0194

SCALE | RELEASED | SHEET

72C0194 A

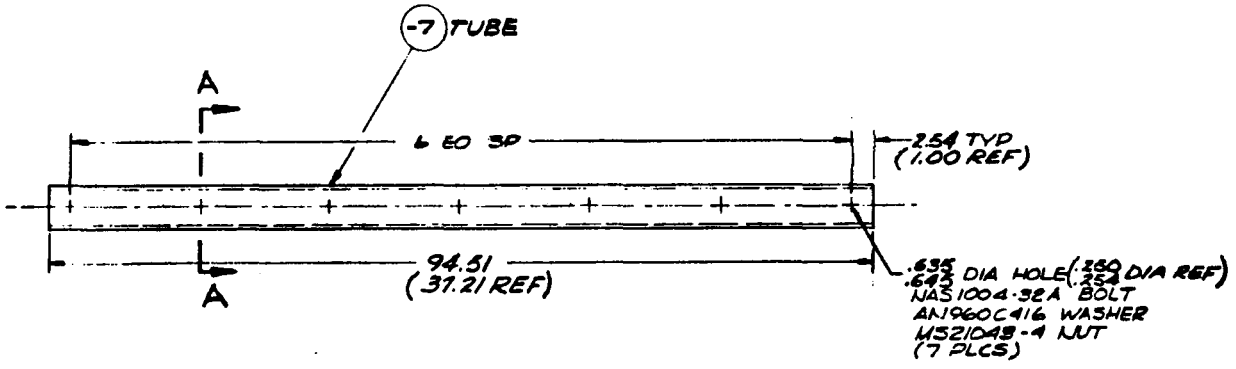

-1 ASSY
SCALE 1/4

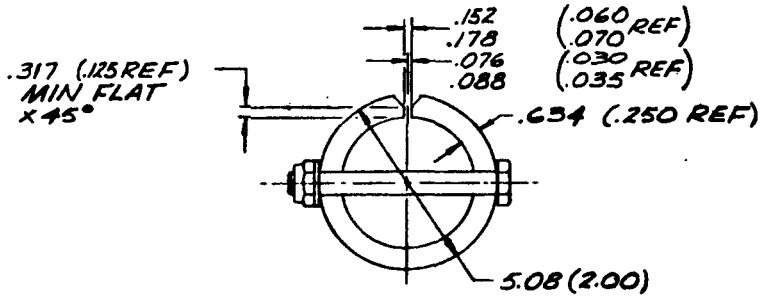

SECTION A-A
SCALE 1/1

MAT'L MS 7220221 ON BMO

FOLDOUT FRAME -2

REVISIONS			
LTR	DESCRIPTION	DATE	APPROVED
A	REVISE DIM OF RING & CHAM.	6-1-73	6-1-73

NOTES:
1. IMPRESSION MARKING OF PART NOT PERMITTED.
2. BREAK SHARP EDGES, .015.
3. ALL DIMENSIONS ARE IN CENTIMETERS.

REF)

REQ PER ASSY / INSTL	UNIT OF MEAS	ITEM OR FIND NO.	CODE IDENT NO.	PART OR IDENTIFYING NUMBER	NOMENCLATURE OR DESCRIPTION	NOTE SYMBOL	NOTE TEXT (STOCK SIZE, MATERIAL, SPECIFICATION, TYPE [TEMPER, ETC.], HEAT TREAT)
7				NAS1004-32A	BOLT		
7				MS21045-4	NUT		
7				AN960C416	WASHER		
1				-7	TUBE	M	2.00 O.D. X 37.5,
-				-1	ASSY	U	NEXT ASSY (AR600)

NOTE SYMBOL: E—END ITEM G—GENERAL NOTE L—LIMIT M—MATERIAL R—REFERENCE DESIGNATION S—STOCK NO. U—USAGE DATA

PARTS LIST

UNLESS OTHERWISE SPECIFIED
ALL MACHINED SURFACES 125√
RIVET BASIC CODE-NAS523
BB—MS20426AD
BJ—MS20470AD

SEE 0-70914 FOR ABBREVIATION, CODE AND SYMBOL REQUIREMENTS

SEE 0-70902 FOR STANDARD MANUFACTURING AND INSTALLATION REQUIREMENTS

ASSOCIATED LIST REQUIRED SEE DOCUMENT SAME NUMBER PREFIXED UL ☐ FOR USAGE LIST

UNLESS OTHERWISE SPECIFIED
DIMENSIONS ARE IN INCHES
TOLERANCES
.X ± .1 .XX ± .03 .XXX ± .010
ANGULAR PER 0-70902

MATL
PROD. ENGR

CHECK
STRESS
QR ENGR
DESIGN
DRAWN
CONTRACT NO.

CONVAIR AEROSPACE DIVISION OF GENERAL DYNAMICS
SAN DIEGO, CALIFORNIA

COMPRESSION PANEL - SIDE SUPPORT

SIZE	CODE IDENT	DRAWING NO.
D	14170	7220221

SCALE NOTED RELEASED SHEET 1 OF 1

SECURITY CLASSIFICATION

A-3/A-4 -B

FOLDOUT FRAME -1

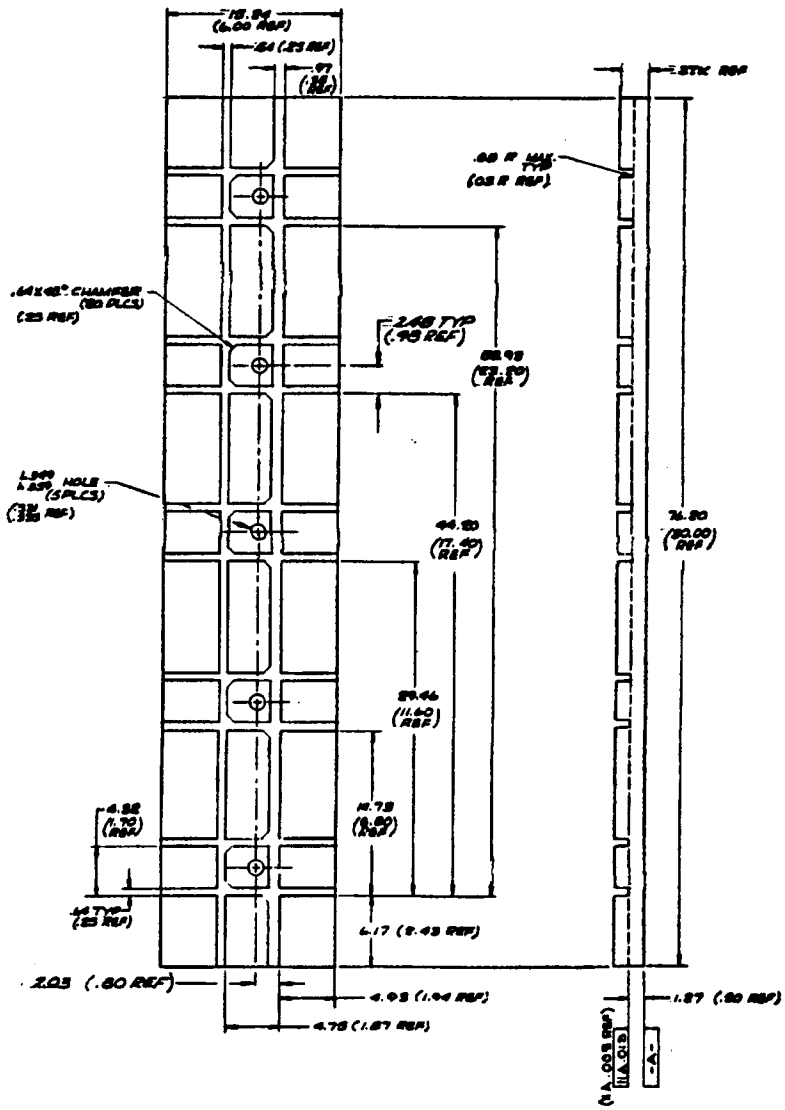

A-5/A-6-A

REVISIONS				REVISIONS				REVISIONS				
ZONE	LTR	DESCRIPTION	DATE	APPROVED	ZONE	LTR	DESCRIPTION	DATE	APPROVED	ZONE	LTR	DESCRIPTION	DATE	APPROVED
										E7	A	RELOCATE HOLES	4-1-2	

FOLDOUT FRAME - 2

NOTES:
1. IMPRESSION MARKING OF PART NOT PERMITTED.
2. BREAK SHARP EDGES, .015
3. MAGNETIC INSPECT. NO CRACKS ALLOWED.
4. ALL DIMENSIONS ARE IN CENTIMETERS.

NEXT ASSY / DISTL	UNIT OF MEAS	ITEM OR FIND NO.	CODE IDENT NO.	PART OR IDENTIFYING NUMBER	NOMENCLATURE OR DESCRIPTION	LTR ZONE	NO.	(STOCK SIZE, MATERIAL, SPECIFICATION, TYPE (TEMPER, ETC.), HEAT TREAT) NOTE YEAR
								(1.00 X 6.0 X 30.0 7EF)
				-7	END PLATE			J 2.54 X 5.9 X 76.2, 4130 STEEL, NORMALIZED
								J NEXT ASSY 72C0194 (2 REQD)

NOTE SYMBOL: E—END ITEM L—LIMIT R—REFERENCE DESIGNATION
G—GENERAL NOTE M—MATERIAL S—STOCK NO. U—USAGE DATA

PARTS LIST

UNLESS OTHERWISE SPECIFIED ALL MACHINED SURFACES 125	SEE B-70914 FOR ABBREVIATION, CODE AND SYMBOL REQUIREMENTS	UNLESS OTHERWISE SPECIFIED DIMENSIONS ARE IN INCHES TOLERANCES .X ±.1 .XX ±.03 .XXX ±.010 ANGULAR PER B-70803	CHECK	CONVAIR AEROSPACE DIVISION OF GENERAL DYNAMICS SAN DIEGO, CALIFORNIA
RIVET BASIC CODE MAS623	SEE B-70900 FOR STANDARD MANUFACTURING AND INSTALLATION REQUIREMENTS		STRESS	
BA—MS20426AD			QR ENGR	
BA—MS20470AD	ASSOCIATED LIST REQUIRED SEE DOCUMENT SAVE NUMBER PREFIXED	MATL	DRAWN	END PLATE - BORON ALUMINUM COMPRESSION PANEL
	UL ☐ FOR USAGE LIST	FINISH	CONTRACT NO.	SIZE E | CODE IDENT 14170 | DRAWING NO. 72C0195
		SECURITY CLASSIFICATION		SCALE — SHEET 1 OF 1

A-5/A-6 - B

FOLDOUT FRAME

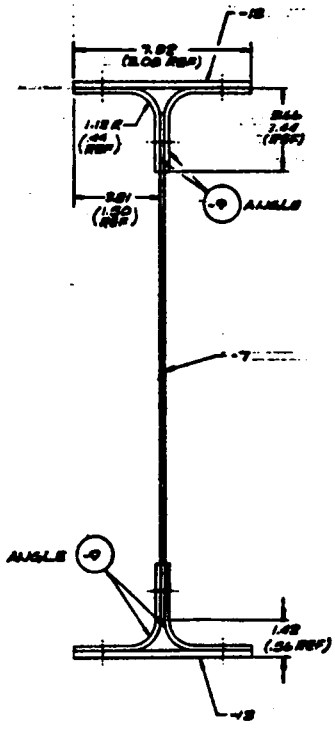

SECT. A-A C3

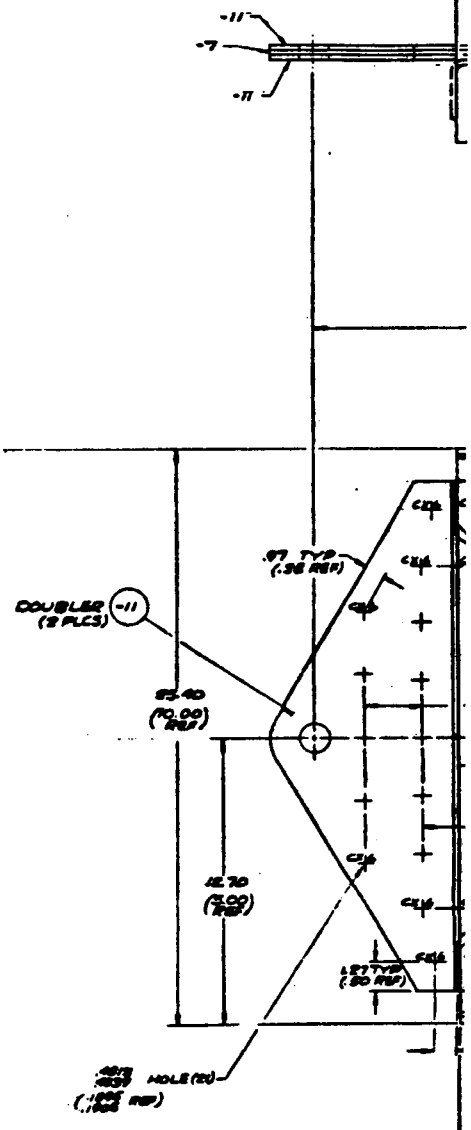

A-7/A-8 A

FOLDOUT FRAME 2

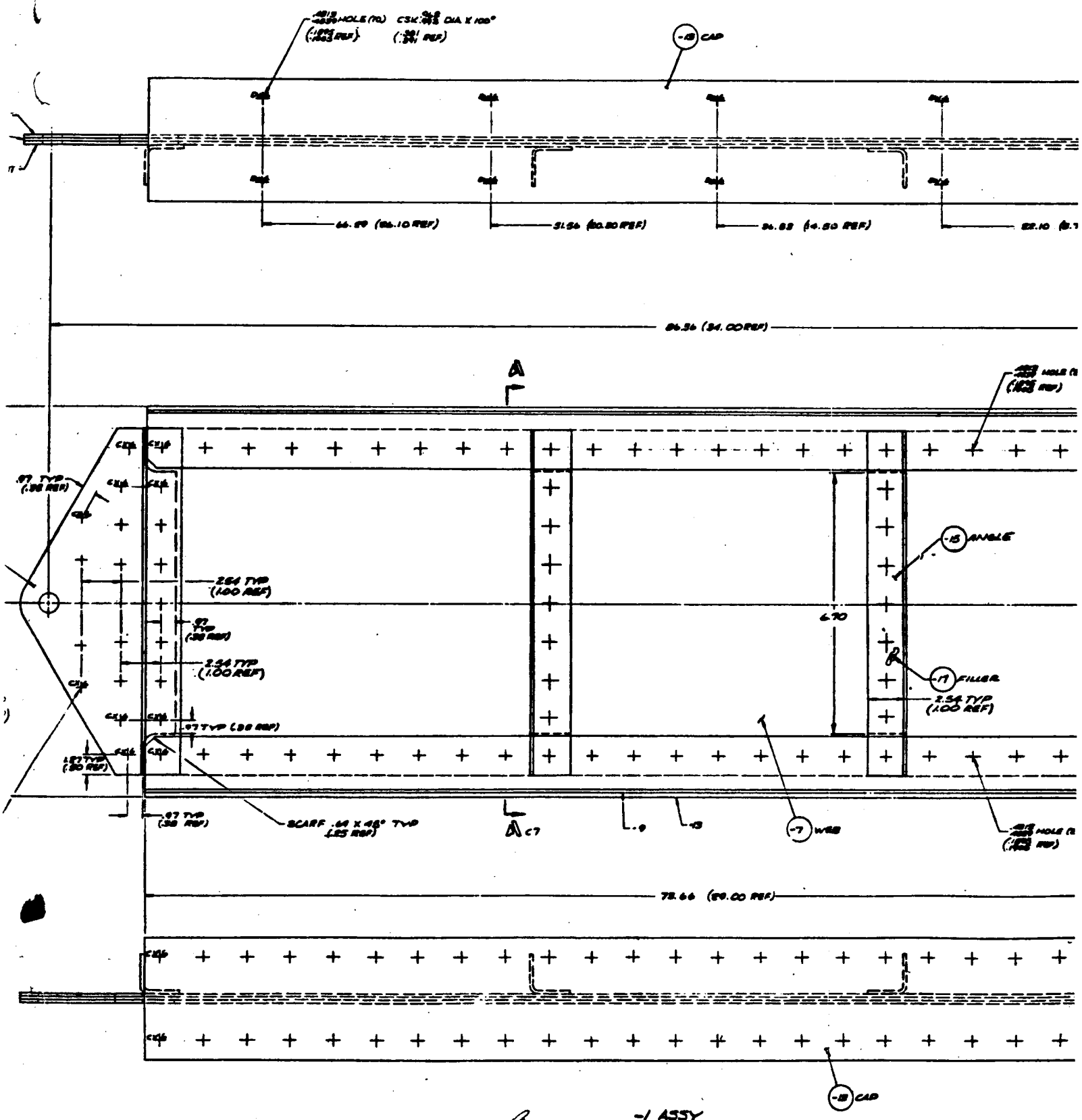

-1 ASSY

B

A-7/A-8

CODE IDENT	SECURITY CLASSIFICATION	DRAWING NO.	SH
14170		72C0196	1

FOLDOUT FRAME 2

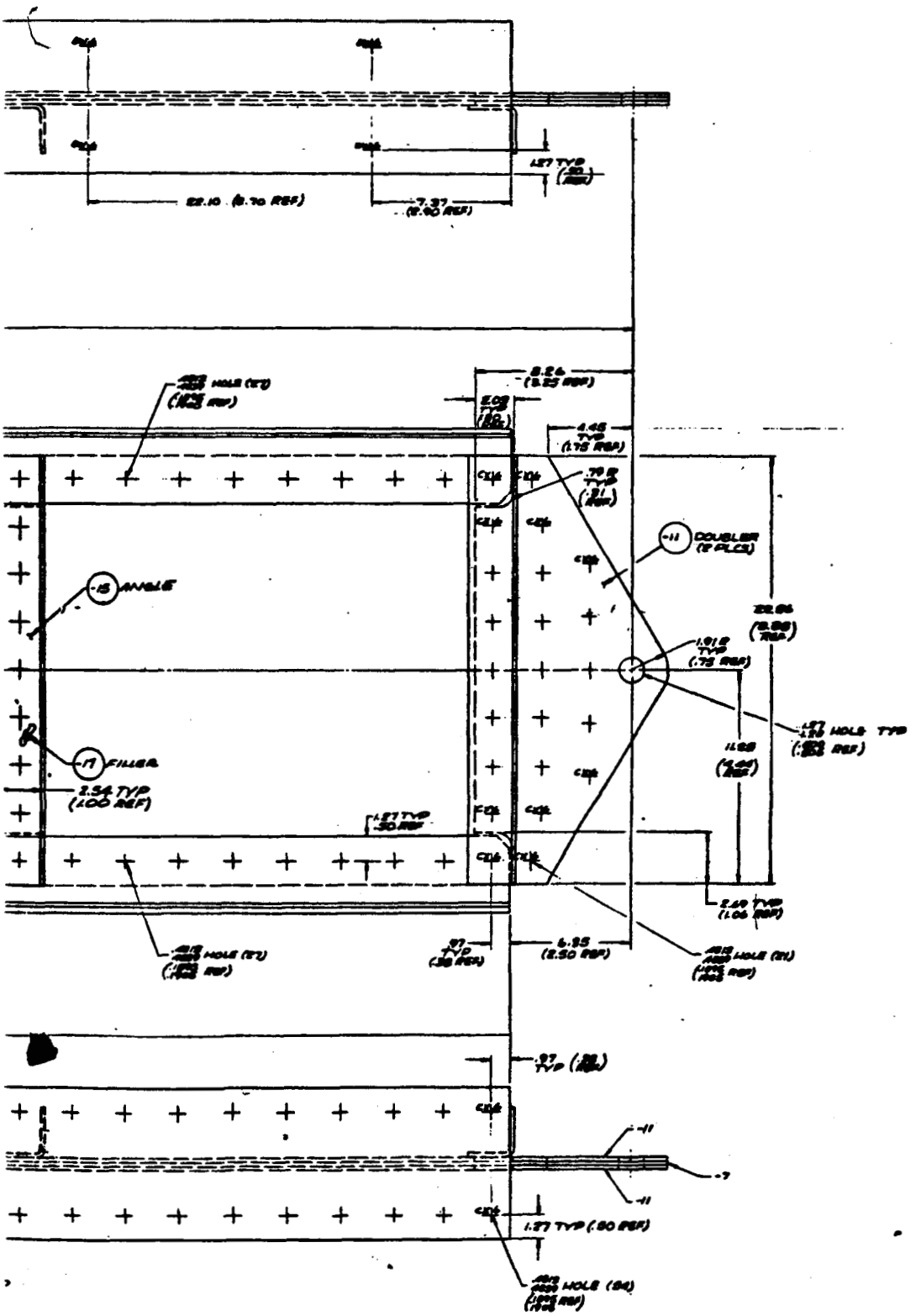

A-7/A-8 C

ZONE	LTR	REVISIONS DESCRIPTION	DATE	APPROVED
E4	A	ADD -15 ANGLE STIFF.	6-1-7[illegible]	[illegible]

FOLDOUT FRAME 4

NOTES:
1. IMPRESSION MARKING OF PART NOT PERMITTED.
2. BREAK SHARP EDGES, .015.
3. ALL FASTENERS ARE EQUALLY SPACED BETWEEN END LOCATION WITHIN ±.03.
4. [illegible] = NAS1466 PIN & NAS 1080 COLLAR.
5. [illegible] = NAS1456 PIN & NAS 1080 COLLAR.
6. ALL DIMENSIONS ARE IN CENTIMETERS.

PARTS LIST

-1	UNIT OF MEAS	ITEM OR FIND NO.	CODE IDENT NO.	PART OR IDENTIFYING NUMBER	NOMENCLATURE OR DESCRIPTION	ZONE LTR	ZONE NO.	NOTE SYMBOL	(STOCK SIZE, MATERIAL, SPECIFICATION, TYPE (TEMPER, ETC.), HEAT TREAT) NOTE TEXT
10				NAS1456-3	PIN				
150				NAS1466-5	PIN				
160				NAS1080-6	COLLAR				
2				-17	FILLER	E	4	M	.203 x 2.54 x 17.01 (.080 x 1.00 x 6.70 REF) 6AL4V TI
4				-15	ANGLE	E	4	M	.203 x 2.54 x 22.56 (.080 x 1.00 x 22.56 REF) 6AL4V TI
2				-13	CLIP	A	4	M	[illegible] REF), 6A 4V TITANIUM
4				-11	DOUBLER	E	3	M	.203 x 10.2 x 22.6 (.080 x 4.0 x 8.9 REF),
4				-9	ANGLE	E	7	M	.203 x 7.7 x 75.7 ([illegible] x 3.0 x 29.8 REF),
1				-7	WEB	C	5	M	[illegible] x 22.6 x [illegible] x 8.9 x 85.5 REF), 6A 4V TITANIUM
[illegible]				-1	ASSY			U	NEXT ASSY 72C0192 (1 REQD)

REQUIREMENTS PER ASSEMBLY/INSTALLATION

NOTE SYMBOL: E—END ITEM; G—GENERAL NOTE; L—LIGHT; M—MATERIAL; R—REFERENCE DESIGNATION; S—STOCK NO.; U—USAGE DATA

UNLESS OTHERWISE SPECIFIED: ALL MACHINED SURFACES 125 √

RIVET BASIC CODE-NAS523

SEE 0-78014 FOR ABBREVIATION, CODE AND SYMBOL REQUIREMENTS

SEE 0-78002 FOR STANDARD MANUFACTURING AND INSTALLATION REQUIREMENTS

ASSOCIATED LIST REQUIRED: SEE DOCUMENT NAME, NUMBER PREFIXED UL ☐ FOR USAGE LIST

UNLESS OTHERWISE SPECIFIED DIMENSIONS ARE IN INCHES
TOLERANCES: .X ±.1, .XX ±.03, .XXX ±.010; ANGULAR PER 0-78002

CHECK / STRESS / GR ENGR / DESIGN / DRAWN / CONTRACT NO.

MATL / FINISH

CONVAIR AEROSPACE DIVISION OF GENERAL DYNAMICS
SAN DIEGO, CALIFORNIA

FRAME ASSY-
COMPRESSION PANEL

SIZE	CODE IDENT	DRAWING NO
J	14170	72C0196

SCALE 1/1 RELEASED. SHEET 1 OF 1

SECURITY CLASSIFICATION

A-71A-8 D